AD NUMBER

AD846415

NEW LIMITATION CHANGE

TO

Approved for public release, distribution unlimited

FROM

Distribution authorized to U.S. Gov't. agencies and their contractors; Administrative/Operational Use; Oct 1966. Other requests shall be referred to Air Force Materials Laboratory, Wright-Patterson AFB, OH 45433.

AUTHORITY

AFML ltr, 7 Dec 1972

AFML-TR-68-292

EVALUATION OF SUPERALLOYS FOR HYPERSONIC VEHICLE HONEYCOMB HEAT SHIELDS

Raj K. Malik

Alvin R. Stetson

Solar Division of International Harvester Company

TECHNICAL REPORT AFML-TR-68-292

October 1968

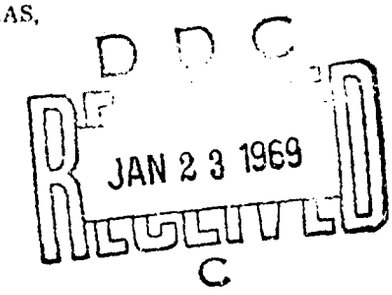

Air Force Materials Laboratory
Air Force Systems Command
Wright-Patterson Air Force Base, Ohio

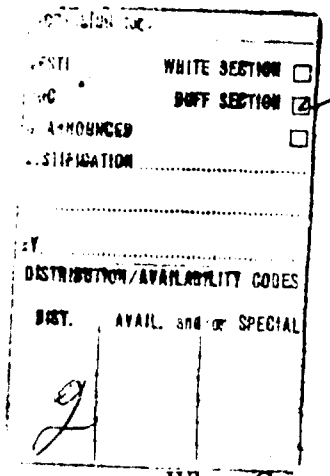

NOTICES

When Government drawings, specifications, or other data are used for any purpose other than in connection with a definitely related Government procurement operation, the United States Government thereby incurs no responsibility nor any obligation whatsoever; and the fact that the Government may have formulated, furnished, or in any way supplied the said drawings, specifications, or other data, is not to be regarded by implication or otherwise as in any manner licensing the holder or any other person or corporation, or conveying any rights or permission to manufacture, use, or sell any patented invention that may be in any way related thereto.

This document is subject to special export controls and each transmittal to foreign governments or foreign nationals may be made only with prior approval of the Materials Support Division, MAAS, Wright-Patterson AFB, Ohio 45433.

Distribution of this document is limited for protection of technical know-how relating to critical products or manufacturing processes, tests and evaluation of military operational weapons systems and installation and other technology restricted by U. S. Export Control Acts.

Copies of this report should not be returned to the Aeronautical Systems Division unless return is required by security considerations, contractual obligations, or notice on a specific document.

EVALUATION OF SUPERALLOYS FOR HYPERSONIC VEHICLE HONEYCOMB HEAT SHIELDS

Raj K. Malik

Alvin R. Stetson

Solar Division of International Harvester Company

FOREWORD

This is the final technical documentary report and covers all the work performed under Contract F33615-67-C-1217. This work was performed in the Research Laboratories of Solar Division of International Harvester Company and was administered under the direction of Air Force Materials Laboratory, with Capt Elvin H. Beardslee, MAAS, Materials Support Division, acting as Project Engineer. This was accomplished under Project 651, Task G.

Mr. R. K. Malik of the Solar Research Laboratories was the Principal Investigator for this program. Mr. A. R. Stetson and Dr. A. G. Metcalfe were joint technical directors of this program and a companion program, F33615-67-C-1211, "Joining of Superalloy Foils for Hypersonic Vehicles". Acknowledgement is made to A. E. Livingstone (specimen preparation and property measurement), C. G. Root (design of the slow cycle test apparatus), and R. Hutting (Metallography specimens).

The manuscript of this report was released by the authors in October 1968 for publication. Solar's internal report number is RDR 1467-4.

This technical report has been reviewed and is approved.

L. N. HJELM, Chief
Space & Missiles Systems Support Branch
Materials Support Division
Air Force Materials Laboratory

ABSTRACT

Objectives of the program were to study the effects of cyclic oxidation exposures on the properties of six superalloy foils in 0.18 (200,000 feet), 10.0 (100,000 feet), and 760 Torr for use in hypersonic vehicle honeycomb heat shields. The six superalloy foils (0.01 inch) were Rene' 41, Inconel 718, Inconel 625, Haynes 25, TD Nickel, and TD Nickel/chromium. Evaluation was by creep tests and before and after reentry simulation exposures by tensile and notch tensile tests at room and elevated temperatures, room temperature high rate tensile tests, and axial fatigue tests at room temperature and at ductility minimum temperature. Weight change data, metallography, X-ray diffraction, gas and electron microprobe analyses were also used.

Based on less than one percent creep under a one ksi stress in 20 hours, the TD Nickel and TD Nickel/chromium alloys were serviceable up to 2400°F; Inconel 625 and Haynes 25 up to 2100°F; and Rene' 41 and Inconel 718 up to 2000°F. However, based on retention of at least 67 percent of initial properties after 760 Torr oxidation exposures for 100 one-hour cycles at different T_{max}, the recommended maximum service temperatures were 2400°F for TD Nickel/chromium; 2200°F for TD Nickel; 2000°F for Haynes 25; and 1800°F for Inconel 625, Inconel 718, and Rene' 41. Rene' 41 and Inconel 718 were eliminated because of higher overall degradation in mechanical properties and oxidation rate than Inconel 625 and Haynes 25 during the 1800°F - 760 Torr - 100-cycle exposure. As a result of the 0.18 Torr - 100 one-hour slow-cycle oxidation exposure, no changes in maximum use temperature of the four alloys were made. No significant effects of decreased pressure were observed except for Haynes 25. Further evaluation for combined effects of stress, temperature, and pressure in profile simulation tests for 100 one-hour slow cycles resulted in final recommendations as follows:

Superalloy Foil (0.01 in.)	Recommended T_{max} (°F)	Most Severe Pressure (Torr)	Maximum Stress for Elongation of 1% in 100 Cycles (ksi)
TD Nickel/ Chromium	2400	760	1.0
TD Nickel	2000	760	4.0
Haynes 25	1800	0.18	2.9
Inconel 625	1800	760	1.0

Effects of temperature, pressure, and stress and identification of surface oxides are described. The degradation in mechanical properties is explained in terms of microstructural changes, internal oxidation, and microhardness values. From the results of various mechanical tests, it was concluded that room temperature tensile or fatigue tests are the most severe for the determination of performance degradation resulting from oxidation exposures. Preoxidizing the program alloy foils improved their high-temperature performance, but only at the sacrifice of room temperature properties.

The distribution of this abstract is unlimited.

CONTENTS

CONTENTS (Cont)

CONTENTS (Cont)

ILLUSTRATIONS

ILLUSTRATIONS (Cont)

ILLUSTRATIONS (Cont)

TABLES

TABLES (Cont)

1

INTRODUCTION

Foil gage superalloys are candidate materials for use in structural and heat shield panels for reentry and hypersonic vehicles. Unlike the coated refractory metals, little attention has been given to the potential environmental effects that may contribute to changes in mechanical properties of foil gage superalloys as a result of the low-pressure and slow-cyclic exposure of a typical hypersonic flight. The objective of this program was to investigate and evaluate operative degradation mechanisms so that reuse capabilities and limitations for promising nickel- and cobalt-base alloy foils (0.01 inch thick) could be predicted. The joining processes for the selected superalloys were selected and evaluated in a companion program at Solar (Contract F33-615-67-C-1217).

Evaluation of superalloys was accomplished by characterization of alloy degradation mechanisms after exposure to slow thermal cycles in dry, atmospheric pressure air and in air at reduced pressure of 0.18 Torr. In addition, environmental simulation tests were conducted by slow thermal cycling of the foil alloys under superimposed levels of stress, at atmospheric pressure, and in reduced pressures of 10.0 Torr and 0.18 Torr, the equivalent pressures at altitudes of 100,000 feet and 200,000 feet, respectively.

The program was divided into the following four phases.

- Phase I - Establish Baseline Data

  In this phase, literature search on candidate nickel- and cobalt-base superalloys and dispersion-strengthened nickel foil alloys was made for identifying alloy availability and heat treatment procedures and for the assessment of available mechanical properties, oxidation and thermal stability data, and also emittance. Based on this literature review and alloy availability, six superalloys were selected for further evaluation. This phase also included verification and supplemental testing, as required, of mechanical property data on the selected six alloy foils (0.01 inch thick). Mechanical testing included tensile tests, notch tensile tests, high rate tensile tests from room temperature to 2400°F; creep tests from 1800 to 2400°F; and fatigue tests at room temperature and at T_{dm}[1]. These tests were performed so that direct correlation could be made to mechanical property test data obtained in subsequent phases of the program.

1. Ductility minimum temperature

- Phase II - Effects of Slow, Cyclic, Atmospheric Pressure Oxidation Exposure

  The effects of cyclic atmospheric pressure oxidation were evaluated by weight change and by other analytical techniques (metallography, electron microprobe, gas analyses, and X-ray diffraction) and by mechanical property testing (similar to that in Phase I). Foil specimens of six superalloys were subjected to 100 one-hour, slow-cycle oxidation exposures at three temperatures (from 1800 to a maximum of 2400°F) in atmospheric pressure dry air. Based on the results of evaluation of the oxidized specimens, four superalloys (Inconel 625, Haynes 25, TD Nickel, and TD Nickel/chromium) and their maximum service temperature (T_{max}) were selected. The four superalloys were further evaluated in Phase III.

- Phase III - Effects of Slow, Cyclic, Low-Pressure Oxidation Exposure

  Foil specimens of the selected four superalloys were subjected to 100 one-hour, slow-cycle oxidation exposures at 0.18 Torr pressure and at their respective T_{max}. The effects of low-pressure oxidation exposure were evaluated by weight change, analytical techniques, and other mechanical property testing as in Phase II.

- Phase IV - Effects of Hypersonic Vehicle Profile Simulation

  This phase differed from Phases II and III because load was included in the mission profile simulation tests. Environmental simulated mission profile tests for the six selected superalloys were conducted for 22 one-hour cycles at different T_{max} (from 1800 to 2400°F) in atmospheric pressure and in reduced pressure (10.0 Torr and 0.18 Torr) air. Selected mission profile exposures at 100 one-hour cycles were also conducted. The effects of the simulated profile exposures were evaluated by room temperature tensile tests and by metallographic analyses.

This final technical documentary report describes the experimental procedures, the effects of oxidation and simulated profile exposures, and the recommendations for service capability of the selected superalloy foils for hypersonic vehicle honeycomb heat shield applications. The experimental procedure for test specimen fabrication, oxidation exposures, mechanical testing, diagnostic techniques, and mission profile simulation tests are given in Section 3. Section 4 presents the mechanical property data and analytical results for superalloy foils in the as-received condition and after atmospheric pressure and low-pressure oxidation exposures (i.e., the results of

Phases I, II, and III). The effects of hypersonic vehicle profile simulation tests (Phase IV) are also covered in Section 4. Results are discussed in Section 5. Conclusions and recommendations are made in Section 6. A comprehensive summary of the entire program is given in Section 2.

2

SUMMARY

Program objectives were accomplished by:

- An investigation to characterize the effects of cyclic oxidation exposures on the mechanical properties of six alloy foils for use as honeycomb heat shields in hypersonic vehicles in atmospheric pressures, and in pressures expected to be encountered at altitudes of 100,000 (10.0 Torr) and 200,000 feet (0.18 Torr).

- A study of the combined effects of temperature, stress, and pressure by different mission profile simulation tests of the program alloy foils.

- An estimation of the reuse capability of foils for honeycomb skins for 100 missions.

On the basis of availability, strengthening mechanism, and a literature search for mechanical property and oxidation and stability data, the six superalloy foils selected for evaluation in this program were:

- Rene' 41 and Inconel 718 (precipitation hardened)
- Inconel 625 and Haynes 25 (solid solution strengthened)
- TD Nickel and TD Nickel/chromium (thoria dispersion strengthened)

Evaluation of the six alloy foils was conducted by creep tests, oxidation rate, mechanical property tests and diagnostic techniques, and by profile simulation tests. The procedures and results are summarized in succeeding paragraphs.

2.1 CREEP TESTS

Creep tests for the six program alloys in the as-received condition in the temperature range 1800 to 2400°F were conducted. The maximum use temperature recommended, based on the temperature at which the creep was less than one percent

under a one ksi stress in 20 hours, was 2400°F for TD Nickel/chromium and TD Nickel, 2100°F for Haynes 25 and Inconel 625, and 2000°F for Inconel 718 and Rene' 41. Creep rate was lowest for TD Nickel/chromium.

2.2 OXIDATION RATE

The six superalloy foils were subjected to 100 one-hour slow-cycle oxidation exposures in 760 or 0.18 Torr at various T_{max} in the slow cycle test furnace (MGR). The different oxidation exposures conducted were:

1800°F - 760 Torr, Rene' 41, Inconel 718, Inconel 625, and Haynes 25

2000°F - 760 Torr, all the six program alloys

2100°F - 760 Torr, Haynes 25

2200°F - 760 Torr, TD Nickel and TD Nickel/chromium

2400°F - 760 Torr, TD Nickel and TD Nickel/chromium

1800°F - 0.18 Torr, Inconel 625

2000°F - 0.18 Torr, Haynes 25

2200°F - 0.18 Torr, TD Nickel and TD Nickel/chromium

Among the four alloys oxidized at 1800°F in 760 Torr, the rate of oxidation was highest for Rene' 41 and lowest for Inconel 625. The oxidation rate was highest for TD Nickel and lowest for TD Nickel/chromium among the six alloys subjected to the 2000°F - 760 Torr oxidation exposure. After oxidation exposure at 2400°F, TD Nickel was embrittled, but TD Nickel/chromium was found to be satisfactory.

2.3 MECHANICAL PROPERTY TESTS AND DIAGNOSTIC TECHNIQUES

The mechanical property tests conducted were tensile tests (standard, notch, and high rate) and fatigue tests at room temperature and at elevated temperatures The diagnostic techniques were optical microscopy; chemical analysis for carbon, oxygen, and nitrogen; microhardness determination; X-ray diffraction and electron microprobe analyses. The maximum service temperature was the temperature that did not produce a loss of more than 33 percent of any mechanical property from the as-received condition.

2.3.1 Precipitation Hardened Alloys (Rene' 41 and Inconel 718)

The 2000°F - 760 Torr - 100-cycle oxidation exposure resulted in 28 and 49 percent loss in room temperature tensile yield strength (F_{ty}), 38 and 50 percent loss

in room temperature fatigue limit (for 5 x 10^6 cycles) for Rene' 41 and Inconel 718, respectively. The loss in tensile properties was highest at T_{dm}[1] compared to that at room temperature or at T_{ox}[2] (2000°F). Therefore, the two alloys were not serviceable at 2000°F. The loss in tensile properties at different test temperatures was greater due to the 2000°F exposure than to the 1800°F exposure because of greater decarburization, intergranular cracking, formation of alloy depletion layer, μ phase instability (for Rene' 41 only), and excessive grain growth (especially for Inconel 718) and higher oxidation rate.

The Rene' 41 and Inconel 718 alloys were eliminated from the remainder of the program because of the higher creep rate, oxidation rate, and overall degradation in tensile properties due to the 1800°F - 760 Torr - 100-cycle exposure than was experienced by Inconel 625 and Haynes 25 alloys.

2.3.2 Solid Solution Strengthened Alloys (Inconel 625 and Haynes 25)

The atmospheric pressure oxidation exposure for 100 one-hour slow cycles at 2100°F for Haynes 25 and at 2000°F for Inconel 625 caused 34 percent loss in room temperature F_{ty} and more than 50 percent loss in room temperature fatigue limit. Decarburization, oxidation attack along grain boundaries, and the formation of an alloy depletion layer were also noted. The loss in properties was highest at room temperature than at any other test temperature. Figures 1A and 1B are bar graphs of F_{ty} and fatigue limits at different test temperatures for Inconel 625 and Haynes 25, respectively, in the as-received condition and after 760 and 0.18 Torr oxidation exposures at 1800°F (Inconel 625) or 2000°F (Haynes 25). The loss in room temperature Fty or fatigue limit was less than 33 percent. Therefore, Inconel 625 and Haynes 25 alloys were considered satisfactory for use up to 1800 and 2000°F, respectively. It should be noted that the F_{ty} at 1800°F was higher in the oxidized conditions for Inconel 625 than in the as-received condition (Fig. 1A); for Haynes 25, the F_{ty} at 2000°F was higher after the 2000°F - 760 Torr - 100-cycle oxidation exposure, but lower after the 2000°F - 0.18 Torr - 100-cycle exposure than in the as-received condition (Fig. 1B). The most severe pressure conditions were 0.18 Torr for Haynes 25 and 760 Torr for Inconel 625.

The surface oxides, as determined by X-ray diffraction analyses, were spinel $NiCr_2O_4$ for Inconel 625 after oxidation at 1800°F and 760 or 0.18 Torr, and for Haynes 25 alloy spinel $CoCr_2O_4$ (760 Torr), α-Cr_2O_3 (0.18 Torr), and α-Cr_2O_3 + $CoCr_2O_4$ (10.0 Torr) after exposure at 2000°F for 100 one-hour cycles.

---

1. T_{dm} - Ductility minimum temperature (1600°F for Rene' 41 and 1300°F for Inconel 718)

2. T_{ox} - Maximum oxidation exposure temperature

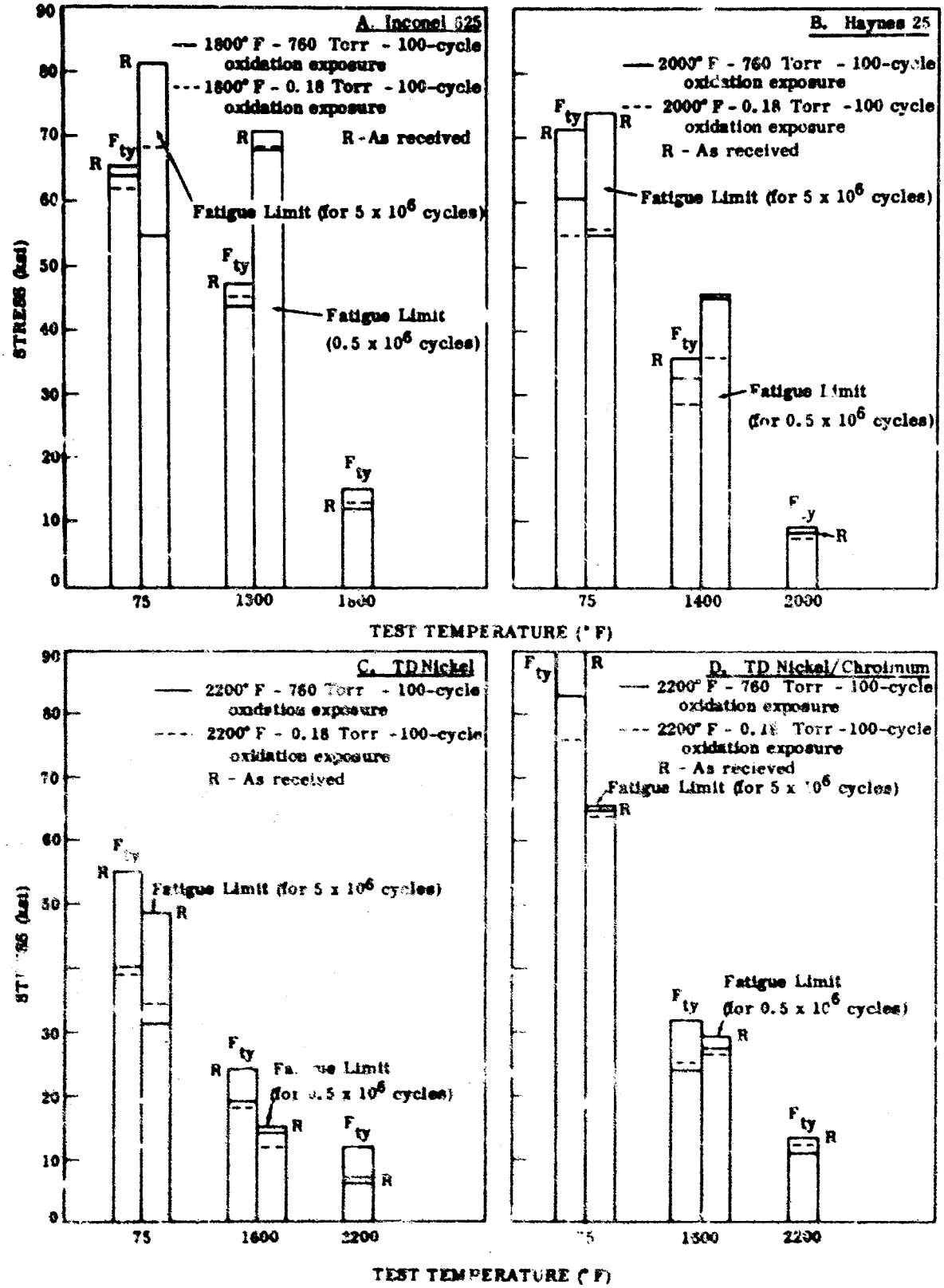

FIGURE 1. STRESS VERSUS TEMPERATURE FOR SOLID SOLUTION AND DISPERSION STRENGTHENED ALLOYS

2.3.3 Dispersion Strengthened Alloys (TD Nickel and TD Nickel/Chromium)

The TD Nickel alloy was severely embrittled and underwent a 72 percent loss in room temperature tensile ultimate strength (F_{tu}) after 760 Torr oxidation exposure at 2400°F. The 2200°F - 760 Torr - 100-cycle exposure for TD Nickel resulted in less than 33 percent loss in tensile properties at different test temperatures (Fig. 1C). The F_{ty} at 2200°F was higher after oxidation than in the as-received condition, most likely because of plasticity of NiO at higher temperatures and increased cross section. Although the loss in room temperature fatigue limit was slightly more than 33 percent, the loss in fatigue limit at T_{dm}[1] was only nine percent. The loss in other properties was less than 33 percent. Therefore, the TD Nickel alloy was considered satisfactory for service up to 2200°F. The thickness of the NiO and the extent of internal NiO was found to increase with increasing oxidation temperature or with increasing pressure.

TD Nickel/chromium was found to be serviceable at 2400°F from the results of mechanical tests (Fig. 1D) or diagnostic evaluation. The oxide at the surface or oxide in the substrate was Cr_2O_3. The extent of internal oxide increased with temperature.

2.4 MISSION PROFILE SIMULATION TESTS

Profile simulation tests were conducted to determine the combined effects of stress, cyclic oxidation, and environmental pressures on the superalloy foils. Two different stress levels and three different pressures, 760, 10.0, and 0.18 Torr, were used for each mission profile. The majority of tests were conducted for 22 one-hour slow cycles. Selected 100 one-hour slow-cycle tests were also performed.

The Haynes 25 specimen ruptured after 65 cycles in the profile simulation test conducted at 2000°F - 0.18 Torr - 1 ksi. There was 60 percent loss in room temperature F_{tu} and about 50 percent loss in substrate thickness for the TD Nickel after 2200°F - 760 Torr - 1 ksi profile simulation tests. Therefore, the recommended maximum service temperatures for Haynes 25 and TD Nickel were reduced to 1800 and 2000°F, respectively. Based on this final evaluation, recommendations on the service capability for the four superalloy foils for use in hypersonic vehicle honeycomb heat shields are contained in the following tabulation.

1. T_{dm} - Ductility minimum temperature from literature search is 1600°F for TD Nickel and TD Nickel/chromium; 1300°F for Inconel 625; and 1400°F for Haynes 25.

Superalloy Foil (0.01 in.)	Recommended T_{max} (°F)	Most Severe Pressure (Torr)	Maximum Stress for Elongation of 1 percent (ksi)
TD Nickel/chromium	2400	760	1.0
TD Nickel	2000	760	~4.0
Haynes 25	1800	0.18	~2.9
Inconel 625	1800	760	~1.0

From the results of mechanical tests, the following observations were made:

- The percent loss in tensile properties as a result of cyclic oxidation exposures was highest at room temperature for Inconel 625, Haynes 25, TD Nickel, and TD Nickel/chromium, and at T_{dm} for Rene' 41 and Inconel 718.

- Preoxidizing the program alloy foils improved the high-temperature performance but impaired the room temperature properties.

- The room temperature tensile or fatigue tests are the most severe tests for the determination of oxidation effects.

- Increasing the test temperature resulted in a high creep rate and a decrease in tensile or fatigue strength. By increasing the oxidation exposure maximum temperature (T_{ox}), the oxidation rate and oxide spalling were increased, and the tensile properties and fatigue life at room temperature and at T_{dm} were decreased, except for TD Nickel/chromium.

- Reduced pressure exposure was most severe on the Haynes 25 alloy. The microstructure showed needles of an unidentified phase after the 2000°F oxidation exposure in the stressed condition and at 0.18 Torr pressure only. For Inconel 625, TD Nickel, and TD Nickel/chromium, the decrease in pressure resulted in reduced oxidation rate, oxide spalling, scale thickness, internal oxidation, nitrogen content, and decarburization. The TD Nickel alloy is serviceable to 2200°F in 0.18 Torr and to 2000°F in 760 Torr, whereas Haynes 25 is serviceable to 2200°F in 760 Torr and only to 1800°F in 0.18 Torr. The maximum stress to which TD Nickel/chromium can be subjected is two ksi at 0.18 Torr but only one ksi at 760 Torr during oxidation at 2400°F for 100 cycles. The reduced pressure essentially decreased the oxidation rate of Inconel 625, TD Nickel, and TD Nickel/chromium with no other deleterious effects.

3

EXPERIMENTAL PROCEDURE

This section contains data leading to the selection of the six candidate superalloys, test-specimen design and fabrication procedures, cyclic oxidation procedures, various mechanical tests, and diagnostic techniques. The procedure for mission profile simulation testing is also described.

3.1 ALLOY SELECTION AND PROCUREMENT

A survey of superalloy suppliers indicated commercial availability of nine superalloys in the form of foil (0.01-inch thick). For the nine superalloys, a comprehensive review of published reports on mechanical properties, oxidation, stability data, and emittance characteristics enabled selection of six superalloys for evaluation in this program. Alloy procurement study, literature search, and selection of alloys are described in the following sections.

3.1.1 Alloy Procurement Study

To broaden the range of alloy chemistries and strengthening mechanisms that were to be studied in the program, the availability of several foil gage superalloys not initially included as candidate program alloys was investigated. (Alloys initially included for consideration in this program were Haynes 25 (L-605), Udimet 700, Udimet 500, Rene' 41, Inconel 718, TD Nickel, TD Nickel/chromium, TD Nickel/molybdenum, Inconel 625, Hastelloy X, and TD Nickel/cobalt.) Two selection criteria were employed:

- Chromium content of the alloy
- Principal strengthening mechanism, i.e., matrix or solid-solution strengthened, precipitation-strengthened, and thoria dispersion strengthened

The selected alloys are categorized according to the most salient of these criteria in Table I.

TABLE I

CATEGORIZATION OF SEVERAL CANDIDATE SUPERALLOY SHEET MATERIALS

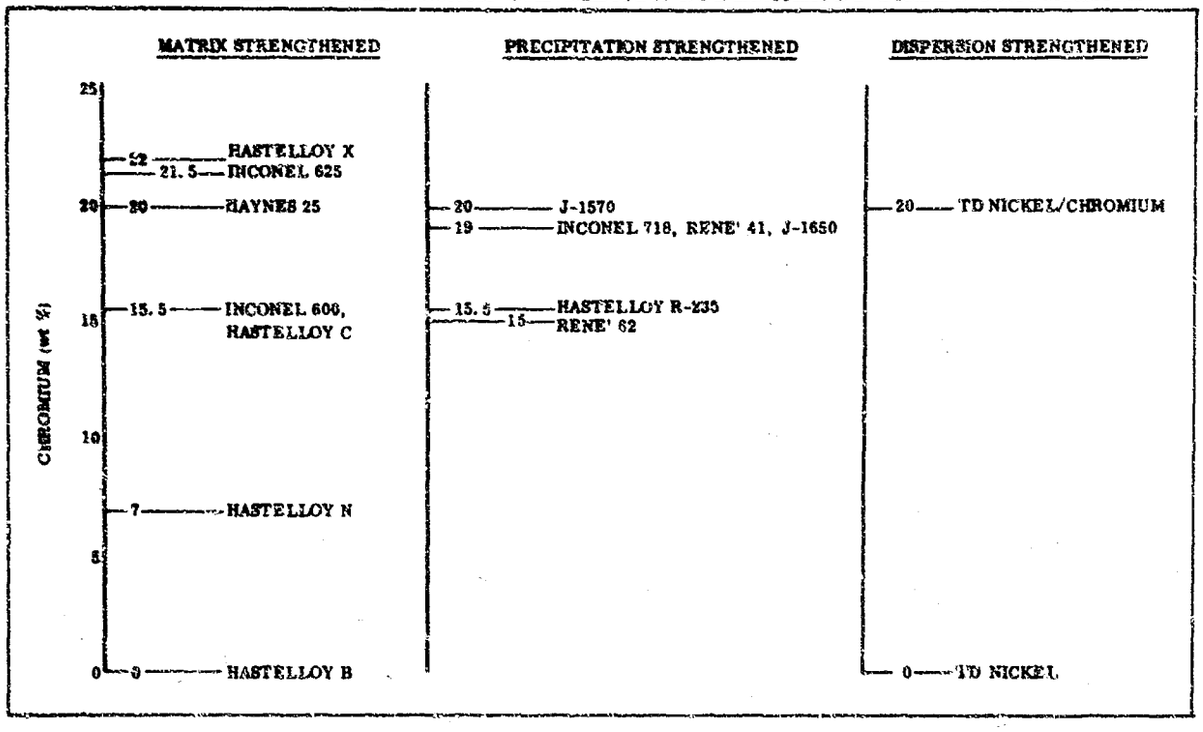

The availability of each alloy in the form of a stress relief annealed coil (0.01 by 0.75 inch) was ascertained by vendor survey. The survey showed that the following nine candidate alloys were available as 0.01-inch foil:

- Matrix Strengthened - Hastelloy X, Inconel 625, Haynes 25, Inconel 600, and Hastelloy C
- Precipitation Hardened - Inconel 718 and Rene' 41
- Dispersion Strengthened - TD Nickel and TD Nickel/chromium

The chemical composition of the nine alloys is summarized in Table II. A literature search is summarized in the succeeding section.

3.1.2 Literature Review and Data Compilation

A literature search for the compilation of data concerning heat treatment procedures, mechanical properties, oxidation and microstructural stability, and emittance characteristics of the nine available superalloys was conducted. This search was necessary to reduce the number of candidate superalloys to six for evaluation, and to provide detailed information that can be used as baseline data for the entire program.

TABLE II

CHEMICAL COMPOSITION - WEIGHT PERCENT

Element	Hastelloy X	Inconel 625	Haynes 25	Inconel 600	Hastelloy C	Inconel 718	Rene' 41	TD Nickel/Chromium	TD Nickel
Carbon	0.05 to 0.15	0.10 max	0.05 to 0.15	0.15 max	0.08 max	0.03 to 0.10	0.12 max	0.05 max	0.02 max
Nickel	Balance	Balance	9.00 to 11.00	Balance	Balance	50.00 to 55.00	Balance	Balance	Balance
Cobalt	0.50 to 2.50	1.00 max	Balance	1.00 max	2.50 max	1.00 max	10.00 to 12.00	--	0.20 max
Chromium	20.50 to 23.00	20.0 to 23.0	19.00 to 21.00	14.00 to 17.00	14.50 to 16.50	17.00 to 21.00	18.00 to 20.00	20	0.05 max
Iron	17.00 to 20.00	5.00 max	3.00 max	6.00 to 10.00	4.00 to 7.00	Balance	5.00 max	--	0.05 max
Aluminum	--	0.40 max	--	0.35 max	--	0.40 to 0.80	1.40 to 1.60	--	--
Titanium	--	0.40 max	--	0.50 max	--	0.65 to 1.15	3.00 to 3.30	--	0.05 max
Molybdenum	8.00 to 10.00	8.00 to 10.00	--	--	15.00 to 17.00	2.80 to 3.30	9.00 to 10.50	--	--
Tungsten	0.20 to 1.00	--	14.00 to 16.00	--	3.00 to 4.50	--	--	--	--
Columbium + Tantalum	--	3.15 to 4.15	--	1.00 max	--	5.00 to 5.50	--	--	--
Boron	--	--	--	--	--	0.002 to 0.006	0.003 to 0.010	--	--
Manganese	1.00 max	0.50 max	1.00 to 2.00	1.00 max	1.00 max	0.35 max	0.10 max	--	--
Silicon	1.00 max	0.50 max	1.00 max	0.50 max	1.00 max	0.35 max	0.50 max	--	--
Phosphorus	0.040 max	--	0.040 max	--	0.040 max	0.015 max	--	--	--
Sulfur	0.030 max	0.05 max	0.030 max	0.015 max	0.030 max	0.015 max	0.015 max	0.02 max	0.02 max
Other	--	-	--	Cu 0.50 max	V 0.35 max	Cu 0.10 max	--	ThO_2 2.0	Th(1.80 to 2.60
Specification	AMS 5536E	Non	AMS 5537B	AMS 5540G	AMS 5[illegible]0C	AMS 5596A	AMS 5545	None	DFN(P)-201B

A bibliography (1963 to February 1967) on the properties of the nine superalloys was requested and received from the Defense Documentation Center. This document contained 186 abstracts of which 32 were pertinent. Additional information sources included DMIC memos and reports, AFML and NASA reports, ASM, AIME, and SAE papers and abstracts, as well as vendor pamphlets on these alloys.

Collected information on the nine available alloys is presented in the Appendix. The data include short-time tensile properties, axial tension-tension fatigue life, creep strength, oxidation resistance, and total normal emittance.

An overall picture of the property data compilation is shown in Table III. Tensile strength versus temperature data were complete for the 0.01-inch Hastelloy X. Rene' 41, and TD Nickel alloys. Data were available for the remaining alloys as follows:

- Inconel 625 - up to 1800°F, unknown thickness
- Haynes 25 - up to 2100°F, 0.062 inch thick
- Hastelloy C - up to 2000°F, 0.109 inch thick
- Inconel 600 - up to 1600°F, 0.250 inch thick
- Inconel 718 - up to 1400°F, 0.063 inch thick
- TD Nickel/chromium - up to 2000°F, unknown thickness

Notch tensile data were available for the 0.01-inch Hastelloy X, Rene' 41, and TD Nickel alloys only.

Tensile-shear versus temperature data were available for the 0.01-inch TD Nickel alloy only.

Impact tensile data were not obtained for any of the alloys. Charpy impact energy was listed where available.

Fatigue data that were available for the candidate alloys are:

- Hastelloy X - Axial tension-tension, room temperature, 0.01 inch thick
- Inconel 625 - Rotating beam, room to 1600°F temperature, 0.625 inch diameter bar
- Haynes 25 - Axial tension-tension, 1500 to 1800°F, unknown thickness

TABLE III

LITERATURE REVIEW SUMMARY

	Hastelloy X	Inconel 625	Haynes 25	Hastelloy C	Inconel 600	Inconel 718	Rene' 41	TD Nickel	TD Nickel/ Chromium
TENSILE Room Temperature High Temperature	■	◪	◪	◪	◪	◪	■	■	◪
NOTCHED TENSILE Room Temperature	■	□	□	□	□	□	■	■	□
TENSILE-SHEAR Room Temperature High Temperature	□	□	□	□	□	□	□	■	□
IMPACT-TENSILE Room Temperature	□	◪	◪	◪	□	□	□	◪	□
FATIGUE Room Temperature High Temperature	◪	◪	□	□	◪	□	◪	◪	□
CREEP High Temperature	◪	◪	◪	◪	◪	◪	◪	◪	◪
OXIDATION High Temperature	■	◪	◪	◪	◪	□	◪	◪	◪
EMITTANCE High Temperature	■	□	■	■	■	□	◪	■	◪

■ Complete information available on 0.010-inch sheet

◪ Qualified information available, i.e., sheet thickness > 0.010 inch, data at particular temperatures missing, data not directly comparable

□ No information available to date

- Hastelloy C - No data available
- Inconel 600 - Rotating-beam, room to 1800°F temperature, unknown thickness
- Inconel 718 - No data available
- Rene' 41 - Axial tension-tension, room temperature, 0.01 inch thick
- TD Nickel - Axial tension-tension, room temperature, 0.01 inch thick; room to 1800°F, 0.060 inch thick
- TD Nickel/chromium - No data available

The creep data collected to date indicated that supplemental testing of all the selected 0.01-inch foils was required.

Data on oxidation resistance of all candidate alloys, except Inconel 718, were available, although not in a directly comparable form.

Emittance data were available for all alloys except Inconel 625 and Inconel 718.

3.1.3 Selection of Six Alloys

Six alloys from the nine available alloys were selected for evaluation in the program. Selection was based on:

- Availability
- Mechanical, oxidation, and optical properties of the foils as revealed by the literature search
- Alloy composition
- Strengthening mechanism

After a thorough study of all the factors, the six alloys selected were:

- Rene' 41 and Inconel 718 - precipitation strengthened
- Inconel 625 and Haynes 25 - solid solution strengthened
- TD Nickel and TD Nickel/chromium - dispersion strengthened

By adopting the philosophy that the alloy selection should result in as broad a scope as possible for the program, two nonmechanical criteria were used - alloy chemistry and principal method of strengthening. The selection of two alloys to represent each of the three strengthening mechanisms yields Rene' 41 and Inconel 718 as the precipitation hardened alloys, TD Nickel and TD Nickel/chromium as the dispersion strengthened alloys, and one cobalt-base, Haynes 25, and one nickel-base alloy as the solid solution strengthened alloys. The Haynes 25 alloy was selected since it is the only candidate cobalt-base solution strengthened alloy, and because of good elevated temperature strength. Among the four remaining solid solution strengthened alloys - Hastelloy X, Hastelloy C, Inconel 625, and Inconel 600 (all nickel-base) - one alloy had to be selected. Inconel 600 was excluded since it has significantly lower elevated temperature strength than the other three matrix strengthened alloys (Fig. 2). The elevated temperature tensile strength of the three remaining alloys was not significantly different (Fig. 2), consequently other selection criteria were employed.

The lack of axial tension-tension fatigue life data for Hastelloy C and Inconel 625 did not permit a direct comparison with Hastelloy X (Table III). Creep data at 1600°F indicated that stresses of 8 and 12 ksi were required to produce one percent creep in approximately 35 hours for Hastelloy X and Inconel 625, respectively. At 1650°F, a stress of eight ksi produced one percent creep in Hastelloy C after 47 hours. Differences in alloy thickness and the unknown conditions of the creep tests did not permit a direct comparison, but it generally can be concluded that the three alloys had similar creep strength. The three alloys showed good retention of tensile properties after oxidation exposure up to 1800°F.

To provide a direct comparison of tensile, fatigue, and creep strength between the three alloys, extensive baseline testing would have been required. Yates (Ref. 1) and Plank (Ref. 2) have stated that of the alloys investigated at Lockheed, for use in the upper surface of a family of hypersonic reentry vehicles (900 to 1800°F), Inconel 625 was the most suitable on the basis of its good tensile and creep properties, fabricability, weldability, thermal stability, and oxidation resistance. The selection of Inconel 625 for study in the program was made to determine its maximum temperature capability. Hence, adopting the broad scope philosophy, the selected alloys were:

- Inconel 625 - A nickel-base alloy containing chromium, molybdenum, columbium, and iron as major alloying elements; solid solution and carbide strengthened.

- Haynes 25 - A cobalt-base alloy containing chromium, tungsten, nickel, and iron as major alloying elements; solid solution and carbide strengthened.

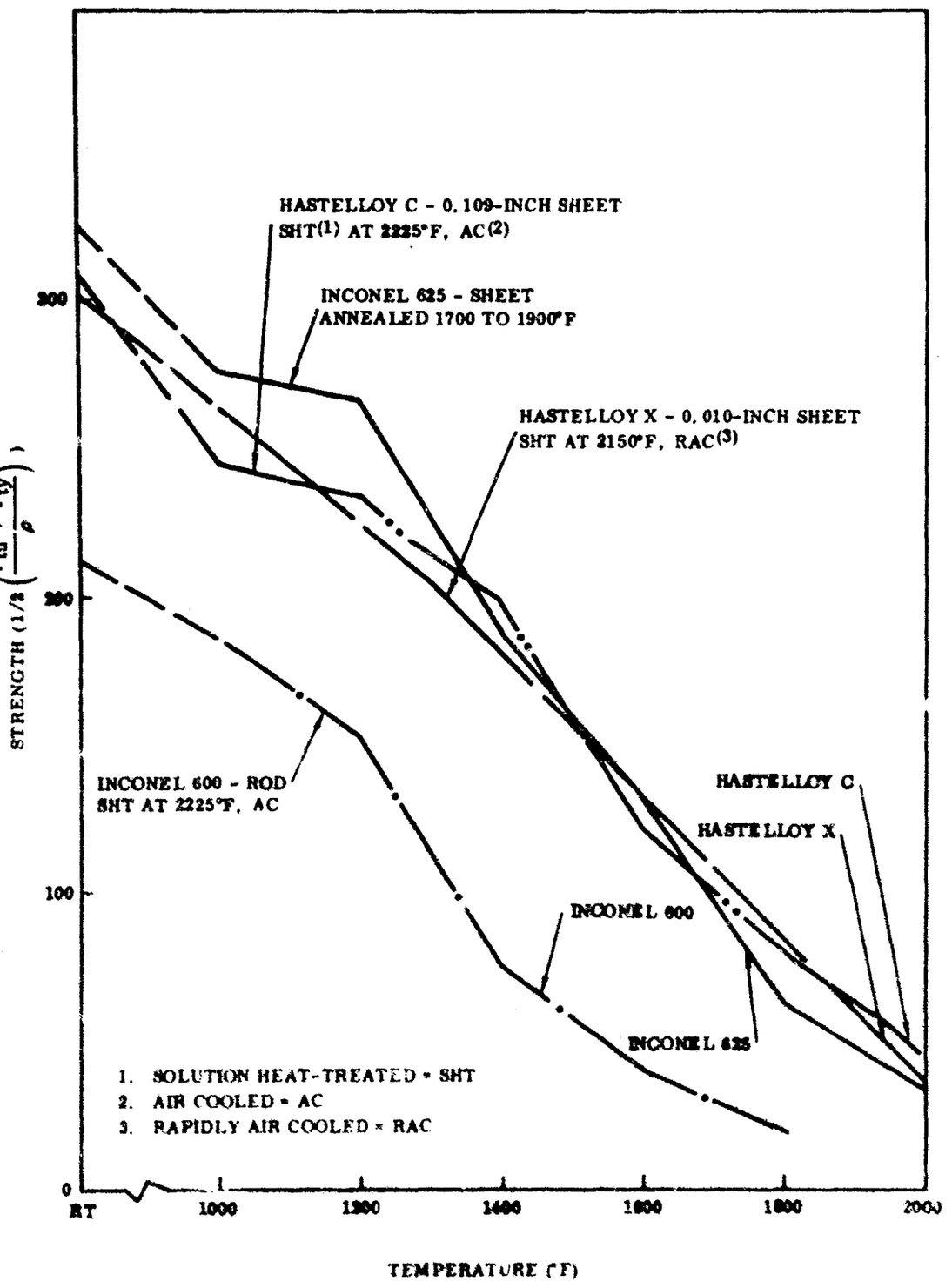

FIGURE 2. ELEVATED TEMPERATURE STRENGTH/WEIGHT RATIO OF THE AVAILABLE MATRIX-STRENGTHENED NICKEL-BASE ALLOYS

- Rene' 41 - A nickel-base alloy containing chromium, cobalt, molybdenum, iron, aluminum, titanium, and boron as major alloying elements; gamma-prime, carbide, and solid solution strengthened.

- Inconel 718 - A nickel-base alloy containing iron, chromium, columbium, molybdenum, aluminum, titanium, cobalt, and boron as major alloying elements; gamma-prime, carbide, and solid solution strengthened.

- TD Nickel - A nickel-base alloy containing thoria as the major alloying constituent; fine thoria dispersion strengthened.

- TD Nickel/chromium - A nickel-base alloy containing chromium and thoria as major alloying constituents; thoria dispersion strengthened.

The six alloys were ordered in 0.01-inch thick sheets in the solution treated or annealed condition. The alloy suppliers, heat numbers, chemical analyses, heat treatments, and typical mechanical properties as provided by the vendors' certification sheets are summarized in Table IV.

Receiving inspection procedures for each alloy included:

- Visual surface appearance
- Surface finish
- Alloy microstructure, microhardness, and grain size in the longitudinal and transverse directions at the start, middle, and end of the coil.

All the alloys received had satisfactory flat surfaces that were free of tears or deep scratches and were bright finished. The average rms surface finishes, as determined with a profilometer, were 12, 7, 15, 25, and 3 microinches (rms) for the Inconel 625, Haynes 25, Rene' 41, Inconel 718, TD Nickel and TD Nickel/chromium alloys, respectively.

Sections from the start, middle, and end of the alloy coils were cut for metallographic examination and the microstructures of the as-received alloys are discussed in Paragraph 4.4.1.

TABLE IV

VENDORS' CERTIFIED DATA ON SIX SUPERALLOY FOILS

Superalloy	Vendor	Heat Number Size (in.) Condition	Chemical Composition (wt %)	Mechanical Properties
Rene' 41	Rodney Metals of California, Inc	72r286, AMS 5545 Cold-rolled Strip (0.010 by 12.0) Annealed at 1975°F	Ni-18.53Cr-9.76Mo-1.46Al-3.07Ti-10.95Co-2.93Fe-0.006B-0.09C-0.02Mn-0.011S-0.33Si	R_B 97 F_{tu} = 143 ksi F_{ty} at 2% offset = 105 ksi Percent elongation in 2 inches = 20 ASTM grain size = 6 Bend Test - OK
Inconel 718	Rodney Metals of California, Inc	4873, AMS 5596A Cold-rolled Strip (0.010 by 12.0) Annealed at 1900°F	18.1Cr-53.3Ni-3.10Mo-0.5Al-0.1Cu-1.07Ti-5.25Cb+Ta-0.41Co-Fe-0.0043B-0.06C-0.10Mn-0.01P-0.004S-0.11Si	R_B 84 F_{tu} = 126.8 ksi F_{ty} = 81.5 ksi Percent elongation in 2 inches = 56.6 Bend test - OK
Inconel 625	Rodney Metals of California, Inc.	NX0144A2 Cold-rolled Strip (0.010 by 12.0) Annealed at 2060°F	22.26Cr-62.10Ni-9.21Mo-0.08Al-0.14Cu-0.20Ti-3.57Cb+Ta-2.26Fe-0.01C-0.04Mn-0.010S-0.10Si	R_B 88 F_{tu} = 130 ksi F_{ty} = 66 ksi Percent elongation in 2 inches = 49.0 Bend test - OK
Haynes 25 (L-605)	Hamilton Precision Metals	B18748, AMS 5537B Cold-rolled (0.010 by 12.0) Coil Annealed at 2250°F	Co-20.14Cr-0.06C-1.95Fe-1.49Mn-10.63Ni-0.04Si-0.013S-14.87W-0.013P	F_{tu} = 137.5 F_{ty} = 67.3 Percent elongation in 2 inches = 28
TD Nickel	E. I. DuPont De Nemours & Company, Inc Baltimore, Md.	2005 Stress-relieved Sheet (0.010 by 10.0 to 12.0)	Ni-2.5ThO_2-0.0055C 0.001Ti-<0.01Fe-<0.01Cr-0.01Co-0.003Cu-0.0023S	F_{tu} (RT) = 65.7, 66.9, 70.9 ksi F_{ty} (RT) = 51.5, 49.7, 52.6 ksi Percent elongation in 1 inch (RT) = 11.2, 11.4, 10.8 F_{tu} (2000°F) = 12.1, 11.2, 12.1 ksi F_{ty} (2000°F) = 11.2, 10.8, 11.6 ksi Percent elongation in 1 inch (2000°F) 3.6, 2.5, 2.5 Bend radius = 1T
TD Nickel/Chromium	E. I. DuPont	2449 Stress-relieved Sheet (0.10 by 6.0)	Ni-1.9ThO_2-0.003N-0.024C-19.90Cr-0.0054S	F_{tu} (RT) = 127.1, 126.1, 128.6, 130.2 ksi F_{ty} (RT) = 85.6, 82.1, 85.2, 85.6 ksi Percent elongation in 1 inch (RT) = 17.5, 16.0, 17.2, 17.5 F_{tu} (2000°F) = 13.9, 15.1, 14.6, 15.5 ksi F_{ty} (2000°F) = 13.9, 14.8, 14.6, 15.5 ksi Percent elongation in 1 inch (2000°F) = 2.0, 1.8, 2.2, 2.3 Stress rupture life at 5.5 ksi exceeds 20 hours Stress rupture percent elongation in 1 inch varies - 6.4, 5.1, 2.2, 8.4 Bend radius = 2T

3.2 TEST SPECIMENS - DESIGN AND FABRICATION

The design of the test specimens for the various mechanical tests (tensile, notch tensile, high-rate tensile, creep, room temperature fatigue, and elevated temperature fatigue), environmental simulation tests, oxidation tests, and emittance measurements are shown in Figure 3. All superalloy specimens except those of TD Nickel/chromium were sheared transverse to the rolling direction. The TD Nickel/chromium specimens were machined longitudinal to the rolling direction. Fabrication procedures for these various test specimens included:

- Shearing nominal sized blanks from the alloy coil stock.
- Stacking 25 similar sized blanks, with 0.25-inch thick mild steel backup plates, into a prefabricated jig for final gang milling of the reduced gage length section. Sharp mill cutters were a necessity for satisfactory milling of the superalloys, particularly the Rene 41 and Haynes 25 alloys.
- Notching the required tensile specimens was performed on a milling machine with a 60-degree, precision ground, 0.01-inch tip, radius mill cutter. The specimens were stacked in the same fixture used to gang mill the reduced gage length section.
- Identifying the specimens by steel stamping the appropriate alloy code and designated test letters and numbers on one end of the specimen. As an example, Rene' 41 specimens to be tensile tested were stamped R-T1, R-T2, R-T3.
- Vapor degreasing the specimens before testing.
- Carefully handling the material to prevent surface scratching and specimen distortion which could lead to inconsistent results.
- The emittance specimens required for oxidation exposures were prepared by the Solar Precision Chemical Milling process (SPCM). Twenty of the $\frac{29}{32}$ inch diameter specimens of each alloy were produced simultaneously by the process. The specimens were flat and stress free.

3.3 CYCLIC OXIDATION TESTING AND OXIDATION RATE

The Merry-Go-Round (MGR) furnace used for cyclic oxidation exposure, the temperature profiles at 760 Torr and at 0.18 Torr, and the procedure for cyclic oxidation exposure and determination of oxidation rate from weight change data are described in following sections.

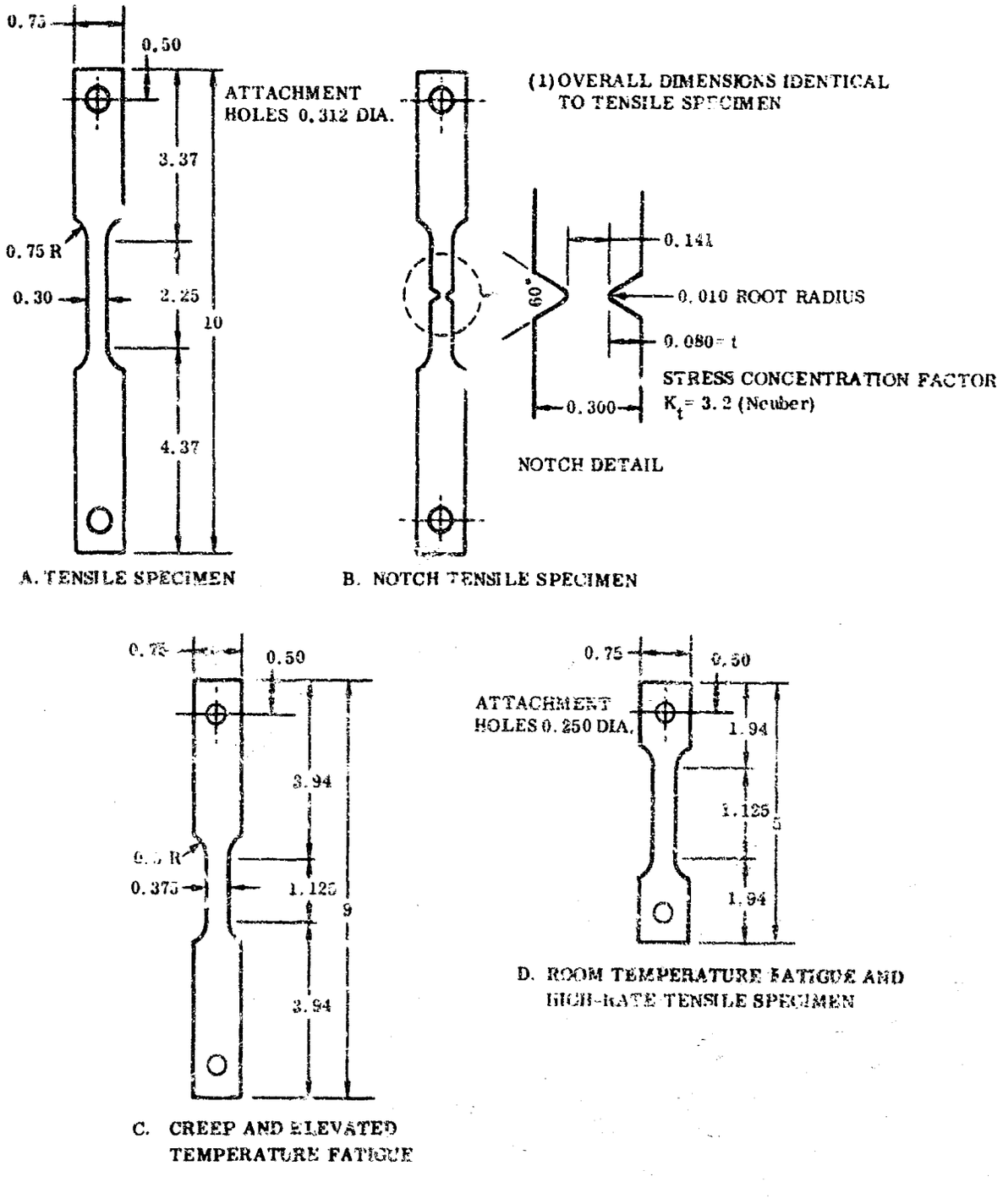

FIGURE 3. TEST SPECIMEN DESIGNS (Sheet 1 of 2)

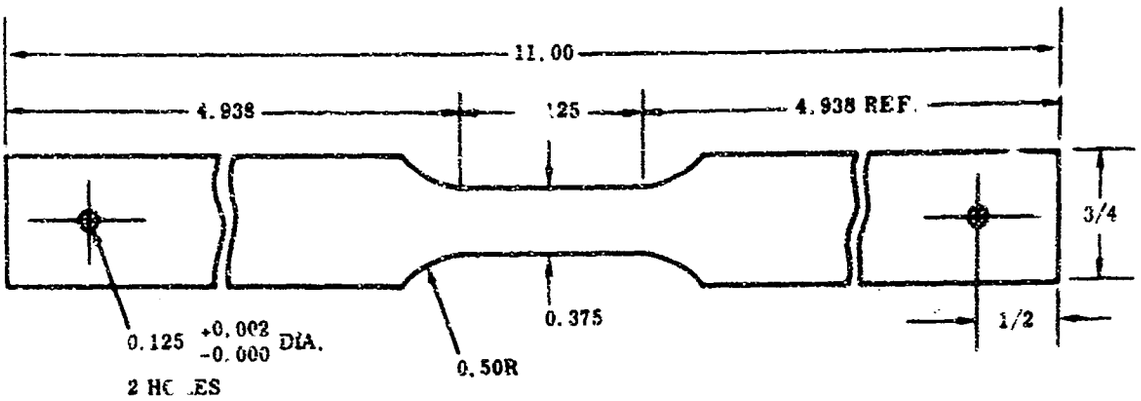

E. ENVIRONMENTAL SIMULATION TEST SPECIMEN

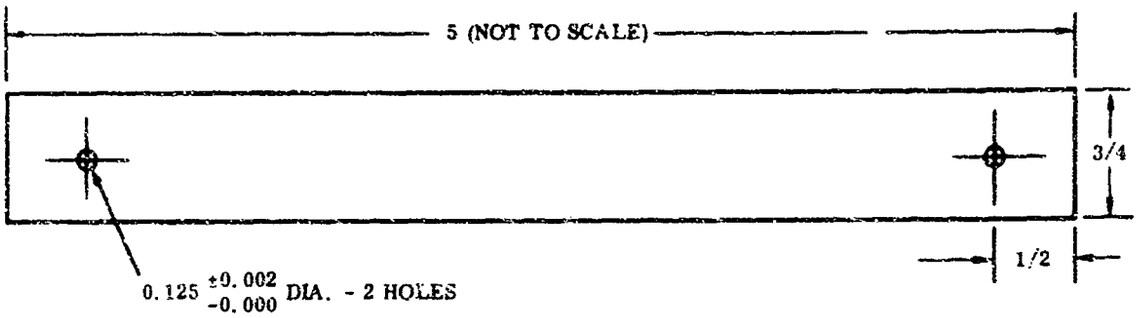

F. OXIDATION TEST SPECIMEN

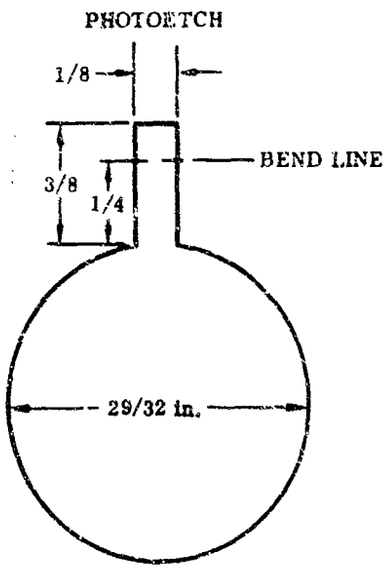

G. EMITTANCE SPECIMEN

NOTES
1. SPECIMENS MACHINED FROM 0.010-INCH SHEET
2. ALL DIMENSIONS IN INCHES

FIGURE 3. TEST SPECIMEN DESIGNS (Sheet 2 of 2)

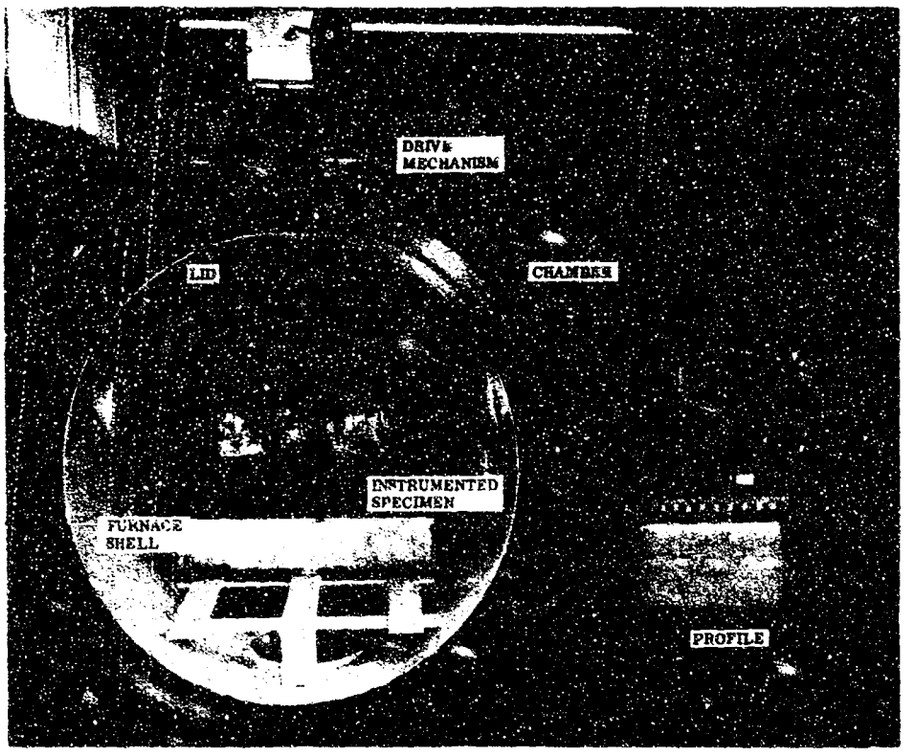

FIGURE 4. ASSEMBLED SLOW-CYCLE TEST APPARATUS

3.3.1 The MGR Furnace

The slow-cycle test apparatus for the oxidation exposures is shown in Figure 4, and a schematic of the apparatus is shown in Figure 5. Furnace heating was achieved by the use of six horizontally positioned silicon carbide heating elements. Power was supplied from a 440-volt, 3-phase, main line through a zero to 510-volt variable autotransformer and a 4:1 stepdown transformer. Temperature was controlled by a proportional band controller which drove the autotransformer by a servomotor. Specimens were supported on Kanthal A-1 wire hooks attached to the furnace lid, which rotated at one revolution/hour. Kanthal A-1 weights (0.1 pound) were attached to the bottom of each specimen to ensure alignment and minimize specimen heating distortion. The specimens were slowly advanced through a preheat section, into a constant temperature zone, and then through a cool-down section to complete the temperature cycle. The front of the MGR furnace was closed with a removable brick structure to minimize heat losses. This furnace allowed easy reproduction of the temperature profiles.

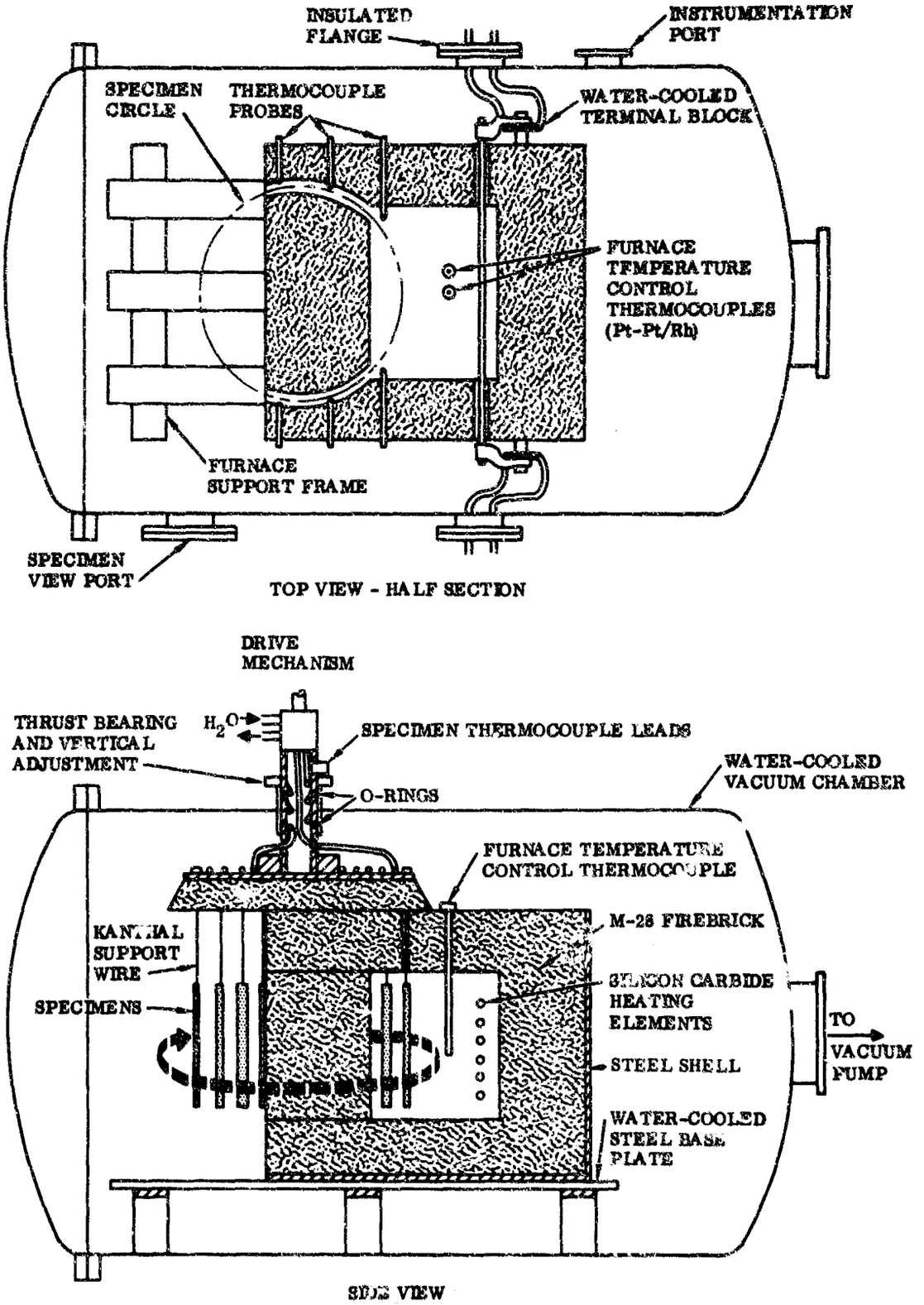

FIGURE 5. CONTROLLED ATMOSPHERE SLOW-CYCLE TEST APPARATUS

3.3.2 The Time-Temperature Profiles

The actual temperature profile in the MGR furnace was determined from thermocouples attached to test specimens. Thermocouples attached to the top, center, and bottom of a 10-inch specimen for the 2000°F T_{max} (760 Torr) profile indicated a temperature gradient of 10 degrees F between the top and center, and a gradient of 40 degrees F between the top and bottom of the specimen, the top being the hottest section. No temperature gradient was detected across the 0.01-inch thickness of the test specimen.

The typical time-temperature profiles with different maximum temperatures of 1800, 2000, 2200, and 2400°F during cyclic oxidation exposure at 760 Torr are shown in Figure 6, and at 0.18 Torr are shown in Figure 7. The approximate soak time (t_1) for temperatures within T_{max} and T_{max}-50 degrees F; the time (t_2) for temperatures above 1100°F; and the area (A) under the time-temperature profile above 1100°F for the different profiles are given in Table V.

The time-temperature profiles for the 760 Torr and 0.18 Torr oxidation were different. The times (t_1 and t_2) for the same T_{max}, were higher for the 0.18 Torr exposure than for the 760 Torr exposure (Table V). This difference in time indicates that the specimens were at temperature for a longer period during the 0.18 Torr oxidation exposure. The longer period was most likely the result of lower heat losses by convection in the 0.18 Torr oxidation than in atmospheric pressure exposure. This longer time at the temperature resulted in approximately a 15 percent increase in area (A) in the 0.18 Torr oxidation exposures at T_{max} of 1800, 2000, or 2200°F over that in the 760 Torr oxidation exposures (Table V). Thus, time-temperature effects would be expected to be about 15 percent (and about 7.8 percent) more severe during the 0.18 Torr oxidation than during the 760 Torr exposure at maximum temperatures up to 2200°F (and at T_{max} of 2400°F respectively).

3.3.3 The Cyclic Oxidation Procedure

The following forty test specimens of each of the six program alloy foils were subjected to atmospheric pressure oxidation exposures for 100 one-hour slow cycles at various T_{max}.

- 3 - Emittance
- 2 - Oxidation standards for weight change and analyses
- 9 - Standard tensile
- 2 to 6 - Notch tensile
- 2 - High-rate tensile (for selected oxidation exposures)
- 20 - Fatigue at room temperature and at T_{dm}

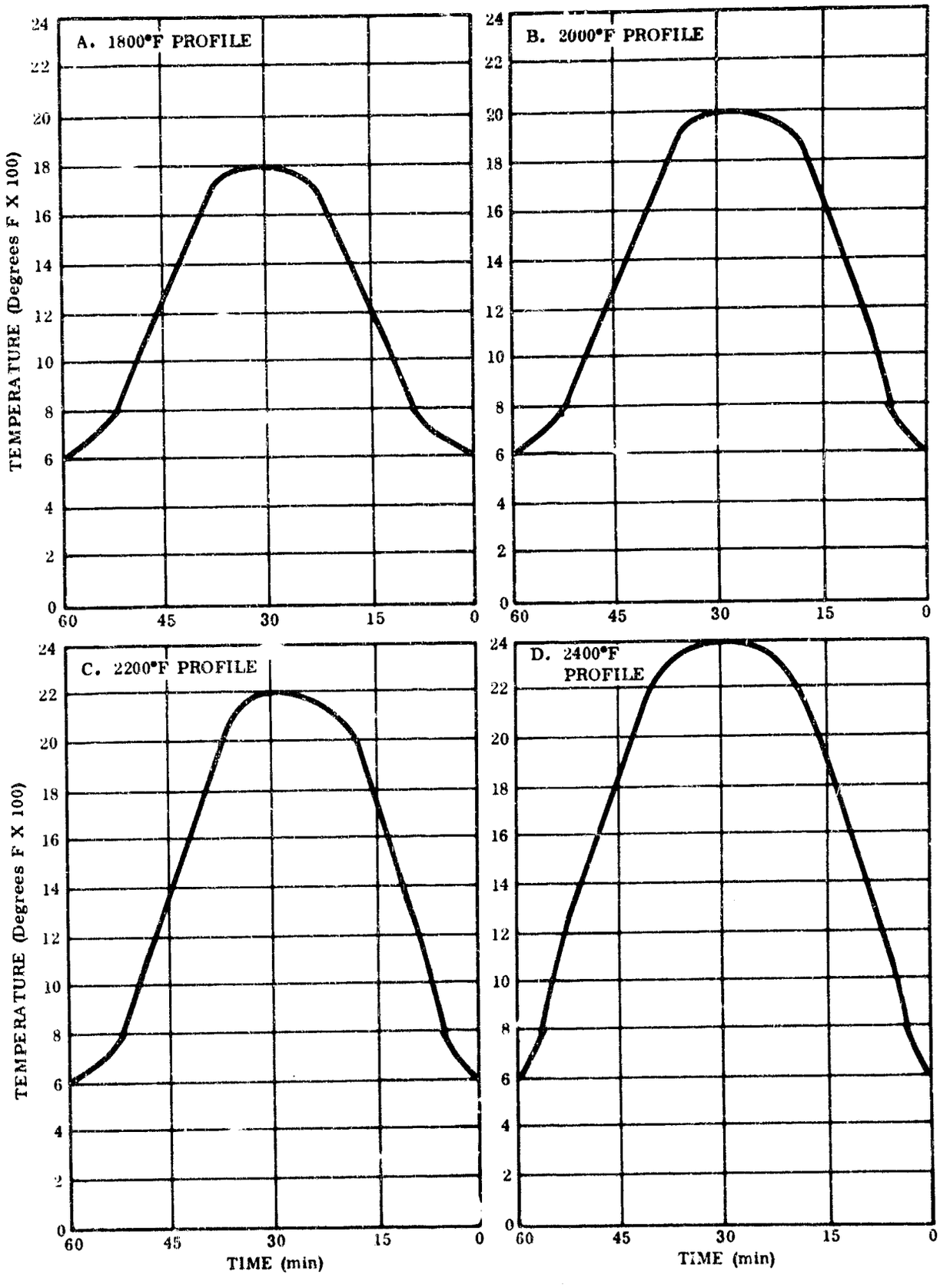

FIGURE 6. TIME-TEMPERATURE PROFILE AT ATMOSPHERIC PRESSURE

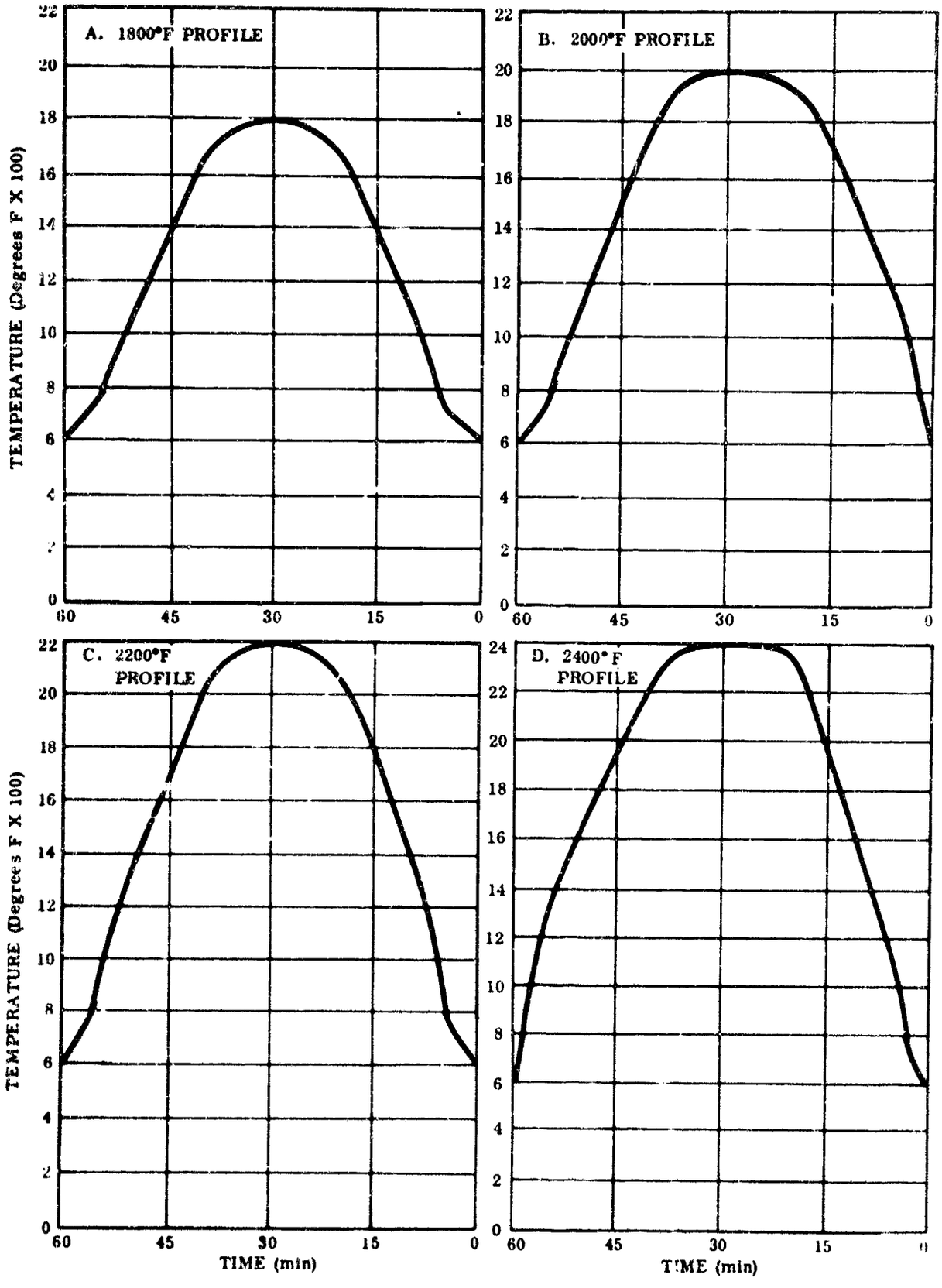

FIGURE 7. TIME-TEMPERATURE PROFILE AT 0.18 TORR PRESSURE

TABLE V

CHARACTERISTICS OF THE DIFFERENT TIME-TEMPERATURE PROFILES

T_{max} (°F)	Pressure (Torr)	t_1[1] (min)	t_2[2] (min)	Area A[3] (10^{-4} deg F x min)	Increase in[4] Area A (%)
1800	760	10	34	1.65	--
2000	760	12	38	2.38	--
2100	760	11	41	2.81	--
2200	760	12	42	3.0	--
2400	760	13	47	4.05	--
1800	0.18	14.5	38	1.91	15.9
2000	0.18	15	45	2.76	15.7
2200	0.18	13	52.5	3.56	17.3
2400	0.18	16	50	4.37	7.8

1. Approximate soak time for temperature within T_{max} and T_{max} -50 degrees F.
2. Time for temperature above 1100°F.
3. Time-temperature profile above 1100°F.
4. Difference between 0.18 Torr and 760 Torr exposure.

The T_{max} for atmospheric pressure oxidation exposures for the program alloys were:

- Rene' 41, Inconel 718, and Inconel 626 - 1800 and 2000°F
- Haynes 25 - 1800, 2000, and 2100°F
- TD Nickel and TD Nickel/chromium - 2000, 2200, and 2400°F

The following four alloys and T_{max} were selected for further evaluation based on previous evaluation of all six program alloys in the as-received condition and after 760 Torr oxidation exposure.

Inconel 625	1800°F
Haynes 25	2000°F
TD Nickel	2200°F
TD Nickel/chromium	2400°F

Forty test specimens (similar to those previously discussed) of each of the four selected superalloys were subjected to low-pressure (0.18 Torr) oxidation exposure for 100 one-hour slow cycles at their recommended T_{max} in the MGR furnace. The oxidation rate in both the atmospheric and low-pressure (0.18 Torr) exposures was estimated from weight change data. The weight change of the program alloys resulting from oxidation exposure was determined from the weights of the two standard test specimens, and from the entire group of test specimens before and after oxidation exposure. Average weight change data expressed as percent, or as mg/cm^2, gave an indication of the oxidation rate of the superalloy foils. In addition to weight change data, mechanical tests and diagnostic techniques described in the following sections were used for evaluating the effects of oxidation exposures.

3.4 MECHANICAL TESTS

Mechanical tests on the superalloy foils in the as-received condition were conducted for verification and for supplemental testing (to the mechanical property data from the literature search) as required. Mechanical tests except creep tests on specimens subjected to 760 Torr and 0.18 Torr oxidation exposure were performed to determine the percentage of degradation in properties. Termination of testing or reduction of T_{max} was considered upon loss of more than 33 percent of the unexposed properties. Mechanical tests conducted were:

- Creep tests
- Tensile tests at room temperature, T_{dm}, and T_{max}
- Notch tensile tests at room temperature, T_{dm}, and T_{max}
- High rate tensile tests at room temperature
- Room-temperature fatigue tests
- High-temperature fatigue tests

The test direction was transverse for all the superalloy foils except TD Nickel/chromium. All testing for TD Nickel/chromium was conducted in the longitudinal direction. The equipment used and the procedural details for these various mechanical tests are described in the following paragraphs.

3.4.1 Creep Tests

Creep testing for the six program alloy foils was conducted in the as-received condition only and at temperatures ranging from 1800 to 2400°F. The stress values required for one percent and five percent creep in a period of 30 hours or less were determined. These data were used to determine the stress necessary for simulated profile exposures, (para 3.6) the selection of the four alloys for low-pressure oxidation exposure, and for recommending their maximum service temperature.

Creep tests were performed in air using the platinum wire resistor tube furnaces shown in Figure 8. The specimens were stressed by direct deadweight loading with lead shots.

The test furnaces consisted of Pt-20Rh wire helically wound and cemented onto a 1.125-inch ID alumina tube. The alumina tube was supported at each end with insulating ceramic bushings attached to a stainless steel case filled with bubbled alumina insulation. The space between the end of the specimen and the furnace tube was loosely packed with Fiber-Frax insulation to reduce thermal end losses and convection currents. A Pt/Pt-13Rh thermocouple, located inside the alumina tube next to the specimen test section, was used for furnace control. A minimum furnace temperature variation was achieved through the use of a proportioning-type temperature controller. Precise temperature calibrations were made with thermocouples welded to the specimen test section.

Calibration tests showed that at 2400°F, the furnace temperature was controlled to within ± 5 degrees F, and the temperature gradient across the specimen test section was approximately 10 degrees F.

Specimen creep was measured and recorded throughout the test using a linear potentiometer in conjunction with a potentiometer-type, strip-chart recorder. The LVDT reading on the strip chart recorder was adjusted to zero after the application of load so that the initial extension was not measured. Correction factors were applied to measured data to obtain the portion of creep applicable to specimen gage length. The correction factor was found to be negligible for Haynes 25 and TD Nickel, and varied from 12 to 18 percent for the other prog. alloys.

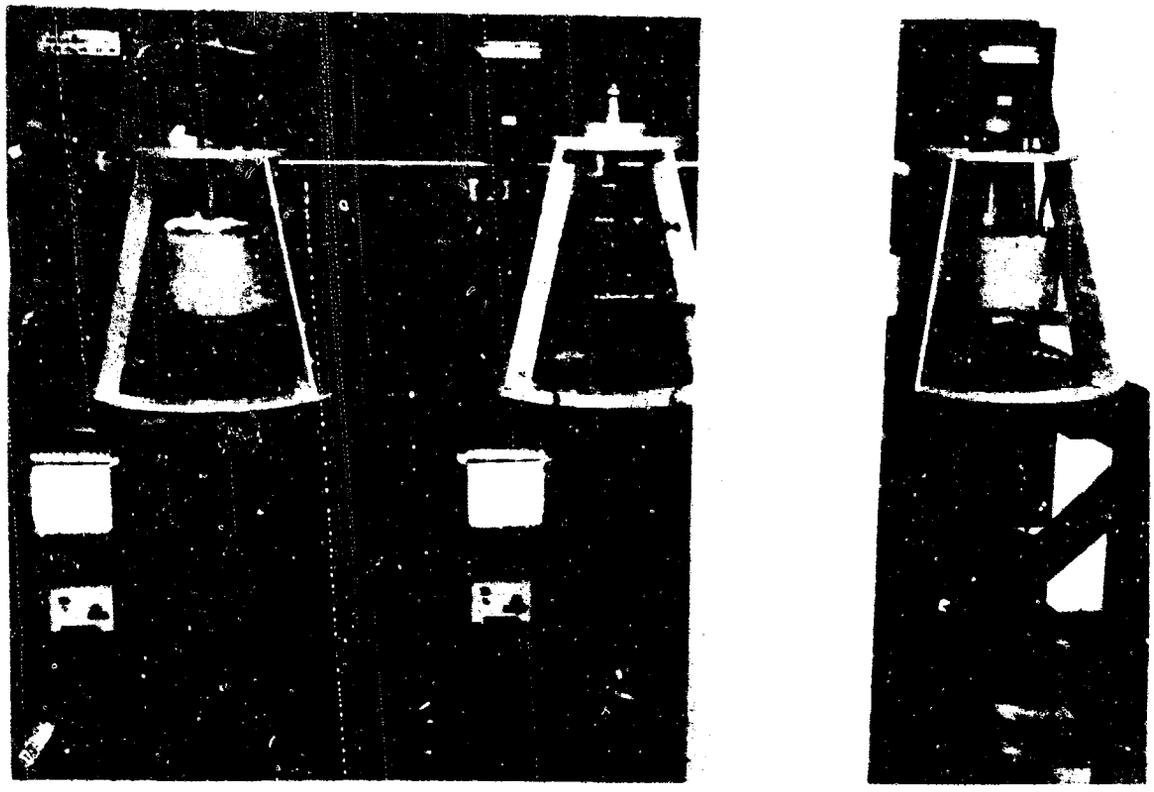

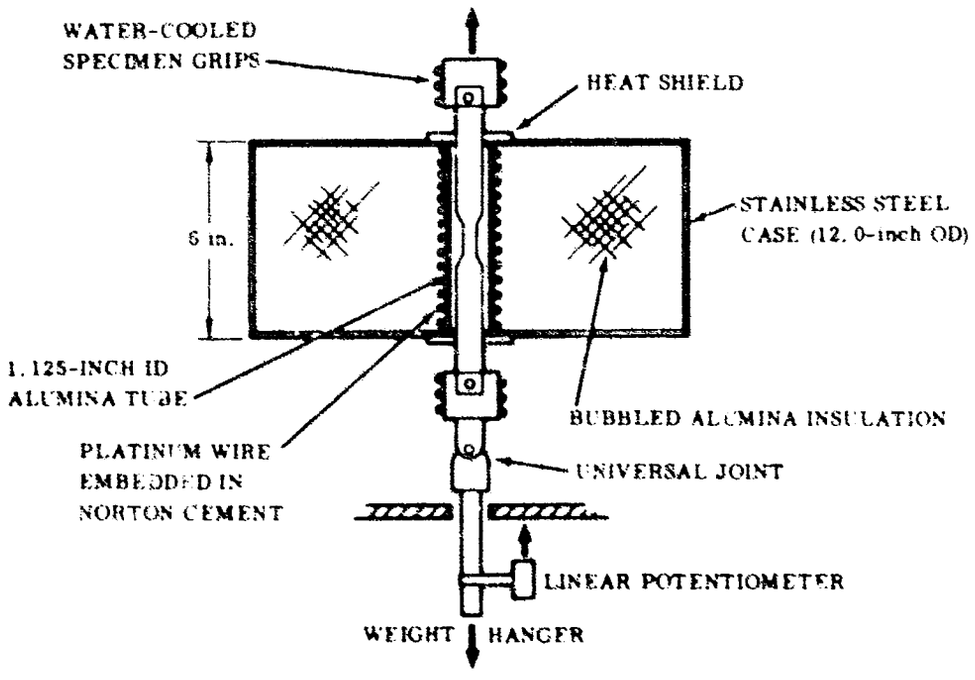

FIGURE 3. CREEP TESTING UNITS

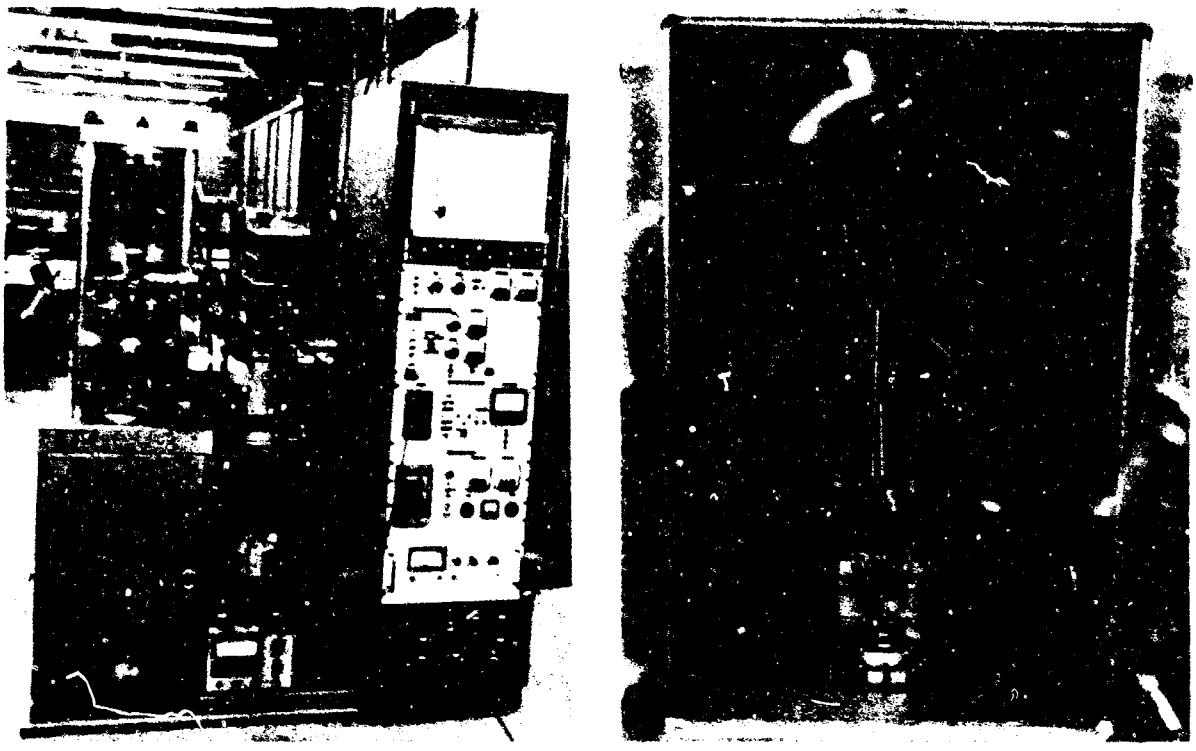

OVERALL ARRANGEMENT HEATING CHAMBER

FIGURE 9. HIGH-TEMPERATURE TENSILE TESTING MACHINE FOR FOIL GAGE SPECIMENS

3.4.2 Tensile Tests

Tensile tests were conducted at room temperature, T_{dm}[1], and oxidation exposure maximum temperature (T_{ox}) for specimens in the as-received condition and after different oxidation exposures at 760 Torr and 0.18 Torr.

Room temperature tensile tests were conducted using the Instron tensile testing machine (Model TTD 20,000 pounds capacity). The high-temperature tensile tests were conducted in vacuum (3×10^{-5} Torr) using the foil testing machine shown in Figure 9 (Ref. 3). This testing system consisted of a screw-driven tensile machine (fitted with a vacuum chamber and furnace) and a console containing instruments for control of temperature, vacuum, load, and strain rate. The frame can sustain a maximum load of 5000 pounds with only 0.001 inch of elastic deflection at the end plates. The specimen load was measured with a series of interchangeable load cells ranging

1. The ductility minimum temperature, as determined from literature review, was 1300°F for Inconel 718 and Inconel 625, 1400°F for Haynes 25, and 1600°F for Rene' 41, TD Nickel, and TD Nickel chromium.

in capacity from 30 to 3000 pounds. Crosshead speed was continuously variable from 0.0005 to 1.0 inch/minute. The heating chamber, with the double-beam extensometer attached to a tensile specimen is also shown in Figure 9. Tensile test data at room temperature obtained from this equipment and from the Instron machine were found to closely agree as shown for Inconel 718.

ROOM TEMPERATURE TENSILE TEST DATA FOR INCONEL 718

Machine	F_{tu} (ksi)	F_{ty} (ksi)	Elongation at F_{tu} (% in 2 in.)	E Modulus -10^3 (ksi)	Specimens Tested
Instron	128.0	61.3	43.5	27.2	2
Thin Gage Testing Machine	133.4	63.5	42.7	28.0	2

For both room temperature and high-temperature tensile tests, a strain rate of 0.005 inch/inch/minute was used up to 0.5 percent elongation, and then the strain rate was increased to 0.05 inch/inch/minute until the specimen failed (for room temperature tests) or until the ultimate strength was reached (for high-temperature tests). Some elevated temperature tests were terminated when the ultimate strength was reached reached, since fracture of specimens could damage the tungsten heating element shown in Figure 9.

Tensile tests for six program alloys at room temperature, T_{dm}, and other elevated temperatures up to 2400°F were conducted. For each data point, duplicate tests were performed. The tensile test specimen configuration shown in Figure 3, 10 inches long with a two-inch gage length, was used.

3.4.3 Notched Tensile Tests

Notched tensile specimens of the selected alloys were tested as received and after exposure at several temperatures and two pressures. Test temperatures were room temperature, T_{dm}, and T_{max}. The specimen dimension and notch characteristics are shown in Figure 3. Room temperature tests were performed on the Instron tensile test machine; whereas, elevated temperature tests were performed on the thin gage foil tester. Calculations of stress were based on the area measured prior to oxidation exposure. The specimen strain rate for these tests, i.e., movement between jaws, was 0.1 inch/minute (crosshead speed).

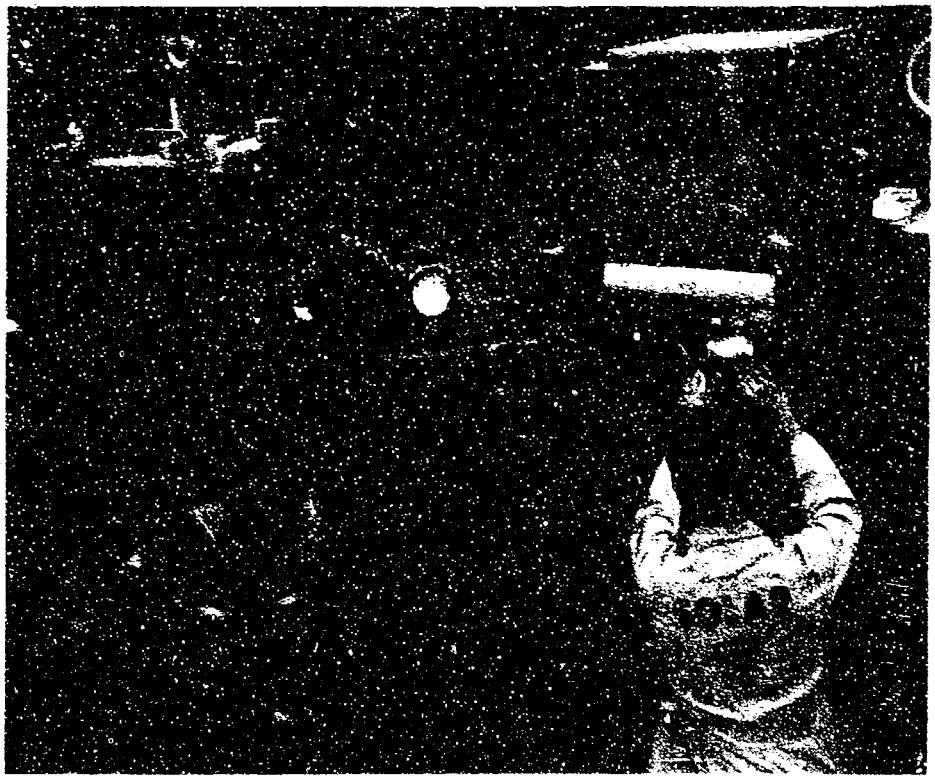

FIGURE 10. MTS FATIGUE TESTING MACHINE

3.4.4 High Strain Rate Tensile Tests

High strain rate tensile tests were conducted with the objective of determining the effect of strain rate on ultimate tensile stress and ductility. The test specimens with 1.0 inch gage length and 5.0 inches overall length were used (Fig. 3). The MTS Machine with a Model 301 loading frame (Fig. 10) and a ram speed of 30 inches/second was used. This loading rate is equivalent to a strain rate of about 25 inch/inch/second and is 30,000 times the strain rate used in standard tensile tests. The tests were conducted at room temperature only on as-received and oxidized superalloy foils. Duplicate tests were performed for each data point.

3.4.5 Room-Temperature Fatigue Tests

Axial tension-tension fatigue tests (room temperature) were conducted using the three tension-tension fatigue machines shown in Figure 11. The specimen (Fig. 3) had a five-inch overall length with a one-inch gage section. The specimens were mounted between a load beam and walking beam with suitable linkage to prevent bending. A fixed rotating eccentric, linked to the walking beam, imparted the motion to

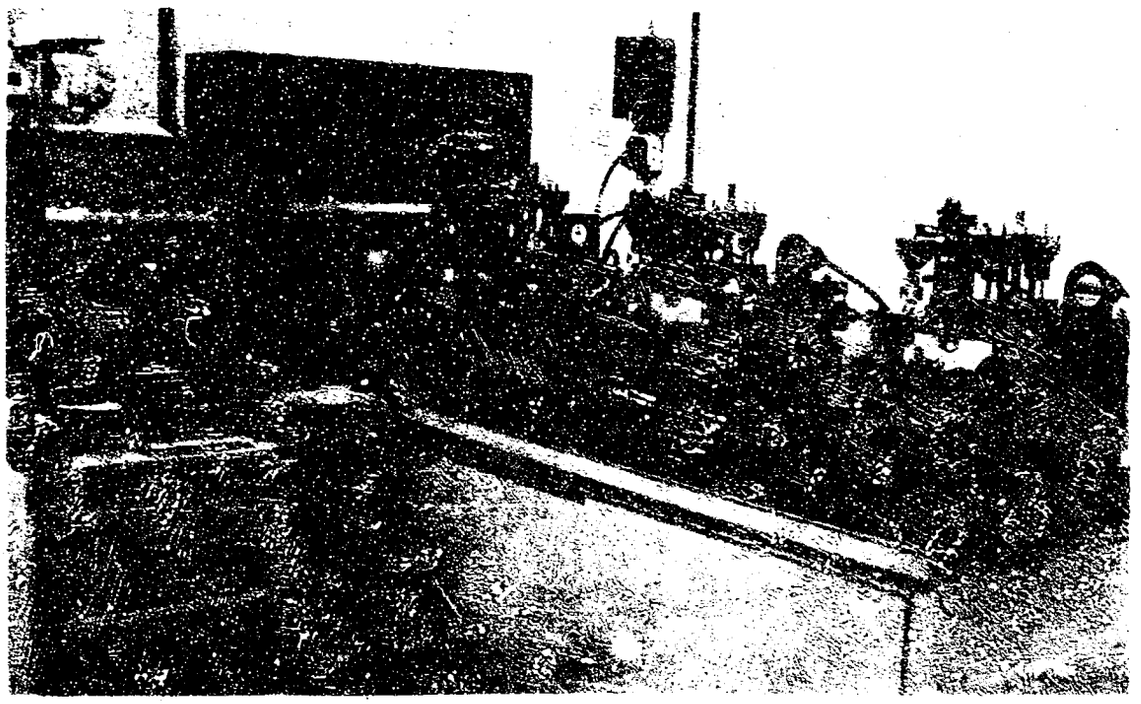

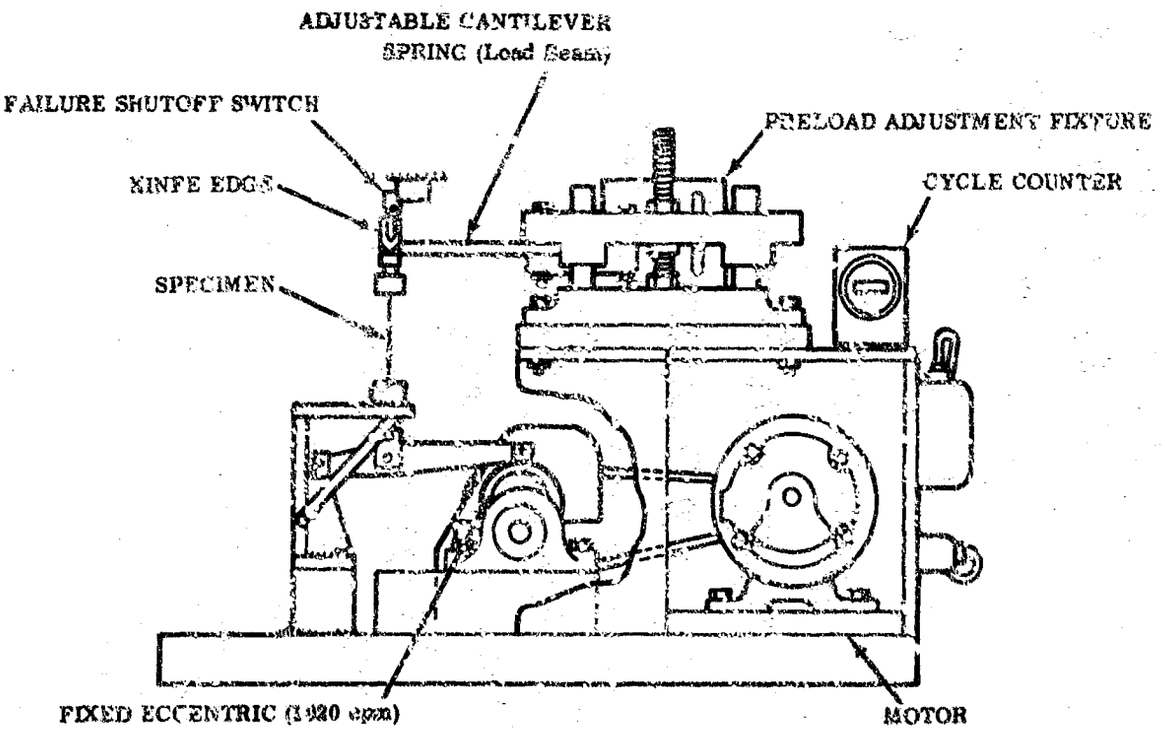

FIGURE 11. TENSILE-TENSION FATIGUE TESTING MACHINE FOR FOIL GAGE SPECIMENS

the specimen at a frequency of 1029 cpm. The load beam, a 0.25-inch thick by 2.0-inch wide spring steel plate, controlled the force imposed on the specimen. This force was measured by strain gages on the beam surface. Dynamic loads were monitored throughout testing on a pen-type oscillograph recorder. The ratio of minimum to maximum stress (R) was held constant at 0.15 for all tests. Tests were performed so that an S-N curve could be established with at least five data points/alloy-temperature condition. Duplicate tests were conducted for at least five different stress values between 0.5 F_{tu} and 0.9 F_{tu}. Tests were terminated if the specimen exhibited a fatigue life of more than five million cycles.

3.4.6 High-Temperature Fatigue Tests

Fatigue tests at the ductility minimum temperature for the four selected alloys (in as-received and oxidized conditions) were performed using the MTS closed-loop, electrohydraulic, fatigue testing machine (Model 301 loading frame) (Fig. 10). This apparatus has capabilities of producing test frequencies ranging from 0.001 to 100 cps with sine, square, triangular, and rampwave load programs available. Fatigue tests performed were tension-tension type using an R of 0.15, a sine wave load program, and a frequency of approximately 3000 cpm (50 cps).

Test specimens were heated in a small resistance furnace. Temperature measurements were made by means of a chromel-alumel thermocouple adjacent to the test specimen. A minimum of temperature variation was achieved by the use of a proportioning-type temperature controller.

The configuration of the test specimen is shown in Figure 3. An 11-inch long specimen was used to permit gripping outside the high-temperature zone of the furnace. This specimen, as in the case of the room-temperature fatigue test specimen, had a gage length of one inch.

In addition to the various mechanical tests described, the superalloy specimens in the as-received and oxidized conditions were also evaluated by various diagnostic techniques described in the next section.

3.5 DIAGNOSTIC TECHNIQUES

To thoroughly identify and characterize oxidation products and changes in alloy microstructure and alloy compositions, various diagnostic and analytical techniques were employed. The different diagnostic techniques were:

- Metallography
- Gas Analyses
- X-Ray Diffraction
- Electron Microprobe

Except for optical metallography, which was performed on a representative specimen in the as-received and all oxidized conditions, the other diagnostic techniques were used on a selected basis as were the metallographic analyses after the various mechanical property tests. The analytical techniques are described in the following sections.

3.5.1 Metallographic Analyses

Metallographic samples were cut from the middle of the standard specimen or from the gage length of the tensile specimens. Cut samples (longitudinal and transverse sections) were mounted in bakelite mounts and ground on sand paper and polished. Specimens were then etched, using the following etchants:

Rene' 41	- $6HCl + 1HNO_3$ or $92HCl + 5H_2SO_4 + 3HNO_3$
Inconel 718	- 10 percent oxalic acid - electrolytic
Inconel 625	- 2 parts HNO_3, 1 part acetic acid - electrolytic
Haynes 25	- HCl + 3 percent H_2O_2
TD Nickel	- Equal parts of 10 percent aqueous solution of $(NH_4)_2SO_4$ + 10 percent NaCN - used during polishing
TD Nickel/chromium	- 10 percent oxalic acid - electrolytic

The specimens were then examined for microstructure, oxide thickness, internal oxidation, and void formation. Microhardness values of the superalloy foils in the as-received and oxidized conditions, using a Knoop indentor and a 200-gram load, were also determined.

3.5.2 Gas Analyses

Chemical analyses for carbon, oxygen, and nitrogen levels of superalloy foils were conducted for the purpose of studying internal oxidation phenomenon and decarburization. Exposed specimens were sandblasted and ground to remove oxide before chemical analyses. Nitrogen and oxygen levels were determined by vacuum fusion analyses. The conductometric method was used for carbon analyses. Duplicate analyses were conducted.

3.5.3 X-ray Diffraction Analyses

X-ray diffraction analyses were conducted to identify the oxidation product for the superalloy foil specimens subjected to different oxidation exposures at their respective T_{max}.

X-ray diffraction patterns were obtained using a Norelco X-ray diffractometer. For Inconel 625, a copper tube with a nickel filter rated at 50 kv and 20 mva was used, resulting in CuKα radiation (λ = 1.5418Å). In the case of Haynes 25, an iron tube with a manganese filter was used resulting in FeKα radiation (λ = 1.936Å). The values of the Bragg angle (θ) and the relative intensity were obtained from X-ray diffraction charts. Using Bragg's law ($2d \sin\theta = \lambda$), "d" values (lattice spacing) were calculated. For the identification of oxides, the X-ray patterns of the oxidized alloys were compared with the standard patterns of various oxides (e.g., cubic Cr_2O_3 and rhombohedral Cr_2O_3, NiO, spinels, CoO).

3.5.4 Electron Microprobe Analyses

Selected electron microprobe analyses were conducted to detect any compsitional changes near the edges of the superalloy specimens exposed to cyclic oxidation at 760 and 0.18 Torr and at T_{max}. Concentration gradients from the center to the specimen edge were mapped for the elements of interest. The superalloy specimens after oxidation exposures and the associated elements analyzed for were:

Inconel 625	Haynes 25	TD Nickel/Chromium
Aluminum	Chromium	Chromium
Titanium	Cobalt	Nickel
Chromium	Manganese	
Columbium	Nickel	
Manganese	Tungsten	
Molybdenum		
Nickel		
Tantalum		

A Norelco AMR-3 microprobe analyzer was used. The method used in microprobe analysis involved a comparison of the beam intensities for elements in the areas of interest with intensities for these elements in alloy or pure element standards.

Concentrations were calculated after accounting for background intensity by multiplying the intensity ratio by the amount present in the standard. The compositions of columbium and tantalum in Inconel 625 were calculated from X-ray intensities compared with pure standards. The chromium composition for TD Nickel/chromium was also similarly determined.

3.6 MISSION PROFILE SIMULATION TESTS

Mission profile simulation tests were conducted to determine the combined effects of temperature, stress, and pressure. The effects of the cyclic oxidation tests at various temperatures and at atmospheric and low pressures were determined under zero stress conditions. However, stressing can conceivably increase gross and intergranular oxidation that may markedly decrease the effective life of foil gage superalloy structures.

The environmental simulators used are shown in Figures 12 and 13 and were developed at Solar under Contract AF33(657)-9443 (Ref. 4). In the test chambers, specimens were simultaneously subjected to the representative mission profile, a constant axial stress, and a constant pressure. The mission profile is a one-hour cycle similar to the profiles in slow-cycle atmospheric pressure oxidation testing (Fig. 6). The mission profiles in different environmental pressures (760, 0.[illegible], and 10 Torr) were found to be similar. This similarity exists because the area values above 1100°F in the mission profile at a particular T_{max} and in various pressures were the same. It is in contrast to the MGR profiles, where the area above 1100°F in the time-temperature profile was greater in the 0.18 Torr pressure than in the 760 Torr pressure (Table V).

The profile simulation test specimens were stressed by direct deadweight loading. Specimen elongation was measured by means of a precision linear variable differential transformer (LVDT) connected to the loading apparatus. Elongation versus time was automatically recorded throughout the test on a strip-chart, potentiometer-type recorder. The strain, thus recorded, was the total strain in the entire specimen.

The temperature profile was achieved by means of a preshaped temperature-time program cam, operating in conjunction with an electronic controller, magnetic modulator, and silicon-controlled rectifier. Test specimens were heated with twelve, 500-watt, clear quartz tubular lamps enclosed in a water-cooled, 3 [illegible]-inch diameter, gold plated reflector assembly. A thermocouple (Pt/Pt-13Rh) adjacent to the surface of the test specimen furnished a feedback signal to the temperature control system. Deviation between specimen and program temperature was automatically corrected in the control system by regulating the power to the quartz lamp heating unit. Continuous recording of specimen temperature was maintained throughout the test period to indicate any deviation from the test program.

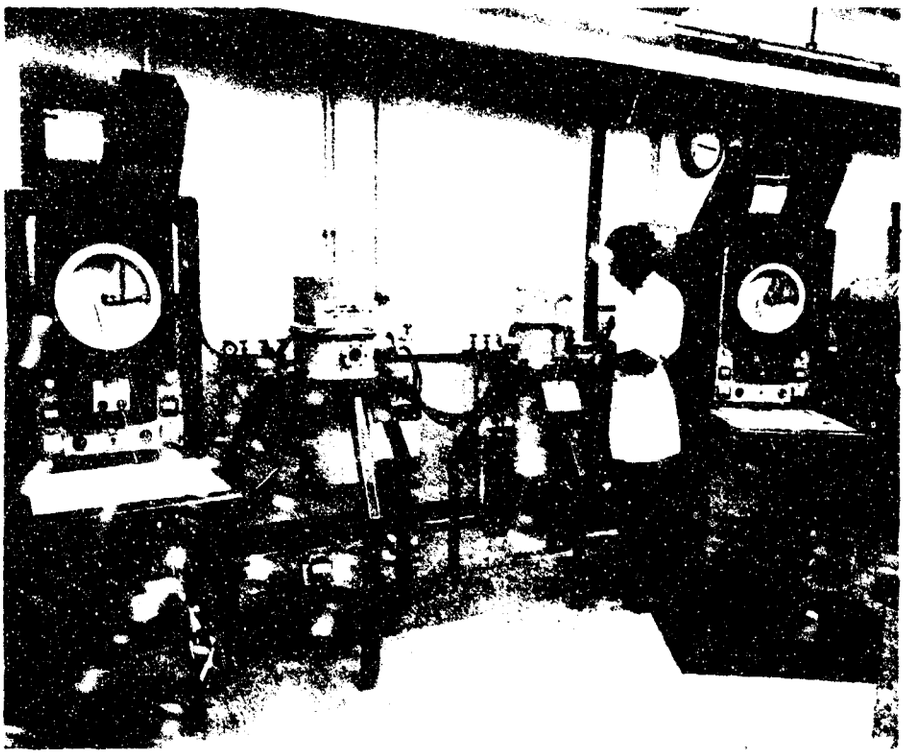

FIGURE 12. ENVIRONMENTAL SIMULATORS

Precise temperature calibrations were made using 0.01-inch thick Haynes 25 alloy foil for the 2000°F T_{max} profile at both 760 Torr and 0.18 Torr. Two thermocouples were used - one Pt/Pt-13Rh held adjacent to the specimen and the other, chromel-alumel, welded to the specimen in the one-inch gage section. The results indicate that there was less than 15 degrees F temperature gradient at 2000°F between the two thermocouples.

TEMPERATURE CALIBRATION RESULTS FOR HAYNES 25

Thermocouples	2000°F - 760 Torr												
Pt/Pt-13Rh (°F)	550	950	1450	1610	1800	2000	1800	1700	1600	1400	1300	1000	650
Chromel-Alumel (°F)	550	940	1440	1600	1800	2000	1800	1700	1600	1405	1305	995	640
	2000°F - 0.18 Torr												
Pt/Pt-13Rh (°F)	500	1000	1250	1650	1800	2000	1700	1400	1250	1000	500		
Chromel-Alumel (°F)	540	1035	1300	1660	1810	2015	1720	1415	1300	1040	550		

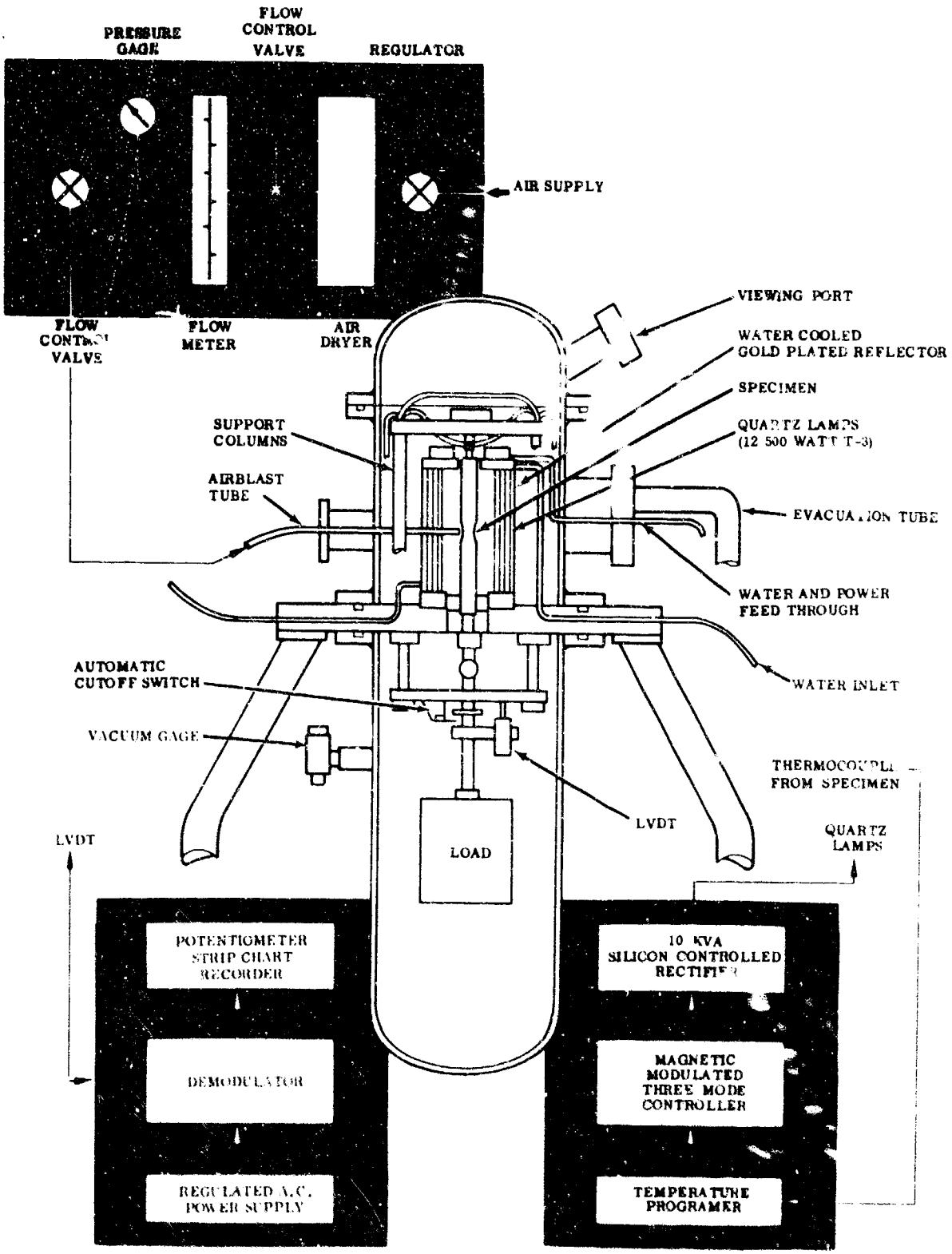

FIGURE 13. SCHEMATIC OF AN ENVIRONMENTAL SIMULATOR TEST UNIT

For low-pressure testing, the chambers were evacuated by means of 15 cfm mechanical vacuum pumps. To ensure dynamic test conditions and as high a flow rate as possible through the test chamber, an adjustable needle valve was used to control the pressure. Pressure in the test chamber was continuously monitored throughout testing by means of thermocouple-type vacuum gages (Veeco Type DV-4AM and DV-1M). These gages were calibrated by means of a Stokes-McLeod mercury manometer.

Both of Solar's environmental simulators have small sight ports used to observe the specimen test section during test. These sight ports are approximately 0.375 inch wide by 1.0 inch long so that the entire test section can be seen from outside the chamber.

The profile simulation test specimen, shown in Figure 3, was 11 inches long and had a one-inch gage length. Eleven-inch long specimens were used to enable gripping outside the hot zone.

ssion profile simulation tests were performed on six superalloy foils at two different stress values, at T_{max} from 1800 to 2400°F and in three different pressures (760, 0.18, and 10 Torr). Two different stress values were used to obtain two different elongation values, viz., about one and five percent. The stresses were selected from creep data. The unfailed mission profile simulation test specimens were evaluated by room temperature tensile tests and by metallographic analyses.

4

RESULTS

The results of creep testing and the effects of 100 one-hour slow-cycle oxidation exposures on the six superalloy foils (0.01-inch thick) as evaluated by weight change measurements, mechanical testing, and various diagnostic techniques, are presented in this section. The effects of simulated profile exposures are also described.

4.1 CREEP TESTING

Creep test data are presented in Table VI. The percent creep versus time for the program alloys for different stress levels and at three constant temperatures (from 1800 to 2400°F) are plotted in Figures 14A through 14F. The creep rates for the program alloys at different test temperatures are given in Table VII. The creep rate, as expected, increased with temperature for all the program alloys.

At 1800 and 2000°F, the creep rate of Rene' 41 and Inconel 718 was higher than that of Haynes 25 and Inconel 625 (Table VII). The creep rate for Haynes 25 and Inconel 625 was about the same for temperatures up to 2100°F. Recommended maximum service temperatures from creep rate considerations (to be able to withstand a minimum stress of one ksi for 30 hours) were:

- For Haynes 25 and Inconel 625 — 2100°F
- For Inconel 718 and Rene' 41 — 2000°F

The creep rate of the four alloys mentioned was much higher than that of TD Nickel and TD Nickel/chromium (Table VII). At 2000 to 2400°F, the creep rate of TD Nickel/chromium was lower than that of TD Nickel. From the point of view of creep, these two alloys (TD Nickel and TD Nickel/chromium) appeared to be useable at temperatures as high as 2400°F.

The creep testing was conducted for the superalloy foil specimens in the as-received condition only and has been described first. The results of the other mechanical tests and the analytical evaluation will be presented after the results of weight change measurements (oxidation rate) in the following section.

TABLE VI

CREEP TEST DATA FOR SUPERALLOY FOILS

Superalloy	Test Temperature (°F)	Stress (ksi)	Fraction of F_{tu} at 1800°F	Time For Elongation		
				1%	5%	X%
Rene' 41	1800	7.8	0.6	-	-	0.7% in 0.5 hr
	1800	5.2	0.4	-	-	0.25% in 1.0 hr
	1800	3.9	0.3	-	-	0.45% in 2.5 hr
	1800	1.95	0.15	12.0 hr	-	2.1% in 32.0 hr
	1800	1.0	-	-	-	0.7% in 20.0 hr
	2000	1.95	-	12 min	50 min	
	2000	1.0	-	50 min	8.0 hr	
Inconel 718	1800	1.5	0.1	14.0 hr	-	1.5% in 23 hr
	2000	1.5	-	1.1 hr	3.2 hr	
Inconel 625	1800	8.5	0.5	9 min	-	3.5% in 25 min
	1800	5.1	0.3	30 min	-	3.5% in 1.7 hr
	1800	3.4	0.2	11.0 hr	-	3.5% in 20.0 hr
	1800	1.7	0.1	-	-	0.7% in 23.0 hr
	2000	1.7	-	-	-	0.7% in 4.5 hr
	2100	1.0	-	45 min	-	4.5% in 6.0 hr
Haynes 25	1800	5.8	0.2	5.7 hr	-	4.25% in 25.0 hr
	1800	4.0	-	12.0 hr	-	4.25% in 28.0 hr
	1800	2.9	0.1	-	-	0.25% in 20.0 hr
	1800	1.1	-	-	-	<0.25% in 26.0 hr
	2000	4.0	-	14 min	1.0 hr	Ruptured after 16% in 2.5 hr
	2000	1.45	-	1.2 hr	12.5 hr	8.5% in 22.3 hr
	2000	1.0	-	5.0 hr	28.0 hr	
	2100	1.0	-	2.5 hr	9.7 hr	
TD Nickel	2000	8.0	-	-	-	Ruptured after 0.9% in 1.0 hr
	2000	7.0	-	-	-	Ruptured after 0.9% in 2.5 hr
	2000	6.0	-	22.0 hr	-	Ruptured after 25.0 hr
	2000	4.0	-	-	-	0.53% in 70.0 hr
	2200	5.0	-	2.2 hr	-	Ruptured after 3.5% in 4.7 hr
	2200	4.0	-	3.1 hr	14.5 hr	Run terminated after 17.0 hr
	2200	3.0	-	12.0 hr	-	1.8% in 64.0 hr
	2400	3.0	-	2.8 hr	24.0 hr	Run terminated after 30.0 hr
	2400	2.0	-	8.0 hr	-	4.4% in 112.0 hr
TD Nickel/chromium	2000	14.0	-	-	-	0.75% in 7.5 hr Ruptured after 9 hr
	2000	13.0	-	-	-	0.75% in 7.75 hr Ruptured after 8.0 hr
	2000	10.0	-	-	-	0.75% in 25.0 hr
	2000	8.0	-	-	-	<0.1% in 21.0 hr
	2200	12.0	-	-	-	Ruptured after 0.75% in 45 min
	2200	10.0	-	9.3 hr	-	Ruptured after 9.3 hr
	2200	9.0	-	13.5 hr	-	Ruptured after 16.6 hr
	2200	8.0	-	-	-	<0.5% in 28.0 hr
	2200	4.0		-	-	0.3% in 30.0 hr
	2400	8.0	-	50 min	-	Ruptured after 1.6% in 1.0 hr
	2400	6.0	-	6.5 hr	9.25 hr	7.5% in 10.25 hr
	2400	5.0	-	-	-	0.54% in 30.0 hr

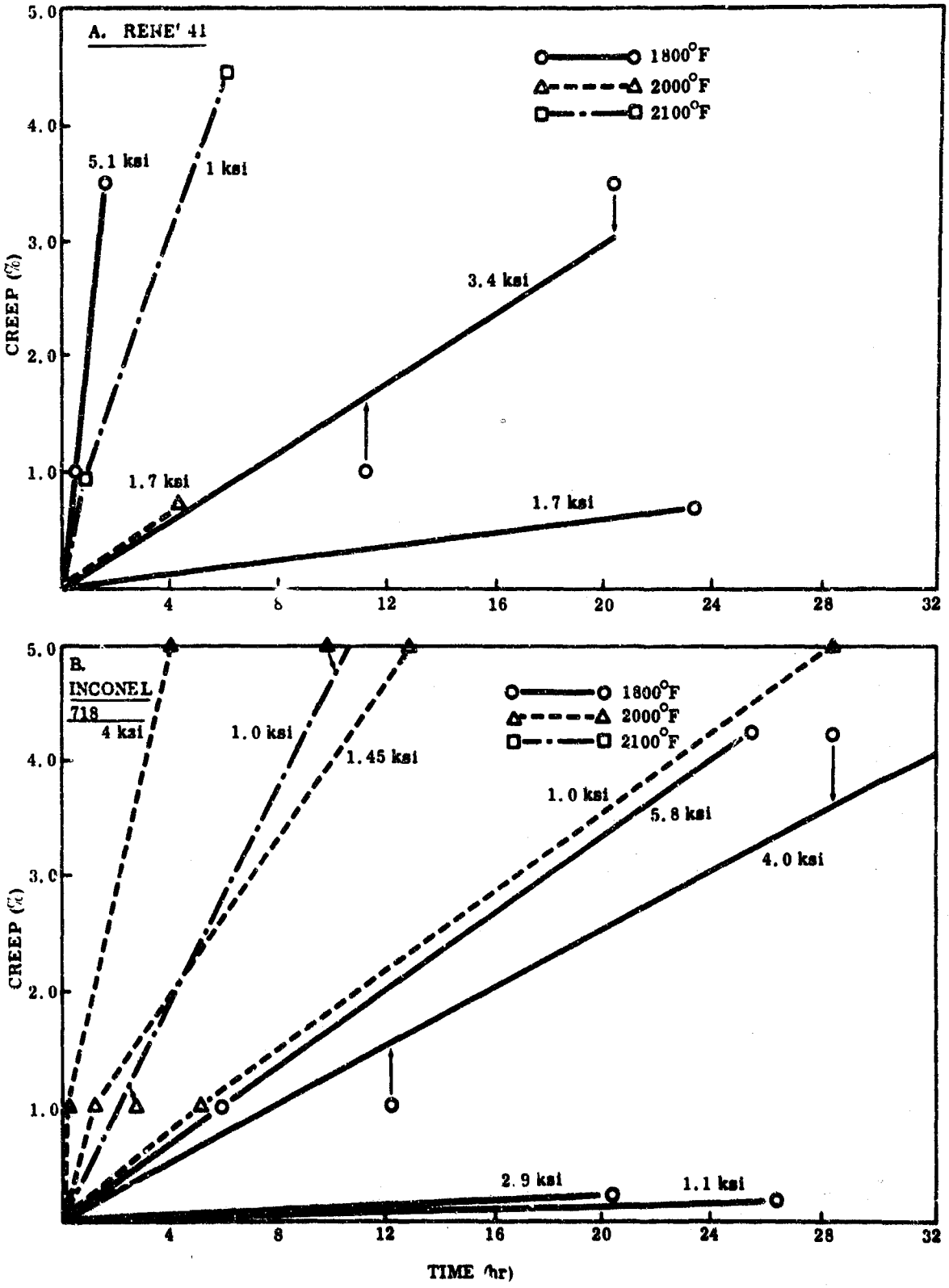

FIGURE 14. CREEP VERSUS TIME FOR THE SIX PROGRAM ALLOYS (Sheet 1 of 3)

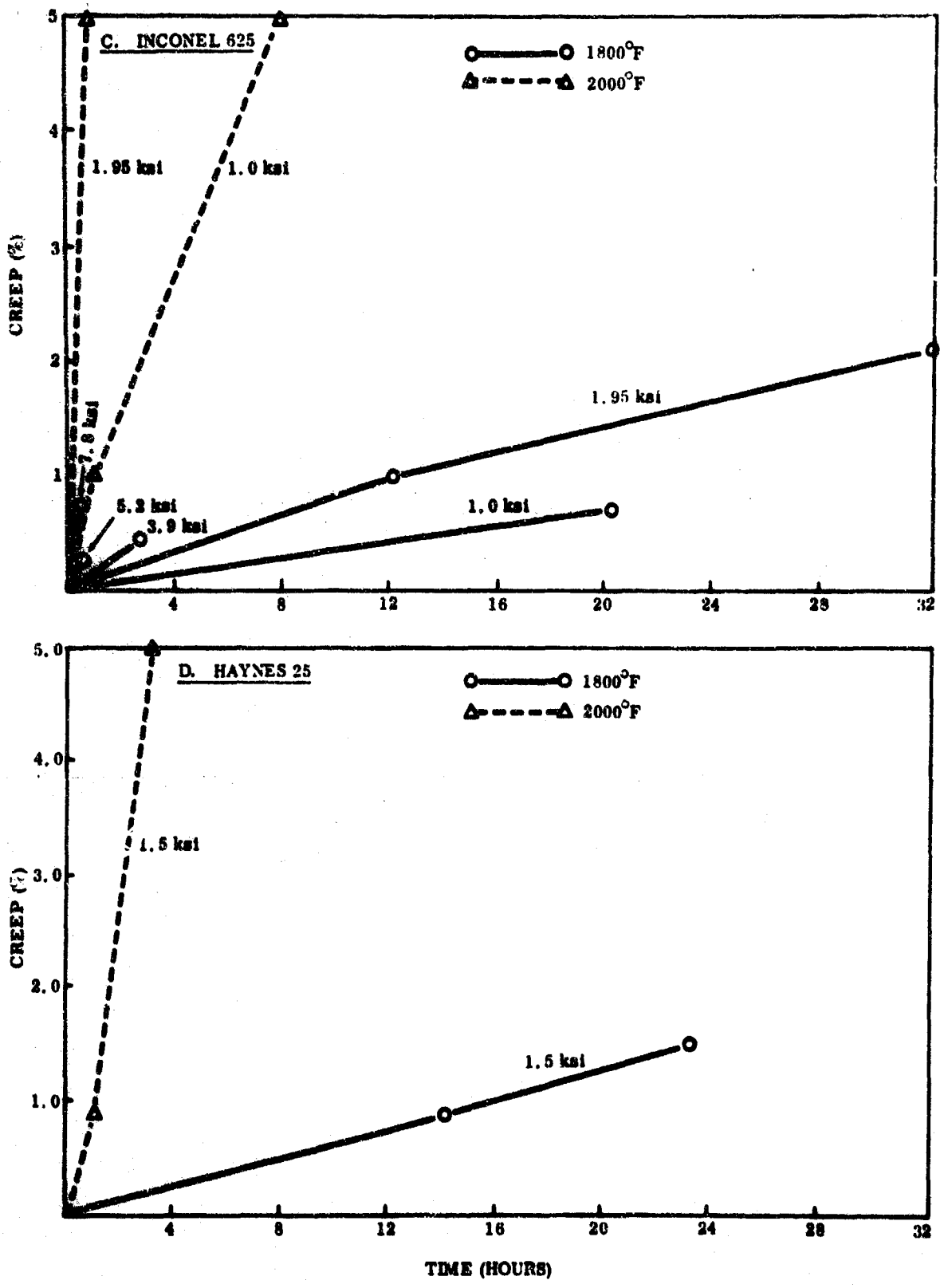

FIGURE 14. CREEP VERSUS TIME FOR THE SIX PROGRAM ALLOYS (Sheet 2 of 3)

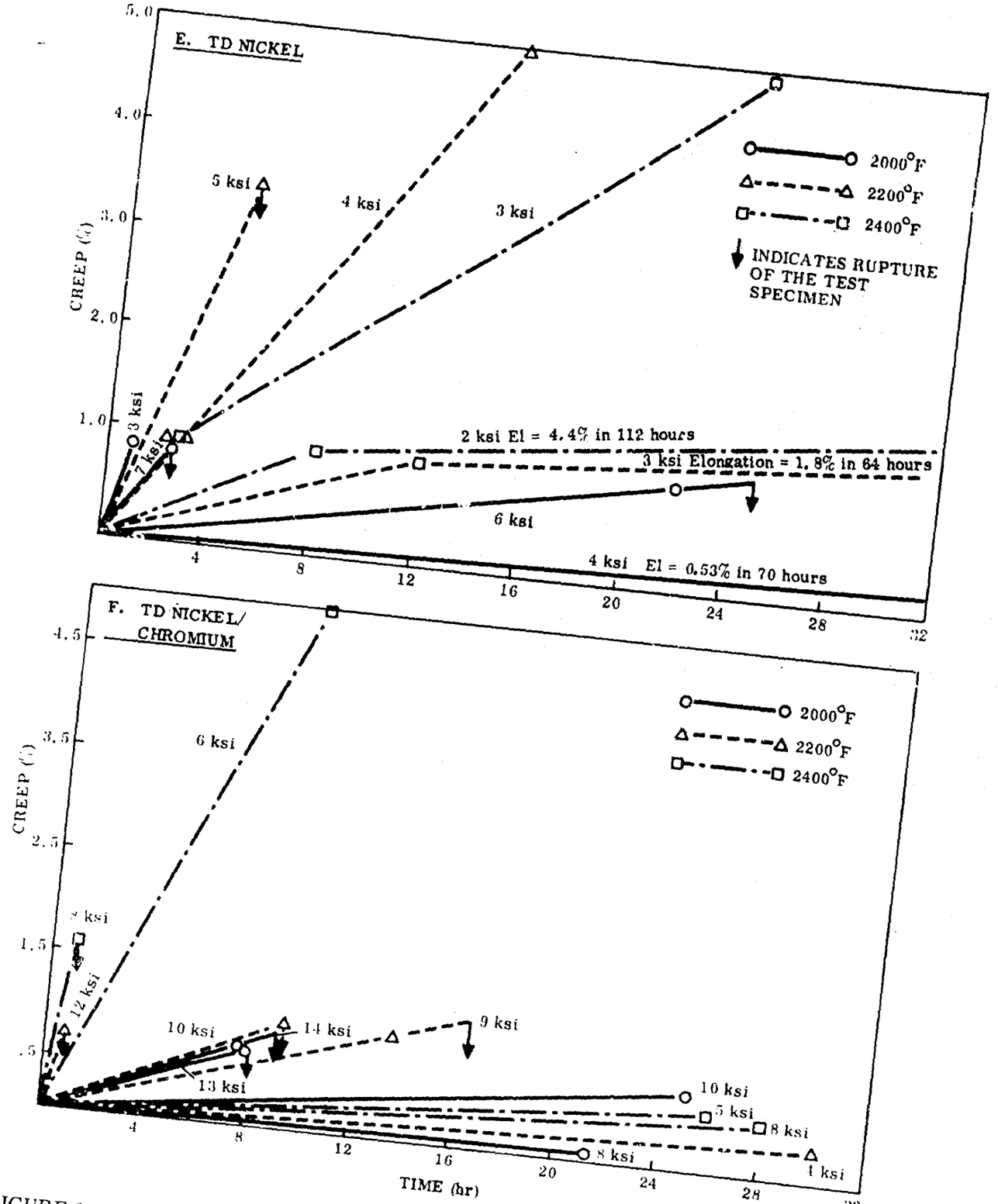

FIGURE 14. CREEP VERSUS TIME FOR THE SIX PROGRAM ALLOYS (Sheet 3 of 3)

TABLE VII

CREEP RATE FOR SUPERALLOY FOILS AT DIFFERENT TEMPERATURES

Test Temperature (°F)	Stress (ksi)	Creep Rate (10^{-4} in. /in. /hr)				Stress (ksi)	Creep Rate (10^{-4} in. /in. /hr)	
		Rene' 41	Inconel 718	Inconel 625	Haynes 25		TD Nickel	TD Nickel/chromium
1800	1.0	3.5	-	-	0.8			
	1.5	-	6.5	-	-			
	1.7	-	-	3.0	-	No creep testing was conducted at 1800°F		
	1.95	6.5	-	-	-			
2000	1.0	51	-	-	17	8.0	90	<0.5
	1.5	-	160	-	-	4.0	0.75	-
	1.7	-	-	15	-	-	-	-
	1.95	600	-	-	-	-	-	-
2100	1.0	-	-	60	54	-	-	-
2200	-	-	-	-	-	8.0	-	1.8
	-	-	-	-	-	4.0	35	1.0
	-	-	-	-	-	3.0	1.5	-
2400	-	-	-	-	-	8.0	-	360
	-	-	-	-	-	5.0	-	1.8
	-	-	-	-	-	3.0	20	-
	-	-	-	-	-	2.0	3.2	-

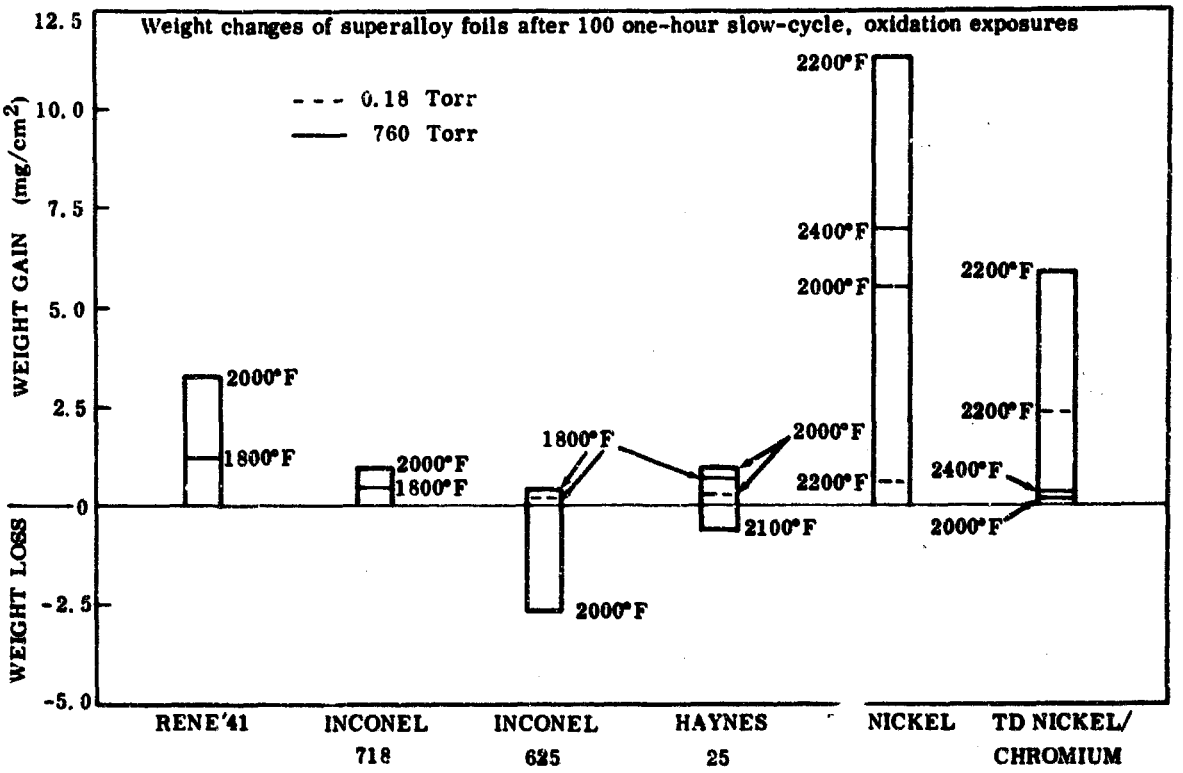

FIGURE 15. WEIGHT CHANGES OF SUPERALLOY FOILS AFTER 100 ONE-HOUR SLOW-CYCLE OXIDATION EXPOSURES

4.2 OXIDATION RATE

The oxidation rates for the six superalloy foils after different atmospheric pressure oxidation exposures and for the four selected alloys after 0.18 Torr exposure are given in Table VIII. The oxidation rate is expressed as average percent weight change and also as mg/cm^2. Comments regarding the specimen's oxidized surface and oxide adherency or exfoliation are included in Table VIII. The oxidation rate data cannot be considered accurate because of oxide spalling during thermal cycling. However, the weight change data gave an indication of the oxidation characteristics of the alloys. The weight changes for the superalloy foils are plotted in bar graph form in Figure 15.

The oxidation rate for the superalloys, in general, was found to increase with increasing T_{max} and to decrease with decreasing environmental pressure (Table VIII). The apparent lower oxidation rate at higher T_{max} (e.g., Inconel 625, Haynes 25, and TD Nickel) was due to the spalling of oxide. Large oxide spalling occurred for all the superalloys except TD Nickel/chromium during atmospheric pressure oxidation exposure at higher oxidation temperatures (2000°F for Rene' 41, Inconel 718, and Inconel 625 - 2100°F for Haynes 25 - 2400°F for TD Nickel). Some spalling of green NiO for TD Nickel occurred during cyclic oxidation exposures (760 Torr as well as 0.18 Torr) at 2200°F.

TABLE VIII

OXIDATION RATE OF SUPERALLOY FOILS

Superalloy	100 One-Hour Slow-Cycle Oxidation Exposures at		Average Weight Change Due to Oxidation Exposure		Comments
	Temperature (°F)	Pressure (Torr)	(%)	(mg/cm^2)	
Rene' 41	1800	760	+1.15	+1.19	Dark gray oxidized surface.
	2000	760	+2.71	+3.17	Large spalling of oxide.
Inconel 718	1800	760	+0.44	+0.47	Dark gray oxidized surface.
	2000	760	+1.69	+0.72	Large spalling of oxide.
Inconel 625	1800	760	+0.30	+0.33	Dark gray oxidized surface.
	2000	760	-0.92	-2.67	Large spalling of oxide.
	1800	0.18	+0.22	+0.23	Oxide adherent.
Haynes 25	1800	760	+0.47	+0.61	Dark gray oxidized surface.
	2000	760	+0.64	+0.91	Dark gray oxidized surface.
	2100	760	-0.42	-0.53	Spalling of oxide - dark oxidized surface.
	2000	0.18	+0.17	+0.21	Oxide adherent.
TD Nickel	2000	760	+4.48	+5.7	Dark greenish oxidized surface.
	2200	760	+8.3	+11.0	Dark greenish oxidized surface.
	2400	760	+6.3	+7.15	Large spalling of green NiO.
	2200	0.18	+0.62	+0.73	Spalling of green NiO.
TD Nickel/ chromium	2000	760	+0.09	+0.11	Dark greenish oxidized surface.
	2200	760	+5.11	+5.93	Dark gray to greenish oxidized surface.
	2400	760	+0.16	+0.19	Dark gray to dark greenish oxidized surface.
	2200	0.18	+1.76	+2.3	Dark gray to dark greenish oxidized surface.
	2400	0.18	-	-	Run not completed due to MGR furnace problems (arc discharge and vaporization of silicon).

\+ Weight Gain

\- Weight Loss

Among the four alloys (Rene' 41, Inconel 718, Inconel 625, and Haynes 25) subjected to 1800°F, 760 Torr, and 100 cycles of oxidation exposure, the rate of oxidation was found to be the highest for Rene' 41 (1.19 mg/cm^2) and least for Inconel 625 (0.23 mg/cm^2) (Fig. 15). The specimens of these four alloys oxidized at 1800°F (760 Torr as well as 0.18 Torr) showed a characteristic dark gray oxidized surface and exhibited no spalling.

Among the six alloys subjected to atmospheric pressure oxidation exposures at 2000°F, the oxidation rate was highest for TD Nickel (5.7 mg/cm^2) and lowest for TD Nickel/chromium (0.09 mg/cm^2) as shown in Table VIII and Figure 15. The TD Nickel specimens were embrittled due to oxidation exposure at 2400°F; therefore, TD Nickel alloy was not considered serviceable at 2400°F. TD Nickel/chromium specimens were found to be satisfactory at temperatures up to 2400°F. In addition to the oxidation rate data, the effects of oxidation exposures on the mechanical properties were also evaluated.

4.3 MECHANICAL PROPERTY DATA

The mechanical property test results for the superalloy specimens in the as-received and oxidized conditions are presented in this section. The tests included tensile, notch tensile, and high-rate tensile properties, room-temperature fatigue, and elevated temperature fatigue strength.

4.3.1 Tensile Test Results

Tensile test data for the six program alloys at room temperature, T_{dm}, and T_{max} in the as-received and oxidized conditions are given in Table IX for Rene' 41 and Inconel 718; in Table X for Inconel 625 and Haynes 25; and in Table XI for TD Nickel and TD Nickel/chromium. These data include average values for F_{tu}, F_{ty}, percent elongation at F_{tu}, percent total elongation and elastic modulus, the percent loss in F_{tu} and F_{ty}, and in elongation due to the different oxidation exposures. Bar graphs of F_{tu}, F_{ty}, and percent elongation at F_{tu} at different test temperatures for the six superalloy foils in the as-received and oxidized conditions are presented in Figure 16 for Rene' 41 and Inconel 718; in Figure 17 for Inconel 625 and Haynes 25; and in Figure 18 for the two dispersion strengthened alloys. These results could not be presented as tensile strength versus temperature curves because the tensile testing was conducted only at three (or a maximum of four) different temperatures.

In the as-received condition and at room temperature, the highest value of F_{ty} (or F_{tu}) was exhibited by Rene' 41 (110 ksi) followed by TD Nickel/chromium, Haynes 25, Inconel 625, Inconel 718, and TD Nickel (54.7 ksi). The room temperature percent total elongation was about the same (~43 percent) for Haynes 25, Inconel 625, and Inconel 718 followed by Rene' 41 (~30 percent), TD Nickel/Chromium (14.5 percent) and TD Nickel (11.0 percent). Thus, the two dispersion strengthened alloys were

TABLE IX

TENSILE TEST DATA FOR RENE' 41 AND INCONEL 718 FOILS (0.01 in.) IN AS-RECEIVED AND OXIDIZED CONDITIONS

Superalloy	Condition			Test Temperature (°F)	F_{tu} (ksi)	Loss in F_{tu} due to Oxidation Exposure (%)	F_{ty} (0.2%) (ksi)	Loss in F_{ty} due to Oxidation Exposure (%)	Elongation at F_{tu} (% in 2 in.)	Loss in Elongation due to Oxidation Exposure (%)	Total Elongation (% in 2 in.)	Loss in Elongation due to Oxidation Exposure (%)	E - Modulus (10^3 ksi)
	R	Oxidized for 100 one-hour cycles: Temperature (°F)	Oxidized for 100 one-hour cycles: Pressure (Torr)										
Rene' 41	R	-	-	RT	177.0	-	110.0	-	30.0	-	30.0	-	28.6
		1800	760	RT	160.0	9.6	107.5	2.3	7.8	74.0	-	-	31.5
		2000	760	RT	113.5	35.9	79.2	28.0	11.0	63.3	-	-	36.0
	R	-	-	1600	88.2	-	72.1	-	2.8	-	16.5	-	-
		1800	760	1600	54.1	38.7	39.9	44.7	-	-	14.5	12.1	-
		2000	760	1600	38.5	56.3	27.1	62.4	0.9	67.8	-	-	-
	R	-	-	1800	38.5	-	26.5	-	1.8	-	12.7	-	-
		1800	760	1800	24.4	36.6	20.05	24.3	-	-	16.0	None	-
	R	-	-	2000	8.6	-	4.4	-	0.9	-	63.0	-	-
		2000	760	2000	10.5	None	5.6	None	0.9	None	12.0	81.0	-
Inconel 718	R	-	-	RT	128.0	-	61.3	-	43.5	-	43.5	-	27.2
		1800	760	RT	130.1	None	61.5	None	35.7	17.9	35.7	17.9	34.9
		2000	760	RT	96.1	24.9	31.1	49.2	34.2	21.4	34.2	21.4	32.4
	R	-	-	1300	126.7	-	86.9	-	16.5	-	20.0	-	21.4
		1800	760	1300	97.4	23.1	65.1	25.1	17.9	None	35.1	None	-
		2000	760	1300	72.9	42.5	58.4	32.8	10.6	35.7	16.3	18.5	26.9
	R	-	-	1800	14.7	-	9.5	-	1.1	-	109.0	-	-
		1800	760	1800	16.0	None	9.8	None	7.6	None	88.4	18.9	-
	R	-	-	2000	7.1	-	4.3	-	0.7	-	16.1	-	6.0
		2000	760	2000	8.1	None	3.9	9.3	10.76	None	28.7	None	7.5
	R	-	-	2100	4.1	-	2.1	-	11.2	-	-	-	6.2

Test direction - Transverse

R - As received

Original area of cross section of unoxidized specimens was used for calculation of F_{tu}, F_{ty}, and E.

TABLE X

TENSILE TEST DATA FOR INCONEL 625 AND HAYNES 25 FOILS (0.01 in.) IN AS-RECEIVED AND OXIDIZED CONDITIONS

Superalloy	Condition R	Oxidized for 100 one-hour cycles: Temperature (°F)	Oxidized for 100 one-hour cycles: Pressure (Torr)	Test Temperature (°F)	F_{tu} (ksi)	Loss in F_{tu} due to Oxidation Exposure (%)	F_{ty} (0.2%) (ksi)	Loss in F_{ty} due to Oxidation Exposure (%)	Elongation at F_{tu} (% in 2 in.)	Loss in Elongation due to Oxidation Exposure (%)	Total Elongation (% in 2 in.)	Loss in Elongation due to Oxidation Exposure (%)	E - Modulus (10^3 ksi)
Inconel 625	R	-	-	RT	131.5	-	66.0	-	43.7	-	43.7	-	29.6
		1800	760	RT	135.8	None	64.9	1.7	42.7	2.3	42.7	2.3	30.2
		1800	0.18	RT	130.3	0.9	63.2	4.2	43.0	1.6	43.0	1.6	30.7
		2000	760	RT	121.9	7.3	43.5	34.1		None	55.0	None	32.6
	R	-	-	1300	90.1	-	45.2	-	23.0	-	65.0	-	39.0
		1800	760	1300	92.4	None	47.9	None	34.7	None	56.8	-	14.6
		1800	0.18	1300	91.0	None	45.7	None	32.0	None	77.0	-	-
		2000	760	1300	79.3	12.0	47.1	None	11.6	50.0	67.8	12.0	22.7
	R	-	-	1800	17.8	-	12.1	-	0.9	-	57.9	-	17.0
		1800	760	1800	19.7	None	13.5	None	2.1	None	58.0	None	-
		1800	0.18	1800	19.35	None	12.85	None	1.2	None	64.8	None	-
	R	-	-	2000	8.6	-	5.1	-	0.8	-	53.4	-	14.0
		2000	760	2000	8.3	3.5	4.4	1.4	0.8	None	27.0	49.5	10.5
	R	-	-	2100	6.1	-	3.35	-	0.7	-	-	-	5.3
Haynes 25	R	-	-	RT	150.0	-	71.1	-	42.7	-	49.0	-	32.1
		1800	760	RT	137.8	8.1	63.3	11.0	35.0	16.3	35.0	28.6	30.2
		2000	760	RT	141.6	5.6	60.2	15.6	50.7	None	50.7	None	34.2
		2000	0.18	RT	125.7	16.2	55.0	22.6	-	-	37.5	25.5	30.7
		2100	760	RT	121.9	7.3	43.5	34.0	55.0	None	34.0	30.0	32.6
	R	-	-	1400	76.2	-	33.8	-	22.0	-	27.0	-	24.8
		1800	760	1400	71.7	None	36.0	None	28.5	None	35.0	None	23.3
		2000	760	1400	71.6	None	36.8	None	25.2	None	25.2	6.7	19.5
		2000	0.18	1400	60.3	20.9	27.8	17.7	26.7	None	26.7	None	-
		2100	760	1400	40.5	46.8	25.5	-	2.0	91.0	-	-	-
	R	-	-	1800	26.1	-	19.8	-	1.25	-	42.7	-	21.5
		1800	760	1800	26.2	None	19.0	4.4	4.7	None	25.8	39.6	15.5
	R	-	-	2000	12.8	-	8.3	-	0.9	-	34.1	-	10.4
		2000	760	2000	12.0	6.2	9.2	None	4.5	None	23.7	30.5	12.2
		2000	0.18	2000	12.2	5.8	7.7	12.5	1.3	None	23.6	30.6	-
	R	-	-	2100	7.9	-	5.4	-	0.8	-	-	-	4.9
		2100	760	2100	7.4	5.7	4.8	11.1	0.8	-	-	-	7.3

Test direction - Transverse

R - As received

Original area of cross section of unoxidized specimens was used for calculation of F_{tu}, F_{ty}, and E.

TABLE XI

TENSILE TEST DATA FOR TD NICKEL AND TD NICKEL/CHROMIUM FOILS (0.01 in.) IN AS-RECEIVED AND OXIDIZED CONDITIONS

Superalloy	Condition			Test Temperature (°F)	F_{tu} (ksi)	Loss in F_{ty} due to Oxidation Exposure (%)	F_{ty} (0.2%) (ksi)	Loss in F_{ty} (%)	Elongation at F_{tu} (% in 2 in.)	Loss in Elongation due to Oxidation Exposure (%)	Total Elongation (% in 2 in.)	Loss in Elongation due to Oxidation Exposure (%)	E - Modulus (10^3 ksi)
	R	Oxidized for 100 one-hour cycles: Temperature (°F)	Oxidized for 100 one-hour cycles: Pressure (Torr)										
TD Nickel	R	-	-	RT	70.1	-	54.7	-	5.75	-	11.0	-	20.2
		2000	760	RT	52.5	25.0	43.9	19.7	3.2	43.5	3.2	70.9	24.4
		2200	760	RT	41.2	41.2	40.0	26.9	2.25	60.8	2.25	79.5	26.0
		2200	0.18	RT	50.3	28.2	39.6	27.6	-	-	6.3	42.7	24.1
		2400	760	RT	19.1	72.7	-	-	-	-	-	-	-
	R	-	-	1600	22.9	-	22.9	-	0.5	-	0.65	-	20.2
		2000	760	1600	20.9	8.7	20.9	8.7	0.3	40.0	0.5	23.0	24.4
		2200	760	1600	19.6	17.0	-	-	0.15	70.0	-	-	12.9
		2200	0.18	1600	18.6	18.8	-	-	-	-	-	-	-
	R	-	-	2000	12.8 (1)	-	11.6 (1)	-	1.0	-	1.8	-	9.6
		2000	760	2000	12 to 14 FS	-	12 to 14 FS	-	0.17	-	0.17	88.9	10.8
	R	-	-	2200	7.6	-	7.4	-	0.30	-	-	-	6.6
		2200	760	2200	18.1	None	13.25	None	0.6	None	1.2	-	15.6
		2200	0.18	2200	7.6	None	7.5	None	0.27	10.0	0.29	-	-
TD Nickel / Chromium	R	-	-	RT	135.5	-	90.[illegible]	-	14.5	-	14.5	-	24.6
		2000	760	RT	117.5	13.3	80.4	11.0	12.0	17.2	11.0	21.4	23.6
		2200	760	RT	126.2	6.9	82.7	8.4	10.3	29.0	10.3	26.4	25.6
		2200	0.18	RT	120.4	11.1	76.0	15.8	-	-	14.0	3.4	22.8
		2400	760	RT	125.3	7.5	77.0	14.7	11.7	19.3	11.7	16.4	26.2
		2400	0.18	RT	115.9	15.1	81.6	9.6	8.0	4.5	8.0	42.8	22.5
	R	-	-	1600	31.3	-	31.3	-	1.1	-	1.8	-	8.2
		2000	760	1600	27.4	12.5	27.2	13.1	0.6	45.0	1.0	44.4	14.8
		2200	760	1600	24.5	21.7	24.1	23.6	[illegible].2	81.8	0.95	-	12.3
		2200	0.18	1600	25.6	18.2	25.2	19.5	[illegible].28	74.0	0.48	-	-
		2400	760	1600	23.75	24.3	23.7	24.3	[illegible].3	72.7	-	-	16.0
	R	-	-	2000	16.4	-	16.1	-	0.2	-	0.2	-	9.6
		2000	760	2000	17.2	None	17.1	None	0.55	None	0.7	None	12.6
	R	-	-	2200	14.4	-	-	-	0.2	-	-	-	8.4
		2200	760	2200	12.2	15.3	-	-	0.[illegible]5	25.0	0.42	-	14.2
		2200	0.18	2200	13.55	6.25	-	-	0.20	-	0.27	-	-

Test direction -

TD Nickel - Transverse

TD Nickel/Chromium - Longitudinal

R - As received

1. Fracture stress

Original area of cross section of unoxidized specimens was used for calculation of F_{tu}, F_{ty}, and E.

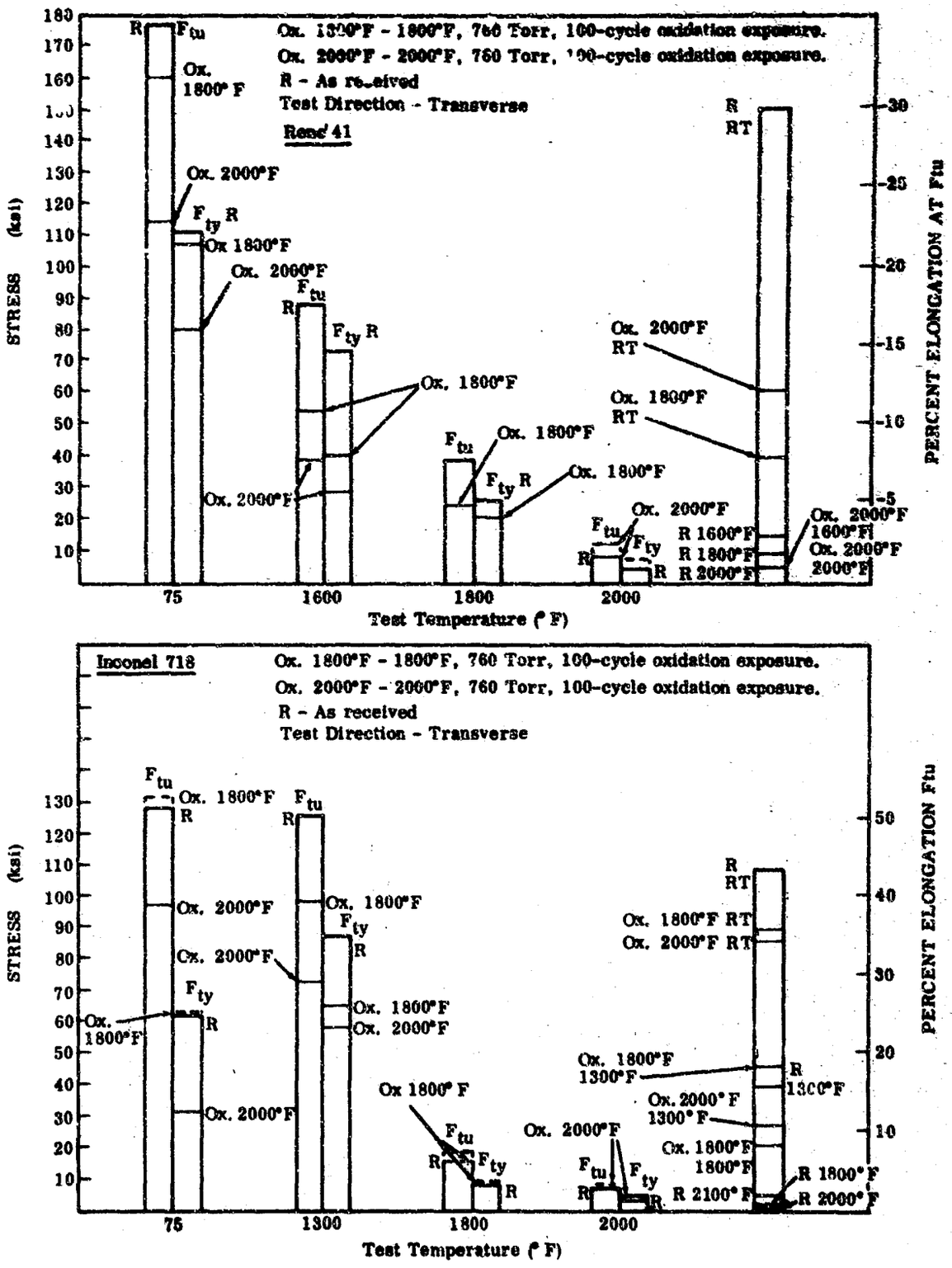

FIGURE 16. TENSILE PROPERTIES AT DIFFERENT TEMPERATURES FOR RENE' 41 AND INCONEL 718 FOILS IN VARIOUS CONDITIONS

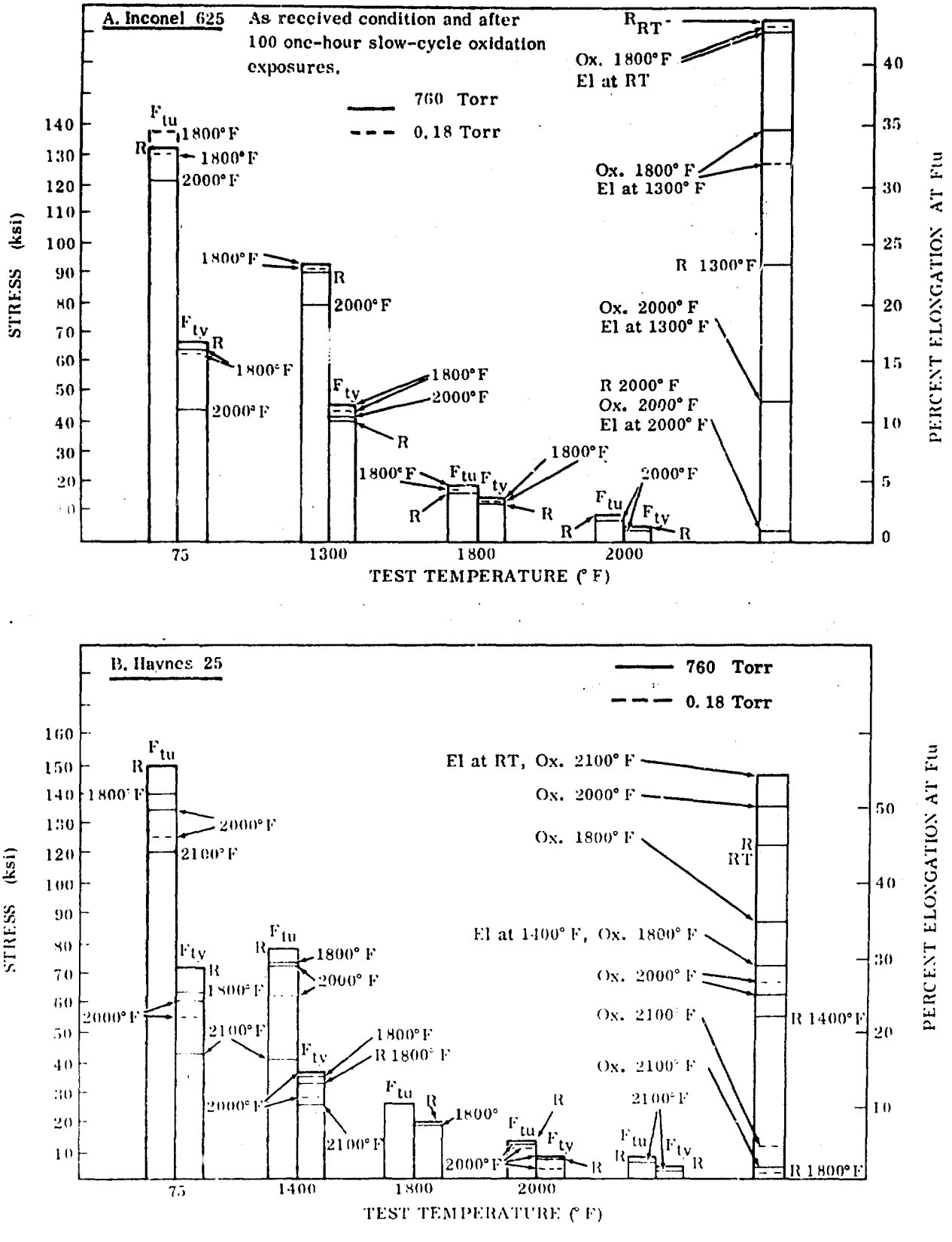

FIGURE 17. TENSILE PROPERTIES AT DIFFERENT TEMPERATURES FOR INCONEL 625 AND HAYNES 25 FOILS IN VARIOUS CONDITIONS

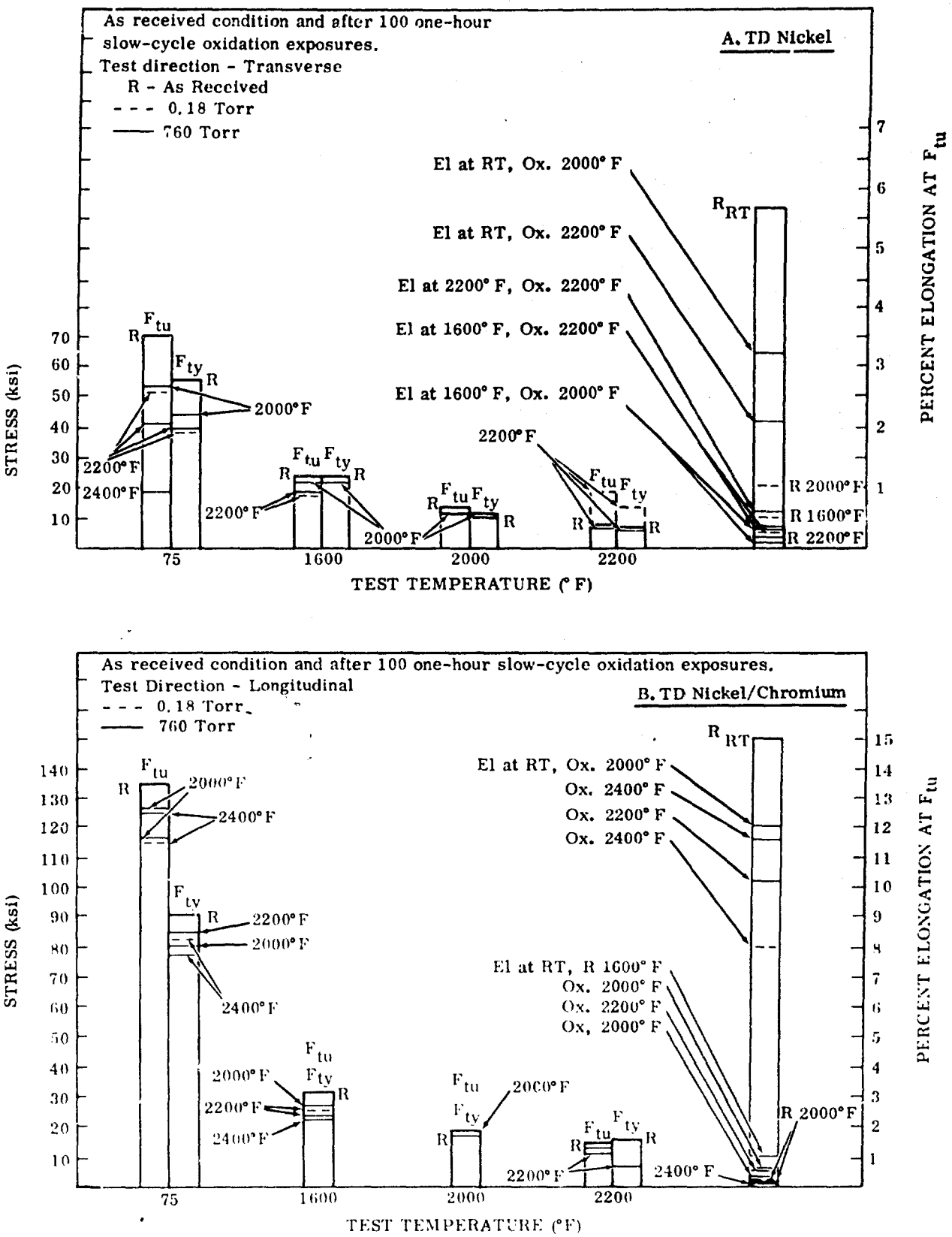

FIGURE 18. TENSILE PROPERTIES AT DIFFERENT TEMPERATURES FOR TD NICKEL AND TD NICKEL/CHROMIUM FOILS IN VARIOUS CONDITIONS

found to have the lowest room temperature ductility; TD Nickel had the lowest F_{tu}, F_{ty}, and elongation values at room temperature among the six superalloys. With increasing temperature, F_{tu}, F_{ty}, and modulus values decrease, as expected, for all six program alloys (Tables IX, X, and XI). Among the six program alloys, at 2000°F, the highest F_{ty} (or F_{tu}) values was exhibited by TD Nickel/chromium (16.1 ksi) followed by TD Nickel (11.6 ksi), Haynes 25 (8.8 ksi), Inconel 625 (5.1 ksi), and Rene' 41 (4.4 ksi) or Inconel 718 (4.3 ksi). Also, at 2000°F, the percent elongation at F_{tu} (not total elongation at failure) was slightly less than one percent for all the superalloys except TD Nickel/chromium, for which the elongation at F_{tu} was 0.2 percent. The percent elongation at F_{tu} values was obtained for all specimens. Only the total elongation values were obtained in some cases because of experimental restrictions. As such, comprehensive comparison of the total elongation values at high temperatures for the superalloys cannot be made. The low modulus values ($\sim 10 \times 10^6$ ksi) for TD Nickel and TD Nickel/chromium at high temperatures (1600°F and higher) were found to be in agreement with the literature (Appendix). The modulus values are qualitative only because of the experimental error associated with obtaining the slope of the linear section of stress-strain curves at elevated temperatures. The effects of oxidation exposures on the tensile properties of the six superalloy foils are discussed in following paragraphs.

Precipitation Hardened Alloys (Rene' 41 and Inconel 718)

The atmospheric pressure oxidation exposures for 100 one-hour slow cycles resulted in loss in tensile properties (F_{tu}, F_{ty}, or percent elongation), the loss being more after the 2000°F T_{max} exposure than after the 1800°F T_{max} exposure (Table IX and Fig. 16). The higher degradation in tensile data due to the 2000°F exposure rather than after the 1800°F exposure for the two alloys, was most likely because of greater decarburization, grain growth, intergranular cracking, and μ phase instability (for Rene' 41 only). The loss, in general, was higher for Rene' 41 than for Inconel 718 which could be the result of extensive intergranular cracking in the case of Rene' 41, as discussed in Paragraph 4.4.1 on metallographic analysis, and to more rapid general oxidation (para 4.2). The decrease in tensile properties was least at T_{ox} (1800 or 2000°F) as compared to that at room temperature or at T_{dm}. (The T_{dm} for Rene' 41 is 1600°F and for Inconel 718 is 1300°F.) Loss in F_{ty} at room temperature after the 2000°F oxidation exposure was higher than 33 percent and, as such, 1800°F was selected as T_{max} for these two alloys.

Although the oxidation effects were more severe for Rene' 41 than for Inconel 718, the residual F_{ty} (or F_{tu}) values after the two oxidation exposures were higher for Rene' 41 than for Inconel 718 at room temperature and at 1800°F (Fig. 16). The F_{ty} values at T_{dm} for the two alloys could not be compared since the T_{dm} for the two alloys were different. But the residual elongation values at F_{tu} were higher for Inconel 718 in the temperature range of room temperature to 2000°F.

The Rene' 41 and Inconel 718 alloys were eliminated from the remainder of the program based on the mechanical property data and the effects of atmospheric pressure oxidation exposure. As such, these two alloys were not subjected to 0.18 Torr oxidation exposure. The remaining four alloys, Inconel 625, Haynes 25, TD Nickel, and TD Nickel/chromium were subjected to both atmospheric and low-pressure cyclic oxidation exposure. The oxidation effects on tensile data are discussed in the next section.

Solid Solution Strengthened Alloys (Inconel 625 and Haynes 25)

The atmospheric pressure cyclic oxidation exposure for 100 cycles with T_{max} = 1800 or 2000°F caused no significant degradation in tensile properties for the Haynes 25 and Inconel 625 alloys, except for a 34 percent loss in room temperature yield strength of Inconel 625 after the 2000°F oxidation exposure (Table X and Fig. 17). The 2100°F atmospheric pressure oxidation exposure for Haynes 25 resulted in a 34 percent loss in room temperature yield strength. Based on this loss and other oxidation effects and creep rate considerations, the temperatures 2000 and 2100°F were considered too high for Inconel 625 and Haynes 25, respectively. The T_{max} selected for Inconel 625 was 1800°F and 2000°F for Haynes 25. The low-pressure (0.18 Torr) oxidation exposure for these two alloys were conducted at their selected T_{max}. The low-pressure (0.18 Torr) oxidation exposure at 1800°F for 100 cycles caused negligible loss in tensile properties of Inconel 625. But the 100-cycle exposure at 2000°F and 0.18 Torr for Haynes 25 resulted in greater loss in tensile properties (less than 33 percent) than the 100-cycle exposure at 2000°F and 760 Torr (Table X and Fig. 17). Thus, Inconel 625 and Haynes 25 were found satisfactory for use up to T_{max} of 1800 and 2000°F, respectively, in both 760 Torr and 0.18 Torr oxidation exposures.

The residual room temperature F_{ty} or percent elongation at F_{tu} after oxidation exposures at 1800 or 2000°F (Table X and Fig. 17), for Inconel 625 and Haynes 25 were about the same. But at 1800 or 2000°F, Haynes 25 exhibited higher residual F_{ty} (or F_{tu}) and percent elongation at F_{tu} than Inconel 625.

Dispersion Strengthened Alloys (TD Nickel and TD Nickel/chromium

The ultimate and yield strength values for oxidized specimens of TD Nickel and TD Nickel/chromium were found to decrease with increasing temperature as was the case with the as-received specimens (Table XI and Fig. 18). In the case of TD Nickel, increasing loss in room temperature tensile properties occurred with increasing oxidation exposure temperature or pressure. This increase was due to loss in cross section and to build up of the brittle nickel oxide. Highest loss occurred in room temperature tensile properties. The degradation in tensile properties was much less at 1600°F than at room temperature. At 2200°F, the F_{ty} values were higher for the

oxidized specimens than for the as-received specimens. These higher values may be explained on the basis that NiO (NaCl structure) exhibited significant ductility at 2000 to 2200°F and carried part of the load. Stress values were calculated based on cross section of the preoxidized specimen. During oxidation exposure, the thickness and area of the TD Nickel specimen increased due to NiO formation. Thus, the use of reduced area values (original area rather than the oxidized area) resulted in higher values for F_{tu} or F_{ty}. For TD Nickel, at the higher oxidation temperature, a greater loss in tensile properties (F_{tu} and percent elongation) occurred at room temperature and at 1600°F (Table XI). However, increasing the oxidation pressure from 0.18 Torr to 760 Torr resulted in greater loss in room temperature tensile properties only, decreased loss in tensile properties at 1600°F, and improvement in tensile properties at 2000 and 2200°F. Results of the increased oxidation pressure are believed to be due to plasticity of NiO at a higher temperature and the increase in the cross section of the specimen after oxidation.

After the 2400°F, 760 Torr oxidation exposure, the TD Nickel specimens were severely oxidized and embrittled, resulting in 72.7 percent loss in room temperature F_{tu}. The TD Nickel alloy showed satisfactory tensile properties after oxidation exposures up to 2200°F in 760 Torr or 0.18 Torr. Thus, the T_{max} for TD Nickel was 2200°F.

In the case of TD Nickel/chromium, the loss in tensile properties was less than 33 percent after the various oxidation exposures up to a T_{max} of 2400°F and in atmospheric or low pressure (0.18 Torr) dry air environment. The 2400°F, 0.18 Torr, and 100-cycle oxidation exposure could not be completed in the MGR because of arc discharge and vaporization of silicon (onto the specimens) from Globar heating elements. One TD Nickel/chromium tensile test specimen was subjected to 2400°F, 100 cycles, and 0.18 Torr exposure in a mission profile environmental simulator (Fig. 12 and 13) without any stress. This oxidized specimen was then evaluated by room temperature tensile test and by metallographic analysis only. Therefore, only the room temperature tensile test data for the TD Nickel/chromium superalloy specimen after a 100-cycle oxidation exposure at 2400°F and 0.18 Torr was obtained. In lieu of 2400°F - 0.18 Torr oxidized specimens, a batch of 40 TD Nickel/chromium specimens was subjected to a 100-cycle oxidation exposure in the MGR furnace at 2200°F and 0.18 Torr. For this oxidized condition, the tensile test data at room temperature, T_{dm}, and T_{max} are included in Table XI. From this tensile test data, TD Nickel/chromium was found satisfactory for service up to 2400°F.

The loss in tensile properties was much lower for TD Nickel/chromium than for TD Nickel. Also, the residual (or as-received) tensile values were found to be higher for TD Nickel/chromium than for TD Nickel.

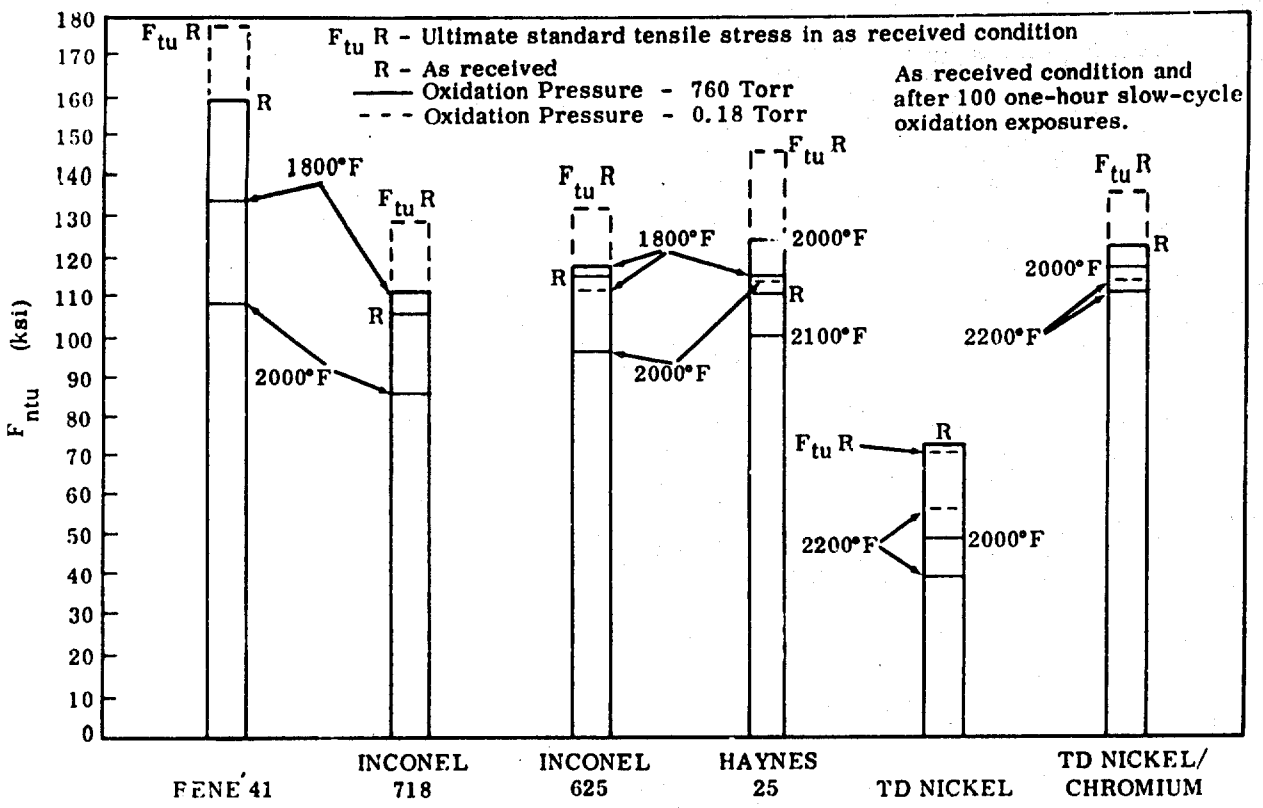

FIGURE 19. NOTCH ULTIMATE TENSILE STRENGTH AT ROOM TEMPERATURE FOR SUPERALLOY FOILS (0.01-Inch Thick) IN VARIOUS CONDITIONS

4.3.2 Notch Tensile Test Results

The results of room temperature notch tensile tests for the six superalloys in the as-received and oxidized conditions, and the elevated temperature notch tensile test results for the four selected alloys (Inconel 625, Haynes 25, TD Nickel, and TD Nickel/chromium) are given in Table XII. The Table includes F_{ntu}, F_{nty}, elongation at F_{ntu}, total elongation, modulus values, notch strength ratio (NSR), and percent loss in F_{ntu} and F_{nty} due to various oxidation exposures. The room temperature notch ultimate strength values for the superalloy foils in the as-received and oxidized conditions are plotted in bar graph form in Figure 19. The notch strength ratio was calculated as

$$NSR = \left(\frac{F_{ntu}}{F_{tu}}\right) \quad \text{or} \quad NSR = \left(\frac{F_{ntu\ oxidized}}{F_{tu\ oxidized}}\right) \quad \text{for the oxidized specimens}$$

The notch tensile specimens of all the six program alloys in the as-received condition exhibited negligible elongation values and the notch yield strength (F_{nty}) values were only slightly less than the notch ultimate strength values (F_{ntu}). The notch tensile test results for the six alloys are discussed in following paragraphs.

TABLE XII

NOTCH TENSILE TEST DATA FOR SUPERALLOY FOILS IN AS-RECEIVED AND OXIDIZED CONDITIONS

Superalloy	Condition			Test Temperature (°F)	F_{ntu} (ksi)	Loss in F_{ntu} due to Oxidation (%)	F_{nty} (ksi)	Loss in F_{nty} due to Oxidation (%)	Elongation at F_{ntu} (% in 2 in.)	Total Elongation (% in 2 in.)	E - Elastic Modulus (10^3 ksi)	NSR
	R	Oxidized for 100 one-hour cycles: T_{max} (°F)	Oxidized for 100 one-hour cycles: Pressure (Torr)									
Rene' 41	R	-	-	RT	158.0	-	146.5	-	0.7	1.1	29.7	0.89
		1800	760	RT	134.7	13.2	-	-	0.1	0.1	31.1	0.84
		2000	760	RT	107.7	31.8	107.7	26.4	0.45	2.1	-	0.94
Inconel 718	R	-	-	RT	105.7	-	79.8	-	1.8	3.8	31.2	0.83
		1800	760	RT	111.8	None	102.7	None	0.4	0.7	32.0	0.86
		2000	760	RT	85.9	18.7	57.0	28.6	1.25	2.1	-	0.89
Inconel 625	R	-	-	RT	114.0	-	98.0	-	1.6	3.5	30.2	0.87
		1800	760	RT	110.5	None	110.9	None	0.6	1.2	26.7	0.86
		1800	0.18	RT	110.4	3.16	87.5	10.7	-	2.0	50.9	0.85
		2000	760	RT	96.9	15.0	66.3	32.2	1.9	3.0	-	0.79
	R	-	-	1300	89.9	-	78.8	-	-	2.0	25.0	0.998
		1800	760	1300	81.6	9.2	65.1	17.4	1.46	1.46	-	0.88
		1800	0.18	1300	81.3	9.6	66.1	16.1	1.29	1.30	-	0.89
	R	-	-	1800	22.4	-	-	-	-	4.5	14.5	1.29
	R	1800	760	1800	29.4	None	19.7	-	0.9	3.3	-	1.49
		1800	0.18	1800	29.4	None	19.65	-	0.9	3.2	-	1.52
Haynes 25	R	-	-	RT	110.0	-	90.7	-	1.9	3.7	34.2	0.73
		1800	760	RT	113.8	None	105.6	None	0.4	0.9	34.4	0.82
		2000	760	RT	124.4	None	93.1	None	1.65	2.5	-	0.88
		2000	0.18	RT	113.5	None	83.6	7.8	-	2.0	63.2	0.90
		2100	760	RT	101.7	7.5	77.1	15.0	1.75	3.25	-	0.94
	R	-	-	1400	59.5	-	53.5	-	-	2.0	22.1	0.78
		2000	760	1400	56.0	5.9	51.5	3.9	0.9	1.9	-	0.79
		2000	0.18	1400	57.8	2.8	45.6	14.8	1.6	2.5	-	0.96
	R	-	-	1800	27.9	-	-	-	-	1.0	-	1.07
	R	-	-	2000	18.6	-	17.9	-	-	-	-	1.66
		2000	760	2000	20.3	None	13.6	24.0	0.9	2.2	-	1.69
		2000	0.18	2000	19.3	None	13.6	24.0	0.9	2.2	17.9	1.60
TD Nickel	R	-	-	RT	71.3	-	68.5	-	0.5	0.75	19.7	1.03
		2000	760	RT	49.0	31.3	49.0	28.5	-	0.5	27.8	0.93
		2200	760	RT	39.7	44.3	-	-	-	0.5	-	0.96
		2200	0.18	RT	56.3	21.0	53.7	21.6	-	1.0	38.8	1.12

TABLE XII (Cont)

NOTCH TENSILE TEST DATA FOR SUPERALLOY FOILS IN AS-RECEIVED AND OXIDIZED CONDITIONS

Superalloy	Condition			Test Temperature (°F)	F_{ntu} (ksi)	Loss in F_{ntu} due to Oxidation (%)	F_{nty} (ksi)	Loss in F_{nty} due to Oxidation (%)	Elongation at F_{ntu} (% in 2 in.)	Total Elongation (% in 2 in.)	E - Elastic Modulus (10^3 ksi)	NSR
	R	Oxidized for 100 one-hour cycles: T_{max} (°F)	Oxidized for 100 one-hour cycles: Pressure (Torr)									
TD Nickel/ chromium	R	-	-	RT	122.5	-	115.5	-	0.5	0.95	24.0	0.90
		2000	760	RT	117.5	4.0	115.5	None	-	0.65	-	1.00
		2200	760	RT	110.0	10.2	106.8	7.5	0.51	0.8	-	0.87
		2200	0.18	RT	113.5	7.3	105.4	8.7	-	1.0	-	0.94
		2400	760	RT	107.4	12.3	105.5	8.6	0.5	0.85	-	0.85
	R	-	-	1600	30.8	-	-	-	-	1.0	15.7	0.95
		2200	760	1600	29.4	4.5	-	-	-	0.33	-	1.20
		2200	0.18	1600	27.21	11.7	-	-	-	0.43	-	1.06
	R	-	-	2200	11.15	-	10.1	-	-	-	9.8	0.77
		2200	760	2200	14.6	None	-	-	-	0.28	-	1.20
		2200	0.18	2200	15.8	None	-	-	-	0.28	-	1.17

Test direction -

Transverse - Rene' 41, Inconel 718, Inconel 625, Haynes 25, and TD Nickel

Longitudinal - TD Nickel/chromium

R - As received

In case of oxidized specimens, the original area of cross section of the unoxidized specimens was used for calculations of F_{ntu}, F_{nty}, and E.

NSR - Notch strength ratio (F_{ntu}/F_{tu})

Precipitation Hardened Alloys (Rene' 41 and Inconel 718)

For these two alloys the percent loss in room temperature F_{ntu} or F_{nty} was more after the 100-cycle exposure at 2000°F and 760 Torr than after an 1800°F exposure. Also this degradation was greater for Rene' 41 than for Inconel 718 (Table XII and Fig. 19). These effects on notch tensile strength values resulting from oxidation exposure were similar to those on standard tensile properties discussed earlier (para 4.3.1). The NSR, a measure of notch sensitivity, was less than unity for both alloys in the as-received or oxidized conditions. There was a slight increase in NSR values due to the oxidation exposure (except for a slight decrease from 0.89 to 0.84 for Rene' 41 after a 100-cycle oxidation exposure at 1800°F and 760 Torr).

Solid Solution Strengthened Alloys (Inconel 625 and Haynes 25)

These two alloys showed no degradation in notch tensile strength values after the 100-cycle oxidation exposure at 1800°F and 760 Torr (Table XII and Fig. 19). But a loss in room temperature notch strength values (F_{nty}) for Inconel 625 was 10.7 percent and 32.2 percent after a 100-cycle oxidation exposure at 1800°F and 0.18 Torr and at 2000°F and 760 Torr, respectively. For Haynes 25, the loss in room temperature F_{nty} after 100 hours of cyclic oxidation exposure at 2000°F and 0.18 Torr, and at 2100°F and 760 Torr was 7.8 percent and 15.0 percent, respectively. Higher loss in room temperature F_{nty} occurred with increasing oxidation temperature and lower pressure (0.18 Torr) for both Inconel 625 and Haynes 25 (similar to the decrease in F_{ty} (Table X). The degradation in notch tensile strength due to different oxidation exposures, in general, was greater for Inconel 625 than for Haynes 25 (Table XII). Also, the residual strength values were higher for Haynes 25 than for Inconel 625 (Fig. 19).

The NSR at room temperature for the two alloys was less than unity in the as-received or oxidized conditions. The NSR at room temperature decreased after different oxidation exposures for Inconel 625 (from 0.87 to 0.79); whereas, it increased for Haynes 25 (from 0.73 to 0.94 - Table XII).

The effects of increasing test temperatures on the notch tensile properties of the two alloys in the as-received or oxidized conditions were:

- A decrease in F_{ntu} and F_{nty}
- Ductility minimum behavior from changes in total percent elongation values
- Increase in NSR values (Table XII), i.e., these two alloy foils were not notch sensitive at temperatures above T_{dm} (1300°F for Inconel 625 and 1400°F for Haynes 25)

There was a definite loss in F_{nty} at T_{dm} of the two alloys because of different oxidation exposures; for Inconel 625 about 17 percent for exposures at 1800°F; for Haynes 25 it was 3.9 and 14.8 percent for exposures at 2000°F and 760 and 0.18 Torr, respectively. At T_{max} (1800°F for Inconel 625 and 2000°F for Haynes 25) there was no decrease in F_{ntu} or F_{nty} for Inconel 625, but the loss in F_{nty} was 24 percent for Haynes 25 after oxidation exposures at 2000°F at both 760 or 0.18 Torr. Low-pressure (0.18 Torr) oxidation exposures, in general, resulted in similar effects on notch tensile test data as the 760 Torr oxidation exposure.

Dispersion Strengthened Alloys (TD Nickel and TD Nickel/Chromium)

For TD Nickel, increasing loss in room temperature F_{ntu} occurred with higher oxidation temperatures or pressures as was the case in standard tensile tests (Tables XI and XII). High-temperature notch tensile tests for TD Nickel were not conducted. For TD Nickel/chromium, less than 10 percent loss in notch tensile yield strength values at room temperature was observed due to oxidation exposures to the T_{max} of 2400°F. The loss in F_{tu} at 1600°F for TD Nickel/chromium after the 2200°F oxidation exposures at 760 Torr and at 0.18 Torr was 4.5 percent and 11.7 percent, respectively. There was no significant degradation in high-temperature (2200°F) properties because of 2200°F oxidation exposures.

The NSR at room temperature was more than unity only in the case of TD Nickel among the six superalloys. Thus, TD Nickel is least notch sensitive. The high-temperature NSR for TD Nickel could not be obtained but the literature values are cited. It is reported (Ref. 5) that for TD Nickel, the ratio of notched to unnotched strength remains greater than unity from 75 to almost 2000°F. Above 2000°F, notched and unnotched tensile strengths are reported to be identical (Ref. 5). The NSR for TD Nickel/chromium in the as-received condition was 0.90 at room temperature and 0.77 at 2000°F. Thus TD Nickel/chromium was found to be more notch sensitive than TD Nickel. At room temperature, the NSR for oxidized TD Nickel/chromium specimens was of the same order of magnitude as for as-received specimens. But at temperatures of 1600°F or higher, the NSR was higher for the oxidized TD Nickel/chromium specimens than for as-received specimens, and was greater than unity (Table XII). In the oxidized conditions, TD Nickel/chromium was found to be not notch sensitive at temperatures of 1600°F or higher.

4.3.3 High Rate Tensile Test Results

High rate tensile test data (room temperature) for F_{tu} and percent elongation (average values) for the superalloy foil specimens in the as-received and oxidized conditions are given in Table XIII. For comparison, the room temperature standard tensile test results are included in Table XIII. Typical load versus elongation oscilloscope traces are reproduced in Figure 20.

TABLE XIII

HIGH STRAIN RATE TENSILE TEST DATA (at RT) FOR SUPERALLOY FOILS (0.01 in.) IN AS-RECEIVED AND OXIDIZED CONDITIONS

Superalloy	Condition			F_{tu} (ksi)	Loss in F_{tu} (%)	Total Elongation (% in 1 in. gage length)	Loss in Elongation (%)
	R	Oxidized for 100 one-hour cycles: Temperature (°F)	Pressure (Torr)				
Inconel 625	R	standard tensile data		136.0	-	49.0	-
	R	-	-	145.6	-	48.8	-
		1800	760	147.4	None	44.5	8.8
		1800	0.18	144.5	0.7	45.5	6.8
Haynes 25	R	standard tensile data		153.0	-	49.0	-
	R	-	-	156.6	-	51.6	-
		1800	760	150.5	None	36.0	30.0
		2000	760	153.6	None	45.5	10.5
		2000	0.18	148.2	9.2	48.0	7.0
TD Nickel	R	standard tensile data		71.5	-	11.0	-
	R	-	-	81.3	-	15.5	-
		2000	760	71.0	12.6	5.3	65.7
		2200	760	62.2	23.5	2.4	84.5
		2200	0.18	73.2	10.0	13.0	12.9
TD Nickel/ chromium	R	standard tensile data		143.0	-	14.0	-
	R	-	-	138.3	-	12.0	-
		2000	760	141.0	None	15.5	None
		2200	760	142.5	None	14.5	None
		2200	0.18	127.9	11.4	12.5	13.8
		2400	760	130.0	6.0	9.1	24.2

Test Direction

Transverse - Inconel 625, Haynes 25, TD Nickel
Longitudinal - TD Nickel/chromium

R - As received

Strain Rate - 1500 in./in./min

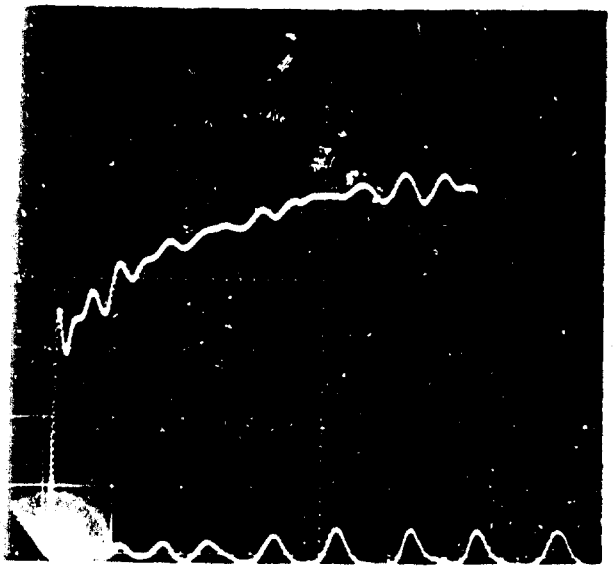

A. As-Received Inconel 625

B. As-Received TD Nickel

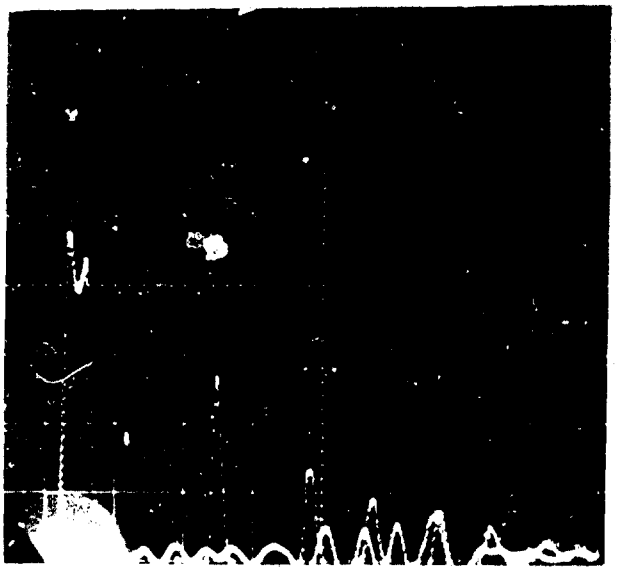

C. TD Nickel
Oxidized 100 Cycles
2200°F
760 Torr
x-axis 1 cm = 0.120 inch
y-axis 1 cm 100 pounds

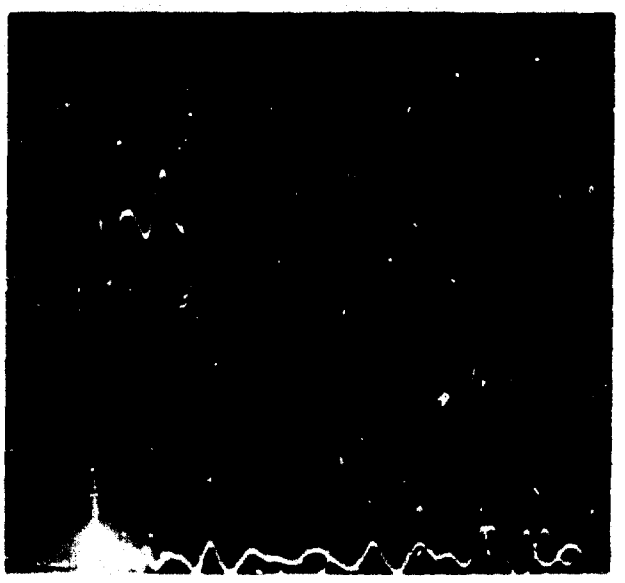

D. TD Nickel
Oxidized 100 Cycles
2200°F
0.18 Torr

FIGURE 20. OSCILLOSCOPE TRACES FOR TYPICAL LOAD VERSUS ELONGATION; As-Received and Oxidized Superalloy Foils (Sheet 1 of 2)

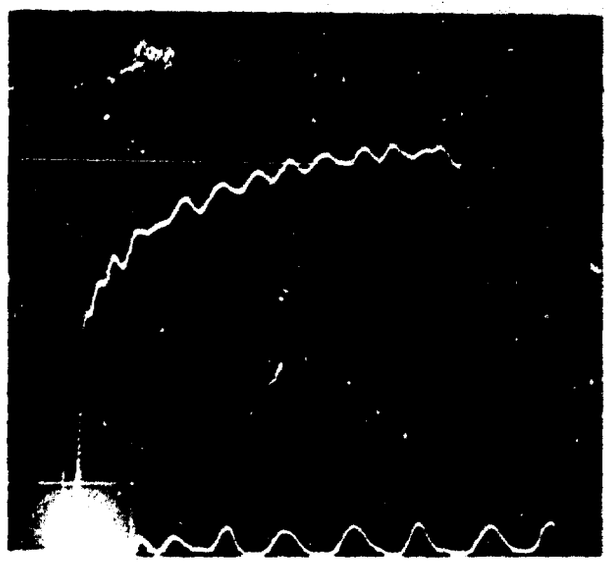

E. Haynes 25
Oxidized 100 Cycles
2000°F
760 Torr

F. As-Received TD Nickel/Chromium

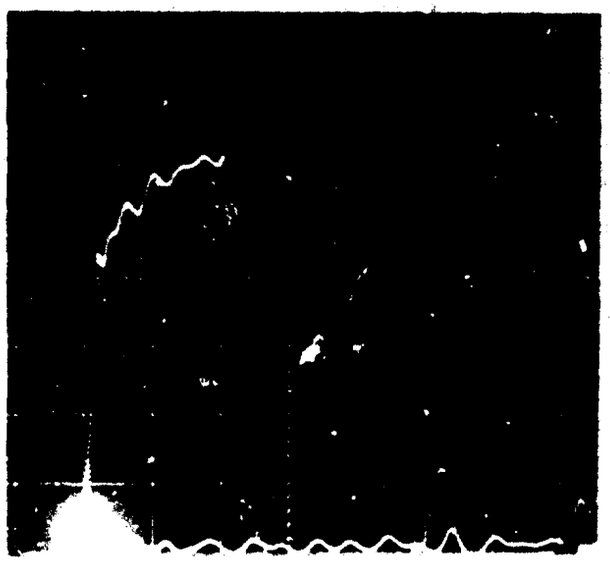

G. TD Nickel/Chromium
Oxidized 100 Cycles
2200°F
760 Torr
x-axis 1 cm = 0.120 inch
y-axis 1 cm = 100 pounds

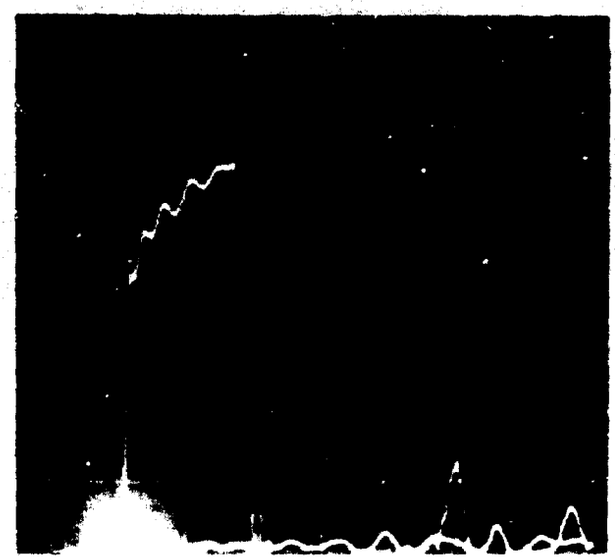

H. TD Nickel/Chromium
Oxidized 100 Cycles
2400°F
760 Torr

FIGURE 20. OSCILLOSCOPE TRACES FOR TYPICAL LOAD VERSUS ELONGATION; As-Received and Oxidized Superalloy Foils (Sheet 2 of 2)

In the as-received condition, the F_{tu} and total elongation values were about the same from the two tensile tests. The F_{tu} and elongation values from the high rate (1500 in. /in. /min) tensile tests were slightly higher for TD Nickel and Haynes 25, and somewhat lower for TD Nickel/chromium than from the standard tensile tests. Among the four superalloy foils, the F_{tu} and elongation values at room temperature were highest for Haynes 25. The elongation values were lowest for TD Nickel/chromium (Table XIII and Figure 20). High strain rate had essentially a negligible effect on the tensile properties of the four superalloy foils.

Because of ringing in the load cell, the load versus elongation oscilloscope traces were not smooth curves (Fig. 20). The traces of Inconel 625 and Haynes 25 (Fig. 20A and 20E) with large elongation values can be easily distinguished from those of TD Nickel and TD Nickel/chromium with small elongation values (Fig. 20B and 20F).

There was no significant loss in high rate tensile strength for the Inconel 625, Haynes 25, and TD Nickel/chromium alloys due to various oxidation exposures. In the case of TD Nickel, maximum loss in F_{tu} (23. 5 percent) and elongation values (84. 5 percent) occurred as a result of exposure at 2200°F and 760 Torr. Exposures at 2200°F and 0. 18 Torr, and 2000°F and 760 Torr had less effect on the F_{tu} for this alloy.

The loss in F_{tu} for the four superalloy foils in the high rate tensile test was less than that in the standard tensile test. For the purpose of determining the degradation resulting from oxidation exposures, the standard tensile test is considered to be a more severe test.

From the load versus elongation oscilloscope traces, the effect of oxidation exposures on ductility of TD Nickel and TD Nickel/chromium can be readily appreciated. In the case of TD Nickel, the elongation was lowest after 2200°F MGR exposure at atmospheric pressure rather than at 0. 18 Torr pressure (Fig. 20B, C, and D).

In all cases necking occurred during high rate tensile tests, but occurred to a greater extent in the case of as-received Inconel 625 and Haynes 25. Shear fracture occurred for the four superalloy foils in the as-received condition. But for the oxidized superalloy specimens, the fracture occurred perpendicular to the test direction.

4. 3. 4 Room Temperature Fatigue Test Results

Results of room temperature fatigue tests for the six superalloy foils (0. 01 inch) in the as-received and oxidized conditions are presented in the form of the S-N (maximum stress, S, in ksi versus fatigue life, N, in cycles) curves. The S-N

curves are plotted in Figure 21 for Rene' 41 and Inconel 718, in Figure 22 for Inconel 625 and Haynes 25 and in Figure 23 for TD Nickel and TD Nickel/chromium. From these S-N curves, the fatigue limit for 5 x 10^6 cycles was determined. The room temperature fatigue limit for the superalloy foils in the as-received condition and after various oxidation exposures are presented in Table XIV, and also in bar graph form in Figure 24. In the as-received condition, the room temperature fatigue limit was highest for Rene' 41 (92.0 ksi) followed by Inconel 718, Inconel 625, Haynes 25, TD Nickel/chromium, and least for TD Nickel (48.0 ksi). The effects of different oxidation exposures on room temperature fatigue life for the superalloys are discussed in succeeding paragraphs.

Precipitation Hardened Alloys (Rene' 41 and Inconel 718)

The atmospheric pressure oxidation exposures caused a decrease in fatigue life for both alloys; the decrease was greater at higher stresses (Fig. 21). The loss in room temperature fatigue limit due to 100 one-hour slow-cycle atmospheric pressure oxidation exposures with T_{max} of 1800 or 2000°F was 17.4 percent and 38 percent, respectively, for Rene' 41, and 11.9 and 50.0 percent, respectively, for Inconel 718 (Table XIV). Thus, greater loss in fatigue limit occurred for Inconel 718 than for Rene' 41 after 2000°F oxidation exposure. The residual room temperature fatigue limit was higher for Rene' 41 than for Inconel 718 (Fig. 24). The loss in fatigue limit, because of a 100-cycle oxidation exposure at 2000°F and 760 Torr was higher than 33 percent for both alloys. Therefore, these two alloys were not considered satisfactory for service at 2000°F.

Solid Solution Strengthened Alloys (Inconel 625 and Haynes 25)

There was a general decrease in fatigue life for both Inconel 625 and Haynes 25 due to the different oxidation exposures, except in the case of Inconel 625 after a 100-cycle exposure at 1800°F and 0.18 Torr. The loss in room temperature fatigue limit because of 100 one-hour cyclic atmospheric pressure oxidation exposures with T_{max} of 1800 or 2000°F was 32.9 and 50.0 percent, respectively, for Inconel 625 and 12.0 and 27.0 percent, respectively, for Haynes 25 (Table XIV). The residual fatigue limit was higher for Haynes 25 than for Inconel (Fig. 22 and 24).

The loss in fatigue limit resulting from atmospheric pressure oxidation exposure at a T_{max} of 2000°F for Inconel 625 and at a T_{max} of 2100°F for Haynes 25 was 50 and 60 percent, respectively (i.e., greater than 33 percent). As such, the recommended T_{max} for Inconel 625 was 1800°F and for Haynes 25 it was 2000°F. The low pressure (0.18 Torr) oxidation exposure at a T_{max} of 1800°F for Inconel 625 and a T_{max} of 2000°F for Haynes 25 resulted in 17.0 and 24.8 percent loss in room temperature fatigue limit, respectively. The percentage losses were less than that due to the similar atmospheric pressure oxidation exposures.

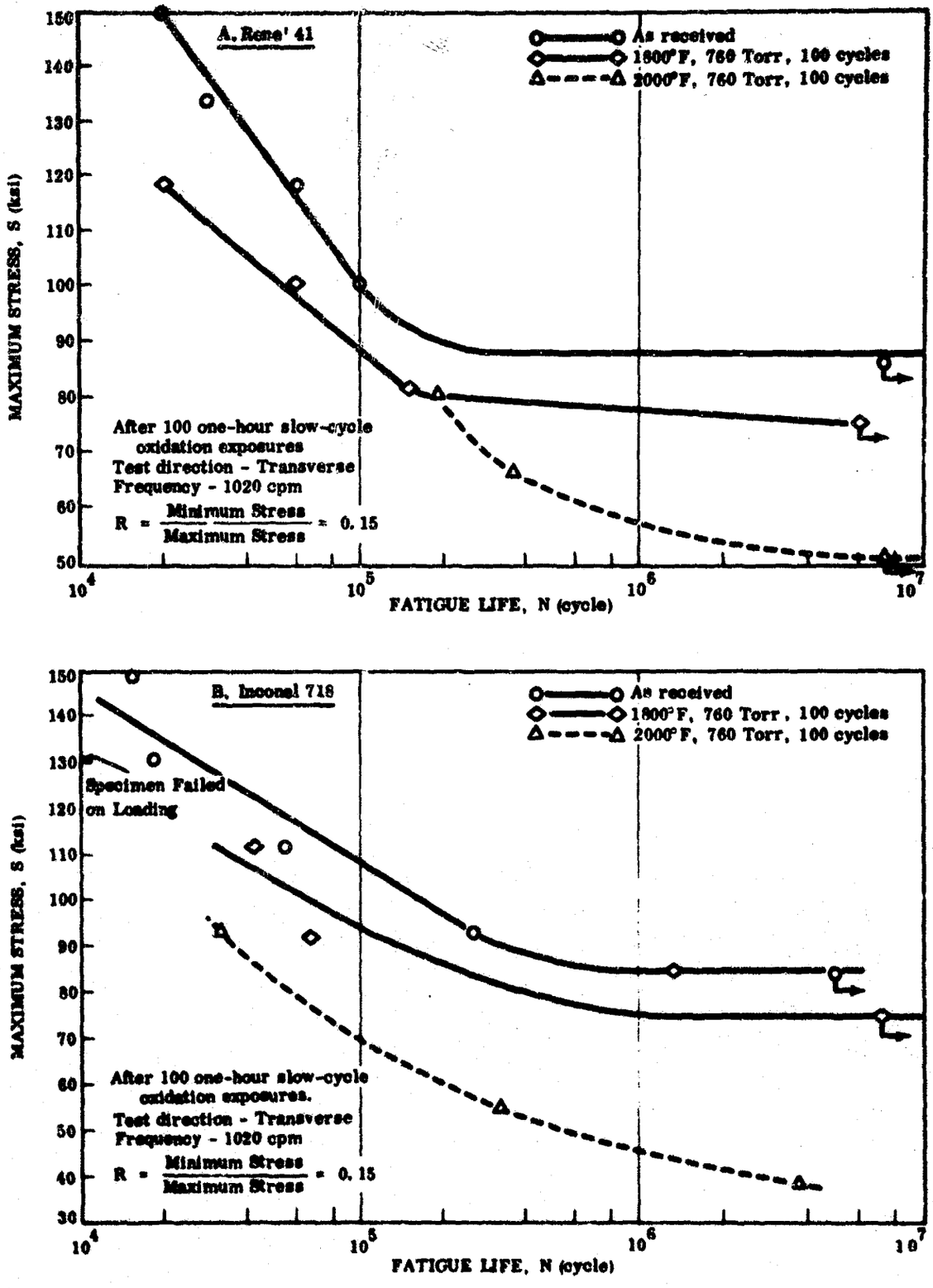

FIGURE 21. ROOM TEMPERATURE FATIGUE CURVES (S-N); Rene' 41 and Inconel 718 Foils

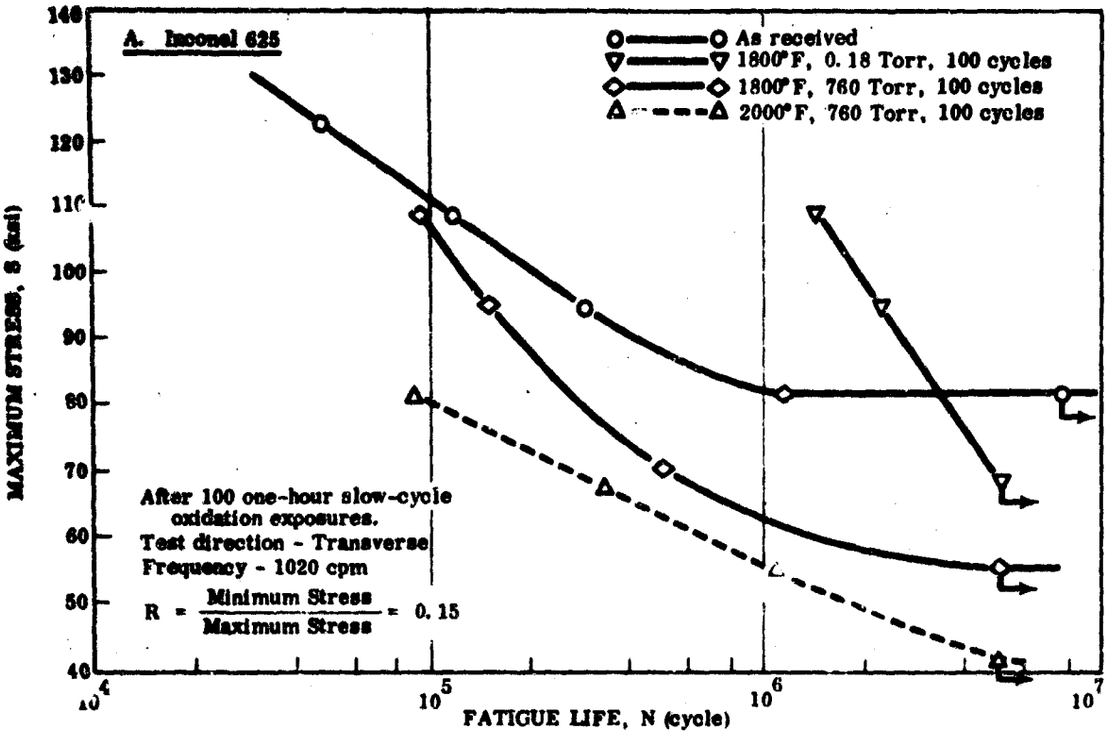

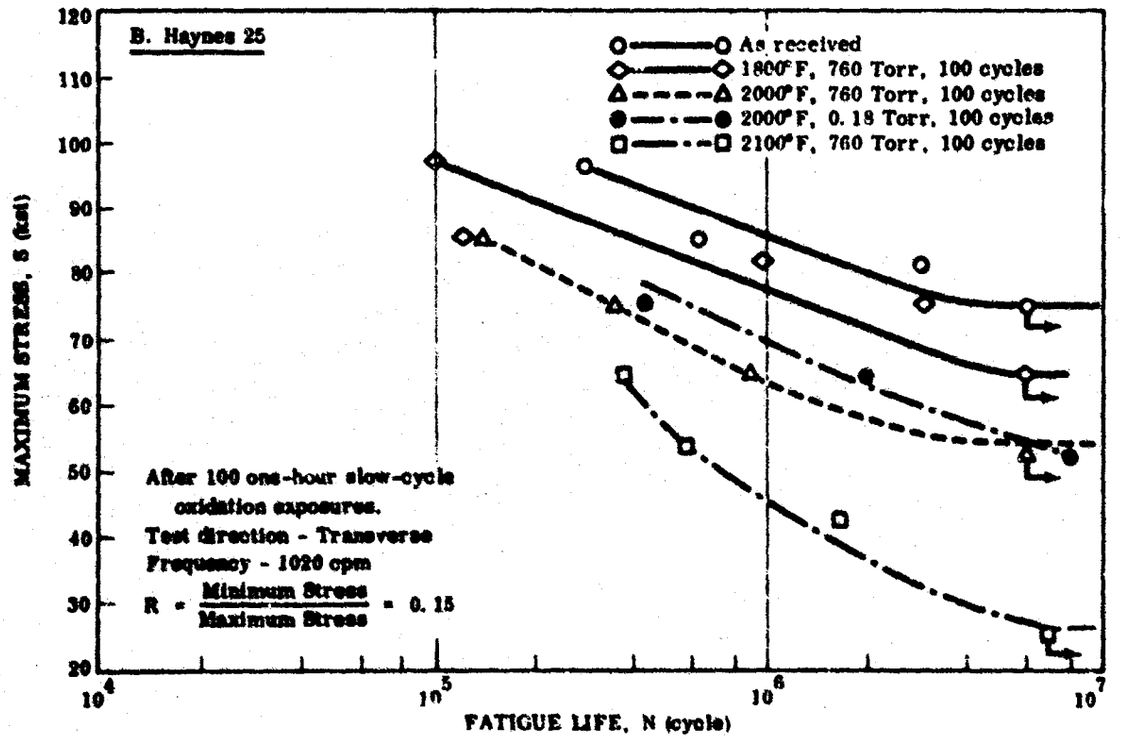

FIGURE 22. ROOM TEMPERATURE FATIGUE CURVES (S-N); Inconel 625 and Haynes 25 Foils

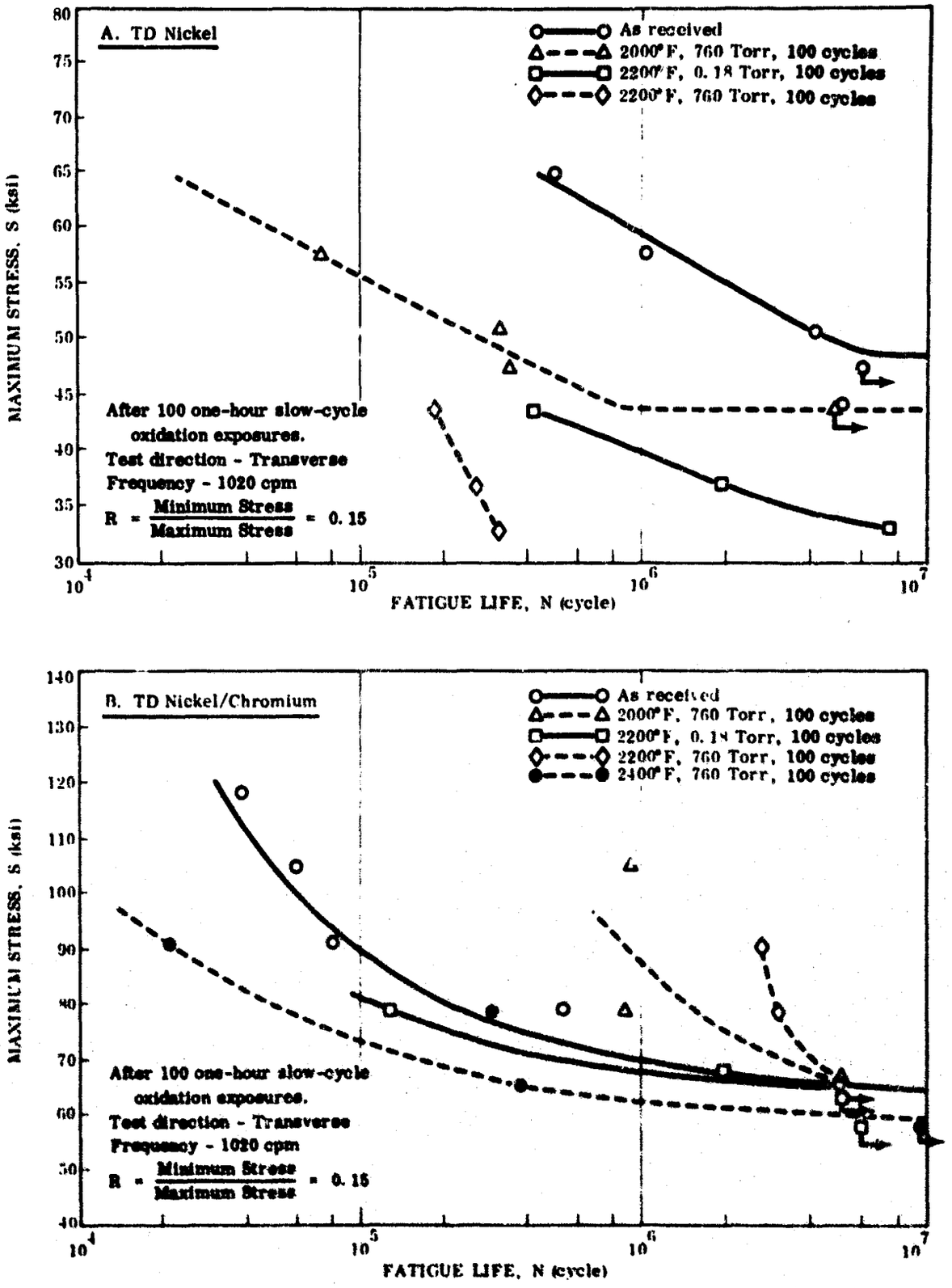

FIGURE 23. ROOM TEMPERATURE FATIGUE CURVES (S-N); TD Nickel and TD Nickel/Chromium Foils

TABLE XIV

RT FATIGUE LIMIT FOR SUPERALLOY FOILS (0.01 in.) IN AS-RECEIVED AND OXIDIZED CONDITIONS

Superalloy	Condition			Room Temperature Fatigue Limit (5×10^6 cycles) (ksi)	Loss in Room Temperature Fatigue Limit due to Oxidation Exposure (%)
	R	Oxidized for 100 one-hour cycles			
		Temperature (°F)	Pressure (Torr)		
Rene' 41	R	-	-	92.0	-
		1800	760	76.0	17.4
		2000	760	51.0	38.0
Inconel 718	R	-	-	85.0	-
		1800	760	75.0	11.9
		2000	760	37.0	50.0
Inconel 625	R	-	-	82.0	-
		1800	760	55.0	32.9
		1800	0.18	68.0	17.0
		2000	760	41.0	50.0
Haynes 25	R	-	-	75.0	-
		1800	760	66.0	12.0
		2000	760	55.0	27.0
		2000	0.18	56.5	24.8
		2100	760	35.0	60.0
TD Nickel	R	-	-	48.0	-
		2000	760	43.2	10.0
		2200	760	32.0	33.3
		2200	0.18	34.0	29.2
TD Nickel/ chromium	R	-	-	65.0	-
		2000	760	65.0	None
		2200	760	65.0	None
		2200	0.18	65.0	None
		2400	760	60.0	7.7

Test Direction

Transverse - Rene' 41 Inconel 718, Inconel 625, Haynes 25, TD Nickel
Longitudinal - TD Nickel chromiun.

R - As received

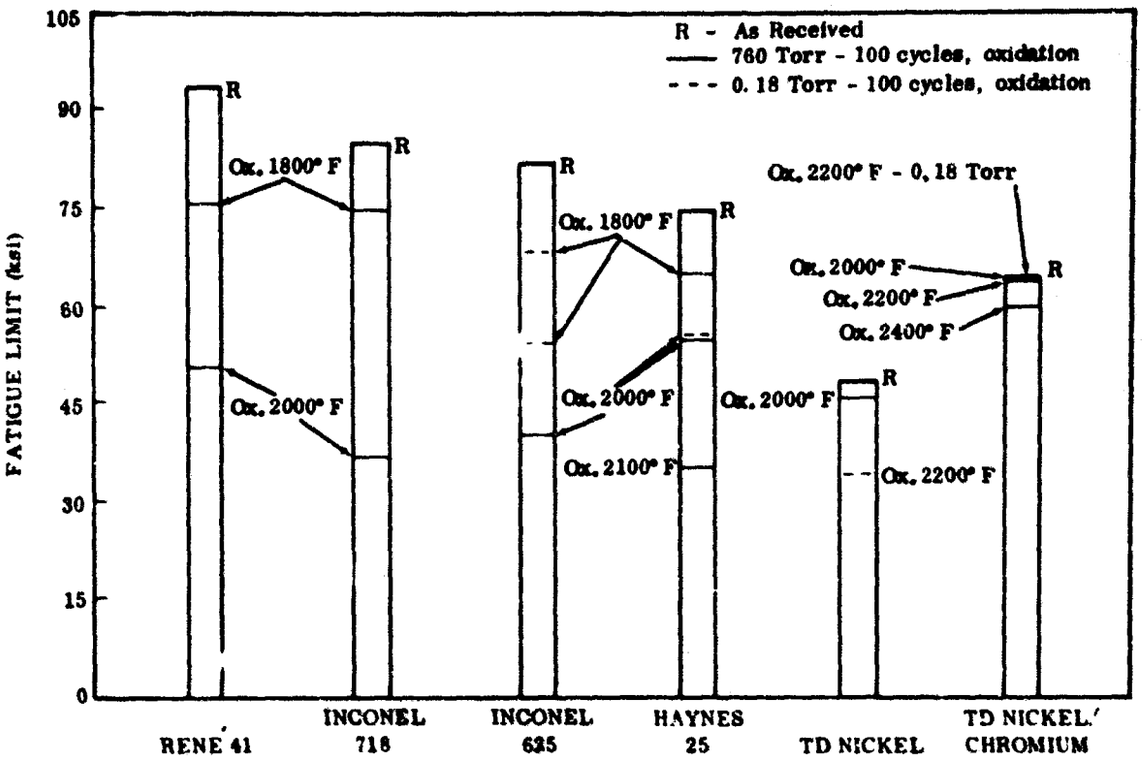

FIGURE 24. ROOM TEMPERATURE FATIGUE LIMIT FOR SUPERALLOY FOILS

Dispersion Strengthened Alloys (TD Nickel and TD Nickel/Chromium)

For TD Nickel, there was an overall decrease in fatigue life because of different oxidation exposures (Fig. 23). For TD Nickel, the loss in room temperature fatigue limit was greater at higher oxidation temperatures (>33.3 percent loss due to exposure at 2200°F and 760 Torr and only 10 percent loss after exposure at 2000°F and 760 Torr) as well as at higher pressures (>33.3 percent loss due to exposure at 2200°F and 760 Torr and 29.2 percent loss after exposure at 2200°F and 0.18 Torr - Table XIV and Fig. 24).

For TD Nickel/chromium, there was only a maximum of 7.7 percent loss in room temperature fatigue limit because of a 100-cycle oxidation exposure at 2400°F and 760 Torr (Table XIV). The other oxidation exposures caused no decrease in fatigue limit for TD Nickel/chromium. As a matter of fact, the fatigue life was improved after a 100-cycle oxidation at T_{max} of 2000 or 2200°F and 760 Torr as indicated by the S-N curves in Figure 23.

Based on overall performance in room temperature fatigue tests, the TD Nickel/chromium alloy was best, followed by Haynes 25, TD Nickel, and Inconel 625. The Inconel 625 alloy had the least residual fatigue limit, and underwent maximum degradation in fatigue strength because of the different oxidation exposures among the four selected alloys (Inconel 625, Haynes 25, TD Nickel, and TD Nickel/chromium).

4.3.5 High Temperature Fatigue Test Results

The tension-tension fatigue test results of the four selected superalloy foils in the as-received and oxidized conditions at the ductility minimum temperature are given in Table XV (Inconel 625 and Haynes 25) and Table XVI (TD Nickel and TD Nickel/chromium). Fatigue tests at T_{dm} for the four selected superalloy foils after 100 one-hour slow-cycle exposures at the respective T_{max} and at 760 and 0.18 Torr were conducted. The S-N curves (maximum stress, S, vs fatigue life, N, cycles) are presented for the two solid solution strengthened alloys in Figure 25A and B) and for the two dispersion strengthened alloys in Figure 25C and D. From these S-N fatigue curves, the fatigue limits (0.5 million cycles) of the alloys were determined and are tabulated together with the F_{tu} at the T_{dm}.

Super Alloy and T_{dm} (same as Test Temperature)	Exposure Condition	Fatigue Limit at T_{dm} (for 0.5×10^6 cycles) (ksi)	F_{tu} at T_{dm} (ksi)
Inconel 625	As Received	72	90.1
1300°F	Ox. 1800°F - 760 Torr	68	92.4
	Ox. 1800°F - 0.18 Torr	68	91.0
Haynes 25	As Received	47	76.2
1400°F	Ox. 1800°F - 760 Torr	55	71.7
	Ox. 2000°F - 760 Torr	47	71.6
	Ox. 2000°F - 0.18 Torr	37	60.3
TD Nickel	As Received	14.6	22.9
1600°F	Ox. 2000°F - 760 Torr	17.9	20.9
	Ox. 2200°F - 760 Torr	14.3	19.0
	Ox. 2200°F - 0.18 Torr	13.3	18.6
TD Nickel/ chromium	As Received	29.0	31.3
1600°F	Ox. 2000°F - 760 Torr	28.5	27.4
	Ox. 2200°F - 760 Torr	27.0	24.5
	Ox. 2200°F - 0.18 Torr	27.0	25.6
	Ox. 2400°F - 760 Torr	26.9	23.7

TABLE XV

ELEVATED TEMPERATURE AXIAL FATIGUE OF INCONEL 625 AND HAYNES 25 FOILS

Superalloy and T_{dm} (same as Test Temperature) (°F)	Maximum Stress, S (ksi)	As Received		Oxidized 1800°F - 760 Torr-100 Cycles		Oxidized 1800°F - 0.18 Torr-100 Cycles		Oxidized 2000°F - 0.18 Torr-100 Cycles	
		N, 10^4 (cycle)	Elongation (%)	N, 10^4 (cycle)	Elongation (%)	N, 10^4 (cycle)	Elongation (%)	N, 10^4 (cycle)	Elongation (%)
Inconel 625	80	4.3	19	2.8	20.0	-	-	-	-
	75	17.5	14	-	-	7.0	18.5	-	-
1300	72	>51.0	13	-	-	-	-	-	-
	70	>51.0	11	43.0	14.0	47.8	14.0	-	-
	68	-	-	>51.0	12.0	>51.0	13.5	-	-
	65	-	-	>51.0	10.0	-	-	-	-
Fatigue Limit(1)		72 ksi		68 ksi		68 ksi			
						Oxidized 2000°F - 760 Torr-100 Cycles			
Haynes 25	74	0.91	17.5	-	-	-	-	-	-
(L-605)	72	1.31	15.0	-	-	-	-	-	-
	70	2.92	16.0	1.52	17.5	-	-	-	-
1400	65	8.5	14.0	6.36	17.5	-	-	-	-
	60	14.9	10.0	17.05	17.0	4.0	15.0	-	-
	57	-	-	20.92	15.0	-	-	-	-
	55	16.0	10.0	51.0	13.0	10.6	13.0	-	-
	50	34.5	8.0	-	-	44.34	10.0	6.82	12.5
	47	51.0	6.5	-	-	>51.0	9.0	-	-
	45	>51.0	6.0	-	-	>51.0	5.5	31.04	9.0
	40	-	-	-	-	-	-	39.85	7.5
	37	-	-	-	-	-	-	>51.0	3.0
	35	-	-	-	-	-	-	>51.0	3.0
Fatigue Limit(1)		47 ksi		55 ksi		47 ksi		37 ksi	

1. Fatigue limit considered to be 50 x 10^4 cycles.

TABLE XVI

AXIAL FATIGUE OF TD NICKEL AND TD NICKEL/CHROMIUM FOILS AT 1600°F

Superalloy and Test Temperature (°F)	Maximum Stress, S (ksi)	As Received		Oxidized 2000°F - 760 Torr-100 Cycles		Oxidized 2200°F - 760 Torr-100 Cycles		Oxidized 2200°F - 0.16 Torr-100 Cycles		Oxidized 2400°F - 760 Torr-100 Cycles	
		N, 10^4 (cycle)	Elongation (%)	N, 10^4 (cycle)	Elongation (%)	N, 10^4 (cycle)	Elongation (%)	N, 10^4 (cycle)	Elongation (%)	N, 10^4 (cycle)	Elongation (%)
TD Nickel	19.0	-	-	3.0	0.5	-	-	-	-		
	18.0	-	-	49.8	0.4	-	-	-	-		
1600	17.1	9.7	-	>52.0	0.2	15.3	0.4	-	-		
	16.2	-	-	-	-	-	-	4.8	0.4		
	15.2	34.9	1.0	>52.0	0.2	20.6	0.4	9.0	0.4		
	14.3	>52.0	0.8	-	-	>52.0	0.1	11.0	0.2		
	13.3	>53.7	0.9	>52.0	0.2	>52.0	0.1	>51.0	0.1		
	12.0	-	-	-	-	-	-	>51.0	0.1		
Fatigue Limit[1]		14.6 ksi		17.9 ksi		14.3 ksi		13.3 ksi			
TD Nickel/ chromium 1600	31.0	2.1	2.0	-	-	-	-	-	-	-	-
	30.0	12.9	1.8	12.0	1.8	-	-	-	-	-	-
	29.5	9.9	1.5	-	-	-	-	-	-	-	-
	29.0	>51.0	1.7	34.3	1.6	23.2	2.0	12.6	2.0	2.5	2.0
	28.0	-	-	>51.0	1.4	38.0	1.6	26.1	2.0	14.5	1.5
	27.0	>51.0	0.6	>51.0	1.4	>51.0	1.8	>51.0	0.5	45.5	1.0
	26.0	-	-	-	-	>51.0	0.9	>51.0	0.5	>51.0	0.7
	25.0	-	-	-	-	>51.0	0.2	-	-	-	-
Fatigue Limit[1]		29.0 ksi		28.5 ksi		27.0 ksi		27.0 ksi		26.9 ksi	

1. Fatigue limit considered to be 50 x 10^4 cycles.

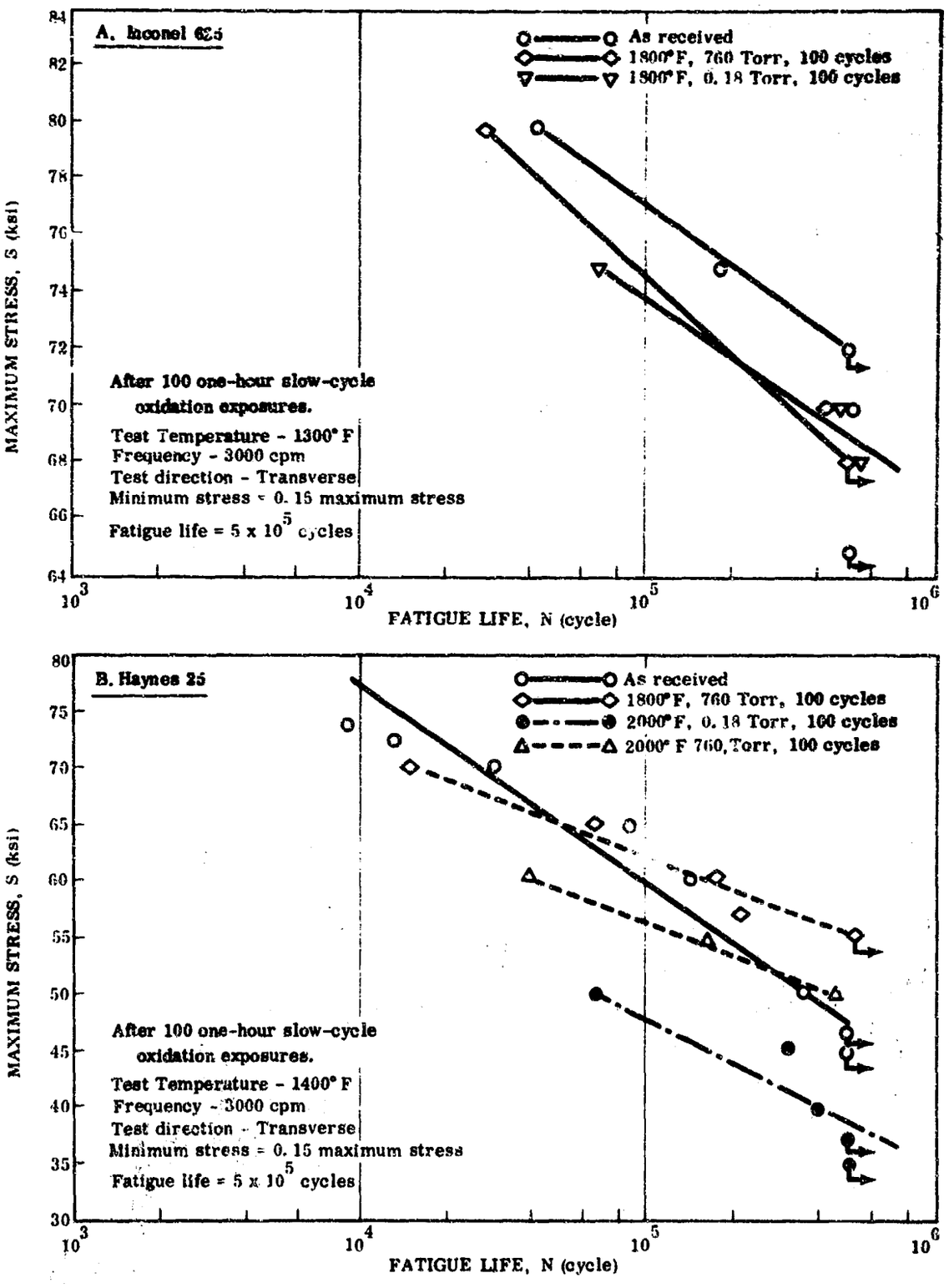

FIGURE 25. ELEVATED TEMPERATURE TENSION-TENSION FATIGUE OF 0.01-INCH INCONEL 625, HAYNES 25, TD NICKEL, AND TD NICKEL/CHROMIUM FOILS (Sheet 1 of 2)

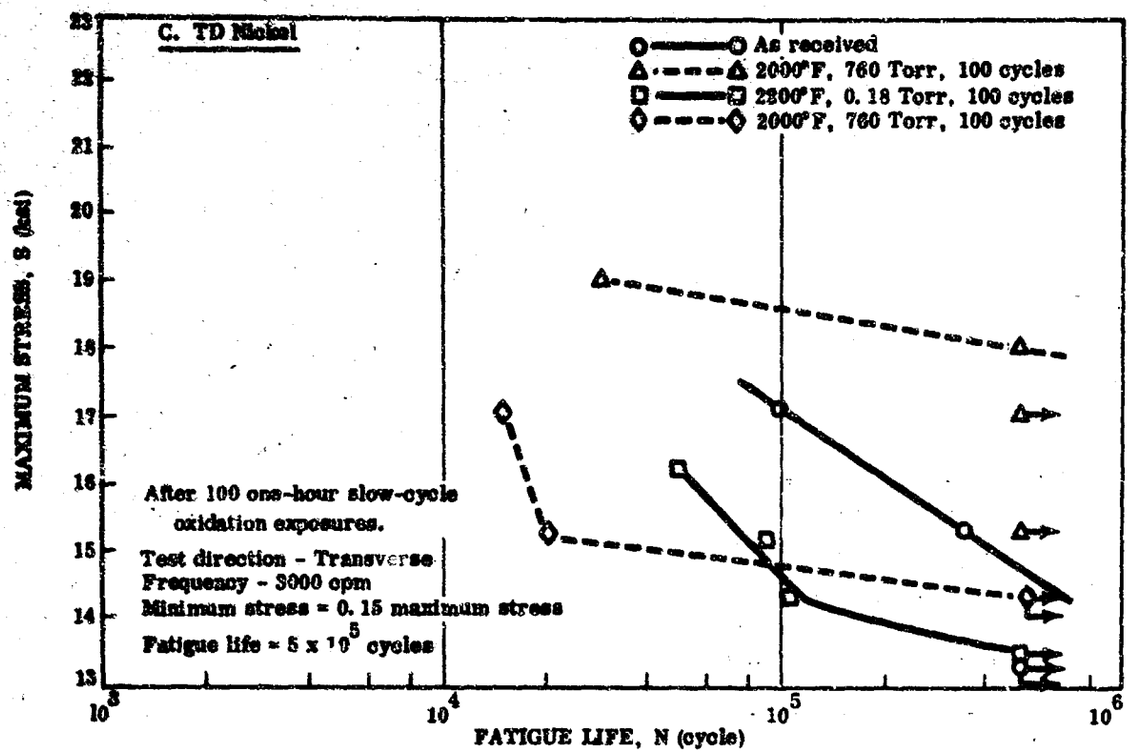

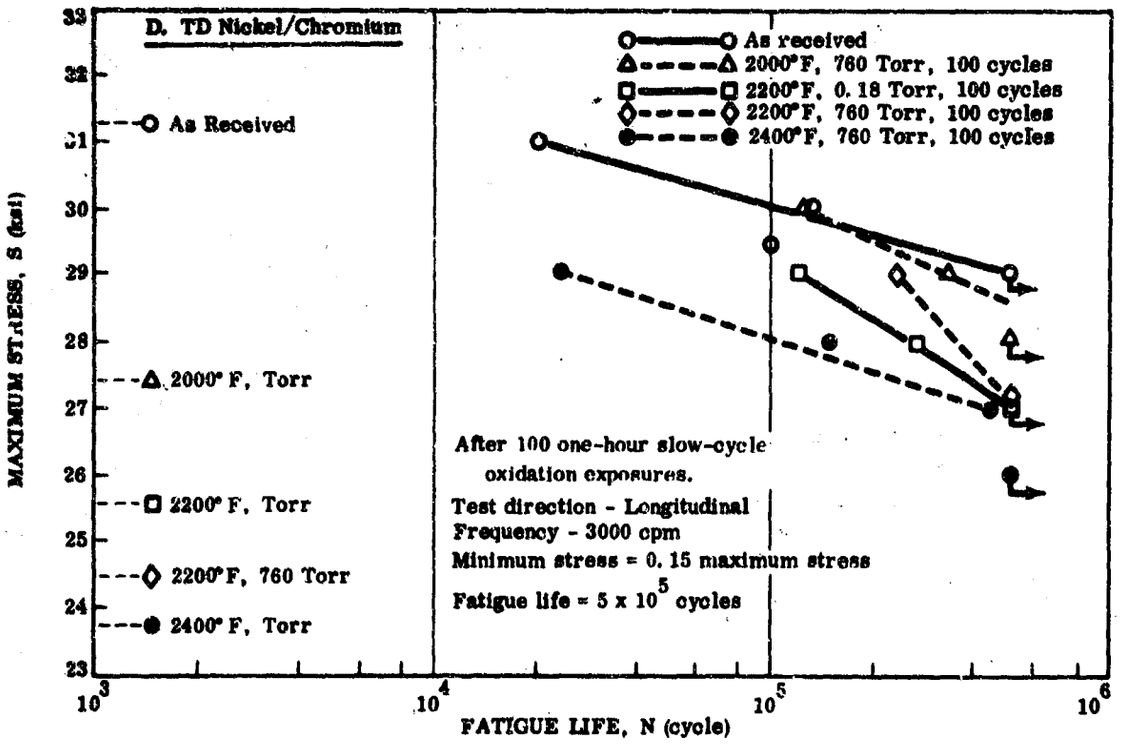

FIGURE 25. ELEVATED TEMPERATURE TENSION-TENSION FATIGUE OF 0.01-INCH INCONEL 625, HAYNES 25, TD NICKEL, AND TD NICKEL/CHROMIUM FOILS (Sheet 2 of 2)

The fatigue limit of the Inconel 625 and Haynes 25 alloys cannot be directly compared because the test temperatures were different. But for the two dispersion strengthened alloys, the fatigue testing was conducted at the same temperature, i. e., 1600°F. The fatigue limit for TD Nickel/chromium was found to be twice as high as that of TD Nickel. The chromium in TD Nickel appears to increase the fatigue limit by about 100 percent.

In the as-received or oxidized conditions, the fatigue limit at T_{dm}, as expected, was lower than F_{tu} at T_{dm} for Inconel 625, Haynes 25, and TD Nickel. But in the case of TD Nickel/chromium, in the oxidized conditions, the fatigue limit at T_{dm} was higher than the respective F_{tu} at T_{dm}. Even in the as-received condition, there was significant cycle life at a stress of 31. 0 ksi, which is very close to the F_{tu} value of 31. 3 ksi (Fig. 25D). This rather unusual characteristic of TD Nickel/chromium, though difficult to account for, could be the result of its strain rate sensitivity. The strain rate used in MTS fatigue tests for a frequency of 3000 cpm was much higher than the strain rate (0. 05 in. /in. /min) used in tensile tests. The higher strain rate could result in higher F_{tu} values than those obtained at a low strain rate of 0. 05 in. /in. /min (although no effects of high strain rate on room temperature tensile data were observed).

There was no significant loss in high temperature fatigue limits (for 0.5×10^6 cycles) for the four superalloy foils due to various oxidation exposures. Considerably higher losses in room temperature fatigue limits (for 5×10^6 cycles) for the superalloys occurred (except TD Nickel/chromium) after different oxidation exposures (Table XIV). Therefore, TD Nickel/chromium is the only alloy of the four superalloys tested which exhibited no loss in room temperature fatigue limit and exhibited less than seven percent loss in high temperature fatigue limit because of oxidation.

The highest loss in elevated temperature fatigue limit was about 20 percent for Haynes 25 after a 100-cycle oxidation exposure at 2000°F and 0. 18 Torr. In the case of Haynes 25, there was no loss in fatigue limit after 100 one-hour slow-cycle atmospheric pressure oxidation exposures at T_{max} of 1800 or 2000°F. Thus for Haynes 25, 0. 18 Torr was found to be a more severe oxidation pressure than 760 Torr. This finding was indicated not only by elevated temperature fatigue data, but also by tensile test data (F_{tu}, F_{ty}) at room temperature and elevated temperatures, notch tensile test data (F_{nty} or F_{ntu}) at room temperature and at 1400°F, and room temperature high-rate F_{tu} value. In the case of room temperature fatigue testing, the loss in fatigue limit after 760 Torr oxidation exposure (27 percent) was slightly higher than that after 0. 18 Torr oxidation exposure (24. 8 percent) at 2000°F for 100 one-hour slow-cycle oxidation exposures (Table XIV).

In the case of TD Nickel, the fatigue limit was higher (though the F_{tu} at 1600°F was lower) in the 2000°F and 760 Torr 100-cycle oxidized condition than in the as-received condition (Figure 25C). Because of oxidation exposures at 2200°F, the fatigue limit decreased, the maximum loss in fatigue limit being about nine percent.

4.4 ANALYTICAL RESULTS

The results of various diagnostic techniques are described in this section. The diagnostic techniques employed were optical microscopy, gas analyses, microhardness determination, X-ray diffraction analyses, and electron microprobe analyses. These analytical techniques were used to evaluate the effects of oxidation exposures on the superalloy foils.

4.4.1 Optical Microscopy

The results of the microscopic examination of the six superalloy foils in the as-received condition and after various oxidation exposures are discussed in the following paragraphs.

Precipitation Hardened Alloys (Rene' 41 and Inconel 718)

The cold rolled foils of Rene' 41 and Inconel 718 alloys were annealed in a protective atmosphere at 1975 and 1800°F, respectively. The microstructure of as-received Rene' 41 and Inconel 718 were similar, the ASTM grain size being 6 and 7, respectively (Fig. 26A and 27A). Carbide stringers were present in both alloys. Rene' 41 exhibited a finer grain structure along the edges than in the middle; Inconel 718 showed uniform grain size all along the specimen. Atmospheric pressure air exposure produced surface scale[1], oxidation attack along grain boundaries, and decarburization (the extent of decarburization being higher at 2000°F than at 1800°F). Grain growth was minor for Rene' 41 due to exposure at temperatures up to 2000°F because of carbide precipitation at grain boundaries (Ref. 7), but extensive grain growth and twinning was observed for Inconel 718 after exposure at 2000°F (Fig. 27C). Alloy depletion (probably carbon, titanium, chromium, and aluminum) removed the rapid etching grain boundaries after the oxidation exposure, particularly for Rene' 41 after the 2000°F exposure (Fig. 26C). Along the edges, extensive intergranular oxidation attack was observed for Rene' 41, especially due to a 2000°F MGR profile exposure. Intergranular oxidation attack for Inconel 718 due to a 2000°F MGR profile exposure was less severe than that for Rene' 41 in the 1800°F profile exposure (Fig. 26B and 27C). For

---

1. For Rene' 41, the surface oxide has been reported to consist of Al_2O_3, Cr_2O_3, $NiCr_2O_4$, and TiO_2 (after oxidation at 1800°F) with traces of NiO after oxidation at 2000°F (Ref. 6).

A. As Received Magnification: 500X

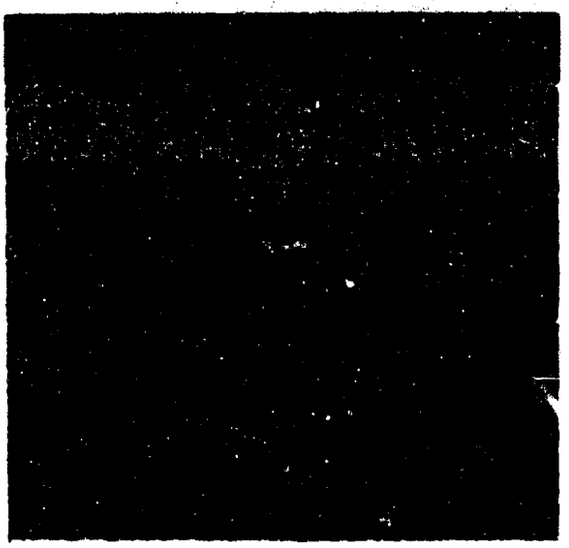

B. Oxidized 1800°F
760 Torr
100 Cycles
Magnification: 500X

C. Oxidized 2000°F
760 Torr
100 Cycles
Magnification: 200X

D. Oxidized 2000°F
760 Torr
100 Cycles
Magnification: 500X

FIGURE 26. MICROSTRUCTURE OF RENE' 41 FOIL IN AS-RECEIVED AND OXIDIZED CONDITIONS

A. As Received Magnification: 500X

B. Oxidized 1800°F
760 Torr
100 Cycles
Magnification: 500X

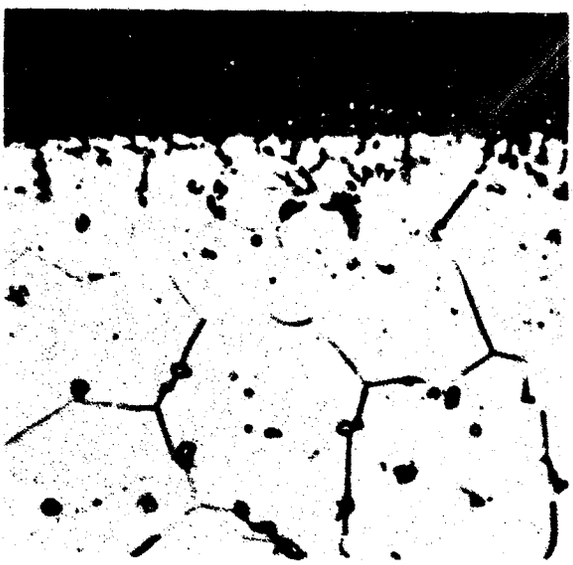

C. Oxidized 1800°F
760 Torr
100 Cycles
Magnification: 500X

FIGURE 27. MICROSTRUCTURE OF INCONEL 718 FOIL IN AS-RECEIVED AND OXIDIZED CONDITIONS

Rene' 41 the remnants of the μ phase particles inside the grains were present after the 1800°F exposure and not after the 2000°F exposure (Fig. 26B and C). The oxidation effects were less pronounced after the 1800°F profile exposure than after the 2000°F profile exposure, and also less severe for Inconel 718 than for Rene' 41.

The effects of aging treatments on the concentration of the minor phases in Rene' 41, and a few other selected alloys (IN-100, B1900, U700, and Unitemp AF2-1D), are discussed in Reference 8. Four minor phases were found in Rene' 41 - μ, MC, M_6C, and $M_{23}C_6$. The μ phase is trigonal and was designated $(Fe, Co)_7(Mo, W)_6$ by P. A. Beck, et al (Ref. 9). The amount of the μ phase increases rapidly with temperature until it reaches a maximum at about 1700°F. The μ phase is the dominant phase from about 1500 to about 1800°F, and becomes completely unstable between 1800 and 1900°F (Ref. 7). This is in agreement with the above metallographic findings; namely the remnants of the μ phase (equiaxed dark etching phase) were present inside the grains only after the 1800°F profile exposure and not after the 2000°F profile exposure (Fig. 26B and 26C). Rene'41 is unstable because it forms the μ phase (Ref. 10).

The solubility limit of γ'-$Ni_3(Al, Ti)$ in Rene' 41 was reported to be between 1900 and 1950°F while that of the M_6C phase was around 2150°F (Ref. 11). The MC phase was the dominant carbide phase at the lower temperature range from 1400 to about 1500°F. The amount of MC remained relatively stable up to about 1600°F and then decreased with temperature until it reached a minimum at about 1800°F (Ref. 10). The amount of M_6C remained relatively stable up to about 1700°F. It then increased with temperature until it reached a maximum between 1900 and 2000°F. The M_6C phase was the dominant carbide phase from about 1800 to about 2100°F and became completely unstable between 2100 and 2200°F. The amount of $M_{23}C_6$ increased with temperature until it reached a maximum at 1600°F. It became completely unstable between 1800 and 1900°F (Ref. 12). Based on the foregoing information and comparison of Figures 26B and C and those in Reference 10, the white precipitates along the grain boundaries of Rene' 41 after 760 Torr exposures were most likely carbides of the M_6C type.

The effects of static atmospheric pressure oxidation exposures for various times up to 100 hours at different temperatures (1650, 1825, 2190, and 2370°F) on Inconel 718 (0.4 to 0.6 cm thick) are discussed in Reference 13. These oxidation exposures resulted in a surface scale formation, intergranular oxidation, and internal oxidation. The surface scale was identified to consist of Cr_2O_3 and the cubic spinel $(Fe, Ni)Cr_2O_4$. Oxidation at 1650°F resulted in the formation of thin needle-like precipitates $Ni_3(Ti, Cb)$ in the matrix. Above 1825°F, the $Ni_3(Ti, Cb)$ precipitates dissolved in the lattice while both the number and size of the inclusions (titanium cyanonitride) increased (Ref. 13). As such, the second-phase particles (Fig. 27B and C) of oxidized Inconel 718 are most likely inclusions of the same type (titanium cyanonitride).

On the basis of metallographic findings, it can be stated that Rene' 41 and Inconel 718 became unstable at temperatures above 1800°F. These findings are in agreement with the mechanical property data of those two alloys (para 4.3).

Solid Solution Strengthened Alloys (Inconel 625 and Haynes 25)

Inconel 625. The Inconel 625 foil was cold rolled from 0.056-inch stock, annealed at 2050°F for one minute in a protective atmosphere, and rapidly air cooled. The resultant microstructure (Fig. 28A and B) indicated recrystallization with some twinning. The ASTM grain size was 6. Carbide particles were noticeably drawn in the longitudinal rolling direction, appearing as small spheroids in the transverse direction. The edges appeared to have retained the rolled microstructure. Because of the atmospheric oxidation exposures to temperature profiles with T_{max} of 1800 and 2000°F, there was slight grain growth, decarburization, oxidation attack along grain boundaries, and the formation of an alloy depletion layer (Fig. 28C, D, E, and F). The decarburization was more after the 2000°F exposure than after the 1800°F exposure. But, in both cases, the carbides were present along the grain boundaries. The microstructures exhibited twinning after the oxidation exposure. The effects of low pressure (0.18 Torr) oxidation exposure at 1800°F on Inconel 625 were similar to those described above, except that the decarburization appeared to be less after the 0.18 Torr exposure (Fig. 28G and H). There could be carbon pickup from the oil vapors of the vacuum pump. The thickness of the alloy depletion layer of Inconel 625 after various oxidation exposures is given in the following tabulation.

100-Cycle Oxidation Exposures	Thickness of Alloy Depletion Layer in Inconel 625 (mil)
1800°F - 760 Torr	0.45
1800°F - 0.18 Torr	0.15
2000°F - 760 Torr	0.85

Thus with increasing oxidation temperature or with increasing environmental pressure, the thickness of the alloy depletion layer was found to increase.

Haynes 25. The Haynes 25 alloy was annealed at 2250°F in a protective atmosphere. The resultant microstructure (Fig. 29A, B, C, and D) indicated complete recrystallization with twinning. Although not as predominant as in the Inconel 625 microstructure, carbide stringers were evident in the longitudinal direction (Fig. 29C and E) and appeared as spheroids in the transverse direction (Fig. 29A and B). There could be a few inclusions in addition to carbides. The ASTM grain size was five and the grains were coarser than those in the as-received Inconel 625. The edges of Haynes 25 had a structure similar to the substrate and were not characterized by a rolled microstructure as in Inconel 625.

Magnification: 200X

A. As Received
Test Direction - Transverse

Magnification: 200X

B. As Received
Test Direction - Longitudinal

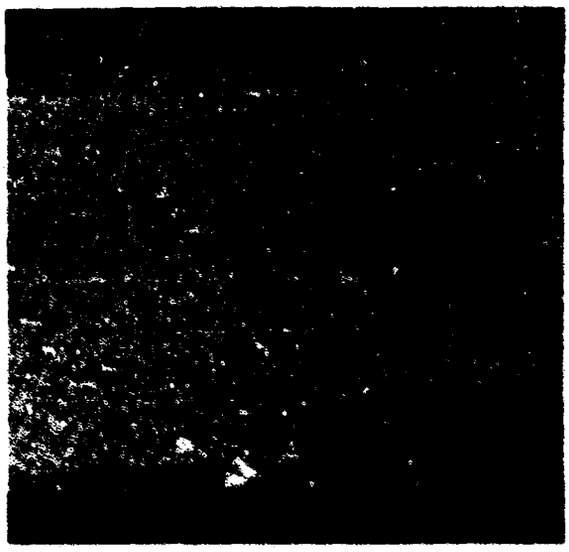

C. Oxidized 1800°F
760 Torr

Magnification: 200X

D. Oxidized 1800°F
760 Torr

Magnification: 500X

FIGURE 28. MICROSTRUCTURE OF INCONEL 625 FOIL IN AS-RECEIVED CONDITION AND AFTER 100-CYCLE OXIDATION EXPOSURE
(Sheet 1 of 2)

E. Oxidized 2000°F 760 Torr Magnification: 200X

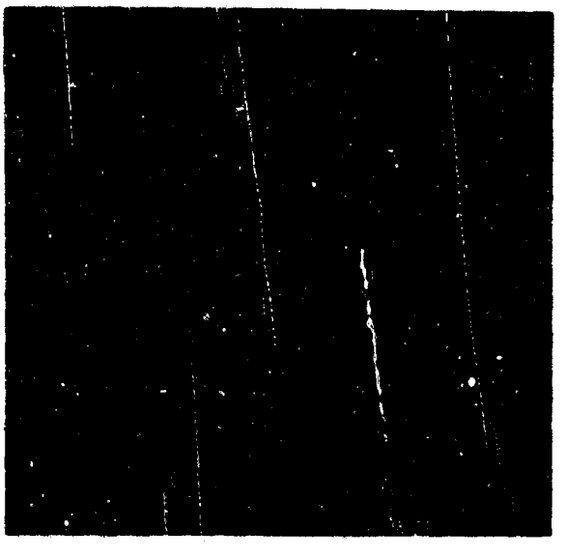

F. Oxidized 2000°F 760 Torr Magnification: 500X

G. Oxidized 1800°F 0.18 Torr Magnification: 200X

H. Oxidized 1800°F 0.18 Torr Magnification: 500X

FIGURE 28. MICROSTRUCTURE OF INCONEL 625 FOIL IN AS-RECEIVED CONDITION AND AFTER 100-CYCLE OXIDATION EXPOSURE (Sheet 2 of 2)

Magnification: 200X

A. As Received
Test Direction - Transverse

Magnification: 500X

B. As Received
Test Direction - Transverse

Magnification: 200X

C. As Received
Test Direction - Longitudinal

Magnification: 500X

D. As Received
Test Direction - Longitudinal

FIGURE 29. MICROSTRUCTURE OF HAYNES 25 FOIL IN AS-RECEIVED CONDITION AND AFTER 100 ONE-HOUR SLOW-CYCLE OXIDATION EXPOSURES (Sheet 1 of 3)

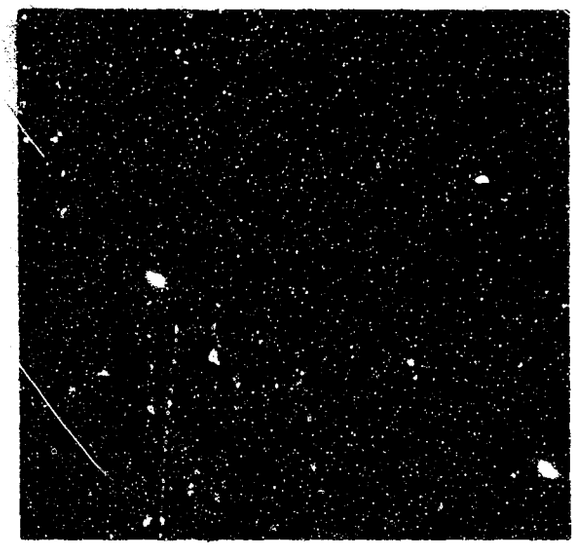

E. Oxidized 1800°F 760 Torr — Magnification: 200X

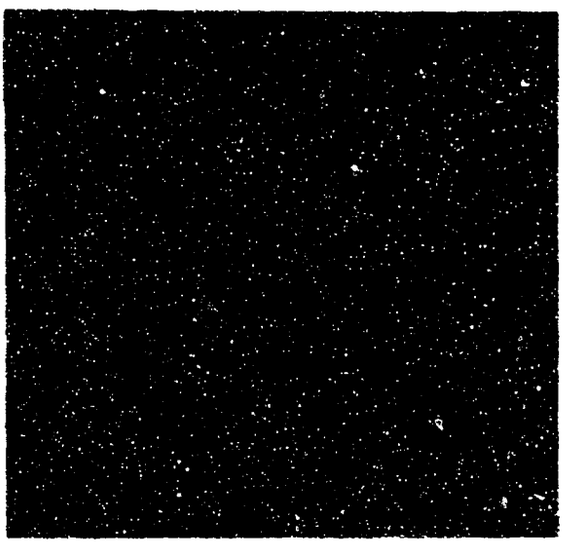

F. Oxidized 1800°F 760 Torr — Magnification: 500X

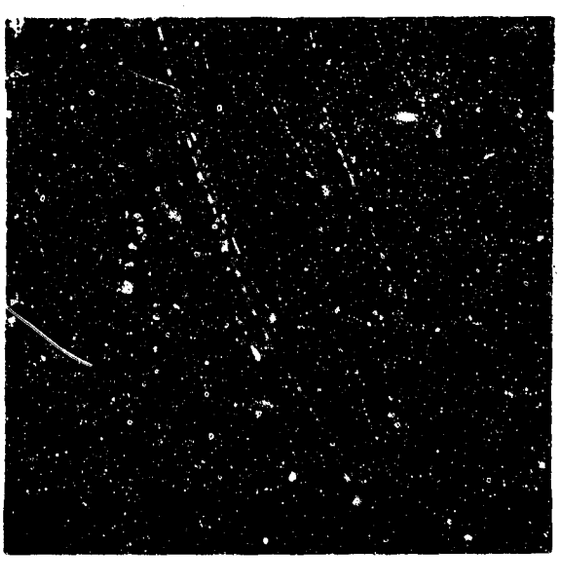

G. Oxidized 2000°F 760 Torr — Magnification: 200X

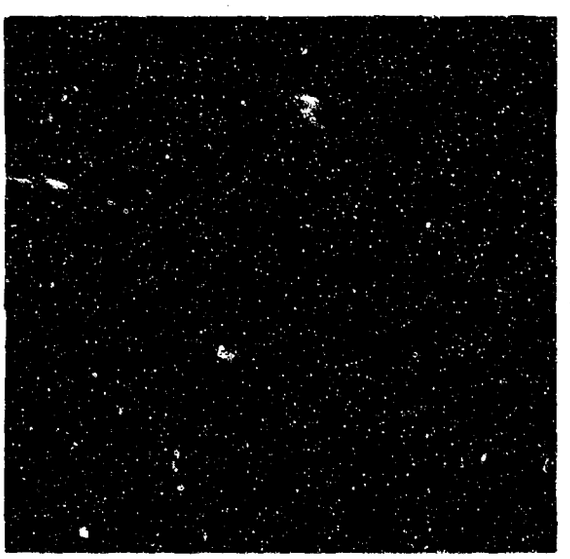

H. Oxidized 2000°F 760 Torr — Magnification: 500X

FIGURE 29. MICROSTRUCTURE OF HAYNES 25 FOIL IN AS-RECEIVED CONDITION AND AFTER 100 ONE-HOUR SLOW-CYCLE OXIDATION EXPOSURES (Sheet 2 of 3)

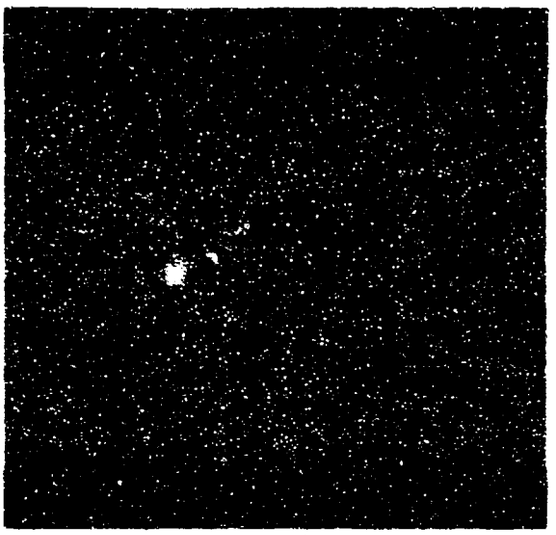

I. Oxidized 2100°F 760 Torr — Magnification: 200X

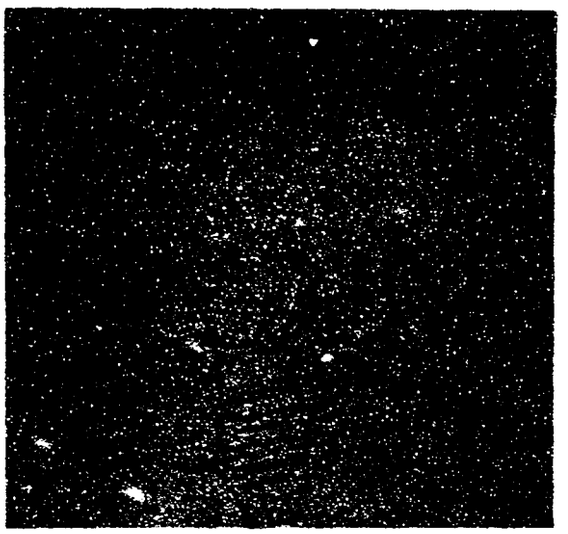

J. Oxidized 2100°F 760 Torr — Magnification: 500X

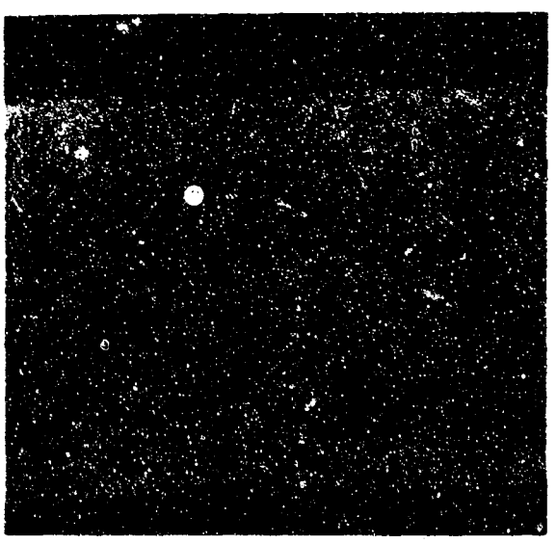

K. Oxidized 2000°F 0.18 Torr — Magnification: 200X

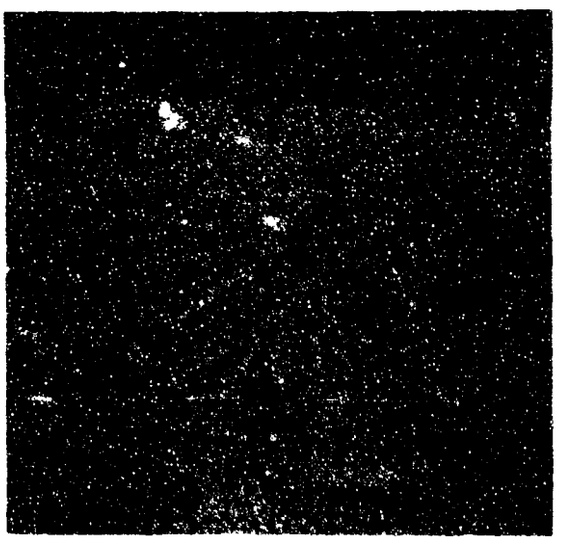

L. Oxidized 2000°F 0.18 Torr — Magnification: 500X

FIGURE 29. MICROSTRUCTURE OF HAYNES 25 FOIL IN AS-RECEIVED CONDITION AND AFTER 100 ONE-HOUR SLOW-CYCLE OXIDATION EXPOSURES (Sheet 3 of 3)

Because of atmospheric pressure oxidation exposures, there was decarburization (para 4.4.2), oxidation attack along grain boundaries, oxide formation at the edges, and the formation of an alloy depletion layer (Fig. 29E, F, G, H, I, and J). In addition, there was grain growth and the grain size increased with increasing oxidation temperature. There were intergranular cracks along the edges, the number and size of which increased with the exposure temperature. During oxidation exposures the carbide particles were found to precipitate, and at higher oxidation temperatures (2000 and 2100°F), the carbide particles agglomerate (Ref. 14). The carbide particle size was maximum after the 100-cycle exposure at 2100°F and 760 Torr. (Fig. 29I and J). The excessive grain growth and intensive grain boundary oxidation attack indicated that 2100°F was too high a service temperature for Haynes 25 (Fig. 29I and J).

The effects of low pressure (0.18 Torr) oxidation exposure at 2000°F appeared to be similar to those effects of atmospheric pressure oxidation exposure at 2000°F (Fig. 29G, H, K, and L). The recrystallization twins were present after the various oxidation exposures. No significant pressure effects could be observed from metallographic analyses.

The alloy depletion layer decreased in chromium and manganese content (para 4.4.5). The thicknesses of the alloy depletion layers after various oxidation exposures are contained in the following tabulation.

100-Cycle Oxidation Exposures	Thickness of Alloy Depletion Layer in Haynes 25 (mil)
1800°F - 760 Torr	0.6
2000°F - 760 Torr	1.0 to 1.2
2000°F - 0.18 Torr	1.0 to 1.2
2100°F - 760 Torr	0.5

During oxidation exposure, the oxides, either spinel (Ni, Mn) Cr_2O_4 at 760 Torr or $(Cr, Mn)_2O_3$ at 0.18 Torr (para 4.4.4) were formed. This formation resulted in depletion of chromium and manganese in layers immediately adjacent to the oxide/metal interface. From internal oxidation effects discussed in Paragraph 4.4.2, the compounds along the grain boundaries could be Cr_2O_3, Cr_2N, or carbides.

Thus, the effects of oxidation exposure on these two solid solution strengthened alloys were somewhat similar - oxidation attack along grain boundaries, oxide formation, formation of an alloy depletion layer, decarburization, and grain growth. Although no significant pressure effects could be observed, definite temperature effects were noted from the metallographic analyses.

Dispersion Strengthened Alloys (TD Nickel and TD Nickel/Chromium)

TD Nickel. The microstructures of TD Nickel in the as-received condition (both longitudinal and transverse) and after various oxidation exposures are shown in Figure 30A through J). The stress relief anneal at 2000°F in a protective atmosphere did not alter the coldworked microstructure of the TD Nickel alloy. The elongation of the grain structure in the extrusion direction was readily evident (Fig. 30A and B). The grains have been reported to be up to 0.001 inch (0.003 cm) long, with a length/width ratio of about 10:1 in the transverse direction (Ref. 15). Marked preferred orientation of grains was especially evident in the transverse direction (Fig. 30G and H).

After the various oxidation exposures, there was considerable surface oxidation (NiO) as well as internal oxide formation. This oxide was quite adherent to the substrate during cyclic oxidation at T_{max} of 2000°F. Spalling of the oxide began during 2200°F cyclic oxidation and was extensive during the 2400°F oxidation exposure. Formation of oxide in the substrate (internal oxidation) is evident in the microstructure of TD Nickel after atmospheric pressure oxidation exposures at 2200 or 2400°F (Fig. 30D, E, and F). Also after low pressure (0.18Torr) oxidation exposure at 2200°F, oxide particles in the substrate were evident (Fig. 30I and J). No appreciable difference in the oxidation characteristics of longitudinal and transverse TD Nickel specimens could be observed (Fig. 30I and J) which is in agreement with the literature (Ref. 15). Intergranular attack by oxidation, often observed in other superalloys, was not observed in TD Nickel. This lack of intergranular attack is a major enabling factor in load carrying ability and useful life at elevated temperatures.

The thicknesses of the unoxidized substrate and of the oxide formed are given below. The thickness values of the oxide are not accurate because of oxide lost by spalling during cyclic oxidation or during mounting for metallographic analyses.

100-Cycles Oxidation Exposure	Thickness (t) for TD Nickel (mil)	
	Oxide/Side	Substrate
As Received	-	10.0
2000°F - 760 Torr	1.0	9.8
2200°F - 760 Torr	2.5	7.5
2200°F - 0.18 Torr	1.2	8.5
2400°F - 760 Torr	5.0	3.7

Magnification: 200X

A. As Received
Test Direction - Longitudinal

Magnification: 500X

B. As Received
Test Direction - Longitudinal

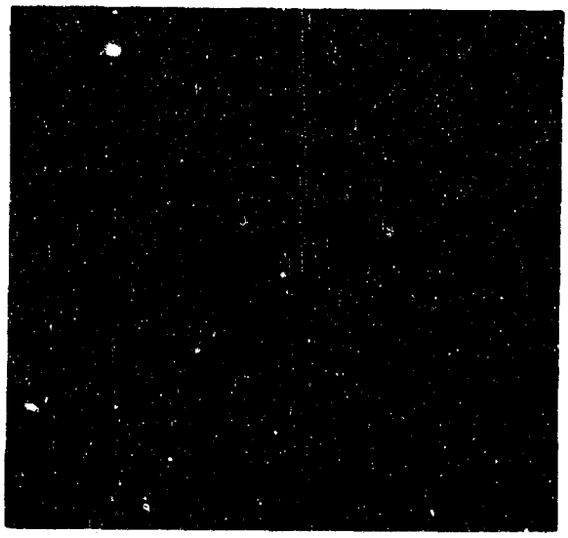

C. Oxidized 2000°F
760 Torr

Magnification: 200X

D. Oxidized 2200°F
760 Torr

Magnification: 200X

FIGURE 30. MICROSTRUCTURE OF LONGITUDINAL TD NICKEL SPECIMENS IN AS-RECEIVED CONDITION AND AFTER 100-CYCLE OXIDATION EXPOSURE (Sheet 1 of 3)

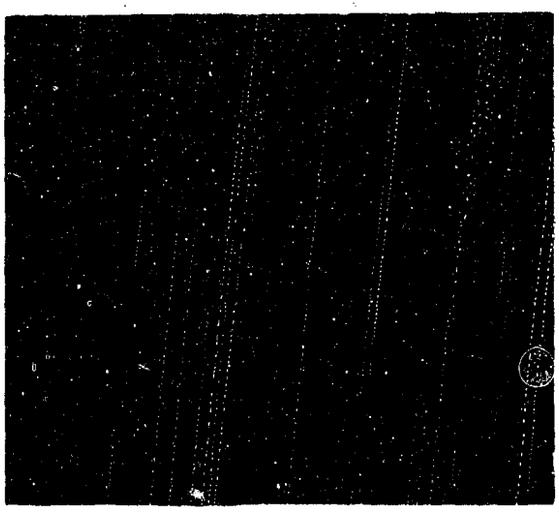

E. Oxidized 2400°F
760 Torr

Magnification: 200X

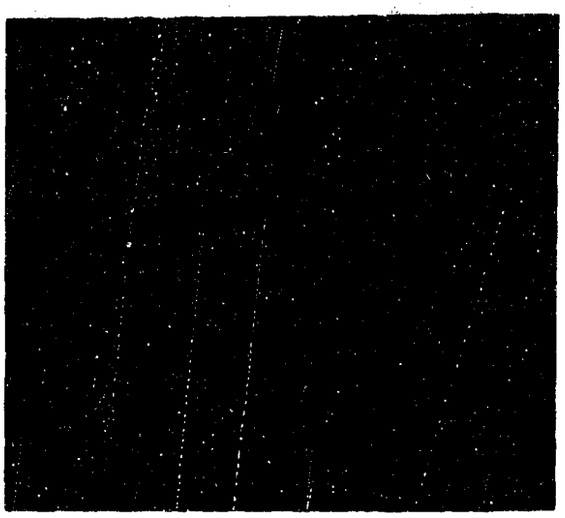

F. Oxidized 2400°F
760 Torr

Magnification: 500X

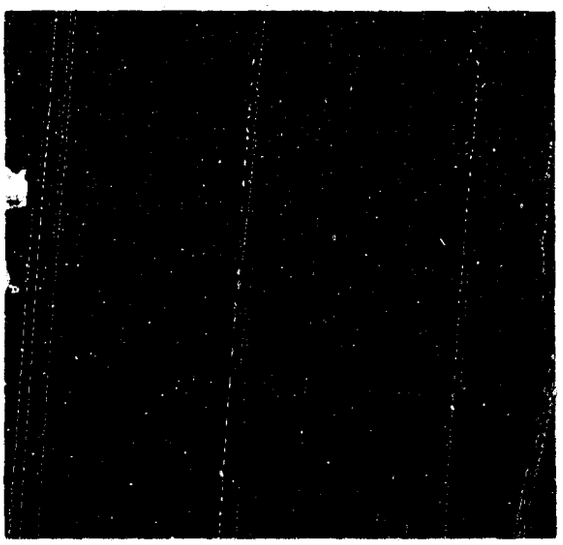

Magnification: 200X

G. As Received
Test Direction - Transverse

FIGURE 30. MICROSTRUCTURE OF LONGITUDINAL TD NICKEL SPECIMENS IN AS-RECEIVED CONDITION AND AFTER 100-CYCLE OXIDATION EXPOSURE (Sheet 2 of 3)

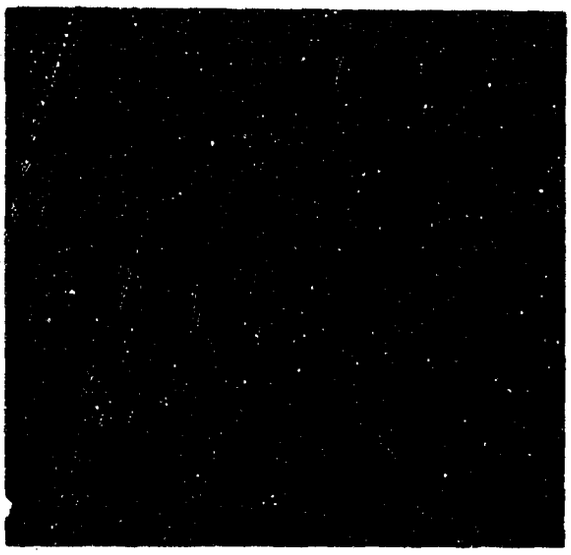

Magnification: 500X

H. As Received
Test Direction - Transverse

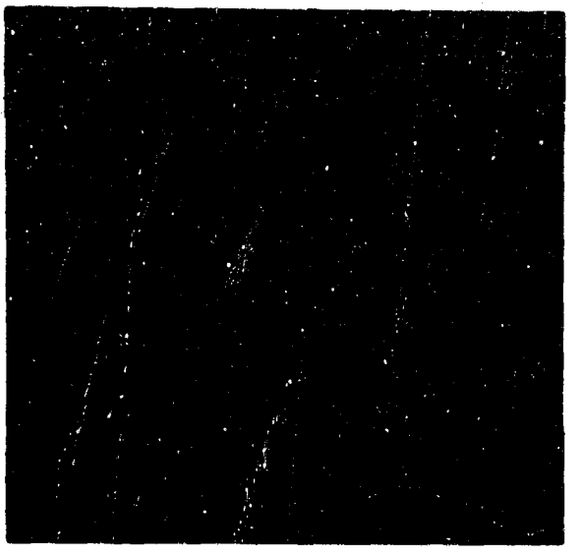

Magnification: 200X

I. Oxidized 2200°F
0.18 Torr
Test Direction - Transverse

Magnification: 200X

J. Oxidized 2200°F
0.18 Torr
Test Direction - Longitudinal

FIGURE 30. MICROSTRUCTURE OF LONGITUDINAL TD NICKEL SPECIMENS IN AS-RECEIVED CONDITION AND AFTER 100-CYCLE OXIDATION EXPOSURE (Sheet 3 of 3)

The severity of oxidation effects increased with increasing temperature as well as with increasing pressure. Also, the formation of an 0.005-inch thick oxide layer after a 100-cycle oxidation exposure at 2400°F and 760 Torr, leaving only 0.0037-inch thick unoxidized substrate (73 percent loss in cross section), showed that TD Nickel is not serviceable at 2400°F. The T_{max} for the TD Nickel alloy is 2200°F.

TD Nickel/Chromium. The microstructure of the TD Nickel/chromium alloy in transverse and longitudinal directions after being cold rolled and stress relief annealed at 2000°F is shown in Figure 31A, B, C, and D. Extremely large grains were present, the structure being quite different from that of the TD Nickel alloy. Grain diameters ranged from 0.010 mm to 0.020 mm (Ref. 16). The structure of the TD Nickel/chromium alloy showed different etch pits which could be due to cold work or they could be oxides (Cr_2O_3 or ThO_2). Unresolved microsized thoria particles were probably present. The microstructure after different oxidation exposures at atmospheric pressure is shown in Figure 31E, F, G, and H and at 0.18Torr in Figure 31I, J, K, and L. These figures show formation of internal oxide (Cr_2O_3) spots. That there was internal oxidation is confirmed from the microprobe data (para 4.4.5). The peaks in chromium trace and the minimum in nickel trace could be only the result of Cr_2O_3 formation. The formation of these internal oxide spots increased with increasing oxidation temperature (Fig. 31E, F, G, and H) and decreased with decreasing pressure (Fig. 31I, J, K, and L). Oxide layers were thin and uniform at 2000°F. Spalling was observed during oxidation exposures at 2200 or 2400°F in association with increased oxide growth and apparent internal oxidation. Spalling of the oxide is in agreement with the observations of other investigators (Ref. 15 and 17). Microstructural changes were minor over the temperature range of 2000 to 2400°F. No intergranular oxidation attack was observed for TD Nickel/chromium or for TD Nickel.

4.4.2 Chemical Analyses for Carbon, Oxygen, and Nitrogen Contents

Chemical analyses to determine the carbon, oxygen, and nitrogen levels in superalloy foils were conducted to study internal oxidation phenomenon and decarburization. Chemical analyses (average values) for the carbon, oxygen, and nitrogen content of the superalloy specimens for various conditions are given in Table XVII.

The carbon analyses of superalloy foil specimens in the as-received condition are compared with those reported by the vendor in Table XVIII. There is a close agreement between the two carbon analyses, except for Inconel 625 and TD Nickel/chromium. The large amount of carbides present in as-received Inconel 625 specimens (Fig. 28A and B) indicated that the carbon content was more likely 0.031 percent than 0.01 percent. The carbon content was least in the case of TD Nickel and maximum for Rene' 41 followed by Haynes 25, Inconel 718, Inconel 625, and TD Nickel/chromium (Table XVIII).

Magnification: 200X

A. As Received
Test Direction - Transverse

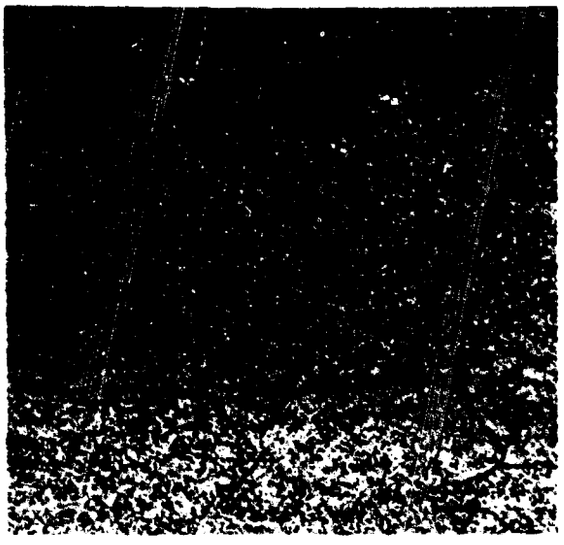

Magnification: 500X

B. As Received
Test Direction - Transverse

Magnification: 200X

C. As Received
Test Direction - Longitudinal

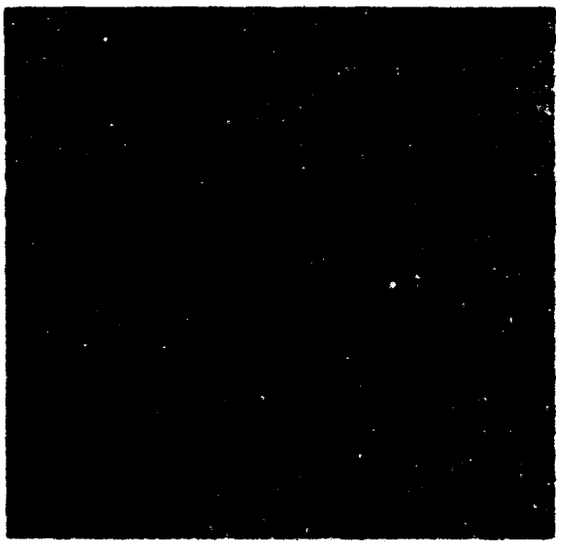

Magnification: 500X

D. As Received
Test Direction - Longitudinal

FIGURE 31. MICROSTRUCTURE OF TD NICKEL/CHROMIUM SPECIMENS IN VARIOUS CONDITIONS (Sheet 1 of 3)

E. Oxidized 2000°F 760 Torr — Magnification: 200X

F. Oxidized 2200°F ,·0 Torr — Magnification: 200X

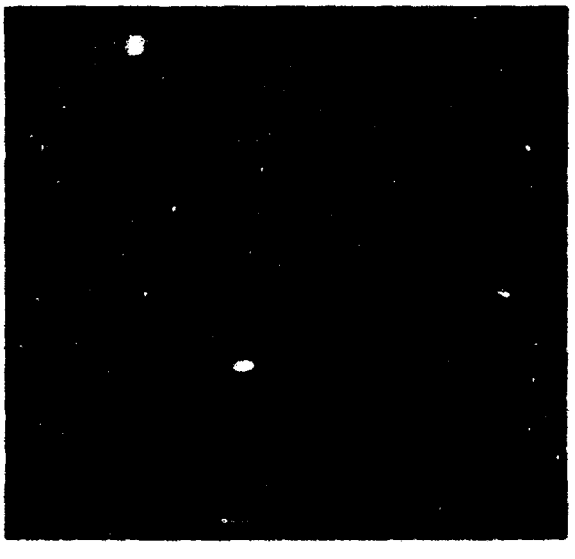

G. Oxidized 2400°F 760 Torr — Magnification: 200X

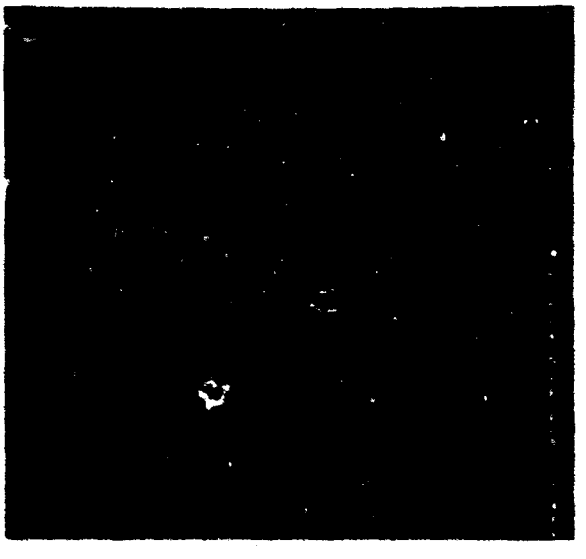

H. Oxidized 2400°F 760 Torr — Magnification: 500X

FIGURE 31. MICROSTRUCTURE OF TD NICKEL/CHROMIUM SPECIMENS IN VARIOUS CONDITIONS (Sheet 2 of 3)

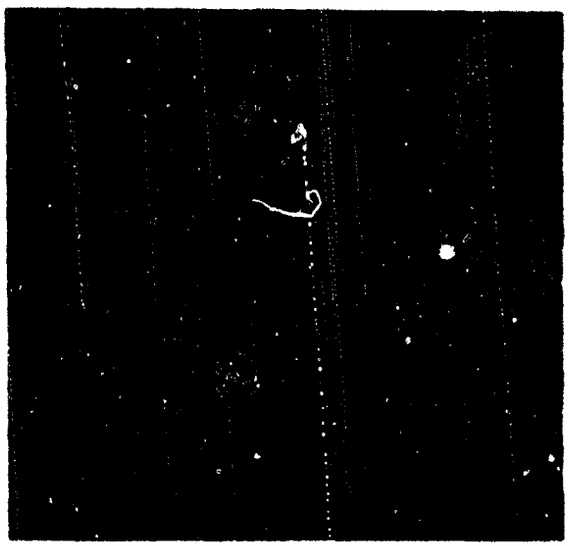

I. Oxidized 2200°F Magnification: 200X
0.18 Torr

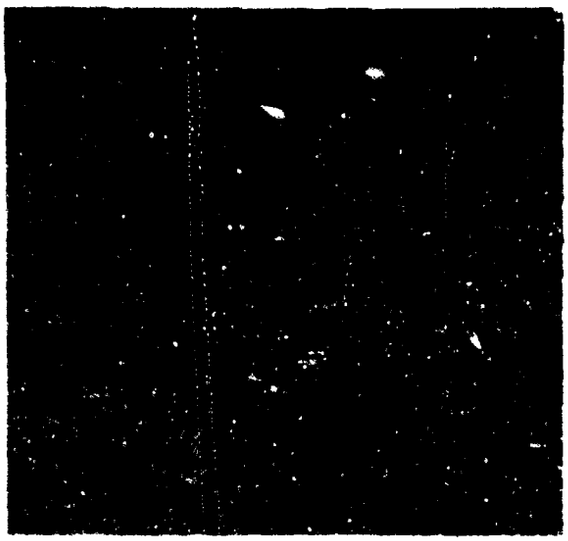

J. Oxidized 2200°F Magnification: 500X
0.18 Torr

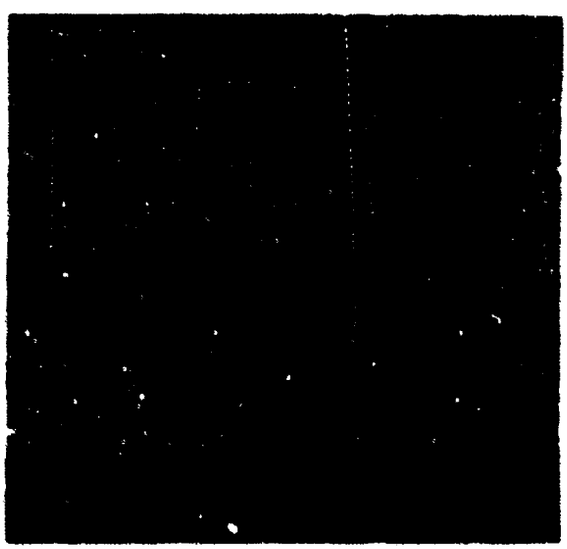

K. Oxidized 2400°F Magnification: 200X
0.18 Torr

L. Oxidized 2400°F Magnification: 500X
0.18 Torr

FIGURE 31. MICROSTRUCTURE OF TD NICKEL/CHROMIUM SPECIMENS IN VARIOUS CONDITIONS (Sheet 3 of 3)

TABLE XVII

RESULTS OF CHEMICAL ANALYSES FOR CARBON, OXYGEN, AND NITROGEN CONTENT OF SUPERALLOY FOILS IN AS-RECEIVED AND OXIDIZED CONDITIONS

Superalloy	Condition			O_2 (%)	N_2 (%)	C (%)	Superalloy	Condition			O_2 (%)	N_2 (%)	C (%)
	R	100 one-hour cyclic oxidation exposures						R	100 one-hour cyclic oxidation exposures				
		T_{max} (°F)	Pressure (Torr)						T_{max} (°F)	Pressure (Torr)			
Rene' 41	R	-	-	0.0081	Nil	0.1014	TD Nickel	R	-	-	0.1307	0.0030	0.0084
		1800	760	0.2399	0.0442	0.1155			2000	760	0.4337	0.0085	0.0059
								(1)	2200	760	0.6019	0.0101	0.0061
Inconel 718	R	-	-	0.0206	Nil	0.0637		(1)	2200	0.18	0.5016	0.0203	0.0111
		1800	760	0.1126	0.0063	0.0673							
							TD Nickel/ Chromium	R	-	-	0.3171	0.0088	0.0153
Inconel 625	R	-	-	0.0160	0.0045	0.0310			2000	760	0.2764	Nil	0.0101
		1800	760	0.0868	0.0157	0.0254			2200	760	0.2730	Nil	0.0085
		1800	0.18	0.1668	0.0063	0.0335			2200	0.18	0.3250	Nil	0.0081
								(1)	2400	760	0.4888	Nil	0.0186
Haynes 25	R	-	-	0.0075	0.0054	0.0787		(2)	2400	0.18	0.3873	Nil	Nil
		1800	760	0.0862	Nil	0.0450							
		2000	760	0.1217	0.0194	0.0547							
		2000	0.18	0.1089	0.0078	0.0430							

R - As received

1. Silicon content was zero in the three specimens analyzed indicating no contamination in the MGR furnace.
2. This oxidation exposure was conducted in the environmental simulator. All other oxidation exposures were conducted in the MGR furnace.

The precipitation hardened alloys (Rene' 41 and Inconel 718) and solid solution strengthened alloys (Haynes 25 and Inconel 625) are also carbide strengthened. The TD Nickel alloy foil in the as-received condition was much lower in oxygen, nitrogen, and carbon than the TD Nickel/chromium (Table XVII). The effects of different oxidation exposures on the carbon, oxygen, and nitrogen contents of superalloys are discussed in succeeding paragraphs.

TABLE XVIII

CARBON CONTENT OF SIX SUPERALLOY FOILS IN AS-RECEIVED CONDITION

Superalloy	Vendor	Carbon Content (%)	
		Vendor	Solar
Rene' 41	Rodney	0.09	0.1014
Inconel 718	Rodney	0.06	0.0637
Inconel 625	Rodney	0.01	0.0310
Haynes 25	Hamilton	0.06	0.0707
TD Nickel	DuPont	0.0055	0.0084
TD Nickel/chromium	DuPont	0.024	0.0153

Precipitation Hardenable Alloys (Rene' 41 and Inconel 718)

For both the Rene' 41 and Inconel 718 alloys, there was an increase in oxygen, nitrogen, and carbon content due to the 1800°F - 760 Torr - 100-cycle oxidation exposure the increase being more for Rene' 41 than for Inconel 718 (Table XVII). The oxygen content increased after the 1800°F oxidation exposure by a factor of 30.0 for Rene' 41 (to 0.24 percent) and by a factor of only 5.5 for Inconel 718 (to 0.113 percent). The oxygen and nitrogen contents in the oxidized Rene' 41 specimen were two and seven times, respectively, when compared to the oxidized Inconel 718 specimen (Table XVII). Therefore, Rene' 41 was much more susceptible to internal oxidation than Inconel 718. No decarburization occurred in these two alloys. There was more oxygen, nitrogen, and carbon in these two alloys after the 1800°F - 760 Torr oxidation exposure than in the as-received condition.

In the case of Rene' 41, the internal oxidation products have been identified as Al_2O_3 and TiN (Ref. 6), and carbides as being of the M_6C + TiC type (para 4.4.1).

Solid Solution Strengthened Alloys (Inconel 625 and Haynes 25)

Both alloys showed an increase in oxygen content and a decrease in carbon content (Table XVII) after 760 Torr and 0.18 Torr air exposures. The slight increase in carbon content for Inconel 625 after the 1800°F - 0.18 Torr - 100-cycle exposure could be due to the carbon pickup from the oil vapors from the vacuum pump. The nitrogen content was lower after the 0.18 Torr exposure than after the 760 Torr exposure at 1800°F (T_{max}) profile for Inconel 625 and at 2000°F (T_{max}) profile for Haynes 25.

Inconel 625, a nickel-base alloy containing only 0.08 percent aluminum, 0.2 percent titanium, 0.1 percent silicon, 22.3 percent chromium, and other metals (Table IV), should preferentially form Al_2O_3, Cr_2O_3, TiO_2, and SiO_2 internally or externally based on free energy data (Table XIX, Ref. 18). (Surface oxides formed were identified by X-ray diffraction to be Cr_2O_3 and spinel $NiCr_2O_4$ - para 4.4.3.) Since this alloy contains only small amounts of aluminum and silicon, the internal oxides formed during oxidation exposure are most likely TiO_2 and Cr_2O_3 with traces of Al_2O_3. Referring to the free energy data for nitrides (Table XIX), the nitrides formed are most likely Cr_2N. Aluminum and titanium are converted readily to the more stable oxides than the nitrides. Since Cr_2N is not a very stable nitride (dissociation pressure of Cr_2N being 4×10^{-4} Torr at 1800°F), it could dissociate during low pressure oxidation exposure (0.18 Torr) resulting in the observed decrease in nitrogen content (Table XVII).

Haynes 25, a cobalt-base alloy containing 20.1 percent chromium, 0.04 percent silicon, 1.49 percent manganese, 1.95 percent iron, 10.63 percent nickel, 14.8 percent tungsten, and small amounts of impurities (Table IV), formed surface oxides identified by X-ray diffraction as spinel $CoCr_2O_4$ after 760 Torr oxidation exposure, and Cr_2O_3 after 0.18 Torr exposure at 2000°F (para 4.4.4). Based on the composition of Haynes 25 and the free energy data for oxides and nitrides (Table XIX), the internal oxides were most likely SiO_2 and/or Cr_2O_3 [1], and the nitride was most likely Cr_2N. For Haynes 25, the oxygen content increased by a factor of 11.5 due to 760 Torr exposure at 1800°F, and by a factor of 16.2 after 760 Torr exposure at 2000°F. Thus, with an increase in the oxidizing T_{max} from 1800 to 2000°F, the oxygen content increased by a factor of about 1.4. Decreasing the exposure pressure from 760 Torr to 0.18 Torr at 2000°F increased the oxygen content to 14.5 times the as-received condition, but not to the extent of exposure at 760 Torr (Table XVII).

1. The oxidation exposures at 1800°F or below have been reported to result in virtually no internal oxidation, and at higher temperatures some internal oxidation of SiO_2 may be encountered (Ref. 19). Smaller amounts of Cr_2O_3 and spinel were also found, the spinel phase being predominant below 2000°F and the α-Cr_2O_3 (rhombohedral) constituent abundant at higher temperatures.

TABLE XIX

THERMODYNAMIC PROPERTIES OF THE OXIDES AND NITRIDES AT 1800°F (Ref. 18)

Element	$\Delta F^{(1)}$	Oxide	$P^{(2)}$	$\Delta F^{(1)}$	Nitride	$P^{(2)}$
Aluminum	-207	Al_2O_3	10^{-36}	-89.1	AlN	3×10^{-16}
Titanium	-177	TiO_2	10^{-31}	-94.6	TiN	4×10^{-17}
Silicon	-161	SiO_2	10^{-28}	-32.0	Si_3N_4	3×10^{-6}
Chromium	-135	Cr_2O_3	10^{-23}	-19.5	Cr_2N	4×10^{-4}
Molybdenum	-102	MoO_3	2×10^{-18}		Unstable	
Iron	- 83.5	Fe_2O_3	3×10^{-15}		Unstable	
Cobalt	- 72.5	CoO	2×10^{-13}		Unstable	
Nickel	- 66.9	NiO	2×10^{-12}		Unstable	
Spinel	-100(3)	$NiCr_2O_4$	4×10^{-15}(3)		Unstable	

1. Free energy of formation/mole of oxygen or nitrogen in Kcal
2. Dissociation pressure in atmospheres
3. Estimated from data on $FeCr_2O_4$

Dispersion Strengthened Alloys (TD Nickel and TD Nickel/Chromium)

For TD Nickel, there was an increase in oxygen and nitrogen content and a decrease in carbon content after the various oxidation exposures (Table XVII). The internal oxide formed was believed to be NiO. The increase in carbon content, because of low-pressure (0.18 Torr) exposure at 2200°F, could be due to the oil vapors from the vacuum pump or to the presence of carbon monoxide from the silicon carbide heating elements used in the MGR furnace.

For TD Nickel/chromium there was no appreciable increase in oxygen or carbon content after various oxidizing exposures at temperatures up to 2200°F, indicating a continuous and stable surface oxide. The oxygen content increased after the exposures at 2400°F, forming islands of Cr_2O_3. The nitrogen content was nil after the different exposures.

4.4.3 Microhardness Values

The microhardness values of the six superalloy foils in the as-received and oxidized conditions are given in Table XX. In the as-received condition, highest microhardness values were exhibited by Rene' 41 followed by TD Nickel/chromium, Haynes 25, Inconel 625, Inconel 718, and TD Nickel. The microhardness values at the edges of the six superalloy foils were lower than those at the center, most likely because of the lack of support at the edge (edge effect). The effects of different oxidation exposures on the microhardness values are discussed below.

Precipitation Hardened Alloys (Rene' 41 and Inconel 718)

The microhardness values at the center of the substrates of Rene' 41 and Inconel 718 increased because of atmospheric pressure oxidation exposures at 1800 or 2000°F (T_{max}). The increased hardness values were most likely the result of:

- Aging effect resulting in γ' precipitation, $Ni_3(Al, Ti)$, in the case of Rene' 41, and $Ni_3(Ti, Cb)$ for Inconel 718 - (para 4.4.1)
- The μ phase formation in the case of Rene' 41 (para 4.4.1)
- Increased carbon, nitrogen, and oxygen contents of the substrate (para 4.4.2 - Table XVII)

For Rene' 41 the hardness value at the center of the substrate after 2000°F oxidation (461 KHN) was of the same order of magnitude as that after 1800°F oxidation (454 KHN - Table XX). This could be because of the instability of γ' and μ phases at temperatures of 1800°F and higher (Fig. 26 and para 4.4.1).

The hardness of Inconel 718 after 2000°F profile exposure (266 KHN) was somewhat less than after the 1800°F profile exposure (289 KHN - Table XX). Probably the dissolution of $Ni_3(Ti, Cb)$ precipitates above 1825°F is responsible for the drop in hardness.

The hardness values of the alloy depletion layer in the case of oxidized Rene' 41 were lower than those of the as-received Rene' 41 (Table XX). The alloy depletion layer for Rene' 41 exhibited lower hardness values after 100 one-hour atmospheric pressure slow-cycle oxidation exposures at 2000°F than at 1800°F. This is most likely due to the decrease in titanium, chromium, and aluminum content in the alloy depletion layer. No appreciable alloy depletion zone was noted in the Inconel 718 after exposure.

TABLE XX

MICROHARDNESS VALUES OF SUPERALLOY FOILS
IN AS-RECEIVED AND OXIDIZED CONDITIONS

Superalloy	Condition			Microhardness Values (KHN 200-gram load)		
		Oxidized for 100 one-hour slow cycles		Substrate		
	R	T_{max} (°F)	Pressure (Torr)	Center	Edge[1]	Alloy Depletion Layer
Rene' 41	R	-	-	390	347, 351	
		1800	760	454	--	285, 292
		2000	760	461	399, 327	175, 257
Inconel 718	R	-	-	241	217, 246	
		1800	760	289	202, 231	
		2000	760	266	210, 178	
Inconel 625	R	-	-	249	246, 228	
		1800	760	279	243, 212	
		1800	0.18	266	263, 269	
		2000	760	246	252, 223	217, 144
Haynes 25	R	-	-	303	272, 266	
		1800	760	331	318, 233	
		2000	760	362	233, 260	
		2000	0.18	219	157, 152	
		2100	760	315	241, 327	
TD Nickel	R	-	-	246	200, 210	
		2000	760	263	206, 228	
		2200	760	214	200, 226	
		2200	0.18	219	157, 152	
		2400	760	185	191, 191	
TD Nickel/ chromium	R	-	-	348	215, 215	
		2000	760	344	219, 257	
		2200	760	339	299, 315	
		2200	0.18	307	289, 299	
		2400	760	353	292, 315	
		2400	0.18	353	335, 348	

R - As received

1. The hardness values determined at one mil below the edge or at the alloy depletion layer are lower than those at the center because of the edge effect

Solid Solution Strengthened Alloys (Inconel 625 and Haynes 25)

For Inconel 625 foil (annealed at 2050°F) there was no significant change in microhardness values resulting from different cyclic oxidation exposures (Table XX). The slight increase in microhardness values after the 1800°F exposures could be caused by oxidation effects, e.g., increase in carbon and oxygen contents (Table XVII). Hardness values for Inconel 625 were slightly lower after 0.18 Torr exposure than after 760 Torr at 1800°F (T_{max}). The decrease values probably resulted from the reduction in nitrogen content.

For Haynes 25, there was an increase in microhardness values (from 303 KHN to 362 KHN) at the center of the substrate after the 2000°F - 760 Torr - 100-cycle oxidation exposure (Table XX). This could be due to internal oxidation (formation of SiO_2 or Cr_2O_3) effects as evidenced by an increase in oxygen and nitrogen contents (Table XVII). The 2000°F - 100-cycle - 0.18 Torr oxidation exposure resulted in a significant decrease in the microhardness values of Haynes 25 (Table XX). This decrease was most likely due to decarburization and reduced nitrogen and oxygen contents as compared to those after the 2000°F - 760 Torr oxidation exposure (Table XVII). After the 2100°F - 760 Torr - 100-cycle oxidation exposure, the microhardness values increased (Table XX).

Dispersion Strengthened Alloys (TD Nickel and TD Nickel/Chromium)

There was, in general, a decrease in microhardness values for TD Nickel after the different oxidation exposures except for the slight increase after the 2000°F - 760 Torr - 100-cycle oxidation (Table XX). The TD Nickel foil after cold rolling was stress relief annealed at 2000°F; therefore, 100 one-hour slow-cycle oxidation exposures at temperatures higher than 2000°F resulted in further stress relief and a decrease in microhardness values. The slight increase in microhardness values after the 2000°F oxidation exposure was due to an increase in oxygen content (Table XVII).

TD Nickel/chromium foils were also stress relief annealed at 2000°F. The different oxidation exposures up to 2200°F resulted in no significant changes in the microhardness values, probably because of some stress relief provided by oxidation exposures at temperatures higher than 2000°F, and because of the negligible increase in oxygen content after oxidation exposures up to 2200°F (Table XVII). The oxygen content increased after the 2400°F oxidation exposures which could account for the slight increase in microhardness values. The carbon and nitrogen contents decreased because of the different oxidation exposures up to 2400°F.

The generally lower microhardness of all four alloys after exposure to 0.18 Torr, as compared to 760 Torr exposure, is probably best explained by the decreaso in internal oxidation and decreased nitrogen content at the lower pressure.

4.4.4 Identification of Surface Oxides by X-ray Diffraction Analyses

X-ray diffraction analyses were conducted to identify the oxidation product for the superalloy foil specimens subjected to 760 Torr and 0.18 Torr oxidation exposures at their respective T_{max}. Only the Inconel 625, Haynes 25, and TD Nickel/chromium alloys were analyzed. No X-ray diffraction analysis was conducted for TD Nickel because the oxide formed due to oxidation exposure is known to be greenish NiO (NaCl structure) from the literature (Ref. 15).

The X-ray diffraction patterns for the three alloys (Inconel 625, Haynes 25, and TD Nickel/chromium) after oxidation exposures are given in Tables XXI through XXVII. The 2θ and d values (lattice spacing), relative intensity, and the identified oxides are included in these tables.

The oxides identified for the three alloys are:

- Inconel 625, oxidized 1800°F - 100 cycles at 760 Torr or 0.18 Torr: α-Cr_2O_3 (rhombohedral) and the spinel, $NiCr_2O_4$. The oxides formed in the case of Inconel 625 were the same after both the 760 Torr or 0.18 Torr oxidation exposures (Tables XXI and XXII).

- Haynes 25, oxidized 2000°F - 100 cycles - 760 Torr - spinel - $CoCr_2O_4$ (Table XXIII).

- Haynes 25, oxidized 2000°F - 100 cycles - 0.18 Torr - α-Cr_2O_3 (rhombohedral) only (Table XXIV).

- Haynes 25, oxidized 2000°F - 22 cycles - 10 Torr - α-Cr_2O_3 (rhombohedral) and $CoCr_2O_4$ (Table XXV).

- TD Nickel/chromium oxidized 2400°F - 100 cycles at 760 Torr or at 0.18 Torr - α-Cr_2O_3 (rhombohedral). No NiO or spinel $NiCr_2O_4$ could be identified. The oxide formed after 760 Torr or 0.18 Torr oxidation exposure was the same (α-Cr_2O_3) (Tables XXVI and XXVII).

It is interesting to note the differences in the nature of the oxides formed for the two solid solution strengthened alloys, Inconel 625 and Haynes 25. After atmospheric pressure oxidation, both Cr_2O_3 (rhombohedral) and spinel were present in the case of Inconel 625; for oxidized Haynes 25, only cubic Cr_2O_3 in the form of complex spinel was identified. For Inconel 625, similar oxides were formed at 760 Torr or at 0.18 Torr environmental pressure, but for Haynes 25, the oxides formed after different oxidation exposures were different depending upon the environmental pressure. After atmospheric pressure oxidation exposure at 2000°F for 100 cycles, a spinel oxide

TABLE XXI

X-RAY DIFFRACTION PATTERN OF INCONEL 625
OXIDIZED 1800°F - 760 TORR - 100 CYCLES
(Cukα Radiation, λ= 1.5418Å, Nickel Filter)

2θ (deg)	d (Å)	Relative Intensity (I/I_1)	Oxide
14.84	5.9344	7	?
18.40	4.8176	6	$NiCr_2O_4$
24.42	3.6419	80	α-Cr_2O_3
30.24	2.9529	10	$NiCr_2O_4$
33.52	2.6711	86	α-Cr_2O_3
36.04	2.4899	100	α-Cr_2O_3, $NiCr_2O_4$
37.44	2.4000	7	$NiCr_2O_4$
44.44	2.1771	14	α-Cr_2O_3
43.50	2.0786	8	$NiCr_2O_4$
50.10	1.8192	36	α-Cr_2O_3
54.70	1.6765	50	α-Cr_2O_3, $NiCr_2O_4$
58.26	1.5823	7	α-Cr_2O_3, $NiCr_2O_4$
63.10	1.4721	21	α-Cr_2O_3
64.84	1.4367	29	α-Cr_2O_3
72.90	1.2964	7	α-Cr_2O_3
76.12	1.2453	4	α-Cr_2O_3
90.42	1.0853	25	$NiCr_2O_4$
95.62	1.0396	7	?
118.00	0.8986	7	α-Cr_2O_3
137.90	0.8253	18	α-Cr_2O_3
138.64	0.8239	9	α-Cr_2O_3
146.44	0.8045	18	α-Cr_2O_3
147.40	0.8025	11	α-Cr_2O_3

The oxides, α-Cr_2O_3 (rhombohedral) and $NiCr_2O_4$ (cubic, spinel type) were identified.

TABLE XXII

X-RAY DIFFRACTION PATTERN OF INCONEL 625
OXIDIZED 1800°F - 0.18 TORR - 100 CYCLES

(Cukα Radiation, λ = 1.5418Å, Nickel Filter)

2θ (deg)	d (Å)	Relative Intensity (I/I_1)	Oxide
18.30	4.8437	15	$NiCr_2O_4$
24.54	3.6244	3	α-Cr_2O_3
30.00	2.9760	5	$NiCr_2O_4$
33.80	2.6496	25	α-Cr_2O_3
35.36	2.5362	60	$NiCr_2O_4$
36.30	2.4727	40	α-Cr_2O_3
41.52	2.1731	15	α-Cr_2O_3
43.00	2.1016	10	$NiCr_2O_4$
44.08	2.0526	60	Substrate
50.22	1.8151	12	α-Cr_2O_3
51.22	1.7820	20	Substrate
54.90	1.6709	20	α-Cr_2O_3
56.82	1.6189	10	$NiCr_2O_4$
62.30	1.4890	15	α-Cr_2O_3
63.34	1.4671	10	$NiCr_2O_4$
63.68	1.4600	10	α-Cr_2O_3
64.90	1.4355	15	α-Cr_2O_3
75.24	1.2618	25	$NiCr_2O_4$
91.40	1.0726	30	$NiCr_2O_4$
139.92	0.8199	10	α-Cr_2O_3
149.02	0.7993	10	α-Cr_2O_3
150.00	0.7974	10	α-Cr_2O_3

The oxides α-Cr_2O_3 (rhombohedral) and $NiCr_2O_4$ (cubic, spinel type, a_o = 8.30-8.34Å) were identified

TABLE XXIII

X-RAY DIFFRACTION PATTERN OF HAYNES 25
OXIDIZED 2000°F - 760 TORR - 100 CYCLES

(Fe kα Radiation, λ = 1.936Å, Manganese Filter)

2θ (deg)	d (Å)	Relative Intensity (I/I_1)	Oxide
23.20	4.8140	23	$CoCr_2O_4$
38.30	2.9508	67	$CoCr_2O_4$
45.30	2.5136	100	$CoCr_2O_4$
65.32	2.0852	17	$CoCr_2O_4$
55.94	2.0639	20	$CoCr_2O_4$
69.24	1.7038	17	$CoCr_2O_4$
74.10	1.6066	17	$CoCr_2O_4$
81.92	1.4766	33	$CoCr_2O_4$
84.30	1.4424	10	$CoCr_2O_4$
00.00	1.2636	23	$CoCr_2O_4$
06.80	1.0874	27	Substrate and $CoCr_2O_4$
Oxide present was the spinel $CoCr_2O_4$			

TABLE XXIV

X-RAY DIFFRACTION PATTERN OF HAYNES 25
OXIDIZED 2000°F - 0.18 TORR - 100 CYCLES

(Fe Kα Radiation, λ = 1.936Å, Manganese Filter

		Relative Intensity (I/I_1)		
2θ (deg)	d (Å)	Oxide Only	Oxide and Substrate	Oxide
30.94	3.6290	60	10	α-Cr_2O_3
42.48	2.6720	100	17	α-Cr_2O_3
45.80	2.4876	100	17	α-Cr_2O_3
52.50	2.1878	50	8	α-Cr_2O_3
55.70	2.0721	-	33	Substrate
64.26	1.8201	50	8	α-Cr_2O_3
65.20	1.7967	-	17	Substrate, α-Cr_2O_3
70.46	1.6780	80	13	α-Cr_2O_3
82.20	1.4225	30	5	α-Cr_2O_3
99.30	1.2701	-	100	Substrate
126.50	1.0840	-	58	Substrate
137 80	1.0375	-	8	Substrate

Oxide present was only α-Cr_2O_3 (rhombohedral). The lattice parameters for pure α-Cr_2O_3 are a = 4954Å, c = 13.584Å

TABLE XXV

X-RAY DIFFRACTION PATTERN OF HAYNES 25
OXIDIZED 2000°F - 10 TORR - 22 CYCLES

		Relative Intensity (I/I_1)		
2θ (deg)	d (Å)	Oxide Only	Oxide and Substrate	Oxide
9.12	9.6883	14	4	
18.18	4.8754	43	13	$CoCr_2O_4$
24.50	3.6302	71	21	α-Cr_2O_3
30.00	2.9760	57	14	$CoCr_2O_4$
33.52	2.6711	71	21	α-Cr_2O_3
35.20	2.5474	100	29	$CoCr_2O_4$
36.04	2.4899	71	17	α-Cr_2O_3
41.30	2.1841	29	8	α-Cr_2O_3
42.72	2.1148	20	6	Substrate
43.90	2.0606	340	100	Substrate, $CoCr_2O_4$
50.10	1.8192	29	8	α-Cr_2O_3
51.10	1.7859	115	33	Substrate, α-Cr_2O_3
54.78	1.6743	57	17	$CoCr_2O_4$
75.12	1.2635	85	25	$CoCr_2O_4$
91.30	1.0771	85	25	$CoCr_2O_4$
96.60	1.0316	29	8	Substrate
Oxides identified were α-Cr_2O_3 (rhombohedral) and spinel $CoCr_2O_4$				

TABLE XXVI

X-RAY DIFFRACTION PATTERN OF TD NICKEL/CHROMIUM
OXIDIZED 2400°F - 760 TORR - 100 CYCLES

(Cukα Radiation, λ = 1.5418Å, Nickel Filter)

2θ (deg)	d (Å)	Relative Intensity (I/I_1)	Oxide
10.92	8.0950	-	Substrate
24.54	3.6241	43	α-Cr_2O_3
27.60	3.2291	-	Substrate
30.54	2.9346	-	Substrate
31.82	2.8098	-	Substrate
33.58	2.6665	100	α-Cr_2O_3
36.22	2.4779	42	α-Cr_2O_3
39.50	2.2794	23	α-Cr_2O_3
41.46	2.1761	16	α-Cr_2O_3
44.20	2.0473	3	α-Cr_2O_3
45.90	1.9751	-	Substrate
50.20	1.8158	18	α-Cr_2O_3
51.56	1.7397	-	Substrate
54.84	1.6726	46	α-Cr_2O_3
63.40	1.4658	15	α-Cr_2O_3
65.02	1.4332	6	α-Cr_2O_3
72.50	1.3026	28	α-Cr_2O_3
83.90	1.1522	6	α-Cr_2O_3
92.40	1.0672	10	α-Cr_2O_3
94.40	1.0498	5	α-Cr_2O_3
120.80	0.8859	-	Substrate
146.80	0.8037	6	α-Cr_2O_3
153.06	0.7920	-	Substrate

Oxide present was only α-Cr_2O_3 (rhombohedral). No NiO or spinel could be identified.

TABLE XXVII

X-RAY DIFFRACTION PATTERN OF TD NICKEL/CHROMIUM OXIDIZED 2400°F - 0.18 TORR - 100 CYCLES

(Cukα Radiation, λ = 1.5418Å, Nickel Filter)

2θ (deg)	d (Å)	Relative Intensity (I/I_1)	Oxide
10.58	8.3544	23	Substrate
24.60	3.6157	31	α-Cr_2O_3
27.62	3.2268	14	Substrate
33.56	2.6650	100	α-Cr_2O_3
36.28	2.4740	20	α-Cr_2O_3
39.60	2.2739	57	α-Cr_2O_3
41.50	2.1741	9	α-Cr_2O_3
44.30	2.0459	158	α-Cr_2O_3
50.28	1.8131	9	α-Cr_2O_3
51.70	1.7666	515	Substrate
54.88	1.6715	29	α-Cr_2O_3
63.20	1.4700	9	α-Cr_2O_3
65.20	1.4296	6	α-Cr_2O_3
72.54	1.3020	43	α-Cr_2O_3
76.00	1.2511	14	?
85.04	1.1397	14	α-Cr_2O_3
92.34	1.0677	36	α-Cr_2O_3
97.60	1.0237	9	α-Cr_2O_3
120.80	0.8859	189	Substrate
152.62	0.7928	57	Substrate

Oxide present was α-Cr_2O_3 (rhombohedral)

$CoCr_2O_4$[1] was formed: whereas, after 2000°F - 100 cycles - 0.18 Torr oxidation exposure, the oxide formed was α-Cr_2O_3. But after the 2000°F - 22 cycles - 10 Torr oxidation exposure, a mixture of the oxides α-Cr_2O_3 and spinel $CoCr_2O_4$ was formed. The higher temperature, 2000°F, for Haynes 25 (compared to 1800°F for Inconel 625), and the lower rate of oxide formation at 0.18 Torr than at 760 Torr, favored the formation of the more stable Cr_2O_3 over spinel. In the case of Inconel 625 at 1800°F, the diffusion rate of chromium was believed to be too slow to prevent the formation of mixture of oxides, α-Cr_2O_3 and spinel. These data are in essential agreement with Wasielewski (Ref. 19).

4.4.5 Selected Electron Microprobe Analyses

Results of microprobe analyses for Inconel 625, Haynes 25, and TD Nickel/chromium after a 100-cycle oxidation exposure at 760 and at 0.18 Torr at their respective T_{max} are presented in Figures 32, 33, and 34, respectively. Elements showing a compositional change near the edge for the three superalloys are:

		Change	
Alloy	Oxidation Exposure	Increase	Decrease
Inconel 625	1800°F - 100 cycles - 760 Torr	Tungsten, columbium, molybdenum, nickel	Chromium, manganese
Inconel 625	1800°F - 100 cycles - 0.18 Torr	Aluminum, molybdenum, nickel, columbium, iron	Chromium, manganese
Haynes 25	2000°F - 100 cycles - 760 Torr	Tungsten, nickel, cobalt	Chromium, manganese
Haynes 25	2000°F - 100 cycles - 0.18 Torr	Tungsten, nickel, cobalt	Chromium, manganese
TD Nickel/ Chromium	2400°F - 100 cycles - 760 Torr	Chromium	Nickel
TD Nickel/ Chromium	2400°F - 100 cycles - 0.18 Torr	Chromium	Nickel

Microprobe analyses for the three alloys are discussed in the following paragraphs.

1. The predominant surface scale constituents are CoO, Cr_2O_3, and a $CoCr_2O_4$ type spinel after oxidation at 1800°F or below, and Cr_2O_3 + spinel at higher temperatures (Ref. 19). Exposures for about one hundred hours at 2200°F produce a scale containing $CoWO_4$, CoO, and Co_3O_4 which, in combination, appeared to be low melting enough to produce catastrophic oxidation at a linear rate (Ref. 19).

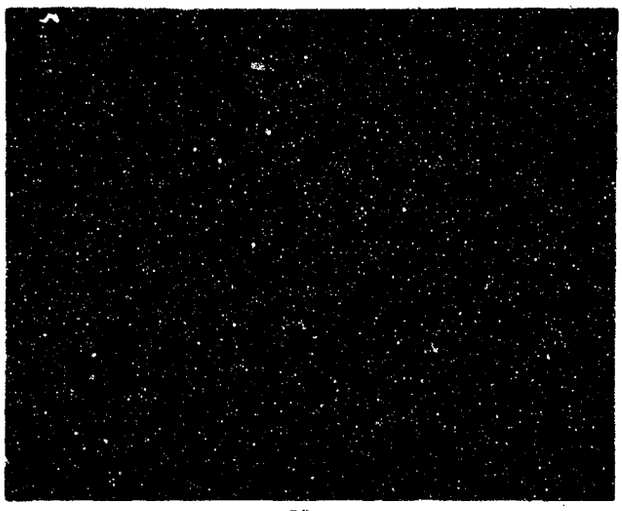

Microprobe trace line is approximate

Oxidized 1800°F
760 Torr
100 Cycles

Magnification: 200X

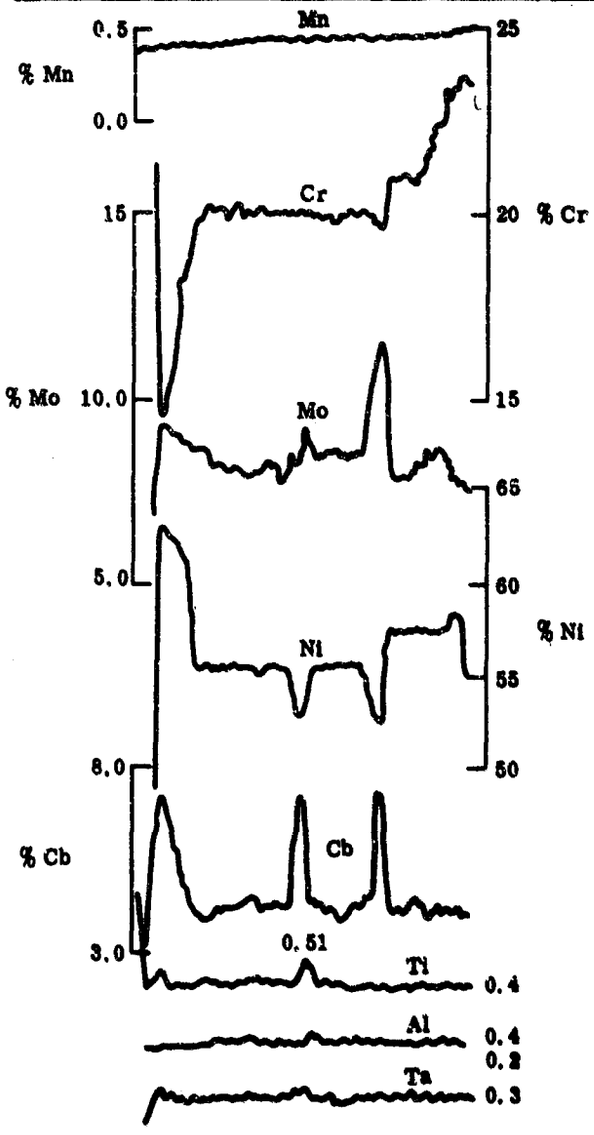

FIGURE 32. ELECTRON MICROPROBE ANALYSES OF THE VARIOUS ELEMENTS IN INCONEL 625 (Sheet 1 of 2)

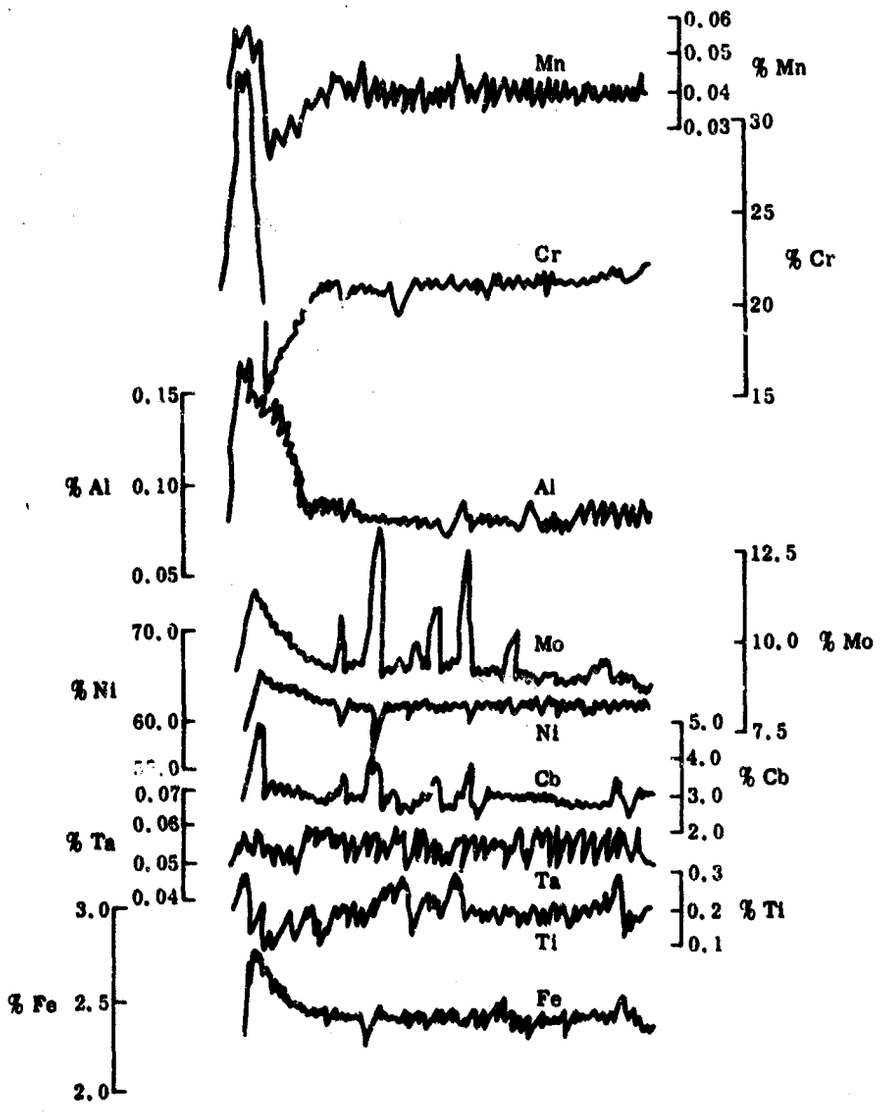

Oxidized 1800°F
760 Torr
100 Cycles

FIGURE 32. ELECTRON MICROPROBE ANALYSES OF THE VARIOUS ELEMENTS IN INCONEL 625 (Sheet 2 of 2)

Microprobe trace line is approximate

Oxidized 2000°F

760 Torr

100 cycles

Magnification: 200X

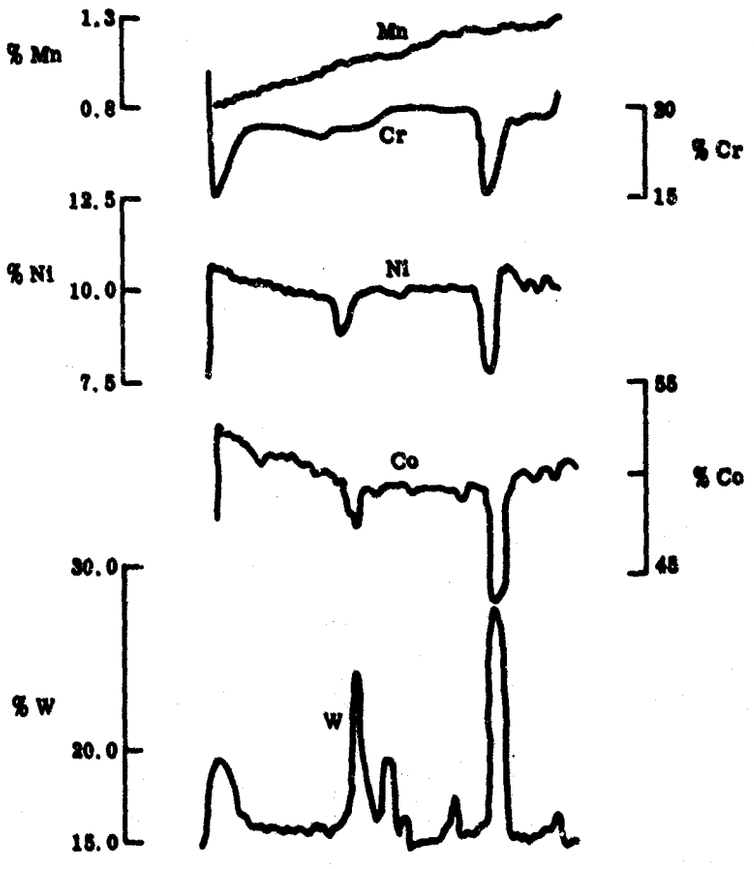

FIGURE 33. ELECTRON MICROPROBE ANALYSES OF THE VARIOUS ELEMENTS IN HAYNES 25 (Sheet 1 of 2)

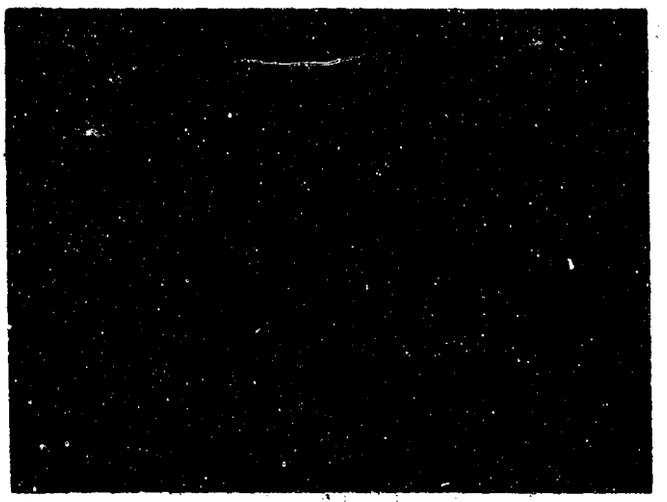

Microprobe trace line is approximate

Oxidized 2000°F
100 Cycles
0.18 Torr

Magnification: 500X

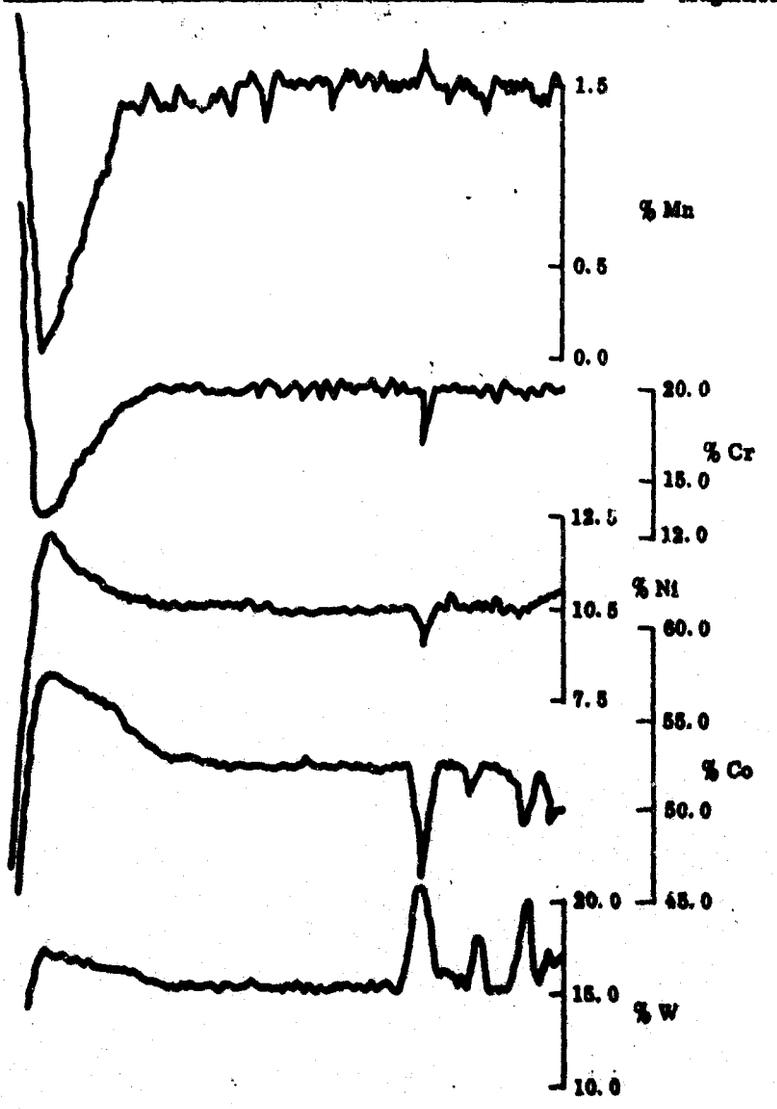

FIGURE 33. ELECTRON MICROPROBE ANALYSES OF THE VARIOUS ELEMENTS IN HAYNES 25 (Sheet 2 of 2)

Microprobe trace line is approximate

Oxidized 2400°F
760 Torr
100 Cycles

Magnification: 200X

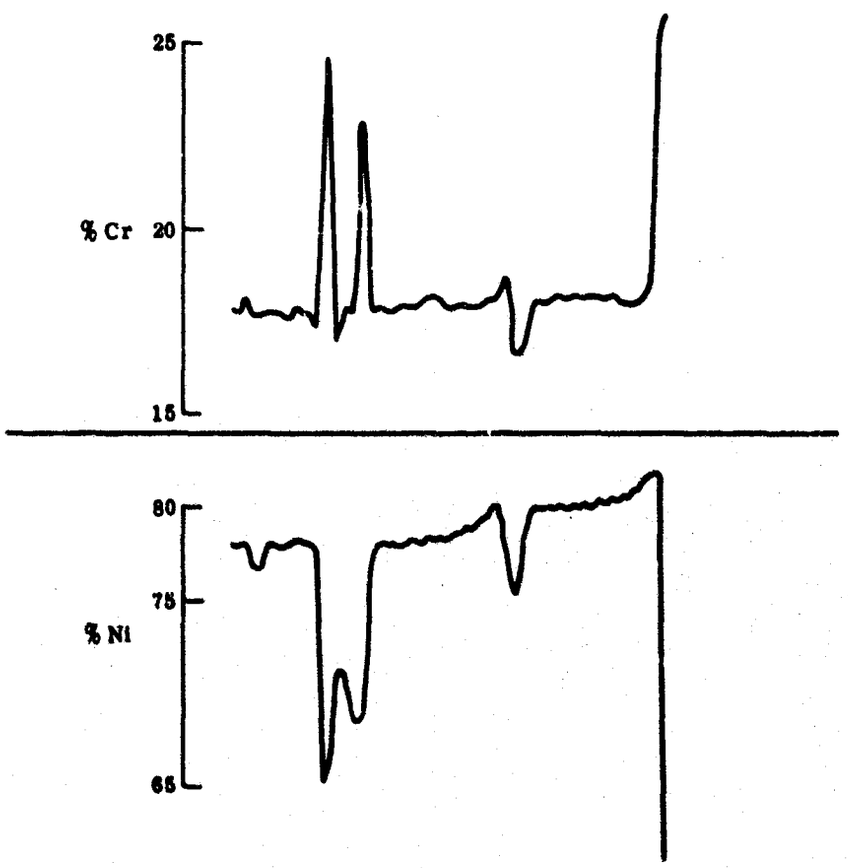

FIGURE 34. ELECTRON MICROPROBE ANALYSES OF CHROMIUM AND NICKEL IN TD NICKEL/CHROMIUM (Sheet 1 of 2)

Microprobe trace line is approximate

Oxidized 2400°F
100 Cycles
0.18 Torr

Magnification: 500X

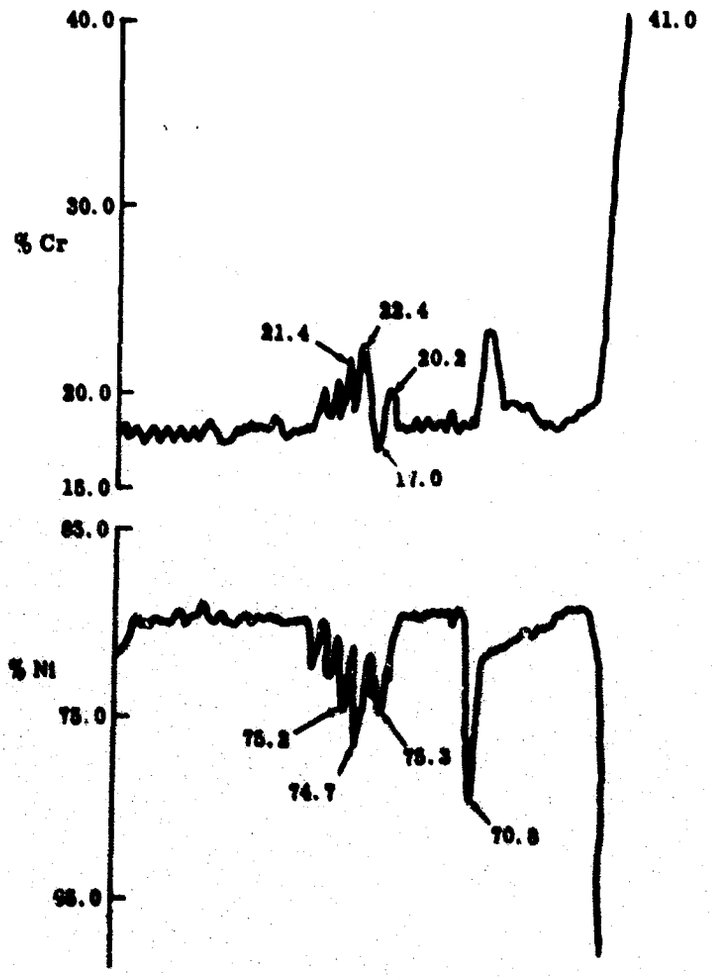

FIGURE 34. ELECTRON MICROPROBE ANALYSES OF CHROMIUM AND NICKEL IN TD NICKEL/CHROMIUM (Sheet 2 of 2)

Inconel 625

For Inconel 625, the microprobe traces for the various elements (Fig. 32A and B) after oxidation exposures at 760 Torr or 0.18 Torr were similar. The peaks in columbium, molybdenum, and the minima in chromium, nickel, and iron could be due to the traverse passing through a carbide. Except for these peaks and minima in traces of the elements, the average composition remained nearly constant in the unaffected base metal. Metals like chromium and manganese showed a decrease in the alloy depletion layer, but an increase in the oxide. The surface oxides, by X-ray diffraction, were identified to be α-Cr_2O_3. Based on microprobe data, the surface oxide formed must be α-$(Cr, Mn)_2O_3$. The metals, aluminum, molybdenum, nickel, columbium, and iron, which exhibited an increase in the alloy depletion layer showed a sudden decrease in the oxide. Thus, the alloy depletion layer was reduced in chromium and manganese, but enriched in the other elements (molybdenum, nickel, columbium, and iron).

Haynes 25

The microprobe traces for various elements (nickel, chromium, cobalt, tungsten) of Haynes 25 oxidized at 2000°F - 760 Torr - 100 cycles (Fig. 33A) were very similar to the alloy oxidized at 2000°F - 0.18 Torr - 100 cycles (Fig. 33B). The peak in tungsten and minima in chromium, nickel, and cobalt could be due to the traverse passing through a carbide. Except for the peak and minima, the average composition remained constant in the substrate after both exposures.

	Percent Element in Substrate	
Element	Haynes 25 Oxidized 2000°F - 760 Torr - 100 Cycles	Haynes 25 Oxidized 2000°F - 0.18 Torr - 100 Cycles
Chromium	20	20.0
Manganese	Varies from 1.3 to 0.8	1.5
Nickel	10	10.5
Cobalt	50	52.5
Tungsten	16	15.0

The manganese traces in Haynes 25 were different after the two oxidation exposures (Fig. 33A and B). The manganese in Haynes 25 exposed at atmospheric pressure at 2000°F continuously decreased from 1.3 percent to 0.8 percent at the edge. At 0.18 Torr pressure, manganese remained nearly constant at about 1.5 percent, decreased in the alloy depletion layer (to almost nil), and then increased in the oxide

(Fig. 33B). In the alloy depletion layer, active metals, e.g., chromium and manganese were decreased and metals like nickel, cobalt, and tungsten were increased. The surface oxides contained chromium and manganese. The surface oxides after 2000°F and 0.18 Torr oxidation exposure by X-ray diffraction (para 4.4.4) were identified to be of the α-Cr_2O_3 type only. Considering microprobe data, the surface oxide was α-$(Cr, Mn)_2O_3$.

TD Nickel/Chromium

The microprobe traces for chromium and nickel in TD Nickel/chromium oxidized at 2400°F and 0.18 Torr for 100 cycles (Fig. 34B) were similar to those for TD Nickel/chromium subjected to atmospheric pressure oxidation at 2400°F for 100 cycles (Fig. 34A). The chromium and nickel remained essentially constant in the substrate at about 18 percent chromium and 80 percent nickel except for the peaks in chromium and the minima in nickel. The peaks[1] in chromium and the minima in nickel were most likely due to the traverse passing through internal oxides (Cr_2O_3). The drop in both chromium and nickel (Fig. 34A) could be the result of the void formation due to decarburization. At the edge (oxide), the chromium level increased and nickel level decreased indicating the formation of Cr_2O_3 essentially free from NiO. (The surface oxides have been identified to be Cr_2O_3 by X-ray diffraction, para 4.4.4.) The lack of a chromium gradient in the alloy indicated that the diffusion rate of chromium in the alloy is greater than the rate of diffusion of oxygen through the oxide. The retained chromium content (18 percent) being well within the range of excellent oxidation resistance indicated that the alloy, TD Nickel/chromium, is serviceable up to at least 2400°F even at low pressures (0.18 Torr). At these low pressures, there was no significant loss in chromium indicating that Cr_2O_3 on the surface hindered chromium vaporization.

4.5 EFFECTS OF PROFILE SIMULATION

Environmental mission profile simulation tests were conducted to determine the combined effects of stress, cyclic oxidation, and environmental pressure on the superalloy foils and to recommend their capability for use as honeycomb heat shields in hypersonic vehicles. Two different stress levels were used for each mission profile. Selected mission profile tests with no stress were also performed. The mission profile tests for 22 one-hour slow cycles were conducted only at 760 Torr for Rene' 41 and Inconel 718. Three different pressures were used (760 Torr, 10 Torr, and 0.18 Torr)

---

1. A polishing abrasive (trade name Cer-Cre) other than Cr_2O_3 was used, so that the peaks in chromium could not be associated with the polishing compound.

for testing the four selected alloys, viz., Inconel 625, Haynes 25, TD Nickel, and TD Nickel/chromium. For these four alloys, 100 one-hour slow-cycle simulated profile tests at their recommended T_{max} and in the most severe pressure condition were also performed.

This section contains a description of the effects of the different simulated profile exposures on the six superalloy foils as evaluated by:

- Creep rate during exposure
- Room temperature tensile tests
- Microscopic examination and microhardness determination
- Comparison to the effects of oxidation exposures without stress (para 4.2, 4.3, and 4.4)

Results of room temperature tensile tests and the microhardness determination after different simulation profiles for 22 one-hour slow cycles for Rene' 41 and Inconel 718 are presented in Table XXVIII, for Inconel 625 and Haynes 25 in Table XXIX, and for TD Nickel and TD Nickel/chromium in Table XXX. The results of 100 one-hour slow-cycle profile exposures for the four selected alloys are given in Table XXXI. For calculation of F_{tu}, F_{ty}, and E values, the original area of cross section of the as-received specimen was used. The total percent elongation and creep rate are included in these tables. The percent elongation versus time for 22 one-hour cycle profile tests are plotted for Rene' 41, for Inconel 718, and for the solid solution strengthened alloys. These results, together with the results of microscopic examination are discussed in following paragraphs.

4.5.1 Profile Simulation Test Results for Rene' 41 and Inconel 718 Alloys

The alloys - Rene' 41 and Inconel 718 - were subjected to simulated profile tests at only one pressure (760 Torr) for 22 one-hour cycles, because these alloys were eliminated early from the program as a result of cyclic oxidation tests.

In the case of Rene' 41, the creep rate at a stress of 1.0 ksi for the 2000°F profile was almost five times higher than that for the 1800°F profile and three times higher than that of Inconel 718 (Table XXVIII and Fig. 35). The creep rate for these two alloys for profiles with T_{max} of 1800 or 2000°F was higher than that for the matrix strengthened (Inconel 625 and Haynes 25) or dispersion strengthened (TD Nickel and TD Nickel/chromium) alloys. Rene' 41 had the highest creep rate of the six selected alloys. This is in agreement with the isothermal creep data (para 4.1). These creep

TABLE XXVIII

RESULTS OF MISSION PROFILE SIMULATION TESTS FOR RENE' 41 AND INCONEL 718 FOILS

Superalloy	Condition					Creep Rate (10^{-3} in./in./hr)	Room Temperature Tensile Test Data							Microhardness Values (KHN 200-gram load)	
	R	22-Cycle Simulated Profile Exposure					F_{tu} (ksi)	Loss in F_{tu} (%)	F_{ty} (ksi)	Loss in F_{ty} (%)	Total Elongation (% in 1.0 in.)	Loss in Elongation (%)	E - Elastic Modulus (-10^3 ksi)	Center	Edges[2]
		T_{max} (°F)	Stress (ksi)	Elongation[1] (%)	Pressure (Torr)										
Rene' 41	R	-	-	-	-	-	182.0	-	114.0	-	34.0	-	31.8	362	292, 315
		1800	None	None	760	-	175.0	3.8	111.0	2.7	15.0	56.0	33.8	557	522, 530
		1800	1.0	2.5	760	1.14	171.5	5.8	114.4	None	15.0	56.0	31.3		
		1800	1.95	5.3	760	2.41	152.5	16.2	113.3	0.6	10.0	70.5	32.0	468	468, 416
		2000	0.63	6.3	760	2.86	141.2	22.4	76.6	32.8	20.0	41.2	32.0		(Alloy depletion layer)
		2000	1.0	11.9	760	5.41	136.6	24.9	99.7	12.5	6.5	80.1	31.1	506	422, 406, 223, 178
Inconel 718	R	-	-	-	-	-	132.0	-	64.8	-	39.0	-	28.0	241	157, 197
		1800	1.5	2.8	760	1.11	117.3	11.1	65.3	None	18.0	54.0	31.9	388	279, 344
		1800	2.25	6.3	760	2.27	Specimen ruptured after 19.5 cycles								
		2000	1.0	4.4	760	1.77	72.5	45.1	39.6	38.9	16.0	59.0	25.4	322	196, 206

1. The elongation was measured by LVDT over the entire specimen length and not in the gage length but percent elongation was calculated over the gage length.

2. The hardness values determined at one mil below the edge or at the alloy depletion layer are lower than those at the center because of the edge effect.

R - As received.

Test direction - Transverse.

For calculation of F_{tu}, F_{ty}, and E values the original area of cross-section of the as-received specimen was used.

TABLE XXIX

RESULTS OF MISSION PROFILE SIMULATION TESTS FOR INCONEL 625 AND HAYNES 25 FOIL (0.01 in. THICK)

Superalloy	Condition					Creep Rate (10^{-3} in./in./hr)	Room Temperature Tensile Test Data							Microhardness Values (KHN 200-gram load)	
	R	22-Cycle Simulated Profile Exposure					F_{tu} (ksi)	Loss in F_{tu} (%)	F_{ty} (ksi)	Loss in F_{ty} (%)	Total Elongation (% in 1.0 in.)	Loss in Elongation (%)	E - Elastic Modulus ($\times 10^3$ ksi)	Center	Edges
		T_{max} (°F)	Stress (ksi)	Elongation[1] (%)	Pressure (Torr)										
Inconel 625	R	-	-	-	-	-	136.0	-	68.0	-	49.0	-	28.5	241	208, 228
		1800	None	None	760	-	133.6	2.2	60.4	1.1	40.0	18.0	34.6	434	422, 441
		1800	2.55	1.25	760	0.50	110.2	19.0	66.1	3.1	19.0	61.2	36.2		
		1800	4.25	3.5	760	1.59	132.5	2.6	66.1	3.1	-	-	36.2	454	410, 372
		1800	2.55	3.9	0.18	1.57	129.5	5.0	63.7	6.3	46.0	6.12	32.9	399	410, 362
		1800	4.25	12.4	0.18	5.0	113.5	16.5	59.6	12.4	26.0	46.9	28.8		
		1800	2.55	2.1	10.0	0.7	133.0	2.26	69.4	None	47.0	4.1	32.6	461	441, 422
		1800	4.25	10.0	10.0	4.1	129.0	5.15	62.1	8.7	42.0	14.3	30.5		
		1800	5.1	5.3	760	-	Specimen ruptured after 12.5 cycles								
		2000	1.0	3.5	760	1.75	116.2	14.5	51.1	24.8	29.0	40.8	30.2	388	226, 272
		2000	1.5	7.2	760	3.0	105.4	22.5	49.3	27.5	19.0	61.0	32.1		
Haynes 25	R	-	-	-	-	-	153.0	-	72.1	-	49.0	-	34.2	322	217, 303
		1800	7.25	3.0	760	1.25	93.8	39.5	67.0	7.1	10.0	79.7	32.5	388	362, 353
		1800	8.7	7.5	760	-	Specimen ruptured after 16.5 cycles								
		2000	None	None	760	-	148.0	3.3	65.1	9.7	23.0	53.1	46.3	566	548, 586
		2000	1.0	1.15	760	0.52	143.2	6.4	62.7	13.1	55.0	None	35.8		
		2000	1.45	2.0	760	0.91	115.1	24.8	62.9	13.0	18.0	63.3	34.8		
		2000	2.9	5.3	760	2.4	77.0	49.7	61.5	14.7	2.0	95.9	33.5	377	276, 246
		2000	1.0	2.7	0.18	0.9	133.0	13.1	58.3	19.1	50.0	None	-	475	434, 468
		2000	1.45	?	0.18	-	131.0	13.7	57.4	20.4	44.0	10.2	-		
		2000	2.9	11.5	0.18	-	Specimen ruptured after 13.5 cycles								
		2000	1.0	1.8	10.0	0.7	144.0	5.9	61.5	14.7	53.0	None	36.6	514	410, 422
		2000	1.45	3.2	10.0	1.43	140.5	8.2	63.8	11.5	47.0	4.1	34.4		
		2000	2.9	7.9	10.0	-	Specimen ruptured after 19.5 cycles								

1. The elongation was measured by LVDT over the entire specimen length and not in the gage length, but percent elongation was calculated over the gage length.

R - As received

Test direction - Transverse

For calculation of F_{tu}, F_{ty}, and E values, original area of cross-section of the as-received specimen was used.

TABLE XXX

RESULTS OF MISSION PROFILE SIMULATION TESTS FOR TD NICKEL AND TD NICKEL/CHROMIUM FOILS

Superalloy	Condition					Creep Rate (10^{-3} in./in./hr)	Room Temperature Tensile Test Data							Microhardness Values (KHN 200-Gram load)	
	R	22-Cycle Simulated Profile Exposure					F_{tu} (ksi)	Loss in F_{tu} (%)	F_{ty} (ksi)	Loss in F_{ty} (%)	Total Elongation (% in 1.9 in.)	Loss in Elongation (%)	E - Elastic Modulus (-10^3 ksi)	Center	Edges
		T_{max} (°F)	Stress (ksi)	Elongation[1] (%)	Pressure (Torr)										
TD Nickel	R	-	-	-	-	-	71.5	-	53.3	-	11.0	-	20.9	194	169, 180
		2000	5.0	0.98	760	0.44	70.8	1.0	55.5	None	3.7	66.9	23.6		
		2000	6.0	1.95	760	0.88	53.4	25.3	53.4	None	2.0	81.5	25.2	226	206, 206
		2000	4.0	1.0	0.18	0.45	77.0	None	58.9	None	13.7	None	23.4		
		2000	5.0	2.1	0.18	0.95	75.7	None	57.0	None	12.0	None	22.4	243	193, 198
		2000	6.0	0.6	0.18	-	Specimen ruptured after 9.5 cycles								
		2000	4.0	1.0	10.0	0.45	72.0	None	54.6	None	-	-	21.6		
		2000	5.0	1.2	10.0	0.54	75.0	None	57.4	None	10.5	4.5	27.1	231	194, 204
		2000	6.0	1.8	10.0	-	Specimen ruptured after 8.3 cycles								
		2200	0.25	0.4	760	-	59.0	17.5	52.6	1.3	1.7	84.0	29.2		
		2200	4.0	3.7	760	1.68	Specimen ruptured after 16.5 cycles								
		2200	3.0	2.6	760	1.18	52.7	26.0	52.2	0.2	2.5	77.0	23.9		
		2200	2.0	2.4	760	1.09	54.7	23.5	45.6	14.4	3.0	73.0	21.0		
		2200	3.0	1.6	0.18	0.73	65.5	8.4	63.5	None	8.0	27.3	26.1		
		2200	2.0	1.3	0.18	0.59	65.6	8.3	53.5	None	9.0	18.1	26.9		
		2200	3.0	1.5	10.0	0.68	66.4	7.1	54.0	None	4.0	63.6	23.7	230	214, 214
		2200	2.0	1.2	10.0	0.54	61.4	14.1	53.0	None	2.0	81.8	-		
TD Nickel/ Chromium	R	-	-	-	-	-	143.0	-	98.9	-	14.0	-	27.4	348	215, 215
		2000	10.0	0.5	760	0.23	106.5	25.5	100.0	None	0.8	94.3	30.6	299	279, 212
		2000	12.0	2.2	760	1.0	40.3	Crack initiated specimen failure during tensile test							
		2000	14.0	3.36	760	1.53	44.5	Crack initiated specimen failure during tensile test							
		2000	6.0	0.0	0.18	-	133.0	7.0	92.0	7.0	10.0	28.6	32.6		
		2000	8.0	1.1	0.18	0.5	120.0	16.1	92.6	6.4	4.0	71.4	30.6	353	331, 344
		2000	10.0	1.8	0.18	-	Specimen ruptured after 6.5 cycles								
		2000	8.0	0.7	10.0	0.32	120.4	16.4	83.5	15.6	10.0	28.6	25.4	404	377, 367
		2000	10.0	2.3	10.0	1.5	Specimen ruptured after 20.5 cycles								
		2200	None	None	760	-	124.9	12.7	86.4	12.6	7.0	50.0	30.4	393	339, 358
		2200	4.0	0.9	760	0.41	92.2	42.0	-	-	1.4	90.0	29.0		
		2200	6.0	1.6	760	0.73	66.7	52.5	-	-	2.0	85.6	24.7		
		2200	4.0	0.9	0.18	0.41	128.8	11.0	74.8	24.4	13.0	7.7	21.6		
		2200	6.0	1.42	0.18	0.64	100.8	29.5	76.5	22.6	5.0	64.0	27.3		
		2200	4.0	0.8	10.0	0.36	117.2	18.0	85.3	13.9	7.0	50.0	36.5		
		2200	6.0	1.5	10.0	0.68	110.0	23.1	64.4	34.9	-	-	23.8		
		2400	2.0	0.5	760	0.23	91.0	36.4	78.1	21.0	2.0	8.6	24.4	315	307, 311
		2400	2.0	1.0	0.18	0.45	124.0	13.3	77.3	21.8	18.0	None	25.0	340	301, 331
		2400	2.0	0.7	10.0	0.32	126.8	11.3	77.8	21.3	15.5	None	29.3	358	359, 348

1 The elongation was measured by LVDT over the entire specimen length and not in the gage length but percent elongation was calculated over the gage length.
R - As received
Test direction - Transverse
For calculation of F_{tu}, F_{ty}, and E values, original area of cross-section of the as-received specimen was used.

TABLE XXXI

RESULTS OF 100 ONE-HOUR CYCLE MISSION PROFILE SIMULATION TESTS FOR THE FOUR SUPERALLOY FOILS

Superalloy	Condition: R	Simulated Profile Exposure for 100 One-Hour Slow Cycles: T_{max} (°F)	Stress (ksi)	Elongation[2] (%)	Pressure (Torr)	Room Temperature Tensile Test Data: F_{tu} (ksi)	Loss in F_{tu} (%)	F_{ty} (ksi)	Loss in F_{ty} (%)	Total Elongation (%): (in 1.0 in.)	Total Elongation (%): (in 2.0 in.)	Loss in Elongation (%)	E - Elastic Modulus (-10^3 ksi)	Microhardness Values (KHN 200-gram load): Center	Microhardness Values (KHN 200-gram load): Edges[3]
Inconel 625	R	-	-	-	-	136.0	-	68.0	-	49.0	-	-	28.5	249	246, 228
	(1)	1800	None	None	760	135.8	Negligible	64.9	4.6	-	42.7	-	30.2	279	243 212
		1800	2.55	17.7	760	66.1	51.4	49.1	27.8	4.0	-	91.8	17.6	276	266, 269
	(1)	1800	None	None	0.18	130.3	4.2	63.2	-	-	43.0	-	30.7	266	263, 269
		1800	2.55	21.0	0.18	94.5	30.5	57.5	15.4	15.0	-	69.4	23.2	311	315, 322
Haynes 25	R	-	-	-	-	153.0	-	72.1	-	49.0	-	-	34.2	303	272, 266
		1800	2.9	7.1	0.18	141.0	7.8	59.8	17.0	34.0	-	30.6	24.4	539	548, 514
	(1)	2000	None	None	0.18	125.7	17.8	55.0	23.7	-	37.5	-	30.7	219	157, 152
		2000	1.0	9.6	0.18	Specimen ruptured after 65.5 cycles								288	173, 263
TD Nickel	R	-	-	-	-	71.5	-	53.3	-	11.0	-	-	20.9	246	200, 210
	(1)	2200	None	None	760	41.2	42.4	40.0	25.0	-	2.25	-	26.0	214	200, 226
		2200	1.0	9.0	760	28.2	60.5	28.0	47.5	0.5	-	95.4	23.3	196	196, 198
TD Nickel Chromium	R	-	-	-	-	143.0	-	98.9	-	14.0	-	-	27.4	348	215, 215
	(1)	2400	None	None	760	125.3	12.4	77.0	22.1	-	11.7	-	28.2	353	292, 315
		2400	2.0	4.9	760	Specimen ruptured after 98.5 cycles									
	(1)	2400	None	None	0.18	115.0	19.6	81.6	17.5	-	8.0	-	22.5	353	335, 348
		2400	2.0	1.0	0.18	122.3	14.5	106.0	None	12.0	-	14.3	31.0	353	344, 348

1. Cyclic oxidation exposures in the MGR furnace with no stress.
2. The elongation was measured by LVDT over the entire specimen length, but percent elongation was calculated over the gage length.

   R - As received

   Test direction - Transverse except longitudinal for TD Nickel/chromium
3. The hardness values determined at one mil below the edge or at the alloy depletion layer are lower than those at the center because of the edge effect.

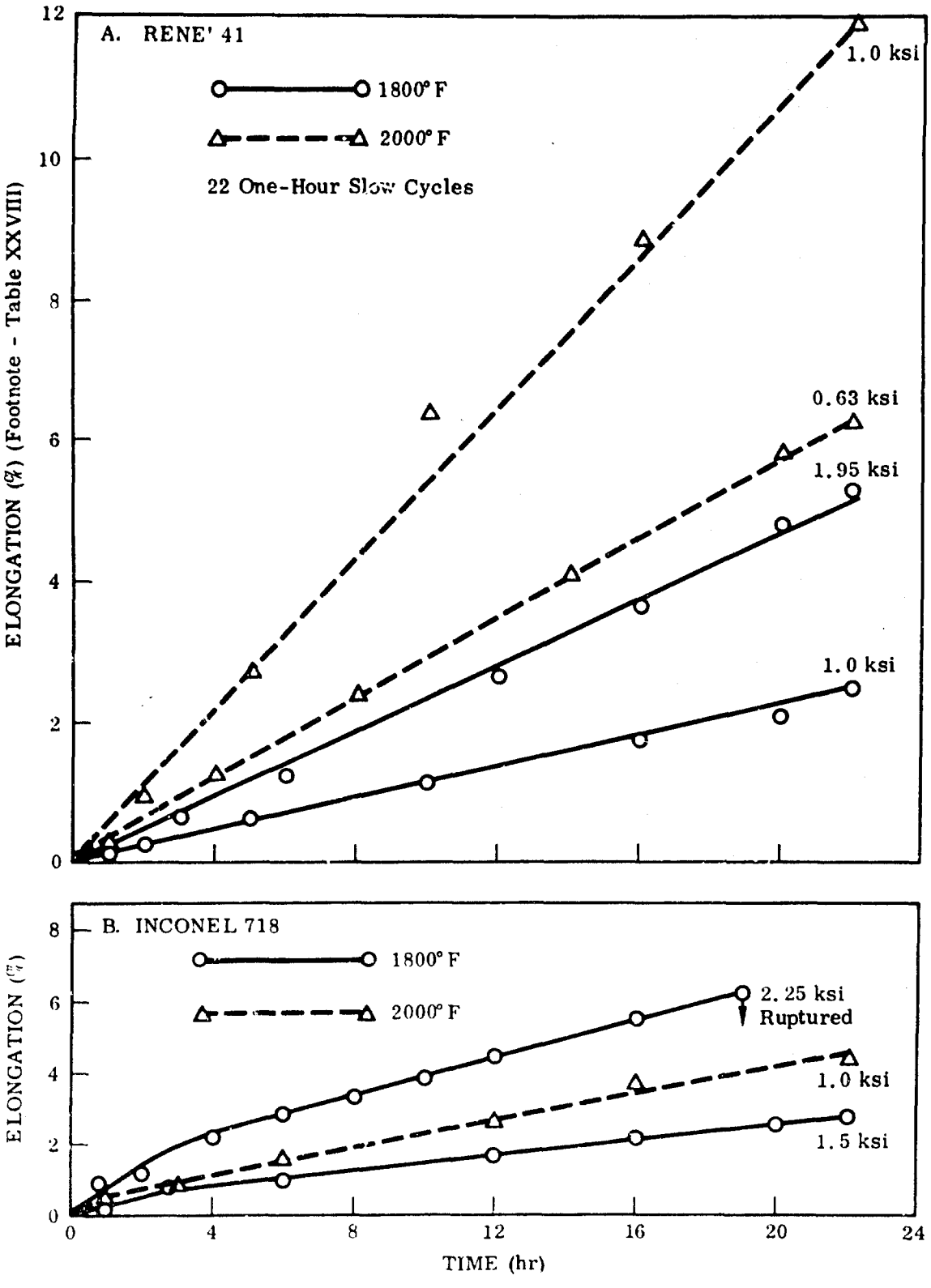

FIGURE 35. PERCENT ELONGATION VERSUS TIME FOR RENE' 41 AND INCONEL 718 FOILS DUE TO 730 TORR SIMULATED PROFILE EXPOSURES

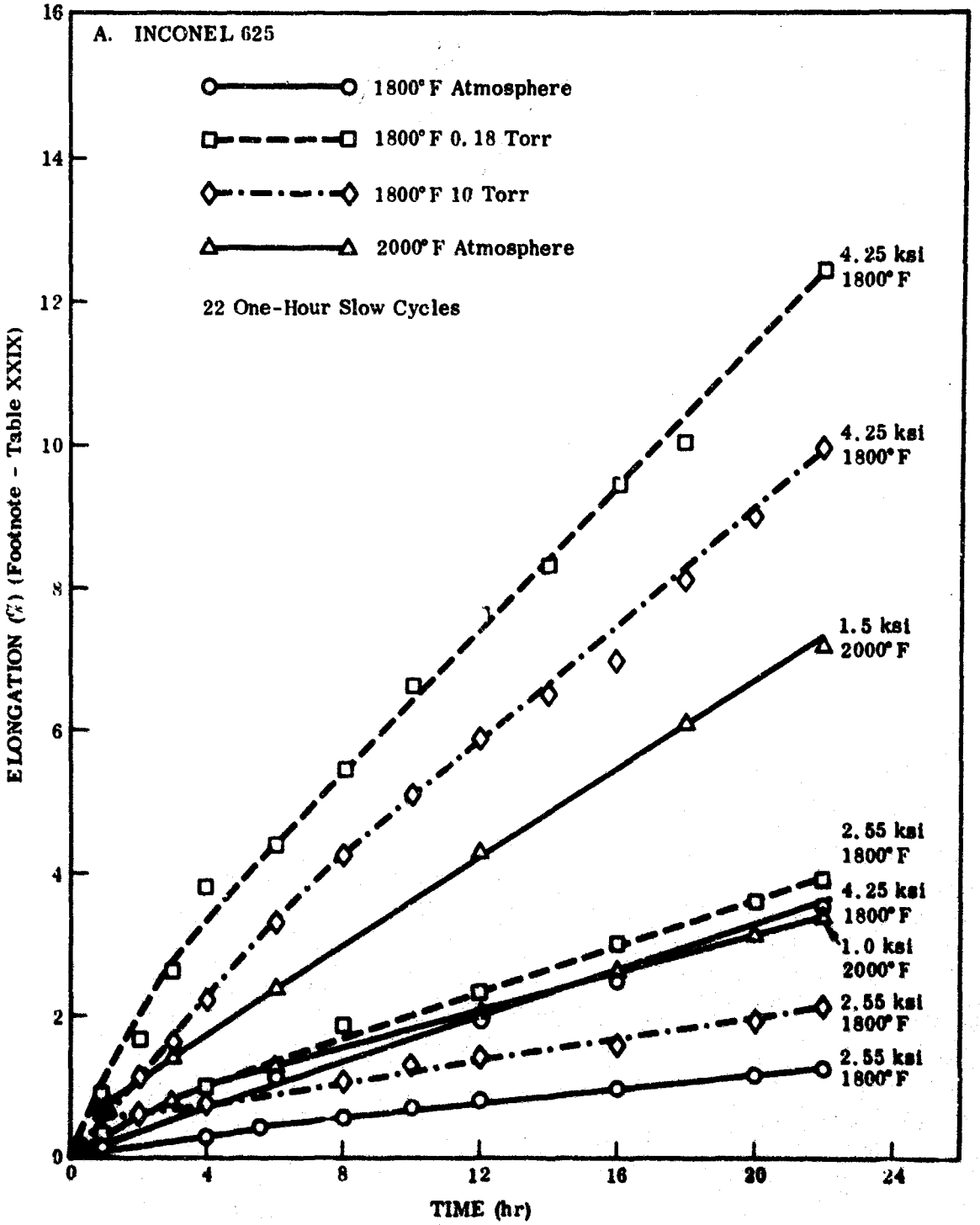

FIGURE 36. PERCENT ELONGATION VERSUS TIME FOR INCONEL 625 AND HAYNES 25 FOILS DUE TO SIMULATED PROFILE EXPOSURES (Sheet 1 of 2)

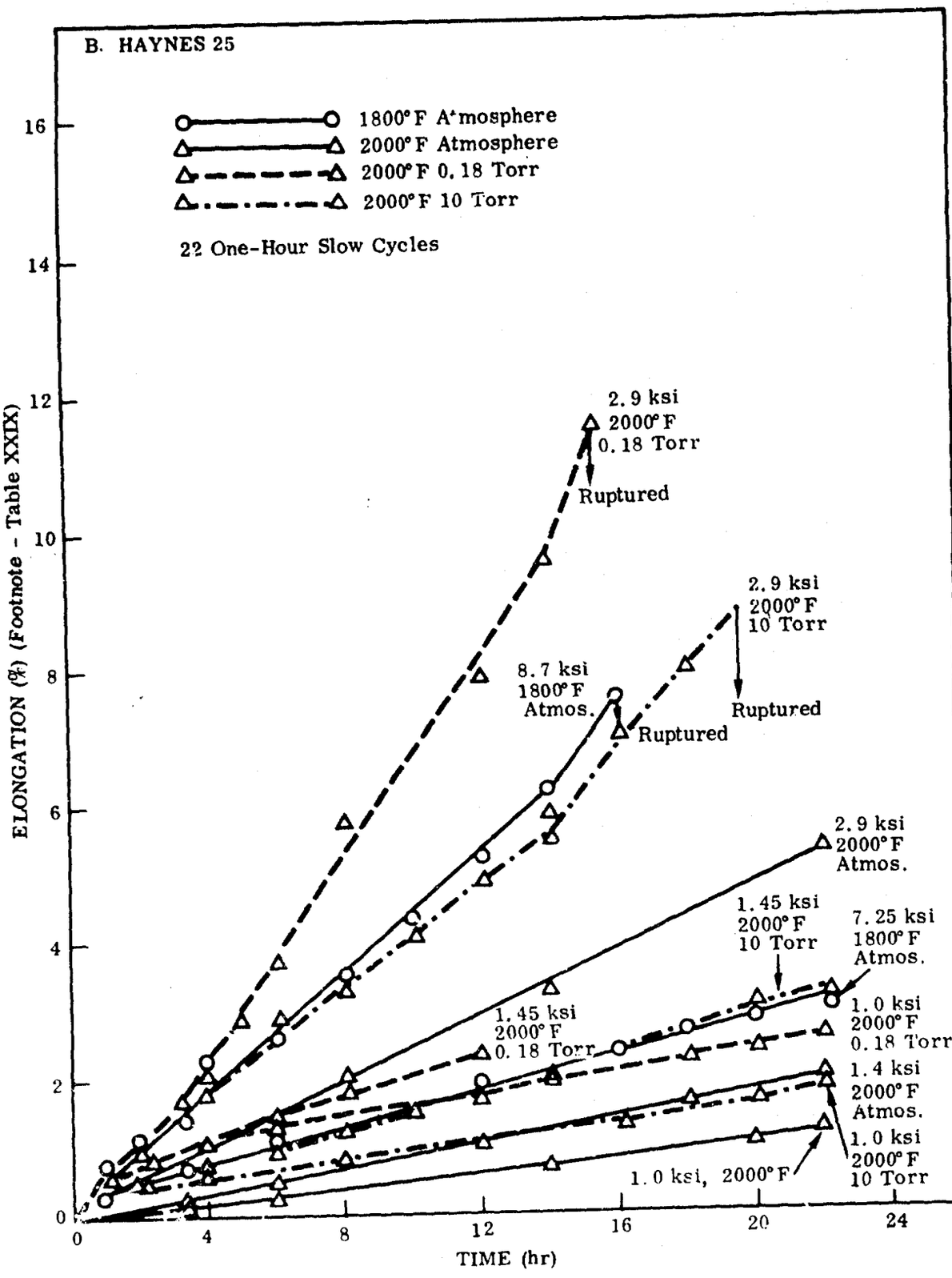

FIGURE 36. PERCENT ELONGATION VERSUS TIME FOR INCONEL 625 AND HAYNES 25 FOILS DUE TO SIMULATED PROFILE EXPOSURES
(Sheet 2 of 2)

rate values (Table XXVIII) were based on elongation in the entire length of the test specimen as measured by a LVDT and were not corrected to correspond to elongation in the gage length of the test specimen as in isothermal creep testing (Table VII). Therefore, the creep rate values in mission profile simulation tests (Tables XXVIII, XXIX, and XXX) cannot be compared with those in Table VII.

The percent loss in room temperature F_{ty} for Rene' 41 and Inconel 718 was negligible (2.7 percent) for the 1800°F profile exposure, and 33 percent or higher for the 2000°F profile (Table XXVIII). There was also considerable loss in percent elongation values. For Rene' 41, increasing stress resulted in increasing loss in F_{tu} and elongation. However, the major loss in elongation is believed to be the result of oxidation effects rather than applied stress, since a 56 percent loss in elongation occurred after the 1800°F simulated mission profile exposure without stress (Table XXVIII).

For Rene' 41 and Inconel 718, the oxidation effects on the microstructure after a simulated profile exposure were similar, but less pronounced than those after the MGR cyclic oxidation exposures described in Paragraph 4.4.1. (Compare Figures 36 and 26 for Rene' 41 and Figures 37 and 27 for Inconel 718.) In the case of Rene' 41 the thickness (0.5 mil) of oxide plus the alloy depletion layer resulting from a 22-cycle simulated profile exposure at 1800°F (Fig. 36) was almost half that after a 100-cycle profile oxidation exposure at 1800°F T_{max} (Fig. 26). Intergranular oxidation attack along the edges was also reduced. The decrease in attack is most likely due to the lower number of cycles, 22 versus 100. The applied stress did not appear to accelerate attack or μ phase formation (Ref. 11).

The Rene' 41 and Inconel 718 foils were appreciably hardened by the simulated profile exposures with T_{max} of 1800 or 2000°F (Table XXVIII). This condition, as explained in Paragraph 4.4.1, could be an aging effect resulting in the formation of γ'-Ni_3(Al, Ti) precipitate in the case of Rene' 41 or of Ni_3 (Cb, Ti) for Inconel 718. The lower hardness of Inconel 718 after the 2000°F T_{max} profile as compared to the hardness after the 1800°F profile is probably the result of dissolution of Ni_3 (Cb, Ti) at temperatures higher than 1800°F (para 4.4.1). The hardness values after the 22 one-hour cycle simulated profile exposures (Table XXVIII) were greater than those after the 100 one-hour slow-cycle MGR oxidation exposure (Table XX).

4.5.2 Profile Simulation Test Results for Inconel 625 and Haynes 25 Alloys

The 22 one-hour slow-cycle atmospheric pressure profile simulation tests for Inconel 625 and Haynes 25 were conducted at two different T_{max}, 1800 and 2000°F (Table XXIX). The reduced pressure (0.18 and 10 Torr) tests were conducted at one T_{max} only, i.e., the recommended maximum service temperature, 1800°F for Inconel 625 and 2000°F for Haynes 25. One hundred one-hour slow-cycle simulated profile

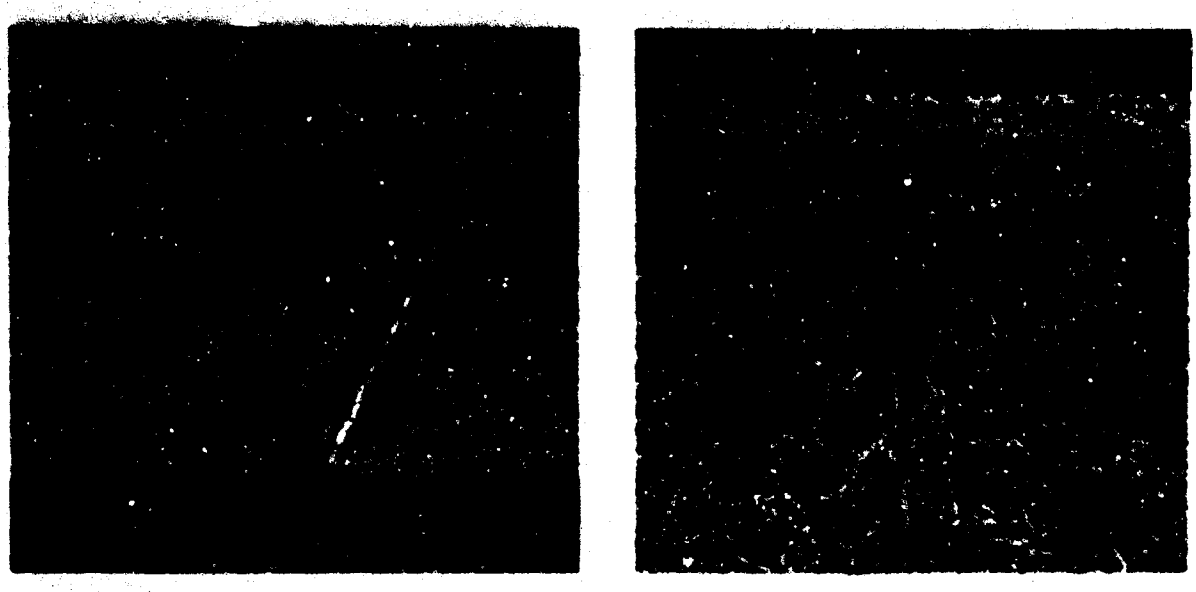

Magnification: 200X

Oxidized 1800°F
760 Torr
Stress: 195 ksi

Magnification 500X

FIGURE 37. MICROSTRUCTURE OF RENE' 41 AFTER SIMULATED MISSION PROFILE EXPOSURE

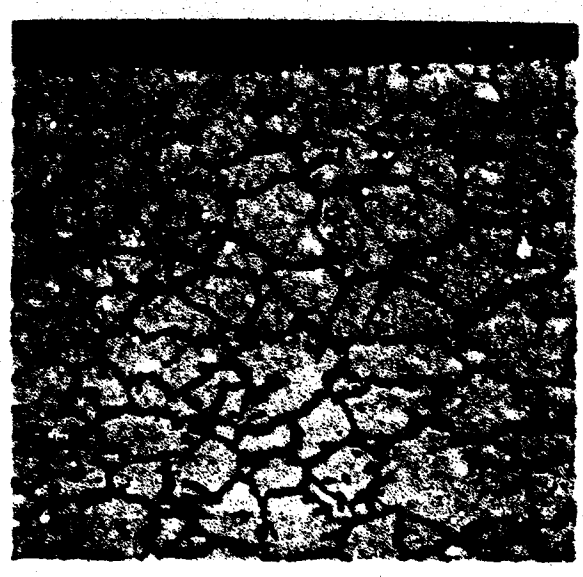

Oxidized 1800°F
Stress: 1.5 ksi
22 Cycles

Magnification: 50X

FIGURE 38. MICROSTRUCTURE OF INCONEL 718 AFTER SIMULATED MISSION PROFILE EXPOSURE

tests at a T_{max} of 1800°F and at 760 and 0.18 Torr pressures for Inconel 625 and at T_{max} of 1800 and 2000°F and 0.18 Torr pressure for Haynes 25 (Table XXXI).

The creep rate for Inconel 625 was higher than that for Haynes 25 at simulated profiles of 760 Torr with T_{max} of 1800 or 2000°F (Table XXIX and Fig. 38). The two matrix strengthened alloys exhibited higher creep rate than the two thoria dispersion strengthened alloys in the mission profile simulation tests as well as in isothermal creep tests (para 4.1). The creep rate for the Inconel 625 and Haynes 25 alloys increased with increasing temperature or increasing stress, and also with a decrease in environmental pressure. The creep rate (or percent elongation) was highest after simulated mission profile exposure at the lowest pressure, 0.18 Torr; the other exposure conditions (profile characteristics, T_{max}, 22 cycles, and applied stress) remaining constant (Table XXIX and Fig. 38). In the case of rupture, the stress rupture time was least at 0.18 Torr. The increase in creep rate with decrease in pressure could be, in part, a result of temperature differences in 760, 10.0, and 0.18 Torr pressures and may not be truly a pressure effect. Temperature calibration indicates that T_{max} may have been 15 to 20 degrees F higher in low pressure tests (para 3.6).

The maximum stress that Inconel 625 can withstand without rupture is between 4.2 and 5.0 ksi at an exposure of 1800°F (T_{max}) for 22 one-hour cycles (Table XXIX). The maximum stress that could be applied to Haynes 25 for 2000°F T_{max} profile for 22 one-hour cycles is greater than 1.45 ksi but less than 2.9 ksi.

The overall loss in room temperature tensile properties (F_{tu}, F_{ty}, and percent elongation) for both Inconel 625 and Haynes 25 was less at 10 Torr than at 760 or 0.18 Torr during the simulated profile exposures with T_{max} of 1800 and 2000°F respectively. Maximum loss in percent elongation (or embrittling) of the two alloys occurred as a result of 760 Torr mission profile exposure.

The 1800°F - 760 Torr - 22-cycle mission profile with no applied stress resulted in 18 percent loss in elongation and negligible loss in F_{tu} and F_{ty} values as compared to as-received tensile properties of Inconel 625. The 2000°F - 760 Torr - 22-cycle mission profile with zero stress caused much higher loss (53 percent) in elongation, but less than 10 percent loss in F_{tu} and F_{ty} values for Haynes 25. Thus, the mission profile with no load resulted principally in loss of ductility. With increasing applied stress, the degradation in room temperature tensile properties was higher (Table XXIX). The decrease in F_{tu} or F_{ty} values and further reduction in ductility was primarily the result of the permanent elongation in the specimen due to application of load.

The microstructure of Inconel 625 after various environmental exposures exhibited oxidation effects similar to those after cyclic oxidation exposure: oxidation attack along grain boundaries, decarburization, slight grain growth, and the formation of an alloy depletion layer (para 4.4.1). For Haynes 25, there were intergranular cracks along the edges, their number and size increased with increasing profile T_{max} and with decreasing environmental pressure (Fig. 39A, B, C, and D). The decarburization for both Inconel 625 and Haynes 25 appeared to be maximum after the 760 Torr exposure. Haynes 25 displayed internal carbide precipitation; the size of carbide particles was found to increase with decreasing pressure for the 2000°F - 22-cycle simulated profile exposures (Fig. 39B, C, and D). The percent of carbides from microstructural analyses was about the same after 0.18 or 10.0 Torr exposures (Fig. 39C and D). After the low-pressure (10.0 Torr or 0.18 Torr) 2000°F - 22-cycle exposure, the carbide precipitates were mostly at the grain boundaries (Fig. 39C and D). Recrystallization twins were present after different mission profile exposures. The elongation of grains, especially in the longitudinal direction due to the applied stress, is evident from the microstructures. The elongation of grains was maximum after 0.18 Torr exposure. The needles of an unidentified phase were present within the grains in the microstructure of Haynes 25 after 0.18 Torr - 2000°F exposure (Fig. 39D).

The Inconel 625 and Haynes 25 were appreciably hardened by the simulated profile exposures, possibly the result of internal oxidation (para 4.4.2) or aging effects. For Inconel 625, the increase in microhardness values after the 2000°F T_{max} profile exposure was less than after the 1800°F T_{max} exposure, and may be the result of a decrease in the N content (para 4.4.2) or to dissolution of γ'.

Simulated Profile Exposures for 100 One-Hour Slow Cycles for Inconel 625 and Haynes 25.

For Inconel 625, large elongation values of 17.7 or 21 percent were obtained after a simulated profile exposure of 100 one-hour slow-cycles with a T_{max} of 1800°F at 760 or 0.18 Torr, respectively (Table XXXI). The elongation and oxidation of the specimen resulted in considerable loss in room temperature F_{tu} and percent elongation values for Inconel 625. The loss in room temperature F_{ty} was less than 33 percent. In general, the loss in room temperature tensile properties after oxidation exposure has been shown to be higher than the loss in high-temperature properties (para 4.3.1). Therefore, Inconel 625 can be still considered satisfactory for service at 1800°F for a stress of at least 2.5 ksi. The most severe pressure condition for Inconel 625 was found to be 760 Torr. Effects on microstructure were similar to those discussed in Paragraph 4.4.1. The Inconel 625 foil was slightly hardened, but the increase in hardness after the 100-cycle profile exposure was less than that after the 22-cycle profile exposure, which could be caused by dissolution of γ' in extended time (100 cycles).

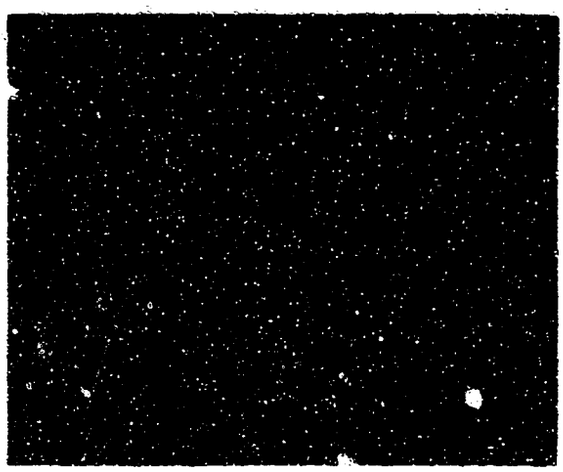

Magnification: 500X

A. Test Direction - Transverse
Oxidized 1800° F
760 Torr
7.25 ksi
22 Cycles
3.0 Percent elongation

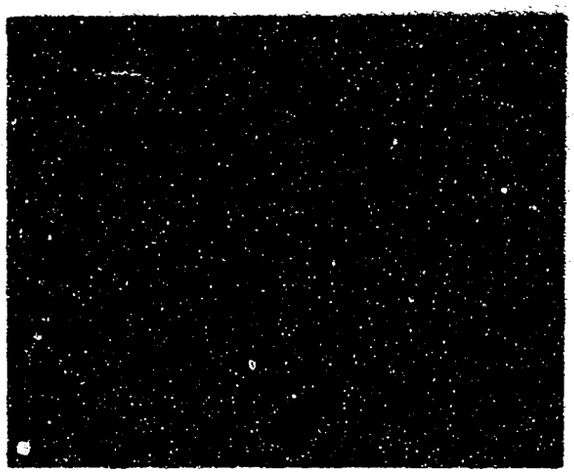

Magnification: 500X

B. Test Direction - Transverse
Oxidized 2000° F
760 Torr
2.9 ksi
22 Cycles
5.3 Percent elongation

Test Direction - Transverse

Magnification: 500X

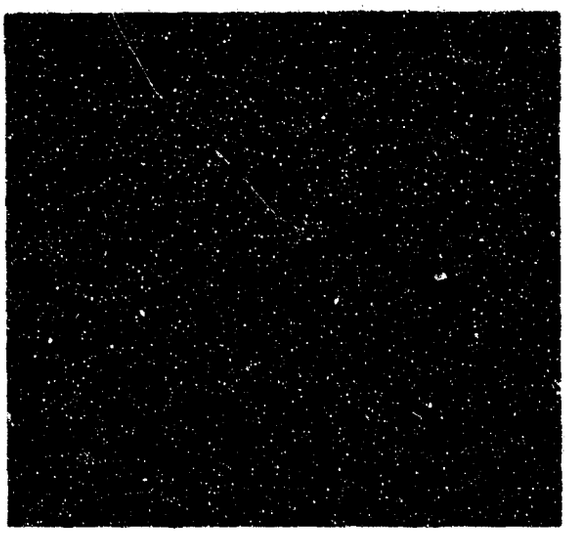

Test Direction - Longitudinal

C. Oxidized 2000° F
10.0 Torr
1.0 ksi
22 Cycles
1.8 Percent elongation

FIGURE 39. MICROSTRUCTURE OF HAYNES 25 FOIL AFTER SIMULATED MISSION PROFILE EXPOSURE (Sheet 1 of 2)

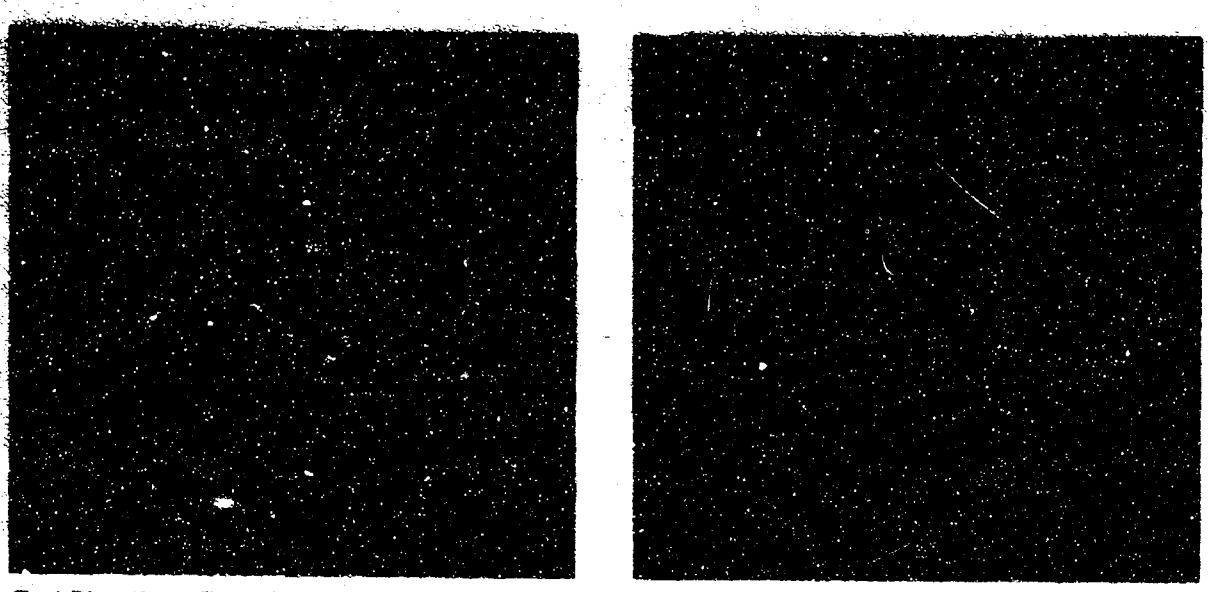

Test Direction - Transverse Magnification: 500X Test Direction - Longitudinal

D. Oxidized 2000° F
0.18 Torr
1.0 ksi
22 Cycles
2.7 Percent elongation

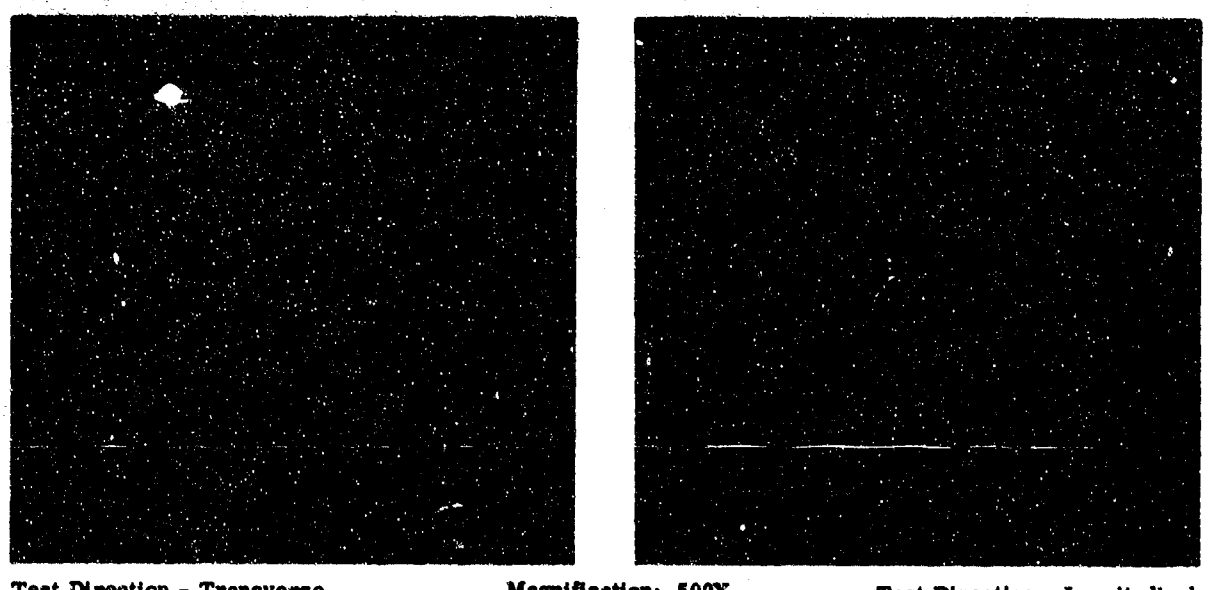

Test Direction - Transverse Magnification: 500X Test Direction - Longitudinal

E. Oxidized 1800° F
0.18 Torr
2.9 ksi
100 Cycles
7.0 Percent elongation

FIGURE 39. MICROSTRUCTURE OF HAYNES 25 FOIL AFTER SIMULATED MISSION PROFILE EXPOSURE (Sheet 2 of 2)

For Haynes 25, the 2000°F mission profile exposure at the most severe pressure (0.18 Torr) and a stress of one ksi caused specimen rupture after 65.5 one-hour slow cycles. Therefore, Haynes 25 is not satisfactory for service at 2000°F. The 1800°F - 0.18 Torr - 100-cycle - 2.9 ksi mission profile exposure resulted in creep of seven percent and a loss in room temperature properties of 17 percent in F_{ty} and 30.6 percent in elongation. Thus, the recommended maximum service temperature for Haynes 25 is 1800°F and not 2000°F.

The microstructure of Haynes 25 after the 1800°F - 0.18 Torr - 100-cycle - 2.9 ksi simulated profile exposure in both longitudinal and transverse directions are shown in Figure 39E. This profile exposure resulted in grain growth, internal precipitation of carbides, cracking along the edges, and intergranular oxidation attack. The cracks were wider in the longitudinal microstructure than in the transverse direction (Fig. 39D and E). Recrystallization twins were present. In addition, there were needles of an unidentified phase (probably Co_3W) within the grains (Fig. 39E). The presence of this phase is also indicated by an increase in the hardness value from 303 to 539 KHN (Table XXXI). The unidentified phase was not observed after the 22-cycle mission profile exposure with T_{max} of 1800°F at 760 Torr, or with T_{max} of 2000°F at 760 Torr or 10.0 Torr (Fig. 39A, B, and C), or after a 100-cycle MGR unstressed oxidation exposure at T_{max} of 1800, 2000, or 2100°F (Fig. 29). The unidentified phase was present after the 0.18 Torr - 2000°F - 22-cycle mission profile exposure (Fig. 29). This presence indicates that the unidentified phase only formed after 0.18 Torr exposure in the stressed condition. Thus it was found that Haynes 25 is stress sensitive and that 0.18 Torr is the most severe pressure condition.

4.5.3 Profile Simulation Test Results for TD Nickel and TD Nickel/Chromium Alloys

The 22 one-hour slow-cycle profile simulation tests were conducted at three different pressures (760, 0.18, and 10.0 Torr) and T_{max} of 2000 and 2200°F for TD Nickel and T_{max} of 2000, 2200, and 2400°F for TD Nickel/chromium (Table XXX). One hundred one-hour slow-cycle mission profile tests at T_{max} of 2200°F in 760 Torr pressure for TD Nickel and at T_{max} of 2400°F in 0.18 Torr pressure for TD Nickel/chromium were also performed (Table XXXI).

The creep rate for TD Nickel was higher than that of TD Nickel/chromium for different mission profiles with T_{max} of 2000 and 2200°F (Table XXX). The two dispersion strengthened alloys exhibited lower creep rate than the two solid solution strengthened alloys or the two precipitation hardened alloys (Tables XXVIII, XXIX, and XXX). Among the six superalloys, the creep rate for TD Nickel/chromium was the lowest. Increasing temperature or stress resulted in a higher creep rate (Table XXX). No definate increase in creep rate with decrease in environmental pressure was noted for the

TD Nickel or TD Nickel/chromium alloys during mission profile exposures with T_{max} of 2000 or 2200°F (Table XXX). But for the 2000°F - 5 ksi - 22-cycle profile exposure for TD Nickel, the highest creep rate occurred during the 0.18 Torr exposure (Table XXX). In the case of TD Nickel/chromium for the 2400°F T_{max} profiles, the highest creep rate occurred during the 0.18 Torr exposure.

The overall loss in room temperature F_{tu} and F_{ty} values of TD Nickel after the different mission profile exposures for 22 cycles with T_{max} of 2000 or 2200°F was less than 33 percent (Table XXX). Loss in elongation values was considerable. The maximum stress to which TD Nickel can be subjected is five and three ksi for simulated mission profile exposures with T_{max} of 2000 and 2200°F, respectively.

Microstructural examination after testing revealed the formation of NiO at the surface and in increase in hardness. The thickness of the oxide formed and of the unoxidized substrate after the different exposures are given in following tabulation.

22-Cycle Simulated Profile Exposure	Thickness (t) of the Oxide/side (mil)	Thickness of the Substrate (T) (mil)
2000°F - 760 Torr - 6 ksi	0.75	9.2
2000°F - 10 Torr - 5 ksi	0.5	9.9
2000°F - 0.18 Torr - 5 ksi	Negligible	10.3
2200°F - 10 Torr - 3 ksi	0.9	8.7

The thickness of the NiO formed was greater at higher temperatures as well as at higher pressures. During the 0.18 Torr - 2000°F - 22-cycle - 5 ksi simulated profile exposure there was negligible oxide formation.

The TD Nickel/chromium alloy exhibited less than 33 percent loss in room temperature F_{ty} or F_{tu} after various simulated mission profile exposures for 22 cycles with T_{max} of 2000, 2200, or 2400°F (except for the 36.4 percent loss in room temperature in F_{tu} after 2400°F - 760 Torr - 2 ksi exposure). Considerable loss in room temperature elongation values occurred (Table XXX). But the loss in tensile properties at elevated temperature would be expected to be much less than that at room temperature. Therefore, the TD Nickel/chromium alloy is considered satisfactory for service at temperatures up to 2400°F for 22 cycles of simulated profile exposure. Based on the data contained in Table XXX, the minimum stresses that can be applied to TD Nickel/chromium foil are eight, six, and two ksi for the 22-cycle mission profile exposure at 2000, 2200, and 2400°F, respectively. The effects of the mission profile exposure on the microstructure of TD Nickel/chromium were similar to those of the cyclic oxidation exposure (para 4.1). There was an increase in the microhardness values after the simulated profile exposures (Table XXX).

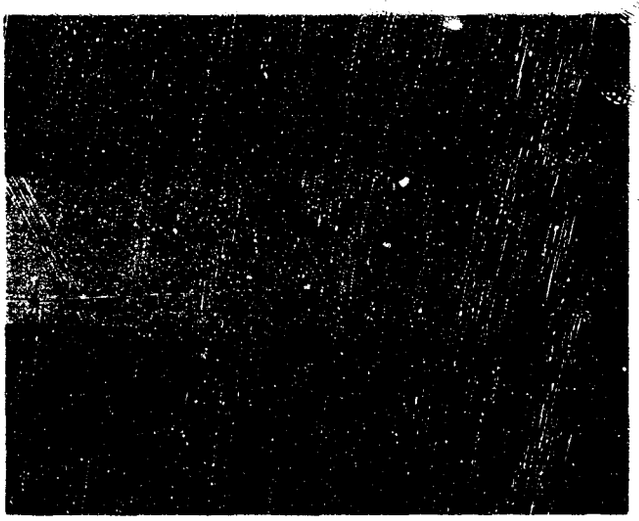

Test Direction - Longitudinal

Oxidized 2200°F
1.0 ksi
760 Torr
100 Cycles
(9.0 Percent elongation)

Magnification: 500X

FIGURE 40. MICROSTRUCTURE OF TD NICKEL FOIL AFTER MISSION PROFILE EXPOSURE

Mission Profile Exposures for 100 One-Hour Slow Cycles for TD Nickel and TD Nickel/Chromium

The 2200°F - 1 ksi - 760 Torr - 100-cycle mission profile exposure for TD Nickel resulted in a nine percent elongation in the specimen and considerable loss in F_{ty} (47.5 percent), F_{tu} (60.5 percent), and elongation (95.4 percent) (Table XXXI). The thickness of the adherent NiO formed was about 3.0 mils and that of the substrate was 5.0 mils (Figure 40). Thus, 50 percent of the cross section area of TD Nickel foil was oxidized; whereas, after the unstressed 2200°F - 760 Torr - 100-cycle MGR exposure, only 25 percent of the area of cross section was converted into NiO (para 4.4.1). The loss in room temperature tensile properties after the mission profile exposure (with a stress of one ksi) was greater than after a similar cyclic MGR oxidation exposure without stress (Table XXXI). The greater reduction in area of the substrate with the stress of one ksi may be part be responsible for the increased property degradations. Thus, ?200°F is too high a service temperature for TD Nickel. The recommended maximum service temperature for TD Nickel is 2000°F.

For TD Nickel/chromium, the 2400°F - 2 ksi - 0.18 Torr - 100-cycle simulated profile exposure resulted in 14.5 percent loss in room temperature F_{tu}, 31 percent loss in elongation, and no loss in F_{ty} (Table XXXI). No adverse microstructural changes were observed. Increase in microhardness values was slight. The TD Nickel/chromium test specimen ruptured after 98 cycles during the mission profile test at 2400°F - 760 Torr - ? ksi (Table XXXI). The TD Nickel/chromium can be subjected to one ksi stress in simulated mission profile tests at 2400°F in 760 Torr. Therefore, TD Nickel/chromium is satisfactory for service at 2400°F.

5

DISCUSSION OF RESULTS

Certain similarities were observed in the effects of cyclic oxidation exposures on the mechanical properties of the program alloy foils at different temperatures. The percent loss in tensile properties and fatigue life of the Inconel 625, Haynes 25, TD Nickel, and TD Nickel/chromium alloys, as a result of 100 one-hour slow-cycle oxidation exposures, was maximum at room temperature and decreased with increasing test temperature. This loss is illustrated in Figure 1 for the four alloys. Figure 1 contains plots of percent loss (due to cyclic oxidation) in F_{ty} or fatigue limit at various test temperatures. The percent loss in tensile properties for Rene' 41 and Inconel 718 foils, resulting from cyclic oxidation, was highest at the ductility minimum temperatures (1600 and 1300°F, respectively), followed by the loss at room temperature and at elevated temperatures (Table VIII). The percent loss in tensile properties after cyclic oxidation was less (and negligible) at the elevated temperatures of 1800 to 2200°F than at other test temperatures for the six program alloys. At the recommended maximum service temperatures, the tensile data (F_{tu}, F_{ty}, and percent elongation) exhibited higher values in the oxidized conditions than in the as-received condition (Tables VIII, IX, and X). Preoxidizing the program alloy foils could thus improve their performance and service capability at high temperatures, but only at the sacrifice in room temperature properties.

The different cyclic oxidation exposures resulted, in general, in a much higher percent loss in room temperature tensile properties or room temperature fatigue life than in high temperature tensile or fatigue tests or any other mechanical tests (high rate tensile and notch tensile tests). The room temperature tensile or fatigue tests are the most severe for the determination of performance degradation resulting from oxidation exposures. Among the room temperature tensile properties, the loss in percent elongation was highest followed by F_{tu} and F_{ty}.

The effects of temperature, pressure, and stress on the properties of the program alloys are discussed in the following paragraphs.

5.1 EFFECTS OF TEMPERATURE

Increasing the test temperature resulted in an increase in creep rate and a decrease in tensile strength (F_{tu} or F_{ty}), notch tensile strength (F_{ntu} or F_{nty}), and fatigue life of the program alloys in as-received or oxidized conditions. For the as-received or oxidized Inconel 625 and Haynes 25 alloys, the notch strength ratio increased (i. e., the notch sensitivity decreased) as a result of increase in the test temperature. The two dispersion strengthened alloys, especially TD Nickel/chromium, exhibited notch sensitivity at high temperatures (>2000°F). The percent total elongation values exhibited ductility minimum behavior at temperatures higher than or equal to the reported T_{dm} of the alloys in as-received or oxidized conditions in both tensile or notch tensile tests. (The high-temperature notch tensile tests were conducted only for the Inconel 625, Haynes 25, and TD Nickel/chromium alloys.) For the as-received or oxidized alloys, Inconel 718, Haynes 25, and TD Nickel, the T_{dm} were the same as in the literature, 1300, 1400 and 1600°F, respectively. The Rene' 41, Inconel 625, and TD Nickel alloys in the as-received or oxidized conditions exhibited T_{dm} of 1800, 2000, and 2200°F, respectively. These temperatures are higher than their reported T_{dm} - 1600, 1300, and 1600°F, respectively.

Increasing the oxidation exposure maximum temperature (T_{ox}) for the six program alloys increased the oxidation rate and the oxide spalling, and decreased the tensile properties at room temperature, at the reported T_{dm}, the room temperature notch tensile strength (F_{ntu} or F_{nty}), and the room temperature fatigue limit. The exception is TD Nickel/chromium for which the room temperature fatigue limit improved after 760 Torr cyclic oxidation exposures at 2000 and 2200°F, but decreased by 7.7 percent after a 2400°F - 760 Torr - 100-cycle oxidation exposure.

The percent loss in fatigue limit at T_{dm} as a result of increase in T_{ox} was much less than that in room temperature fatigue limit for the four program alloys (Inconel 625, Haynes 25, TD Nickel, and TD Nickel/chromium). The room temperature notch sensitivity decreased (or the NSR increased) as a result of increase in T_{ox} for all the program alloys except Inconel 625. Increasing T_{ox} had a pronounced effect on the micro-structure, e. g.:

- Intergranular oxidation attack for Rene' 41, Inconel 718, Inconel 625, and Haynes 25. There was no intergranular oxidation attack for the thoria dispersed alloys.
- Grain growth for Inconel 718 and Haynes 25.
- Decarburization for Rene' 41, Inconel 718, Inconel 625, and Haynes 25.
- Formation of an alloy depletion layer for Rene' 41, Inconel 625, and Haynes 25. The thickness of the alloy depletion layer was found to increase with increasing T_{ox}

- Oxide formation at the edges for all the program alloys.
- Internal oxidation especially for Rene' 41, Haynes 25, TD Nickel, and TD Nickel/chromium.

The amount of internal oxides formed (NiO for TD Nickel and Cr_2O_3 in the case of TD Nickel/chromium) increased with increasing T_{ox}. There was an increase in oxygen content with increasing T_{ox} for the Haynes 25, TD Nickel, and TD Nickel/chromium alloys (Table XVII). The nitrogen content was found to increase for Haynes 25 and TD Nickel (but it decreased for TD Nickel/chromium) as a result of an increase in T_{ox}.

Microhardness values for the program alloys exhibited interesting changes (Table XX). With an increase in T_{ox} from 1800 to 2000°F, the microhardness value at the center decreased for Inconel 718 and Inconel 625, probably due to the dissolution of γ' and/or reduction in nitrogen content. The hardness values increased for Haynes 25 because of internal oxidation (formation of SiO_2 or Cr_2O_3) as evidenced by an increase in oxygen content (Table XVII). For Rene' 41, the microhardness values at the center were about the same after a 760 Torr - 100-cycle oxidation exposure with T_{ox} of 1800 or 2000°F because of instability of γ' and μ phase at 1800°F and higher temperatures. The microhardness values, for the two dispersion strengthened alloys, decreased with an increase in T_{ox} because of additional stress relief provided at higher exposure temperatures.

5.2 EFFECTS OF PRESSURE

The time-temperature profile effects were about 15 percent more severe during the 0.18 Torr oxidation exposure than during the 760 Torr exposure (para 3.3.2). For the four alloys (Inconel 625, Haynes 25, TD Nickel, and TD Nickel/chromium), the decrease in pressure from 760 Torr to 0.18 Torr (for a 100-cycle oxidation exposure for the profiles with T_{max} of 1800, 2000, 2200, and 2400°F, respectively) resulted in:

- Decrease in oxidation rate
- Reduction in spalling of the oxides
- Increase in room temperature fatigue limit by about 25 percent for Inconel 625, three percent for Haynes 25, and more than six percent for TD Nickel. For TD Nickel/chromium there was a slight reduction in room temperature fatigue life, but this was offset by 15 percent increased severity of time-temperature effects during cycling oxidation at 0.18 Torr.
- Decrease in fatigue limit at T_{dm} by 25 percent for Haynes 25 and seven percent for TD Nickel. For Inconel 625 and TD Nickel/chromium, there was no change in fatigue limit at T_{dm} as a result of the decrease in pressure from 760 to 0.18 Torr.

There was no significant effect of reduced oxidation pressure (0.18 Torr) on the residual tensile or notch tensile properties at room temperature or at high temperatures for Inconel 625 and TD Nickel/chromium foils. The percent loss in tensile or notch tensile properties at different temperatures for Haynes 25 was greater after the 0.18 Torr - 2000°F - 100-cycle oxidation exposure than after the 760 Torr - 2000°F - 100-cycle oxidation exposure (Tables X and XII). For TD Nickel, the percent residual tensile or room temperature notch tensile properties were higher after the 0.18 Torr - 2200°F oxidation exposure than after the 760 Torr - 2200°F oxidation exposure at room temperature, but were lower at 1600 and 2200°F (Tables XI and XII). This appears to be due to the plasticity of NiC (para 4.3.1) at high temperatures which allows both the oxide and the alloy to bear load. The NSR at various test temperatures for Inconel 625 and Haynes 25 was not significantly affected by reduction in oxidation pressure, but the room temperature NSR increased from 0.96 to 1.12 for TD Nickel and from 0.87 to 0.94 for TD Nickel/chromium (Table XII).

The microstructural effects for the four alloys, because of oxidation at 0.18 or 760 Torr pressures, were similar except for the following effects at 0.18 Torr:

- Less decarburization for Inconel 625 and Haynes 25
- Decrease in thickness of alloy depletion layer for Inconel 625 and Haynes 25
- About 50 percent decrease in thickness of NiO for TD Nickel
- Less internal oxides in the case of TD Nickel/chromium
- Reduced nitrogen content and a general decrease in internal oxidation can explain generally lower microhardness values of all the four alloys after exposure to 0.18 Torr as compared to 760 Torr.

The oxides formed after 760 or 0.18 Torr oxidation exposures were the same for Inconel 625, TD Nickel, and TD Nickel/chromium but not for Haynes 25. The oxides on Haynes 25 after the 2000°F - 100-cycle exposure at different pressures were:

760 Torr - $CoCr_2O_4$

10.0 Torr - $-Cr_2O_3 + CoCr_2O_4$

0.18 Torr - $\alpha-Cr_2O_3$

The lower rate of oxide formation at 0.18 Torr than at 760 Torr favored the formation of more stable Cr_2O_3 over spinel.

Interesting microstructural effects were observed for Haynes 25 in mission profile simulation tests at 0.18 Torr pressure. The needles of an unidentified phase (probably Co_3W) were formed only after 0.18 Torr exposure in the stressed condition. The elongation of grains and the size of internal carbides were greater after 0.18 Torr pressure than after 760 or 10.0 Torr pressure. Therefore, the most severe pressure for Haynes 25 is 0.18 Torr.

5.3 EFFECTS OF STRESS

The main effects of increasing applied stress in the mission profile test were the increased permanent elongation and increased loss in room temperature tensile properties for all six program alloys. The applied stress in mission profile tests for 22 one-hour slow cycles resulted in higher hardness values than after 100 one-hour slow-cycle oxidation exposures (without stress) for the program alloys except TD (Nickel/chromium (Tables XXVIII, XXIX, XXX, and XXXI). The effects of applied stress on microstructure, observed only for Haynes 25 and TD Nickel, were:

- Formation of needles of an unidentified phase after the 2000°F - 0.18 Torr exposure for 22 cycles or 100 cycles (Fig. 39D and E) for Haynes 25 only in the stressed condition.
- The thicknesses of the substrate of TD Nickel foil were 7.5 mil and 5.0 mil after oxidation exposures at 2200°F - 100 cycles - 760 Torr with no stress and a stress of 1.0 ksi, respectively.

The degradation in various mechanical properties as a result of different oxidation exposures for the six program alloys was accounted for by their oxidation rate, scale thickness, extent of internal oxidation, microstructural analyses, microhardness determination, and other diagnostic techniques. Based on the results of various tests and evaluation, the selected four alloys, in order of preference, their recommended maximum service temperature, the most severe pressure condition and the maximum stresses that the foils can withstand are:

Superalloy Foil (0.01 in.)	Recommended T_{max} (°F)	Most Severe Pressure (Torr)	Maximum Stress for Elongation of 1 percent (ksi)
TD Nickel/chromium	2400	760	1.0
TD Nickel	2000	760	~4.0
Haynes 25	1800	0.18	~2.9
Inconel 625	1800	760	~1.0

6

CONCLUSIONS AND RECOMMENDATIONS

The six superalloy foils (0.01 inch thick) selected for extensive evaluation on the basis of availability and strengthening mechanisms, and upon a literature review for mechanical properties and oxidation and stability data were:

- Rene' 41 and Inconel 718 (precipitation hardened)
- Inconel 625 and Haynes 25 (solid solution strengthened)
- TD Nickel and TD Nickel/chromium (thoria dispersion strengthened)

The intent of this study was to investigate and characterize the effects of cyclic oxidation exposures on mechanical properties of the six alloy foils for use as honeycomb heat shields in hypersonic vehicles in atmospheric pressure and in pressures expected to be encountered at 100,000 and 200,000 feet altitudes. Recommendations regarding maximum service temperature of the alloys for use as honeycomb heat shields were also desired.

Evaluation was conducted by mechanical property testing and by diagnostic analyses of the superalloy foils in the as-received and the oxidized conditions. The maximum use temperature was determined as the temperature that did not produce a loss of more than 33 percent of any mechanical property from the as-received condition in 100 slow cycles or the temperature at which the alloy would creep less than one percent under a one ksi stress in 20 hours. Based on the results of extensive evaluations, the following conclusions are made.

6.1 CONCLUSIONS

The alloys, Rene' 41 and Inconel 718, although serviceable at temperatures up to 1800°F in atmospheric pressure condition, were eliminated from the program because:

- The overall degradation in tensile properties due to 1800°F - 760 Torr - 100-cycle oxidation is higher than that for Inconel 625 and Haynes 25 alloys.
- The creep rate and oxidation rates are higher than for Inconel 625 and Haynes 25.

The selected four alloys, in order of preference, their recommended maximum service temperature, the most severe pressure condition, and the maximum stresses that the foils can withstand in 100 one-hour cycles are:

Superalloy Foil (0.01 in.)	Recommended T_{max} (°F)	Most Severe Pressure (Torr)	Maximum Stress for Elongation of 1 percent (ksi)
TD Nickel/chromium	2400	760	1.0
TD Nickel	2000	760	~4.0
Haynes 25	1800	0.18	~2.9
Inconel 625	1800	760	~1.0

The ductility minimum temperatures for the six superalloy foils from literature search and as determined in this program are:

Alloy	T_{dm} From Literature (°F)	Approximate T_{dm} This Program[1] (°F)
Rene' 41	1600	1800
Inconel 718	1300	1300
Inconel 625	1300	2000
Haynes 25	1400	1400
TD Nickel	1600	1600
TD Nickel/chromium	1600	2200

1. In as-received or oxidized conditions.

The percent loss in tensile properties as a result of cyclic oxidation exposures was highest at room temperature for Inconel 625, Haynes 25, TD Nickel, and TD Nickel/chromium, and at T_{dm} (1600 and 1300°F) for Rene' 41 and Inconel 718.

The room temperature tensile or fatigue tests are the most severe tests to determine the degradation in performance due to oxidation exposures. The room temperature elongation of the program alloys is the property most affected by oxidation exposure.

Increasing the test temperature resulted in higher creep rates and a decrease in tensile properties and fatigue life.

Increasing the oxidation exposure maximum temperatures (T_{ox}) increased the oxidation rate and oxide spalling, decreased the tensile properties and fatigue life at room temperature and at T_{dm} for each of the four alloys, except TD Nickel/chromium. Microstructural effects such as intergranular oxidation attack; decarburization for Rene' 41, Inconel 718, Inconel 625, and Haynes 25; grain growth for Inconel 718 and Haynes 25; formation of an alloy depletion layer for Rene' 41, Inconel 625, and Haynes 25; and oxide formation at the edges for all the six alloys were also more pronounced with higher T_{ox}.

Decrease in exposure pressure from 760 to 0.18 Torr decreased the oxidation rate and spalling of the oxides, and increased the room temperature fatigue limit for the four program alloy foils, but decreased the fatigue limit at T_{dm} by 25 percent for Haynes 25 and seven percent for TD Nickel. The main effects of reduced oxidation pressure (0.18 Torr) were on the Haynes 25 foil. The most severe pressure condition for TD Nickel was 760 Torr. For Inconel 625 and TD Nickel/chromium there were no significant effects of reduced oxidation pressure.

The main effects of stress in mission profile tests were the increased creep and the loss in room temperature tensile properties for the six program alloys. For Haynes 25, the microstructure showed needles of an unidentified phase after the 2000°F - 0.18 Torr oxidation exposure in the stressed condition. For TD Nickel, an applied stress of one ksi in the 2200°F - 760 Torr - 100-cycle oxidation exposure resulted in a five-mil thick substrate compared to the 7.5-mil thick substrate after a similar oxidation exposure with no stress.

6.2 RECOMMENDATIONS

The following selected areas of investigation that will enhance the knowledge of the limitation of foil gage alloys for use in reentry structures are:

- Study the specific cause for high-percentage loss in tensile properties at room temperature for Inconel 625, Haynes 25, TD Nickel, and TD Nickel/chromium, and at T_{dm} for Rene' 41 and Inconel 718
- Investigate preoxidation as a means of increasing the high-temperature properties of foil alloys.
- Study the mechanism of internal oxidation of TD Nickel foil.
- Study the metallurgical effect of TD Nickel/chromium that results in a fatigue limit (for 0.5×10^6 cycles) at 1600°F which is higher than its F_{tu} at 1600°F. The study of high strain rate tensile tests at elevated temperatures may provide an insight into the phenomenon.

- A detailed investigation of the effects of reduced pressure on the creep rate of the superalloy foils. There is an indication that creep rates may increase with decreasing pressure.

An evaluation of the effects of stress and low pressure (0.18 Torr) on the formation of an unidentified phase (probably Co_3W) in the microstructure of Haynes 25 during oxidation exposure at 1800 or 2000°F is recommended.

REFERENCES

1. Yates, L., Selection of Refractory Materials for High L/D Re-entry Vehicles. SAE Preprint 660658, presented at Aeronautic and Space Engineering and Manufacturing Meeting, Los Angeles, California (Oct. 3-7, 1966).

2. Plank, P. P., Hypersonic Thermal-Structural Concept Trends. Paper presented at Twelfth Refractory Composites Working Group Meeting, Denver, Colorado (Oct. 17-19, 1966).

3. Rose, F. K., Advanced Methods to Test Thin Gage Materials, Third Year Summary Technical Report on Contract AF33(615)-1709 (October 1966). Solar Division of International Harvester Company.

4. Moore, V. S. and Stetson, A. R., Evaluation of Coated Refractory Metal Foils. Technical Documentary Report, RTD-TDR-63-4006, Part II, Contract AF33(657)-9443, Solar Division of International Harvester Company.

5. Stuart, R. E., "New Design Data on TD-Nickel" Materials in Design Engineering (August 1963), pp. 81-83.

6. Wlodek, S. T., "The Oxidation of Rene' 41 and Udimet 700". Trans. AIME, Vol. 230 (August 1964), pp. 1078-1090.

7. Sims, C. T., "A Contemporary Review of Nickel-Base Superalloys". Journal of Metals (October 1966), pp. 1119-1130.

8. Collins, H. E., Microstructural Instability of Nickel Base Superalloys. Progress Report No. 4, Contract AF33(615)-5126, (July 1967).

9. Beck, P. A., et al, "Intermediate Phases in the Mo-Fe-Co, Mo-Fe-Ni and Mo-Ni-Co Ternary Systems", AIME Trans. Vol. 215 (1959), p. 648.

10. Collins, H. E., Microstructural Instability of Nickel Base Superalloys. Progress Report No. 1, Contract AF33(615)-5126, (October 1966).

11. Beattie, J. H. Jr., and Hagel, W. C., "Intergranular Precipitation of Intermetallic Compounds in Complex Austenitic Alloys". Trans. AIME Vol. 221 (February 1961), pp. 28-35.

REFERENCES (Cont)

12. Collins, H. E., Microstructural Instability of Nickel Base Superalloys. Progress Report No. 5, Contract AF33(615)-5126 (October 1967).

13. Kvernes, I., Studies on the Behavior of Nickel Base Superalloys at High Temperatures. USAF Contract F61052 67 C0057, Central Institute for Industrial Research, Blindern, Oslo, Norway. (1 November 1966 - 31 October 1967).

14. Cole, F. W., Padden, J. B., and Spencer, A. R., Oxidation Resistant Materials for Transpiration Cooled Gas Turbine Blades. NASA CR-930, Bendix Corporation (February 1968).

15. Sims, C. T., "Structural Stability in Ni-2ThO_2 Alloy". Trans. AIME Vol. 220 (December 1963), pp. 1455-1457.

16. DMIC Technical Note "TD Nickel-Chromium". Battelle Memorial Institute, Columbus, Ohio 43201 (November 2, 1967).

17. Johnson, R., Jr., Dispersion Strengthened Metal Structural Development. Douglas Aircraft Company, Contract F33615-67-C-1319, Interim Progress Report No. 3 (November 1967).

18. Wasielewski, G. E., Nickel-Base Superalloy Oxidation. Contract AF33(615)-2861, Final Report, General Electric Co. (January 1967).

19. Wasielewski, G. E., Oxidation of Nickel and Cobalt Superalloys. State-of-the-Art Review, General Electric Co., Cincinnati, Ohio, Report No. R68AEG141.

APPENDIX

A SUMMARY OF SEVERAL PROPERTIES OF THE AVAILABLE PROGRAM ALLOYS FROM PHASE I LITERATURE REVIEW

A SUMMARY OF SEVERAL PROPERTIES OF THE AVAILABLE PROGRAM ALLOYS FROM PHASE I LITERATURE REVIEW

Collected data concerning the nine available superalloy foils are presented in groups of five tables for each alloy.

1. Short-Time Tensile Property Summaries - This includes ultimate, yield, notch tensile, tensile-shear, and impact strengths at room temperature and elevated temperatures, before and after oxidation exposures.

2. Axial Tensiln-Tension Fatigue Life Property Summaries - This includes room temperature and elevated temperature fatigue life (cycles x 10^3) at various stress levels. Where no axial tension-tension fatigue data are available, rotating-beam fatigue life is presented (where available).

3. Creep Strength Property Summaries - Presentation of creep data has been oriented to determine the stress required to produce one percent and five percent total strain in 30 to 40 hours at elevated temperatures.

4. Oxidation Resistance Property Summaries - Rate constants and the extent of internal oxidation and alloy depletion have been listed where available. In some cases oxidation is reported as a percent weight change or the amount of surface recession after various times at several temperatures.

5. Total Normal Emittance Property Summaries - The condition of the alloy surface, the test method employed, and the calculated total normal emittance at several temperatures are listed where the data are available.

TABLE 1-A

SHORT-TIME TENSILE PROPERTY SUMMARY - HASTELLOY X
(References 1, 2)

Condition	Thickness (in.)	Test Direction	Test Temperature (F)	F_{tu} (ksi)	F_{ty} (ksi)	Elongation (% in 2 in.)	Elastic Modulus (10^6 psi)	Notched F_{tu} (ksi)	Notched/ Unnotched Ratio	Tensile-shear (ksi)	Impact Tensile	Charpy Impact Energy (ft-lb)
SOLUTION HEAT-TREATED (SHT) FOR 30 MIN AT 2150 F AND RAPIDLY AIR COOLED (RAC)	0.010	L	75	118	65	41		96	0.81			
		T	75	119	61	36	27	103	0.87			
		T	1300	78	44	18	20					
		L	1600	29	27	16						
		T	1600	44	35	16	21					
		T	1900	17	15	16	15					
		T	2200	5	5	5	5					
SHT, RAC, OXIDIZED(1)												
10 hr/1600 F	0.010	T	70	113	53	31	28					
10 hr/1900 F		T	70	105	48	26	27					
5 hr/2200 F		T	70	80	28	28	24					
SHT, RAC, OXIDIZED(2)												
25 cycles - 0 load	0.010	T	72	111	53	34	26					
- 1/2 F_{tu}		T	75	110	55	27	27					
- 2/3 F_{tu}		T	74	77	52	8	26					
50 cycles - 0 load		T	71	108	52	27	27					
- 1/2 F_{tu}		T	74	95	52	18	26					
100 cycles - 0 load		T	72	112	50	32	26					
- 1/2 F_{tu}		T	74	76	51	8	27					
SHT, RAC, OXIDIZED(3)												
6 cycles - 10 to 25% F_{ty}		L	75	110	63	31		94	0.85			
		T	75	112	60	30		93	0.83			
		L	1600	28	25	34						
25 cycles - 10 to 25% F_{ty}		L	75	95	59	17						
		L	1600	25	23	27						

1. Isothermally oxidized at indicated temperature for indicated time
2. Cycled in air between 500 and 1900 F for indicated number of cycles at indicated load (length of cycle not given)
3. Cycled hourly in air between room temperature and 1800 F for indicated number of cycles at 10 percent to 25 percent of room temperature F_{ty} (65 ksi)

TABLE 2-A

AXIAL TENSION - TENSION FATIGUE LIFE PROPERTY SUMMARY - HASTELLOY X
(References 1, 2)

Condition	Thickness (in.)	Test Direction	Test Temperature (F)	Maximum Stress (ksi)	Number of Cycles(2) (x 10^3)
SOLUTION HEAT-TREATED (SHT) AT 2150 F AND RAPID AIR COOLED	0.010	L	70	65	7000
		T	70	65	1600
		L	70	100	50 (115)
		T	70	100	70
SHT, OXIDIZED(1)					
26 cycles - 0.1 to 0.25% F_{ty}		L	75	100	39

1. Cycled hourly in air between room temperature and 1800 F for indicated number of cycles at 10 percent to 25 percent of room temperature F_{ty} (65 ksi)
2. 1560 cpm

TABLE 3-A

CREEP STRENGTH PROPERTY SUMMARY - HASTELLOY X
(References 1, 2)

Condition	Thickness (in.)	Test Direction	Test Temperature (F)	Stress (ksi)	Time (hr)	Strain (%)
SOLUTION HEAT-TREATED (SHT) AT 2150 F AND RAPIDLY AIR COOLED (RAC)	0.010	L	75	5.5	100	1.05
		T	1600	5.9	79	0.79
		T	1600	8.0	30	1.0
		T	1600	10.0	12	1.0
		T	1900	0.5	35	1.0
		T	1900	1.0	23	1.0
		T	1900	1.8	5	1.0
		T	1900	3.0	3	1.0
		T	1900	4.9	1	1.0
		T	1900	5.9	0.6	1.0
SHT, OXIDIZED[1]						
6 cycles - 0.1 to 0.25 F_{ty}		L	75	5.5	100	0.48

1. Cycled hourly in air between room temperature and 1800 F at 10 percent and 25 percent of room temperature F_{ty} (65 ksi)

TABLE 4-A

OXIDATION PROPERTY SUMMARY - HASTELLOY X
(Reference 3)

Condition	Thickness (in.)	Temperature (F)	Observed Rate Constants				I O[1] in 100 hours	A D[2] in 100 hours
			K_{L_I} ($mg/cm^2/sec$)	$K_{L_{II}}$ ($mg/cm^2/sec$)	K_{P_I} ($mg^2/cm^4/sec$)	$K_{P_{II}}$ ($mg^2/cm^4/sec$)		
COMMERCIAL SHEET	0.030	1600	3.17×10^{-6} (t<600 min)	2.07×10^{-6}			<0.5 mil	<1.0 mil
		1700	1.02×10^{-5} (t<400 min)		2.26×10^{-6}		<0.5 mil	<1.0 mil
		1800	1.53×10^{-5} (t<200 min)		3.02×10^{-6}		0.5 mil	1.5 mils
		1900			1.32×10^{-5} (t<400)	7.89×10^{-6}	1.0 mil	2.2 mils
		2000			2.85×10^{-5} (t<400)	1.35×10^{-5}	>1.0 mil	3.0 mils
		2200			1.68×10^{-4} (t<150)	7.6×10^{-5}	>1.0 mil	>3.0 mils

1. Internal Oxidation (I O) defined as depth to which oxide phases could be resolved in the subscale region
2. Alloy Depletion (A D) defined as depth to which original structure is affected by oxidation, as determined by etching

TABLE 5-A

TOTAL NORMAL EMITTANCE PROPERTY SUMMARY - HASTELLOY X
(References 1, 2, 4)

Condition	Test Method	Test Temperature (F)	Calculated Total Normal Emittance
SOLUTION HEAT-TREATED (SHT) AT 2150 F AND RAPIDLY AIR COOLED	Normal spectral reflectance 0.3 to 32μ range integrated with blackbody curves	RT	0.186 (0.31)
		1400	0.336
		1700	0.353
		2000	0.368
OXIDIZED[1] 6 cycles	Normal spectral reflectance 0.3 to 32μ range integrated with blackbody curves	RT	0.613
		1400	0.701
		1700	0.712
		2000	0.722
STABLY OXIDIZED AT 2000 F	Hemispherical total emittance, comparison blackbody	1000	0.86
		1600	0.88
		2000	0.88
STABLY OXIDIZED AT 2200 F	Hemispherical total emittance, comparison blackbody	80	0.72

1. Cycled hourly in air between room temperature and 1800 F at 10 percent and 25 percent of room temperature F_{ty} (65 ksi)

TABLE 1-B.

SHORT-TIME TENSILE PROPERTY SUMMARY - INCONEL 625
(Reference 5)

Condition	Thickness (in.)	Test Direction	Test Temperature (F)	F_{tu} (ksi)	F_{ty} (ksi)	Elongation (% in 2 in.)	Elastic Modulus[1] (10^6 psi)	Notched F_{tu} (ksi)	Notched/ Unnotched Ratio	Tensile-shear, F_{su} (ksi)	Impact Tensile (ksi)	Charpy Impact Energy (ft-lb)
COLD ROLLED, MILL ANNEALED 1700 TO 1900F	Unknown	Unknown	RT	136	63	50	30					49
			800	120	43	51						
			1000	120	48	56	26					
			1200	115	47	47	24					
			1300	100	45	40						
			1400	71	44	67	23					
			1600	40	40	104						
			1800	17								
HOT ROLLED, MILL ANNEALED 1700 TO 1900F, AND OXIDIZED FOR 100 HOURS AT												
1200F	Unknown	Unknown	RT	172	121	35						
1400F			RT	148	92	35						
1600F			RT	143	80	37						
1800F			RT	130	53	55						

1. Elastic modulus determined on bar stock; size unknown

TABLE 2-B.

AXIAL TENSION-TENSION FATIGUE LIFE PROPERTY SUMMARY - INCONEL 625

No data available to date.

TABLE 3-B.

ROTATING-BEAM FATIGUE LIFE PROPERTY SUMMARY, INCONEL 625
(Reference 5)

Condition	Thickness (in.)	Test Direction	Test Temperature (F)	Maximum Stress (ksi)	Number of Cycles ($\times 10^3$)
HOT-ROLLED BAR Solution annealed at 2100F	0.625 dia.	Unknown	85	72	100
			85	68	1,000
			85	67	10,000
			1000	64	100
			1000	63	1,000
			1000	62	10,000
			1200	58	100
			1200	55	1,000
			1200	55	10,000
			1400	50	100
			1400	45	1,000
			1400	45	10,000
			1600	39	1,000
			1600	32	10,000

TABLE 4-B

CREEP STRENGTH PROPERTY SUMMARY - INCONEL 625
(Reference 5)

Condition	Thickness (in.)	Test Direction	Test Temperature (F)	Stress (ksi)	Time (hr)	Strain (%)
SHEET Solution annealed at 2100F	Unknown	Unknown	1200	52	100	1
			1200	56	100	5
			1400	18	100	1
			1400	22	100	5
			1600	5	100	1
			1600	8	100	5

TABLE 5-B

OXIDATION RESISTANCE PROPERTY SUMMARY - INCONEL 625
(Reference 5)

Condition	Thickness (in.)	Hours of Cyclic Exposure(1)	Test Temperature (F)	Change in Weight (%)
Unknown	Unknown	100	1800	+0.086
		100	2000	-0.182
		200	1800	+0.065
		200	2000	-1.086
		300	1800	+0.065
		300	2000	-3.335
		400	1800	+0.048
		400	2000	-5.399
		500	1800	+0.021
		500	2000	-6.566
		600	2000	-10.066

1. Cycles of 15 minutes heating, 5 minutes cooling

TABLE 6-B

TOTAL NORMAL EMITTANCE PROPERTY SUMMARY - INCONEL 625

No data available to date.

TABLE 1-C

SHORT-TIME TENSILE PROPERTY SUMMARY - HAYNES 25
(References 6. 7. 8)

Condition	Thickness (in.)	Test Direction	Test Temperature (F)	F_{tu} (ksi)	F_{ty} (ksi)	Elongation (% in 2 in.)	Elastic Modulus (x 10^6 psi)	Notched F_{tu} (ksi)	Notched/ Unnotched Ratio	Tensile-shear, F_{su} (ksi)	Impact Tensile (ksi)	Charpy Impact Energy (ft-lb)
SOLUTION HEAT-TREATED (SHT)	0.010	L	70	108	65	30						193
AT 2225F AND RAPIDLY AIR	0.010	T	70	113	64	30						
COOLED (RAC)	0.020	L	70	143	73	49	34					
		T	70	148	72	48	36					
	0.062	T	70	161	86	47	35					
		T	1000	131	54	40	29					201
		T	1200	94	55	29						170
		T	1650	46	32	27						
		T	1800	29	28	35	22					106
		T	2000	12	8	20						
		T	2100	8	5	18						
SHT 2225F, RAC OXIDIZED[1]												
10 hr/1600F	0.020	Unknown	70	117	71	16						
10 hr/1800F			70	141	71	14						
10 hr/2000F			70	105	51	12						
10 hr/2000F			2000	10	9	12						
10 hr/2200F			70	61	40	21						
UNKNOWN HEAT TREATMENT, OXIDIZED[1]												
5 hr/1200F	0.032	Unknown	1200	90	42	45	24					
25 hr/1200F			1200	93	45	47	23					
50 hr/1200F			1200	89	-	40	-					
5 hr/1500F			1500	78	34	39	21					
25 hr/1500F			1500	80	34	32	20					
50 hr/1500F			1500	82	35	26	23					
5 hr/1800F			1800	34	25	25	17					
25 hr/1800F			1800	41	27	33	17					
50 hr/1800F			1800	38	25	30	17					
UNKNOWN HEAT TREATMENT, OXIDIZED[2]												
96 hr/1600F - 760 Torr	Unknown	Unknown	75	126	67	16	30					2
- 8.5 Torr			75	126	65	15	33					2
- 0.15 Torr			75	128	65	15	33					2
96 hr/2000F - 760 Torr			75	108	47	48	29					35
- 8.5 Torr			75	114	51	55	31					50
- 0.15 Torr			75	116	50	48	34					42

1. Isothermally oxidized for indicated time at indicated temperature
2. Isothermally oxidized at indicated temperature in indicated air atmosphere. As received properties - F_{tu} 143 ksi, F_{ty} 70 ksi, Elongation 53 percent, E 30 x 10^6 psi, Charpy 36.0 foot-pounds

TABLE 2-C

AXIAL TENSION-TENSION FATIGUE LIFE PROPERTY SUMMARY - HAYNES 25
(Reference 9)

Condition	Thickness (in)	Test Direction	Test Temperature (F)	Maximum Stress (ksi)	Number of Cycles (x 10^3)
Unknown	Unknown	Unknown	1500	30	100,000
			1500	40	10,000
			1800	13	100,000
			1800	15	10,000
			1800	20	1,000

TABLE 3-C

CREEP STRENGTH PROPERTY SUMMARY - HAYNES 25
(Reference 9)

Condition	Thick-ness (in)	Test Direction	Tempera-ture (F)	Stress (ksi)	Time (hr)	Strain (%)
SOLUTION HEAT-TREATED AT 2250F AND RAPIDLY AIR COOLED	Unknown	Unknown	1500	19	10	0.74
			1500	19	50	2.00
			1500	21.5	50	4.73
			1600	12	10	0.45
			1600	12	50	1.14
			1700	10	10	0.38
			1700	10	50	1.25
			1800	6	10	0.46
			1800	6	50	1.28

TABLE 4-C

OXIDATION RESISTANCE PROPERTY SUMMARY - HAYNES 25
(Reference 10)

Condition	Thickness (in.)	Temperature (F)	Exposure Time (hr)	Total Penetration (uniform and intergranular) mils
Unknown	Sheet	1600	50	0.13
			100	0.20
		1800	50	1.25
			100	1.62
		2000	25	2.00
			100	

TABLE 5-C

TOTAL NORMAL EMITTANCE PROPERTY SUMMARY - HAYNES 25
(Reference 4)

Condition	Test Method	Test Temperature (F)	Calculated Total Normal Emittance
STABLY OXIDIZED AT 2000F	Hemispherical total emittance, comparison blackbody, measured in air	1000	0.85
		1200	0.86
		1400	0.86
		1600	0.87
		1800	0.88
		2000	0.88

TABLE 1-D

SHORT-TIME TENSILE PROPERTY SUMMARY - HASTELLOY C
(References 7, 11)

Condition	Thickness (in.)	Test Direction	Test Temperature (F)	F_{tu} (ksi)	F_{ty} (ksi)	Elongation (% in 2 in.)	Elastic Modulus (10^6 psi)	Notched F_{tu} (ksi)	Notched/ Unnotched Ratio	Tensile-Shear (ksi)	Impact Tensile	Charpy Impact Energy (ft-lb)
SOLUTION HEAT-TREATED (SHT) AT 2225F AND RAPIDLY AIR COOLED (RAC)	0.050	Unknown	RT	129	68	49						
SHT 2225F, WATER QUENCHED (WQ)	0.109	Unknown	RT	121	58	48	30					
			1000	99	44	52	25					
			1200	97	43	55	25					
			1400	79	41	50	23					
			1600	56	3[illegible]	47	20					
			1800	32	18	49	15					
			2000	18	10	36	11					
UNKNOWN HEAT TREATMENT, OXIDIZED[1]												
7 hr/1200F	0.025		1200	98	49	41	25					
25 hr/1200F			1200	-	50	-	23					
50 hr/1200F			1200	94	51	-	23					
5 hr/1500F			1500	79	52	33	21					
25 hr/1500F			1500	87	60	35	20					
50 hr/1500F			1500	86	60	25	20					
5 hr/1800F			1800	-	27	-	17					
25 hr/1800F			1800	37	24	28	15					
50 hr/1800F			1800	37	25	26	14					

1. Isothermally oxidized in air (30 cfh) for indicated time at indicated temperature

TABLE 2-D

AXIAL TENSION-TENSION FATIGUE LIFE PROPERTY SUMMARY - HASTELLOY C

No data available to date.

TABLE 3-D

CREEP STRENGTH PROPERTY SUMMARY – HASTELLOY C
(Reference 11)

Condition	Thickness (in.)	Test Direction	Test Temperature (F)	Stress (Ksi)	Time (hr)	Strain (%)
SOLUTION HEAT-TREATED AT 2225 F AND RAPIDLY AIR COOLED	0.050	Unknown	1200	45	41	1.0
			1200	45	342	5.0
			1350	20	56	1.0
			1350	30	12	1.0
			1350	30	103	5.0
			1500	12	22	1.0
			1500	18	54	5.0
			1650	8	47	1.0
			1650	12	33	5.0

TABLE 4-D

OXIDATION RESISTANCE PROPERTY SUMMARY – HASTELLOY C
(Reference 12)

Condition	Thickness (in.)	Exposure Time (hr)	Test Temperature (F)	Change in Weight (%)	Alloy Consumed (mils)
Unknown	Unknown	7	1200	0.00	0.1
		50	1200	0.04	0.4
		5	1500	0.00	0.4
		50	1500	0.04	0.2
		5	1800	0.08	0.5
		50	1800	0.21	0.5

TABLE 5-D

TOTAL NORMAL EMITTANCE PROPERTY SUMMARY - HASTELLOY C
(Reference 4)

Condition	Test Method	Test Temperature (F)	Calculated Total Normal Emittance
POLISHED, 8 MICROINCHES RMS AVERAGE	Normal total emittance, resistance-heated specimens, comparison blackbody, measured in vacuum	400	0.13
		1000	0.20
		1400	0.27
		1600	0.32
		1700	0.35
STABLY OXIDIZED AT 2000 F	Hemispherical total emittance, comparison blackbody, measured in air	600	0.90
		1000	0.90
		1200	0.91
		1400	0.92
		1600	0.93
		1800	0.95
		2000	0.96
		2100	0.97

TABLE 1-E

SHORT-TIME TENSILE PROPERTY SUMMARY -- INCONEL 600
(References 13, 14)

Condition	Thickness (in.)	Test Direction	Test Temperature (F)	F_{tu} (ksi)	F_{ty} (ksi)	Elongation (% in 2 in.)	Elastic Modulus (10^6 psi)	Notched F_{tu} (ksi)	Notched/ Unnotched Ratio	Tensile-Shear (ksi)	Impact Tensile	Charpy Impact Energy (ft-lb)
SOLUTION HEAT-TREATED (SHT) AT 2225 F AND AIR COOLED (AC)	0.250	Unknown	80	80	30	38	31					
			1000	62	22		25					
			1200	53	20		24					
			1400	34	16							
			1600	16	10							
SHT 2225 F, AC BAR STOCK		Unknown	RT	90	35	47	31[1]					
			1000	84	28	47	27					
			1200	65	26	39	26					
			1400	27	17	46	25					
			1600	15	9	80	23					
			1800	8	4	118						

1. Dynamic modulus reported for bar stock

TABLE 2-E

AXIAL TENSION-TENSION FATIGUE LIFE PROPERTY SUMMARY – INCONEL 600

No data available.

TABLE 3-E

ROTATING-BEAM FATIGUE LIFE PROPERTY SUMMARY – INCONEL 600
(Reference 13)

Condition	Thickness (in.)	Test Direction	Test Temperature (F)	Maximum Stress (ksi)	Number of Cycles[1] (x 10^3)
SOLUTION HEAT-TREATED AT 2225 F AND AIR COOLED	Unknown	Unknown	RT	49	100,000
			1000	42	100,000
			1200	27	100,000
			1400	16	100,000
			1600	10	100,000
			1800	7	100,000

1. 3450 rpm

TABLE 4-E

CREEP STRENGTH PROPERTY SUMMARY – INCONEL 600
(Reference 14)

Condition	Thickness (in.)	Test Direction	Test Temperature (F)	Stress (ksi)	Time (hrs)	Strain (%)
SOLUTION HEAT-TREATED AT 2225 F AND AIR COOLED, BAR	Sheet	Unknown	1300	17	100	rupture
			1400	12	100	rupture
			1600	5	100	rupture
			1800	3	100	rupture
			2000	1	100	rupture

TABLE 5-E

OXIDATION RESISTANCE PROPERTY SUMMARY – INCONEL 600
(Reference 5)

Condition	Thickness (in.)	Hours of Cyclic Exposure(1)	Test Temperature (F)	Change in Weight (%)
Unknown	Unknown	100	1800	+0.154
		100	2000	-0.144
		200	1800	+0.179
		200	2000	-2.962
		300	1800	+0.185
		300	2000	-10.789
		400	1800	+0.163
		400	2000	-19.718
		500	1800	+0.029
		500	2000	-27.189
		600	2000	-34.957
		700	1800	-1.223
		1000	1800	-2.877

1. Cycles of 15 minutes heating, 5 minutes cooling

TABLE 6-E

TOTAL NORMAL EMITTANCE PROPERTY SUMMARY – INCONEL 600
(Reference 4)

Condition	Test Method	Test Temperature (F)	Calculated Total Normal Emittance
AS ROLLED	Normal total emittance, resistance-heated specimens, comparison blackbody, measured in air	800	0.27
		1000	0.29
		1200	0.40
		1400	0.59
STABLY OXIDIZED AT 2000F	Normal total emittance, resistance-heated specimens, comparison blackbody, measured in air	800	0.76
		1000	0.78
		1200	0.81
		1400	0.83
		1600	0.85
		1800	0.87
		2000	0.90

TABLE 1-F

SHORT-TIME TENSILE PROPERTY SUMMARY – INCONEL 718
(References 6, 15)

Condition	Thickness (in.)	Test Direction	Test Temperature (F)	F_{tu} (ksi)	F_{ty} (ksi)	Elongation (% in 2 in.)	Elastic Modulus (x 10^6 psi)	Notched F_{tu} (ksi)	Notched/ Unnotched Ratio	Tensile-Shear F_{su} (ksi)	Impact Tensile (ksi)	Charpy Impact Energy (ft-lb)
MILL ANNEALED 30 MIN AT 1750 F IN PROTECTIVE ATMOSPHERE, AIR COOLED (AC), SOLUTION HEAT-TREATED 1 HR AT 1700 F, AC, AGED 16 HR AT 1325 F, AC	0.063	-	RT	187	144	21						
			800	158	126	22						
			1000	150	124	21						
			1200	148	123	17						
			1300	128	117	7						
			1400	97	92	17						
UNKNOWN HEAT TREATMENT, OXIDIZED[1]												
96 hr - 1600 F - 760 Torr	Unknown	Unknown	75	126	66	21	27					10
- 8.5 Torr			75	144	76	26	27					7
- 0.15 Torr			75	126	54	36	26					7
96 hr - 2000 F - 760 Torr			75	103	57	51	25					41
- 8.5 Torr			75	100	46	34	25					39
- 0.15 Torr			75	141	110	29	26					24

1. Isothermally oxidized at indicated temperature in indicated air atmosphere. As received properties - F_{tu} 114 ksi, F_{ty} 54 ksi, Elongation 56 percent, E 27 x 10^6 psi, Charpy 36 foot-pounds

TABLE 2-F

AXIAL TENSION-TENSION FATIGUE LIFE PROPERTY SUMMARY – INCONEL 718

No data available to date.

TABLE 3-F

CREEP STRENGTH PROPERTY SUMMARY – INCONEL 718
(Reference 15)

Condition	Thickness (in.)	Test Direction	Test Temperature (F)	Stress (ksi)	Time (hr)	Strain (%)
MILL ANNEALED PLUS SOLUTION HEAT-TREATED 1 HR AT 1700F, AIRCOOLED AND AGED FOR 16 HR AT 1325F, AIR COOLED	0.063	Unknown	1150	100	120	0.5
				100	170	1.0
				100	230	5.0
			1250	50	79	0.2
				50	230	0.5
			1300	25	123	0.2
				25	317	0.4

TABLE 4-F

OXIDATION RESISTANCE PROPERTY SUMMARY – INCONEL 718

No data available to date.

TABLE 5-F

TOTAL NORMAL EMITTANCE PROPERTY SUMMARY – INCONEL 718

No data available to date.

TABLE 1-G

SHORT-TIME TENSILE PROPERTY SUMMARY - RENE 41
(References 2, 6, 7, 16)

Condition	Thickness (in.)	Test Direction	Test Temperature (F)	F_{tu} (ksi)	F_{ty} (ksi)	Elongation (% in 2 in.)	Elastic Modulus (10^6 psi)	Notched F_{tu} (ksi)	Notched/ Unnotched Ratio	Tensile-shear, F_{su} (ksi)	Impact Tensile (ksi)	Charpy Impact Energy (ft-lb)
SOLUTION HEAT-TREATED (SHT) AT 2150F, AIR COOLED (AC), AND AGED FOR 4 HR AT 1650F, AC.	0.010	L	70	103	95	4	27	104	k_t=2.97			
		T	70	116	102	4	27	103				
		T	800					101				
		T	1300	101	87	19	24					
		T	1600	64	60	3	16					
		T	1900	11	11	11	5					
		T	2200	5	4	8	2					
SHT, AC, OXIDIZED[1]												
5 hr/1600F	0.010	T	70	116	102	4	27					
10 hr/1600F		T	70	119	104	3	29					
5 hr/1900F		T	70	96	62	12	26					
10 hr/1900F		T	70	78	48	10	26					
5 hr/2200F		T	70	42	32	5	22					
SHT 30 MIN/1950F IN VACUUM, AGED 16 HR/1400F IN AIR, AND OXIDIZED [1]												
50 hr/1200F	0.028	Unknown	1200	174	135	9	27					
50 hr/1500F			1500	140	115	8	23					
50 hr/1800F			1800	44	28	16	15					
SHT, AC, AGED, AC, OXIDIZED[2]												
10 A-cycles, 3 ksi; load	0.063	Unknown	70	107	80	12	30					
100 A-cycles, 3 ksi; load			70	97	76	7	28					
10 A-cycles, 3 ksi; load			1400	97	75	12	23					
100 A-cycles, 3 ksi; load			1400	79	72	5	22					
10 B-cycles, 6 ksi; load			70	109	86	6	29					
100 B-cycles, 6 ksi; load			70	102	73	5	29					
100 B-cycles, 6 ksi; load			1400	103	76	7	22					
UNKNOWN HEAT TREATMENT, OXIDIZED [3]												
96 hr-1600F-760 Torr	Unknown	Unknown	75	181	113	15	31					2
-8.5 Torr			75	167	93	18	31					5
-0.15 Torr			75	168	93	21	31					3
96 hr-2000F-760 Torr			75	140	87	37	27					29
-8.5 Torr			75	114	70	29	28					38
-0.15 Torr			75	163	97	31	29					26

1. Isothermally oxidized at indicated temperature for indicated time
2. Cycle A - 1 hour/1350F, heat to 1875F in 30 seconds, 15 seconds/1875F, cool to 1350F in 30 seconds
   Cycle B - 1 hour 1350F, heat to 1750F in 30 seconds, 15 seconds/1750F, cool to 1350F in 30 seconds
3. Isothermally oxidized at indicated temperature in indicated air atmosphere. As received properties - F_{tu} 152 ksi, F_{ty} 95 ksi, Elongation 43 percent, E 28 x 10^6 psi, Charpy 17 foot-pounds

TABLE 2-G

AXIAL TENSION-TENSION FATIGUE LIFE PROPERTY SUMMARY - RENÉ 41
(Reference 2)

Condition	Thickness (in.)	Test Direction	Test Temperature (F)	Maximum Stress (ksi)	Number of Cycles(1) (x 10^3)
SOLUTION HEAT-TREATED AT 2150F, AIR COOLED, AGED 4 HR AT 1650F, AND AIR COOLED	0.010	T	72	40	6300
				45	1246
				50	955
				55	551
				60	320
				70	193
				80	96
				85	84
				95	59
				105	20
				109	5

1. 1560 cpm

TABLE 3-G

CREEP STRENGTH PROPERTY SUMMARY - RENE 41
(Reference 2)

Condition	Thick-ness (in.)	Test Direction	Test Temper-ature (F)	Stress (ksi)	Time (hr)	Strain (%)
SOLUTION HEAT-TREATED AT 2150F, AIR COOLED, AGED 4 HR AT 1650F, AND AIR COOLED	0.010	T	1600	15	100	0.9
			1600	16	81	1.0
			1600	17	37	1.0
			1600	19	39	1.0
			1600	20	34	1.0
			1600	22	16	1.0
			1600	23	14	1.0
			1900	1	95	1.0
			1900	2	18	1.0
			1900	3	17	1.0
			1900	4	6	1.0
			1900	7	1	1.0
			1900	13	<0.1	failed

TABLE 4-G

OXIDATION RATE PROPERTY SUMMARY - RENE 41
(Reference 17)

Condition	Thickness (in.)	Test Temperature (F)	Observed Rate Constants				I O[1] in 100 hours	A D[2] in 100 hours
			K_{L_I} (mg/cm^2/sec)	$K_{L_{II}}$ (mg/cm^2 sec)	K_{P_I} (mg^2/cm^4 sec)	$K_{P_{II}}$ (mg^2/cm^4 sec)		
SOLUTION HEAT-TREATED FOR 3d MED AT 2150°F, AGED 4 HR AT 1600°F	0.032 to 0.062	1600	4.3×10^{-6} (t < 150 min)		1.3×10^{-6}		<1.0 mil	<1.0 mil
		1800	1.2×10^{-4} (t < 23 min)		3.1×10^{-5} (t < 600 min)	2.9×10^{-5}	>1.0 mil	2.0 mils
		2000			4.0×10^{-4} (t < 110 min)		>1.0 mil	>4.0 mils

1. Internal Oxidation (I O) defined as depth to which oxide phases could be resolved in the subscale region
2. Alloy Depletion (A D) defined as depth to which original structure is affected by oxidation, as determined by etching

TABLE 5-G

TOTAL NORMAL EMITTANCE PROPERTY SUMMARY - RENE 41
(Reference 2)

Condition	Test Method	Test Temperature (F)	Calculated Total Normal Emittance
SOLUTION HEAT-TREATED (SHT) AT 2150F, AIR COOLED (AC), AGED 4 HR AT 1650F, AND AIR COOLED	Calculated by taking the specimen to black reference ratio of radiometer outputs in millivolts. Corrected for nonlinearity of the cold radiometer and the 0.95 emittance of the black reference	80	0.36
SHT, AIR COOLED, AGED 4 HR AT 1650F, AIR COOLED, AND STABLY OXIDIZED 2200F	Calculated by taking the specimen to black reference ratio of radiometer outputs in millivolts. Corrected for nonlinearity of the cold radiometer and the 0.95 emittance of the black reference	80	0.63

TABLE 1-H

SHORT-TIME TENSILE PROPERTY SUMMARY – TD Ni
(References 1, 2, 6, 18)

Condition	Thickness (in.)	Test Direction	Test Temperature (F)	F_{tu} (ksi)	F_{ty} (ksi)	Elongation (% in 2 in.)	Elastic Modulus (10^6 psi)	Notched F_{tu} (ksi)	Notched/ Unnotched Ratio	Tensile - Shear, F_{su} (ksi)	Impact Tensile (ksi)	Charpy Impact Energy (ft-lb)
ANNEALED (time and temperature not given)	0.010	L	70	77	47	17	29	71	0.97			
		T	70	72	39	15	29	70	1.00	50		
		T	1200	25	22	3	23			18		
		L	1600	20	19	1						
		T	1600	18	19	1	21			17		
		T	1900	14	14	2	8			10		
		T	2200	11	11	2	6			6		
ANNEALED, OXIDIZED[1]												
6 hr/1600F	0.010	L	75	63	44	8		67	1.07			
6 hr/1600F		T	75	64	39	6		69	1.07			
6 hr/1600F		L	1600	15	-	1						
10 hr/1600F		L	75	54	37	5						
10 hr/1600F		T	75	70	43	8	27					
10 hr/1600F		L	1600	16	16	1						
5 hr/1900F		T	75	58	38	7	24					
16 hr/1900F		T	75	56	36	6	23					
5 hr/2200F		T	75	50	35	6	22					
ANNEALED, OXIDIZED[2]												
25 cycles - 0 load	0.010	T	75	71	40	11	27					
- 1/2 F_{tu}		T	75	70	41	11	27					
- 2/3 F_{tu}		T	75	71	40	14	28					
50 cycles - 0 load		T	75	72	41	11	27					
- 1/2 F_{tu}		T	75	69	39	13	28					
100 cycles - 0 load		T	75	70	43	9	28					
- 1/2 F_{tu}		T	75	66	40	9	28					
ANNEALED, OXIDIZED[3]												
96 hr - 1800F - 760 Torr	Unknown	Unknown	75	59	35	11	16					21
- 8.5 Torr			75	60	36	18	18					19
- 0.15 Torr			75	63	38	18	16					18
96 hr - 2000F - 760 Torr			75	51	33	15	16					17
- 8.5 Torr			75	59	36	19	19					19
- 0.15 Torr			75	63	37	18	17					21

1. Isothermally oxidized at indicated temperature for indicated time
2. Cycled in air between 500 and 1900F for indicated number of cycles at indicated load (length of cycle not given)
3. Isothermally oxidized at indicated temperature in indicated air atmosphere. As received properties - F_{tu} 62 ksi, F_{ty} 42 ksi, Elongation 17 percent, E 16 x 10^6 psi, Charpy 14 foot-pounds

TABLE 2-H

AXIAL TENSION-TENSION FATIGUE LIFE PROPERTY SUMMARY - TD Ni
(References 1, 2, 19)

Condition	Thickness (in.)	Test Direction	Test Temperature (F)	Maximum Stress (ksi)	Number of Cycles[1] (x 10^3)
ANNEALED	0.010	L	70	74	1
			70	74	10
			70	70	100
			70	58	1000
			70	50	5000
		T	70	72	5
			70	69	10
			70	62	100
			70	54	1000
			70	48	5000
	0.060	T	RT	64	1
			RT	63	10
			RT	59	100
			RT	50	1000
			RT	45	5000
			1600	23	1
			1600	22	10
			1600	21	100
			1600	18	1000
			1600	16	5000
			1800	17	1
			1800	17	10
			1800	16	100
			1800	14	1000
			1800	12	5000
ANNEALED AND OXIDIZED[2] 6 cycles - 0.1 to 0.25 F_{ty}	0.010	L	75	65	8

1. 1560 cpm
2. Cycled hourly in air between room temperature and 2160F for indicated number of cycles at 10 percent and 25 percent of room temperature F_{ty} (47 ksi)

TABLE 3-H

CREEP STRENGTH PROPERTY SUMMARY – TD Ni
(References 1, 2)

Condition	Thickness (in.)	Test Direction	Test Temperature (F)	Stress (ksi)	Time (hr)	Strain (%)
ANNEALED	0.010	L	75	8	100	0.14
		T	1600	8	100	0.67
			1600	9	86	0.52
			1600	10	10	0.50
			1600	11	4	0.39
			1600	12	0.6	0.53
			1600	15	0.3	0.60
			1900	6	57	0.68
			1900	7	7	0.86
			1900	8	<1	0.21
ANNEALED AND OXIDIZED(1)						
6 cycles - 0.1 to 0.25 F_{ty}	0.010	L	75	8	100	0.04

1. Cycled hourly in air between room temperature and 1800F for indicated number of cycles at 10 percent to 25 percent of room temperature

TABLE 4-H

OXIDATION RATE PROPERTY SUMMARY – TD Ni
(Reference 20)

Condition	Thickness (in.)	Temperature (F)	Observed Rate Constants K_p, ($mg^2/cm^4/sec$)	Surface Recession in 100 Hours (mils/side)
ANNEALED 1 HR AT 1868F IN VACUUM	0.030	1652	2.8×10^{-2}	
		1832	2.2×10^{-1}	
		2012	8.7×10^{-1}	1.9
		2192	4.5	3.4
		2372	13.4	6.8

TABLE 5-H

TOTAL NORMAL EMITTANCE PROPERTY SUMMARY – TD Ni
(Reference 1)

Condition	Test Method	Test Temperature (F)	Calculated Total Normal Emittance
ANNEALED	Normal spectral reflectance 0.3 to 32μ range integrated with blackbody curves.	RT	0.076
		1400	0.187
		1700	0.224
		2000	0.245
OXIDIZED[1]			
6 cycles	Normal spectral reflectance 0.3 to 32μ range integrated with blackbody curves.	RT	0.485
		1400	0.574
		1700	0.592
		2000	0.612

1. Cycled hourly in air between room temperature and 2160F for indicated number of cycles at 10 percent and 25 percent of room temperature F_{ty} (47 ksi)

TABLE 1-J

SHORT-TIME TENSILE PROPERTY SUMMARY – TD NiC
(References 21, 22)

Condition	Thickness (in.)	Test Direction	Test Temperature (F)	F_{tu} (ksi)	F_{ty} (ksi)	Elongation (% in 2 in.)	Elastic Modulus (10^6 psi)	Notched F_{tu} (ksi)	Notched/ Unnotched Ratio	Tensile – Shear, F_{su} (ksi)	Impact Tensile (ksi)	Charpy Impact Energy (ft-lb)
UNKNOWN, PROBABLY ANNEALED 1 TO 2 HR AT 2000F IN HYDROGEN	Unknown	Unknown	RT	130	90	18						
			1200	65	54	6						
			1500	35	30	7						
			2000	17	15	4						
UNKNOWN, PROBABLY ANNEALED 1 TO 2 HR AT 2000F IN HYDROGEN, OXIDIZED[1]	0.026 to 0.029	T	RT	128	84		23					
96 hr – 1800F – 760 Torr	0.026 to 0.028	T	RT	125	84		23					
96 hr – 1900F – 760 Torr			RT	128	82		23					
– 0.15 Torr			RT	125	78		21					
96 hr – 2200F – 760 Torr			RT	127	78		21					
– 0.15 Torr			RT	105	66		20					
UNKNOWN, PROBABLY ANNEALED 1 TO 2 HR AT 2000F IN HYDROGEN, OXIDIZED[2]												
100 hr/2400F	Unknown	T	2200F	18								
½ hr/2400F in air plus 100 hr/ 2400F in hydrogen	Unknown	T	2200F	18								
100 hr/2400F in argon	Unknown	T	2200F	17								

1. Isothermally oxidized at indicated temperature in indicated air atmosphere
2. Isothermally oxidized at indicated temperature in air except where noted. As received properties - F_{tu} 16 ksi

TABLE 2-J

AXIAL TENSION-TENSION FATIGUE LIFE PROPERTY SUMMARY – TD NiC

No data available to date.

TABLE 3-J

CREEP STRENGTH PROPERTY SUMMARY – TD NiC
(Reference 21)

Condition	Thickness (in.)	Test Direction	Test Temperature (F)	Stress (ksi)	Time (hr)	Strain (%)
Unknown	Sheet	L	1200	28	100	rupture
		T	1200	23	100	rupture
		L	1400	21	100	rupture
		T	1400	18	100	rupture
		L	1600	17	100	rupture
		T	1600	13	100	rupture
		L	1800	12	100	rupture
		T	1800	10	100	rupture
		L	2000	9	100	rupture
		T	2000	7	100	rupture

TABLE 4-J

OXIDATION RATE PROPERTY SUMMARY – TD NiC
(Reference 22)

Condition	Thickness (in.)	Test Temperature (F)	Test Pressure Torr	Exposure Time (hr)	Avg Thickness Change (%)	Weight Change (%)
Unknown	0.024 to 0.028	1600	760	96	+1.6	+0.05
		1900	760	24	+0.6	+0.10
		1900	760	96	+0.6	-13.90
		1900	0.18	24	+1.8	-0.20
		1900	0.18	96	+2.2	-3.45
		2200	760	24	+3.4	+0.20
		2200	760	96	+6.2	+0.05
		2200	0.18	24	+2.6	-0.45
		2200	0.18	96	+1.0	-0.15

TABLE 5-J

TOTAL NORMAL EMITTANCE PROPERTY SUMMARY – TD NiC
(Reference 21)

Condition	Test Method	Test Temperature (F)	Calculated Total Normal Emittance
HEATED IN AIR	Unknown	600	0.08
		800	0.15
		1000	0.16
		1200	0.18
		1500	0.30
		1700	0.44
		2000	0.57

REFERENCES

1. Kerr, J. R., and Cox, J. D., Effect of Environmental Exposure on Mechanical Properties of Several Foil Gage Refractory Alloys and Superalloys, Technical Report AFML-TR-65-92 (General Dynamics/Convair Report No. GDC 63-0817-5, 1965).

2. Leggett, H., et al., Mechanical and Physical Properties of Superalloy and Coated Refractory Alloy Foils, Technical Report No. AFML-TR-65-147, Douglas Aircraft Co. Report No. SM-48760 (August 1965).

3. Wlodek, S. T., "The Oxidation of Hastelloy X", Trans. A.I.M.E. 230 177-184 (February 1964).

4. Wood, W. D., Deem, H. W. and Lucks, C. F., The Emittance of Iron, Nickel, and Cobalt and Thin Alloys, DMIC Memorandum 119 (July 25, 1961).

5. Engineering Properties of Inconel 625, Bulletin T-42, Huntington Alloy Products Division (1966).

6. Wurst, J. C., Monthly Letter Report No. 30 on Contract AF33(615)-1312, University of Dayton Research Institute (November 1966).

7. Rabensteine, A. S., Oxidation Characteristics of Various Structural Materials for Ramjets and Heat Exchangers, Report PR 281-4Q-1 Contract AF33(657)-8706. Marquardt Corporation (June 15, 1963).

8. Slunder, C. J., Short-Time Tensile Properties of the Co-20Cr-15W-10Ni Cobalt-Base Alloy (L-605), DMIC Memorandum 179 (September 27, 1963).

9. Haynes Alloy No. 25, Bulletin, Union Carbide, Stellite Division (June 1962).

10. Lund, C. H. and Wagner, H. J., Oxidation of Nickel and Cobalt Base Superalloys, DMIC Report 214, March 1, 1965.

11. Hastelloy Alloy C. Bulletin, Union Carbide, Stellite Division (May, 1966).

12. The Processing and Properties of Hastelloy C, Redstone Scientific Information Center, RSK-28, May 1964.

13. Favor, R. J., Roberts, D. A. and Achbach, W. P., Design Information on Nickel-Base Alloys for Aircraft and Missiles, DMIC Report 132 (July 20, 1960).

14. High Temperature, High Strength, Nickel Base Alloys, INCO Bulletin (1964).

15. Popp, H. G., Benbow, J. M., Materials Property Data Compilation, Part I, Inconel 718, Second Quarterly Report, Contract AF33(657)-8017, General Electric Company (August 10, 1962).

16. Moon, D. P., Van Echo, J. A., Simmons, W. F., and Barker, J. F., Structural Damage in Thermally Cycled René 41 and Astroloy Sheet Materials, DMIC Report 126 (February 29, 1960).

17. Wlodek, S. T., "The Oxidation of René 41 and Udimet 700", Trans. A.I.M.E. 230, 1078-1090 (August 1964).

18. Metcalfe, A. G., Rose, F. K., and Zumbrunnen, A., Final Report on Diffusion Bonding of Refractory Metals and TD Nickel, AFML-TR-64-394, Volume II (December 1964).

19. Fatigue Properties of TD Nickel Sheet, DMIC Data Sheets (September 29, 1966).

20. Pettit, F. S., and Felten, E. J., "The Oxidation of Ni-2ThO_2 Between 900° and 1400°C", Journ. Electrochem. Soc. 111 135-139 (February 1964).

21. TD NiC Interim Data Sheets, E. I. DuPont Company (August 26, 1966).

22. Cherry, J. A., Engineering Test Memorandum No. 18 on Contract AF33(615)-1312, University of Dayton Research Institute (November 30, 1966).

UNCLASSIFIED

Security Classification

DOCUMENT CONTROL DATA - R&D

(Security classification of title, body of abstract and indexing annotation must be entered when the overall report is classified)

1 ORIGINATING ACTIVITY (Corporate author)
Solar Division of International Harvester Company
San Diego, California

2a REPORT SECURITY CLASSIFICATION
UNCLASSIFIED

2b GROUP

3 REPORT TITLE
EVALUATION OF SUPERALLOYS FOR HYPERSONIC VEHICLE HONEYCOMB HEAT SHIELDS

4 DESCRIPTIVE NOTES (Type of report and inclusive dates)
Summary Technical Report

5 AUTHOR(S) (Last name, first name, initial)
Malik, Raj K.
Stetson, Alvin R.

6 REPORT DATE	7a. TOTAL NO. OF PAGES	7b. NO. OF REFS
October 1968	196	41

8a CONTRACT OR GRANT NO.	9a. ORIGINATOR'S REPORT NUMBER(S)
F33615-67-C-1217	RDR 1467-4
b. PROJECT NO. 651-G	
c	9b. OTHER REPORT NO(S) (Any other numbers that may be assigned this report)
d	AFML-TR-68-292

10 AVAILABILITY/LIMITATION NOTICES
This document is subject to special export controls and each transmittal to foreign governments or foreign nationals may be made only with prior approval of the Materials Support Division, MAAS, Wright-Patterson AFB, Ohio

11 SUPPLEMENTARY NOTES	12. SPONSORING MILITARY ACTIVITY
	Air Force Materials Laboratory, Wright-Patterson AFB, Ohio 45433

13 ABSTRACT

The effects of reentry simulation exposures in 0.18 (200,600 feet), 10 (100,000 feet), and 760 Torr on the mechanical and structural properties of six 0.01-inch thick superalloy foils (Rene' 41, Inconel 718, Inconel 625, Haynes 25, TD Nickel, and TD Nickel/chromium) were determined.

Rene' 41 and Inconel 718 were eliminated from the program because of higher overall degradation in mechanical properties and oxidation rate due to 1800°F, 760 Torr, 100 cycles exposure than Inconel 625 and Haynes 25. Based on retention of at least 67 percent of initial properties after 760 or 0.18 Torr oxidation exposures for 100 one-hour slow cycles at different maximum temperatures (1800 - 2400°F), the recommended maximum use temperatures were 2400°F for TD Nickel/chromium, 2200°F for TD Nickel, 2000°F for Haynes 25, and 1800°F for Inconel 625. The further evaluation for combined effects of stress, temperature, and pressure in profile simulation tests for 100, one-hour slow cycles resulted in recommended maximum service temperatures of 2400, 2200, 2000, and 1800°F for TD Nickel/chromium, TD Nickel, Haynes 25, and Inconel 625, respectively. The most severe pressure was 0.18 Torr for Haynes 25 and 760 Torr for the other alloys.

The distribution of this abstract is unlimited.

DD FORM 1473

UNCLASSIFIED

Security Classification

14. KEY WORDS	LINK A		LINK B		LINK C	
	ROLE	WT	ROLE	WT	ROLE	WT
Rene' 41 Foil						
Inconel 718 Foil						
Inconel 625 Foil						
Haynes 25 Foil						
TD Nickel Foil						
TD Nickel/Chromium Foil						
Simulated Profile Oxidation						
Mechanical Tests						
Structural Properties						

INSTRUCTIONS

1. ORIGINATING ACTIVITY: Enter the name and address of the contractor, subcontractor, grantee, Department of Defense activity or other organization *(corporate author)* issuing the report.

2a. REPORT SECURITY CLASSIFICATION: Enter the overall security classification of the report. Indicate whether "Restricted Data" is included. Marking is to be in accordance with appropriate security regulations.

2b. GROUP: Automatic downgrading is specified in DoD Directive 5200.10 and Armed Forces Industrial Manual. Enter the group number. Also, when applicable, show that optional markings have been used for Group 3 and Group 4 as authorized.

3. REPORT TITLE: Enter the complete report title in all capital letters. Titles in all cases should be unclassified. If a meaningful title cannot be selected without classification, show title classification in all capitals in parenthesis immediately following the title.

4. DESCRIPTIVE NOTES: If appropriate, enter the type of report, e.g., interim, progress, summary, annual, or final. Give the inclusive dates when a specific reporting period is covered.

5. AUTHOR(S): Enter the name(s) of author(s) as shown on or in the report. Enter last name, first name, middle initial. If military, show rank and branch of service. The name of the principal author is an absolute minimum requirement.

6. REPORT DATE: Enter the date of the report as day, month, year, or month, year. If more than one date appears on the report, use date of publication.

7a. TOTAL NUMBER OF PAGES: The total page count should follow normal pagination procedures, i.e., enter the number of pages containing information.

7b. NUMBER OF REFERENCES: Enter the total number of references cited in the report.

8a. CONTRACT OR GRANT NUMBER: If appropriate, enter the applicable number of the contract or grant under which the report was written.

8b, 8c, & 8d. PROJECT NUMBER: Enter the appropriate military department identification, such as project number, subproject number, system numbers, task number, etc.

9a. ORIGINATOR'S REPORT NUMBER(S): Enter the official report number by which the document will be identified and controlled by the originating activity. This number must be unique to this report.

9b. OTHER REPORT NUMBER(S): If the report has been assigned any other report numbers *(either by the originator or by the sponsor)*, also enter this number(s).

10. AVAILABILITY/LIMITATION NOTICES: Enter any limitations on further dissemination of the report, other than those imposed by security classification, using standard statements such as:

(1) "Qualified requesters may obtain copies of this report from DDC."

(2) "Foreign announcement and dissemination of this report by DDC is not authorized."

(3) "U. S. Government agencies may obtain copies of this report directly from DDC. Other qualified DDC users shall request through _____."

(4) "U. S. military agencies may obtain copies of this report directly from DDC. Other qualified users shall request through _____."

(5) "All distribution of this report is controlled. Qualified DDC users shall request through _____."

If the report has been furnished to the Office of Technical Services, Department of Commerce, for sale to the public, indicate this fact and enter the price, if known.

11. SUPPLEMENTARY NOTES: Use for additional explanatory notes.

12. SPONSORING MILITARY ACTIVITY: Enter the name of the departmental project office or laboratory sponsoring *(paying for)* the research and development. Include address.

13. ABSTRACT: Enter an abstract giving a brief and factual summary of the document indicative of the report, even though it may also appear elsewhere in the body of the technical report. If additional space is required, a continuation sheet shall be attached.

It is highly desirable that the abstract of classified reports be unclassified. Each paragraph of the abstract shall end with an indication of the military security classification of the information in the paragraph, represented as *(TS)*, *(S)*, *(C)*, or *(U)*.

There is no limitation on the length of the abstract. However, the suggested length is from 150 to 225 words.

14. KEY WORDS: Key words are technically meaningful terms or short phrases that characterize a report and may be used as index entries for cataloging the report. Key words must be selected so that no security classification is required. Identifiers, such as equipment model designation, trade name, military project code name, geographic location, may be used as key words but will be followed by an indication of technical context. The assignment of links, rules, and weights is optional.